WASH - 1136
EANDC(US) - 122 U
INDC(US) - 14 U
INDC-317

Reports to . . .

THE AEC NUCLEAR CROSS SECTIONS ADVISORY COMMITTEE

Meeting at

RICE UNIVERSITY
HOUSTON, TEXAS

September 18-19, 1969

Compiled by . . .

R.E. Chrien, Secretary, NCSAC

BROOKHAVEN
NATIONAL
LABORATORY

WASH - 1136
EANDC(US) - 122 U
INDC(US) - 14 U

Reports to . . .

THE AEC NUCLEAR CROSS SECTIONS ADVISORY COMMITTEE

Meeting at

Rice University
Houston, Texas

September 18-19, 1969

Compiled by . . .

R. E. Chrien, Secretary, NCSAC

BROOKHAVEN
NATIONAL
LABORATORY

PREFACE

The reports in this document were submitted to the AEC Nuclear Cross Sections Advisory Committee (NCSAC) at the meeting at Houston, Texas, on September 18 and 19, 1969. The reporting laboratories are those having a substantial effort in measuring neutron and nuclear cross sections of relevance to the U. S. applied nuclear energy program. The material contained in these reports is to be regarded as comprised of informal statements of recent developments and preliminary data. Appropriate subjects are listed as follows:

1. Microscopic neutron cross sections relevant to reactor development, including shielding. Inverse reactions where pertinent are included.

2. Charged particle cross sections, especially as appropriate in developing and testing nuclear models.

3. Gamma-ray production, radioactive decay, and theoretical developments in nuclear structure.

4. Proton and alpha-particle cross sections, at energies of up to 1 GeV, which are of interest to the space program.

These reports cannot be regarded as a complete summary of the nuclear research effort of the AEC. A number of laboratories, whose research is less programmatically oriented do not submit reports; neither do the submitted reports reflect all the work related to nuclear cross sections in progress at the submitting laboratory.

Persons wishing to make use of these data should contact the individual experimenter for further details. The data which appear in this document should be quoted only by permission of the contributor and should be referenced as private communication, and not by this document number.

This compilation has been produced almost completely from master copies prepared by the individual contributors listed in the Table of Contents. It is a pleasure to acknowledge their help in the preparation of these reports.

R. E. Chrien
Secretary, NCSAC
Brookhaven National Laboratory
Upton, New York 11973

TABLE OF CONTENTS

Previously submitted Reports to the AEC Nuclear Cross Sections Advisory Committee include the following:

April 1969 Meeting at Oak Ridge, Tennessee	WASH-1127 EANDC(US)120 U INDC(US)10U
October 1968 Meeting at Columbia University	WASH-1124 EANDC-US-111 U INDC-US-9 U
April 1968 Meeting at Los Alamos, New Mexico	WASH-1093 EANDC-US-105 U INDC-US-2 U
October 1967 Meeting at Idaho Falls, Idaho	WASH-1079 EANDC-US-104 U INDC-US-12U
April 1967 Meeting at Brookhaven, New York	WASH-1074 EANDC-US-99 U INDC-US-9 U
November 1966 Meeting at Argonne, Illinois	WASH-1071 EANDC-US-91 U INDC-US-5 U
March 1966 Meeting at Washington, D. C.	WASH-1068 EANDC-US-85 U INDC-US-3 U
October 1965 Meeting at Duke University	WASH-1064 EANDC-US-79 U
March 1965 Meeting at National Bureau of Standards	WASH-1056 EANDC-US-72 U
October 1964 Meeting at Oak Ridge National Laboratory	WASH-1053 EANDC-US-70 U
June 1964 Meeting at Columbia University	WASH-1048 EANDC-US-57 U
January 1964 Meeting at Savannah River Laboratory	WASH-1046 EANDC-US-50 U

An index to measurements in WASH-1136 pertinent to requests listed in WASH-1078 "Compilation of Requests for Nuclear Cross Section Measurements" (June 1967). A CINDA-type index has been prepared by L. T. Whitehead of the Division of Technical Information Extension, Oak Ridge; and follows on page viii.

REQUEST NO.	MATERIAL	X-SECTION TYPE	WASH-1136 PAGE
1	D-2	DEL	117, 215
2	D-2	DEL	117, 215
4	T-3	DEL	117
13	LI-6	NA	6
27	BE-NAT	GPR	193
29	BE-9	MIS	193
31	B-10	TOT	6
34	C-NAT	DEL	24
37	C-NAT	GPR	120, 193
38	N-NAT	DEL	98
39	N-NAT	SIN	98
40	N-NAT	GPR	196
41	N-NAT	GPR	196
42	N-NAT	GPR	196
44	N-NAT	ABS	98
45	N-NAT	ABS	98
50	O-NAT	GPR	137, 196
54	O-NAT	NA	137
59	NA-NAT	RPR	28
65	AL-NAT	GPR	35, 120
66	AL-NAT	GPR	35, 120
71	SI-NAT	GPR	189
76	TI-NAT	SIN	1
77	TI-NAT	EM	1
79	TI-46	NP	55
80	TI-47	NP	55
81	TI-48	NP	55
84	V-NAT	NG	144
87	CR-NAT	NG	144
88	CR-NAT	GPR	196
90	MN-NAT	NG	22
91	MN-NAT	NG	22
92	MN-NAT	NG	22
95	FE-NAT	SIN	24
96	FE-NAT	SIN	24
97	FE-NAT	SIN	24
100	FE-NAT	GPR	35

REQUEST NO.	MATERIAL	X-SECTION TYPE	WASH-1136 PAGE
101	FE-NAT	GPR	35
102	FE-NAT	GPR	35
103	FE-NAT	GPR	35
107	CO-NAT	TOT	28
110	NI-NAT	DEL	24
111	NI-NAT	SIN	24
115	NI-NAT	GPR	196
116	NI-NAT	GPR	196
124	ZR-NAT	NG	22
125	ZR-NAT	GPR	202
153	NB-NAT	GPR	202
154	NB-NAT	GPR	202
155	NB-94	NG	57
156	NB-94	NG	52
157	NB-95	NG	57
158	MO-NAT	SIN	1
161	RH-103	NG	30, 33, 34, 114
183	PM-147	NG	50
197	EU-151	NG	28
198	EU-153	NG	28
205	GD-NAT	NG	28, 33
207	GD-155	NG	28, 33, 34
209	GD-157	NG	34
210	GD-158	NG	28
213	ER-166	NG	28
214	ER-167	NG	10, 28
215	ER-170	NG	28
216	TM-169	NG	30
217	TM-170	NG	44
231	W-NAT	GPR	185
233	W-NAT	GPR	185, 189, 202
234	W-NAT	GPR	189, 202
239	PB-NAT	NG	78, 83
240	PB-NAT	GPR	78, 83
244	TH-NAT	NG	30, 55
246	TH-232	N2N	55
253	U-233	NG	30
254	U-233	NG	30
259	U-233	NF	65
270	U-234	NG	110
271	U-234	NG	110
281	U-235	GPR	107
285	U-235	RPR	93, 145

REQUEST NO.	MATERIAL	X-SECTION TYPE	WASH-1136 PAGE
286	U-235	NF	4
287	U-235	NF	4
288	U-235	NF	4
300	U-236	NG	110
301	U-236	NG	110
303	U-237	NF	126
307	U-238	SIN	2
308	U-238	NG	33, 110
309	U-238	NG	4, 33, 110
310	U-238	GPR	35, 185, 189
311	U-238	GPR	35
312	U-238	FR	4
315	NP-237	NG	110, 114
316	NP-237	NG	110, 114
317	NP-237	NF	110
330	PU-239	DEL	3
331	PU-239	DEL	3
332	PU-239	SIN	3
334	PU-239	NG	97
337	PU-239	RPR	97
338	PU-239	GPR	19, 185, 189
341	PU-239	NF	4, 74
342	PU-239	NF	4, 61, 97, 110
343	PU-239	FR	4
355	PU-240	SIN	3
357	PU-240	NG	143
358	PU-240	NG	143
364	PU-240	FR	143
373	PU-242	NG	110
380	AM-241	NG	53
383	AM-243	NG	110
387	CM-243	NF	95, 110
388	CM-244	NG	54, 110
389	CM-244	NF	110
394	CM-245	NF	110
398	CM-247	NF	110
400	BK-249	TOT	95
404	CF-252	NG	110

ELEMENT S	A	QUANTITY	TYPE	ENERGY MIN	ENERGY MAX	DOCUMENTATION REF	VOL	PAGE	DATE	LAB	COMMENTS	SERIAL NO.
H	001	TOTAL XSECT	EXPT-PROG	1. 6	2. 7	WASH1136	149		9/69	RPI	STOLER+,TOF,TO BE DONE	48059
H	001	TOTAL XSECT	EXPT-PROG	1.5 6	1.5 7	WASH1136	133		9/69	NBS	SCHWARTZ+,NO STRUCTURE SEEN,CURVE	48091
H	001	N,GAMMA	EXPT-PROG	2.5-2		WASH1136	31		9/69	COL	COKINOS+,ABSOL VALUE GIVN,.2PC ERROR	47872
D	002	DIFF ELASTIC	EXPT-PROG	2.2 7		WASH1136	117		9/69	LAS	HOPKINS+,VDG,TOF,POLARIZATION MEASD	47974
D	002	DIFF ELASTIC	EXPT-PROG	8. 6		WASH1136	215		9/69	DKE	TAYLOR+ POL NEUTS,THETA#40-70DEG,TBP	48031
D	002	POLARIZATION	EXPT-PROG	2.2 7		WASH1136	117		9/69	LAS	HOPKINS+,VDG,TOF,ASYMM 40-118.5DEG	47976
D	002	POLARIZATION	EXPT-PROG	8. 6		WASH1136	215		9/69	DKE	TAYLOR+ POL NEUTS,THETA#40-70DEG,TBP	48030
T	003	DIFF ELASTIC	EXPT-PROG	2.2 7		WASH1136	117		9/69	LAS	HOPKINS+,VDG,TOF,POLARIZATION MEASD	47975
T	003	POLARIZATION	EXPT-PROG	2.2 7		WASH1136	117		9/69	LAS	HOPKINS+,VDG,TOF,ASYMM 40-118.5DEG	47977
HE	003	N,GAMMA	EXPT-PROG	0.	8. 6	WASH1136	87		9/69	LRL	BERMAN+,INVERSE REACTION,CURVE	47967
HE	004	DIFF ELASTIC	EXPT-PROG	1.8 7	2.3 7	WASH1136	119		9/69	LAS	WALTER+ ANG DIST,3ES,20-140DEG,NDG	47979
HE	004	DIFF ELASTIC	EXPT-PROG	8. 6		WASH1136	214		9/69	DKE	STAMMBACH+ POL NEUTS,NO DATA,TBP	48032
HE	004	POLARIZATION	EXPT-PROG	8. 6		WASH1136	214		9/69	DKE	STAMMBACH+ POL NEUTS,NO DATA,TBP	48029
LI		ABSORPTION	EXPT-PROG	THR		WASH1136	6		9/69	ANL	MEADOWS+,0.025EV VALUE GIVEN	47755
LI	006	ABSORPTION	EXPT-PROG	THR		WASH1136	6		9/69	ANL	MEADOWS+,0.025EV VALUE GIVEN	47754
BE	009	THRMLSCATLAW	THEO-PROG			WASH1136	39		9/69	GA	BORGONOVI,CURVE,DETAILS IN GA-9364	47903
BE	009	N,PROTON	EXPT-PROG	1.5 7		WASH1136	193		9/69	TNC	NELLIS+,GAMMA SPEC SHOWN,478KEV PEAK	48117
B	010	ABSORPTION	EXPT-PROG	THR		WASH1136	6		9/69	ANL	MEADOWS+,OKS BNL325,.025EV VALU GIVN	47756
C		TOTAL XSECT	EXPT-PROG	1. 5	1.5 6	WASH1136	7		9/69	ANL	MEADOWS+,2.5KEV RESOL,LEAST-SQRS FIT	47757
C		DIFF ELASTIC	EXPT-PROG	4.0 4	5.6 6	WASH1136	24		9/69	CSE	LINDOW+,3ES,THETA#25-148DEG,NO DATA	47795
C		INELST GAMMA	EXPT-PROG	5. 6	1.5 7	WASH1136	193		9/69	TNC	MARTIN+,2ES,PRODUCTN SIGS 4.43MEV G	48116
C	012	INELST GAMMA	EXPT-PROG		1.4 7	WASH1136	120		9/69	LAS	DRAKE+,4.44-MEV LVL EXCITED,NO DATA	48059
N		NONEL GAMMAS	EXPT-PROG	1.5 7		WASH1136	196		9/69	TNC	BUCHANAN+,TO BE COMPLETED	48115
N		NONEL GAMMAS	EXPT-PROG	1.5 7		WASH1136	196		9/69	TNC	BUCHANAN+,TO BE COMPLETED	48114
O	016	TOTAL XSECT	EXPT-PROG	2.4 6		WASH1136	26		9/69	COL	KALYNA+,VDG+TOF,ABSOL MEAST TBC	47796
O	016	RESON PARAMS	EXPT-PROG	1.8 6		WASH1136	137		9/69	ORL	FOWLER+,J+PI GIVEN FROM SCAT MEASTS	48090
O	016	NONELASTIC	EXPT-PROG	6.7 6	1.1 7	WASH1136	137		9/69	ORL	DICKENS+,SUM OF PARTIAL SIGS,NO DATA	48098
O	016	INELST GAMMA	EXPT-PROG	6.7 6	1.1 7	WASH1136	137		9/69	ORL	DICKENS+,GE(LI),GAM SPEC+SIG,TBP NSE	48079
O	016	N,ALPHA	EXPT-PROG	6.7 6	1.1 7	WASH1136	137		9/69	ORL	DICKENS+,GE(LI),GAM SPEC+SIG,TBP NSE	48078
NA	023	TOTAL XSECT	EXPT-PROG	1. 0	5. 4	WASH1136	28		9/69	COL	CAMARDA+,NO DATA GIVEN,TO BE COMPLTD	47797
NA	023	RESON PARAMS	EXPT-PROG	1. 0	5. 4	WASH1136	28		9/69	COL	CAMARDA+,NO DATA GIVEN,TO BE COMPLTD	47819
NA	023	STRNTH FNCTN	EXPT-PROG	1. 0	5. 4	WASH1136	28		9/69	COL	CAMARDA+,NO DATA GIVEN,TO BE COMPLTD	47838
AL	027	NONEL GAMMAS	EXPT-PROG	TR	1.6 7	WASH1136	35		9/69	GA	HOOT+,GE(LI) DET,TOF,TO BE COMPL,NDG	47899
AL	027	NONEL GAMMAS	EXPT-PROG	4. 6	7.5 6	WASH1136	120		9/69	LAS	DRAKE+,ALSO 6MEV,TABLES,TO BE PUBLSH	47979
AL	027	N,PROTON	EXPT-PROG	FISS		WASH1136	55		9/69	MTR	SCHUMAN+,ACTIVATION ONLY,NO DATA	47926
AL	027	N,ALPHA	EXPT-PROG	FISS		WASH1136	55		9/69	MTR	SCHUMAN+,ACTIVATION ONLY,NO DATA	47925
AL	027	N,ALPHA	EXPT-PROG	FISS		WASH1136	55		9/69	MTR	SCHUMAN+,ACTIVATION,VALUE GIVEN	47931
AL	027	N,ALPHA	EXPT-PROG	1.3 7	1.5 7	WASH1136	89		9/69	LRL	WARNOCK+,TO BE COMPLETED,CURVE	47968
SI		NONEL GAMMAS	EXPT-PROG	5. 6	1.1 7	WASH1136	189		9/69	TNC	TUCKER+,SEE REPORT DASA-2333	48119
S	034	TOTAL XSECT	EXPT-PROG	4	5	WASH1136	208		9/69	DKE	SEIBEL+ TO BE PUBLISHED,NO DATA GIVN	48053
S	034	RESON PARAMS	EXPT-PROG	4	5	WASH1136	208		9/69	DKE	SEIBEL+ TO BE PUBLISHED,NO DATA GIVN	48050
CL		SPECT NGAMMA	EXPT-PROG	NDG		WASH1136	231		9/69	DKE	PEAK+ NO DATA GIVEN,TO BE PUBLISHED	48028
AR		TOTAL XSECT	EXPT-PROG	1. 0	5. 4	WASH1136	28		9/69	COL	CAMARDA+,NO DATA GIVEN,TO BE COMPLTD	47798
AR		RESON PARAMS	EXPT-PROG	1. 0	5. 4	WASH1136	28		9/69	COL	CAMARDA+,NO DATA GIVEN,TO BE COMPLTD	47819
AR		STRNTH FNCTN	EXPT-PROG	1. 0	5. 4	WASH1136	28		9/69	COL	CAMARDA+,NO DATA GIVEN,TO BE COMPLTD	47839
AR	040	TOTAL XSECT	EXPT-PROG	4	5	WASH1136	208		9/69	DKE	SEIBEL+ TO BE PUBLISHED,NO DATA GIVN	48054
AR	040	RESON PARAMS	EXPT-PROG	4	5	WASH1136	208		9/69	DKE	SEIBEL+ TO BE PUBLISHED,NO DATA GIVN	48051
CA	048	TOTAL XSECT	EXPT-PROG	4	5	WASH1136	208		9/69	DKE	SEIBEL+ TO BE PUBLISHED,NO DATA GIVN	48052

ELEMENT S A	QUANTITY	TYPE	ENERGY MIN	ENERGY MAX	DOCUMENTATION REF VOL PAGE	DATE	LAB	COMMENTS	SERIAL NO.
CA 048	RESON PARAMS	THEO-PROG	NDG		WASH1136 210	9/69	DKE	DIVADEENAM+ SHELL-MODEL CALC,NO DATA	48036
CA 048	RESON PARAMS	EXPT-PROG	4	5	WASH1136 208	9/69	DKE	SEIBEL+ TO BE PUBLISHED,NO DATA GIVN	48049
CA 048	STRNTH FNCTN	THEO-PROG	NDG		WASH1136 210	9/69	DKE	DIVADEENAM+ SHELL-MODEL CALC,NO DATA	48035
TI	TOTAL XSECT	EXPT-PROG	1. 5	1.5 6	WASH1136 1	9/69	ANL	SMITH+,ANAL TO BE COMPLETED,NO DATA	47719
TI	DIFF ELASTIC	EXPT-PROG	1. 5	1.5 6	WASH1136 1	9/69	ANL	SMITH+,ANAL TO BE COMPLETED,NO DATA	47720
TI	DIFF INELAST	EXPT-PROG	1. 5	1.5 6	WASH1136 1	9/69	ANL	SMITH+,ANAL TO BE COMPLETED,NO DATA	47721
TI 046	N2N REACTION	EXPT-PROG	FISS		WASH1136 55	9/69	MTR	SCHUMAN+,ACTIVATION,VALUE GIVEN	47948
TI 046	N,PROTON	EXPT-PROG	FISS		WASH1136 55	9/69	MTR	SCHUMAN+,ACTIVATION,VALUE GIVEN	47945
TI 047	N,PROTON	EXPT-PROG	FISS		WASH1136 55	9/69	MTR	SCHUMAN+,ACTIVATION,VALUE GIVEN	47946
TI 048	N,PROTON	EXPT-PROG	FISS		WASH1136 55	9/69	MTR	SCHUMAN+,ACTIVATION,VALUE GIVEN	47947
TI 050	N,GAMMA	EXPT-PROG	FISS		WASH1136 55	9/69	MTR	SCHUMAN+,ACTIVATION,VALUE GIVEN	47949
V	RESON PARAMS	EXPT-PROG	0	1. 6	WASH1136 144	9/69	RPI	STIEGLITZ+,CAPT+TRANS MEAST,ANAL TBC	48074
V 051	RESON PARAMS	THEO-PROG	4.2 0	1.7 1	WASH1136 149	9/69	RPI	LUBERT+,J+WN SRESON COLUMBIA DATA	48058
CR	INELST GAMMA	EXPT-PROG	5. 6	1.5 7	WASH1136 196	9/69	TNC	BUCHANAN+,2ES,SPECTRA+SIGS GIVEN	48113
CR 050	RESON PARAMS	EXPT-PROG	0	1. 6	WASH1136 144	9/69	RPI	STIEGLITZ+,FROM CAPT MEASTS,ANAL TBC	48072
CR 052	RESON PARAMS	EXPT-PROG	0	1. 6	WASH1136 144	9/69	RPI	STIEGLITZ+,FROM CAPT MEASTS,ANAL TBC	48071
CR 053	RESON PARAMS	EXPT-PROG	0	1. 6	WASH1136 144	9/69	RPI	STIEGLITZ+,FROM CAPT MEASTS,ANAL TBC	48070
CR 054	RESON PARAMS	EXPT-PROG	0	1. 6	WASH1136 144	9/69	RPI	STIEGLITZ+,FROM CAPT MEASTS,ANAL TBC	48069
MN 055	RESON PARAMS	EXPT-PROG	0	1	WASH1136 22	9/69	BNL	CHRIEN+,QUALITAT DATA FROM CAPT SPEC	47780
MN 055	N,GAMMA	EXPT-PROG	3		WASH1136 30	9/69	COL	ARBO+,TO BE DONE	47864
MN 055	SPECT NGAMMA	EXPT-PROG	0	1	WASH1136 22	9/69	BNL	CHRIEN+,CAPT IN FIRST SRESON,NO DATA	47779
FE	TOTAL XSECT	EXPT-PROG	5. 5	1.5 7	WASH1136 133	9/69	NBS	SCHWARTZ+,STRUCTURE SEEN,CFD OTHERS	48090
FE	NOVEL GAMMAS	EXPT-PROG	TR	1.6 7	WASH1136 35	9/69	GA	HOOT+,GE(LI) DET,TOF,TO BE COMPL,NDG	47898
FE	N,GAMMA	EXPT-PROG	3		WASH1136 30	9/69	COL	ARBO+,TO BE DONE	47869
FE	N,PROTON	EXPT-PROG	FISS		WASH1136 55	9/69	MTR	SCHUMAN+,ACTIVATION ONLY,NO DATA	47927
FE 054	DIFF ELASTIC	EXPT-PROG	4.0 6	5.6 6	WASH1136 24	9/69	CSE	LINDOW+,3ES,THETA#25-148DEG,NO DATA	47787
FE 054	DIFF INELAST	EXPT-PROG	4.0 6	5.6 6	WASH1136 24	9/69	CSE	LINDOW+,3ES,THETA#25-148DEG,NO DATA	47791
FE 056	DIFF ELASTIC	EXPT-PROG	4.0 6	5.6 6	WASH1136 24	9/69	CSE	LINDOW+,3ES,THETA#25-148DEG,NO DATA	47788
FE 056	DIFF INELAST	EXPT-PROG	4.0 6	5.6 6	WASH1136 24	9/69	CSE	LINDOW+,3ES,THETA#25-148DEG,NO DATA	47792
CO 059	TOTAL XSECT	EXPT-PROG	1. 0	5. 4	WASH1136 28	9/69	COL	CAMARDA+,NO DATA GIVEN,TO BE COMPLTD	47799
CO 059	TOTAL XSECT	EXPT-PROG		1. 6	WASH1136 108	9/69	LOK	FISHER+,POLARIZED TARGET,TO BE DONE	47972
CO 059	RESON PARAMS	EXPT-PROG	1. 0	5. 4	WASH1136 28	9/69	COL	CAMARDA+,NO DATA GIVEN,TO BE COMPLTD	47820
CO 059	STRNTH FNCTN	EXPT-PROG	1. 0	5. 4	WASH1136 28	9/69	COL	CAMARDA+,NO DATA GIVEN,TO BE COMPLTD	47840
NI	INELST GAMMA	EXPT-PROG	4. 6	1.5 7	WASH1136 196	9/69	TNC	BUCHANAN+,2ES,SPECTRA+SIGS GIVEN	48112
NI	N,GAMMA	EXPT-PROG	3.3-2	2.7-1	WASH1136 22	9/69	BNL	BRUNHART+,MOXON-RAE DET,ANAL TBC	47782
NI 058	DIFF ELASTIC	EXPT-PROG	4.0 6	5.6 6	WASH1136 24	9/69	CSE	LINDOW+,3ES,THETA#25-148DEG,NO DATA	47789
NI 058	DIFF INELAST	EXPT-PROG	4.0 6	5.6 6	WASH1136 24	9/69	CSE	LINDOW+,3ES,THETA#25-148DEG,NO DATA	47793
NI 058	N,PROTON	EXPT-PROG	FISS		WASH1136 55	9/69	MTR	SCHUMAN+,ACTIVATION,VALUE GIVEN	47942
NI 060	RESON PARAMS	EXPT-PROG	0	1. 6	WASH1136 144	9/69	RPI	STIEGLITZ+,CAPT+TRANS MEAST,ANAL TBC	48073
NI 060	DIFF ELASTIC	EXPT-PROG	4.0 6	5.6 6	WASH1136 24	9/69	CSE	LINDOW+,3ES,THETA#25-148DEG,NO DATA	47790
NI 060	DIFF INELAST	EXPT-PROG	4.0 6	5.6 6	WASH1136 24	9/69	CSE	LINDOW+,3ES,THETA#25-148DEG,NO DATA	47794
NI 061	N,PROTON	EXPT-PROG	FISS		WASH1136 55	9/69	MTR	SCHUMAN+,ACTIVATION	47943
NI 064	N,GAMMA	EXPT-PROG	FISS		WASH1136 55	9/69	MTR	SCHUMAN+,ACTIVATION	47944
NI 064	N,PROTON	EXPT-PROG	NDG		WASH1136 107	9/69	LOK	GRENCH+,TO BE COMPLETED,NO DATA GIVN	47983
CU	NOVEL GAMMAS	EXPT-PROG	1.4 7		WASH1136 32	9/69	COL	STAMATELATOS+,GAMMA SPEC,NO DATA	47877
CU	N,GAMMA	EXPT-PROG	3.3-2	2.7-1	WASH1136 22	9/69	BNL	BRUNHART+,MOXON-RAE DET,ANAL TBC	47783
CU 065	RESON PARAMS	EXPT-PROG	2.3 2		WASH1136 147	9/69	PPI	YAMAMURO+,J+PI ASSIGNED TO S-WAVE	48066
ZN 064	N,GAMMA	EXPT-PROG	FISS		WASH1136 55	9/69	MTR	SCHUMAN+,ACTIVATION,VALUE GIVEN	47936

ELEMENT S A	QUANTITY	TYPE	ENERGY MIN	ENERGY MAX	DOCUMENTATION REF VOL PAGE	DATE	LAB	COMMENTS	SERIAL NO.
ZN 064	N,PROTON	EXPT-PROG	FISS		WASH1136 55	9/69	MTR	SCHUMAN+,ACTIVATION,VALUE GIVEN	47937
ZN 067	N,PROTON	EXPT-PROG	FISS		WASH1136 55	9/69	MTR	SCHUMAN+,ACTIVATION,VALUE GIVEN	47938
ZN 068	N,GAMMA	EXPT-PROG	FISS		WASH1136 55	9/69	MTR	SCHUMAN+,ACTIVATION,TO ZN69M,VALUE	47941
ZN 068	N,ALPHA	EXPT-PROG	FISS		WASH1136 55	9/69	MTR	SCHUMAN+,ACTIVATION,VALUE GIVEN	47939
ZN 070	N,GAMMA	EXPT-PROG	FISS		WASH1136 55	9/69	MTR	SCHUMAN+,ACTIVATION,TO ZN71M,VALUE	47940
AS 075	N,ALPHA	EXPT-PROG	1.3 7	1.5 7	WASH1136 89	9/69	LRL	WARNOCK+,CURV,STRUCTURE SEEN,TBC	47969
SR 088	RESON PARAMS	THEO-PROG	NDG		WASH1136 210	9/69	DKE	DIVADEENAM+ SHELL-MODEL CALC,NO DATA	48037
SR 088	STRNTH FNCTN	THEO-PROG	NDG		WASH1136 210	9/69	DKE	DIVADEENAM+ SHELL-MODEL CALC,NO DATA	48034
ZR	NONEL GAMMAS	EXPT-PROG	1.4 7		WASH1136 32	9/69	COL	STAMATELATOS+,GAMMA SPEC,NO DATA	47879
ZR	INELST GAMMA	EXPT-PROG	1.6 6	1.5 7	WASH1136 202	9/69	TNC	MARTIN+,4ES,SPECTRA+SIGS GIVEN	48111
ZR	N,GAMMA	EXPT-PROG	3.3-2	2.7-1	WASH1136 22	9/69	BNL	BRUNHART+,MOXON-RAE DET,ANAL TBC	47781
ZR 090	RESON PARAMS	THEO-PROG	NDG		WASH1136 210	9/69	DKE	DIVADEENAM+ SHELL-MODEL CALC,NO DATA	48036
ZR 090	STRNTH FNCTN	THEO-PROG	NDG		WASH1136 210	9/69	DKE	DIVADEENAM+ SHELL-MODEL CALC,NO DATA	48033
NB 093	RESON PARAMS	EXPT-PROG	NDG		WASH1136 114	9/69	LAS	HARLOW+,PHYSICS -8 SHOT,ANAL TBC	47986
NB 093	INELST GAMMA	EXPT-PROG	7.5 5	1.0 6	WASH1136 202	9/69	TNC	WILLIAMS,13ES,GAMMA YLDS GIVN,TBC	48110
NB 093	RES INT ABS	EXPT-PROG	THR		WASH1136 52	9/69	MTR	SCHUMAN,VALUE GIVEN	47917
NB 093	N,GAMMA	EXPT-PROG	THR		WASH1136 52	9/69	MTR	SCHUMAN,VALUE GIVEN	47915
NB 093	SPECT NGAMMA	EXPT-PROG	NDG		WASH1136 114	9/69	LAS	HARLOW+,PHYSICS -8 SHOT,ANAL TBC	47985
NB 094	TOTAL XSECT	EXPT-PROG	NDG		WASH1136 57	9/69	MTR	YOUNG+,ANAL TBC,NO DATA BUT RES PARS	47950
NB 094	RESON PARAMS	EXPT-PROG	1.2 1	2.3 1	WASH1136 57	9/69	MTR	YOUNG+,WN WG FOR 2 RESON,ANAL TBC	47952
NB 094	RES INT ABS	EXPT-PROG	THR		WASH1136 52	9/69	MTR	SCHUMAN,VALUE GIVEN	47910
NB 094	N,GAMMA	EXPT-PROG	THR		WASH1136 52	9/69	MTR	SCHUMAN,VALUE GIVEN	47916
NB 095	TOTAL XSECT	EXPT-PROG	NDG		WASH1136 57	9/69	MTR	YOUNG+,NO RESON BELO 50EV,ANAL TBC	47951
MO	N,GAMMA	EXPT-PROG	1. 0	1. 3	WASH1136 33	9/69	GA	LOPEZ+,TOF,TO BE COMPLETED,NO DATA	47880
MO 092	TOTAL XSECT	EXPT-PROG		1.5 6	WASH1136 1	9/69	ANL	SMITH+,TO BE COMPLETED,NO DATA GIVEN	47732
MO 092	RESON PARAMS	EXPT-PROG	0	1	WASH1136 19	9/69	BNL	CHRIEN+,J+PI FOR 346EV RESONANCE	47776
MO 092	RESON PARAMS	EXPT-PROG	8.5 3	5.8 4	WASH1136 209	9/69	DKE	DIVADEENAM+ J+PI+WN GIVN FOR 23RESON	48029
MO 092	DIFF ELASTIC	EXPT-PROG		1.5 6	WASH1136 1	9/69	ANL	SMITH+,ANAL TO BE COMPLETED,NO DATA	47722
MO 092	DIFF INELAST	EXPT-PROG		1.5 6	WASH1136 1	9/69	ANL	SMITH+,ANAL TO BE COMPLETED,NO DATA	47727
MO 092	SPECT NGAMMA	EXPT-PROG	0	1	WASH1136 19	9/69	BNL	CHRIEN+,RESONANT CAPT,NO DATA GIVEN	47775
MO 094	TOTAL XSECT	EXPT-PROG		1.5 6	WASH1136 1	9/69	ANL	SMITH+,TO BE COMPLETED,NO DATA GIVEN	47733
MO 094	DIFF ELASTIC	EXPT-PROG		1.5 6	WASH1136 1	9/69	ANL	SMITH+,ANAL TO BE COMPLETED,NO DATA	47723
MO 094	DIFF INELAST	EXPT-PROG		1.5 6	WASH1136 1	9/69	ANL	SMITH+,ANAL TO BE COMPLETED,NO DATA	47728
MO 096	TOTAL XSECT	EXPT-PROG		1.5 6	WASH1136 1	9/69	ANL	SMITH+,TO BE COMPLETED,NO DATA GIVEN	47734
MO 096	DIFF ELASTIC	EXPT-PROG		1.5 6	WASH1136 1	9/69	ANL	SMITH+,ANAL TO BE COMPLETED,NO DATA	47724
MO 096	DIFF INELAST	EXPT-PROG		1.5 6	WASH1136 1	9/69	ANL	SMITH+,ANAL TO BE COMPLETED,NO DATA	47729
MO 098	TOTAL XSECT	EXPT-PROG		1.5 6	WASH1136 1	9/69	ANL	SMITH+,TO BE COMPLETED,NO DATA GIVEN	47735
MO 098	DIFF ELASTIC	EXPT-PROG		1.5 6	WASH1136 1	9/69	ANL	SMITH+,ANAL TO BE COMPLETED,NO DATA	47725
MO 098	DIFF INELAST	EXPT-PROG		1.5 6	WASH1136 1	9/69	ANL	SMITH+,ANAL TO BE COMPLETED,NO DATA	47730
MO 100	TOTAL XSECT	EXPT-PROG		1.5 6	WASH1136 1	9/69	ANL	SMITH+,TO BE COMPLETED,NO DATA GIVEN	47736
MO 100	DIFF ELASTIC	EXPT-PROG		1.5 6	WASH1136 1	9/69	ANL	SMITH+,ANAL TO BE COMPLETED,NO DATA	47726
MO 100	DIFF INELAST	EXPT-PROG		1.5 6	WASH1136 1	9/69	ANL	SMITH+,ANAL TO BE COMPLETED,NO DATA	47731
RH 103	RESON PARAMS	EXPT-PROG	NDG		WASH1136 34	9/69	GA	CARLSON+,NO DATA GIVEN,TO BE COMPLTD	47894
RH 103	ELASTIC	EXPT-PROG	2.5 1	1. 5	WASH1136 114	9/69	LAS	HOFFMAN+,PHYSICS-8 SHOT,ANAL TBC	48024
RH 103	RES INT ABS	EXPT-PROG	NDG		WASH1136 34	9/69	GA	CARLSON+,NO DATA GIVEN,TO BE COMPLTD	47896
RH 103	N,GAMMA	EXPT-PROG	3		WASH1136 30	9/69	COL	ARBO+,TO BE DONE	47861
RH 103	N,GAMMA	EXPT-PROG	1. 0	1. 3	WASH1136 33	9/69	GA	LOPEZ+,TOF,TO BE COMPLETED,NO DATA	47881
RH 103	N,GAMMA	EXPT-PROG	NDG		WASH1136 34	9/69	GA	CARLSON+,NO DATA GIVEN,TO BE COMPLTD	47895

x

ELEMENT S A	QUANTITY	TYPE	ENERGY MIN	ENERGY MAX	DOCUMENTATION REF VOL PAGE DATE	LAB	COMMENTS	SERIAL NO.
RH 103	N,GAMMA	EXPT-PROG	2.5 1	1. 5	WASH1136 114 9/69	LAS	HOFFMAN+,PHYSICS-8 SHOT,ANAL TBC	48025
AG 107	N,GAMMA	EXPT-PROG	3		WASH1136 22 9/69	COL	ARBO+,TO BE DONE	47867
AG 109	N,GAMMA	EXPT-PROG	3		WASH1136 22 9/69	COL	ARBO+,TO BE DONE	47868
IN	N,GAMMA	EXPT-PROG	FISS		WASH1136 55 9/69	MTR	SCHUMAN+,ACTIVATION ONLY,NO DATA	47929
IN 113	INELST GAMMA	EXPT-PROG	1.4 7		WASH1136 135 9/69	NEL	TEMPERLEY+,ACT,SIG TO IN113M GIVEN	48099
IN 113	NON REACTION	EXPT-PROG	1.4 7		WASH1136 135 9/69	NEL	TEMPERLEY+,ACT,SIGS TO IN112G,M GIVN	48089
IN 115	TOTAL XSECT	EXPT-PROG	1. 0	5. 4	WASH1136 28 9/69	COL	CAMARDA+,NO DATA GIVEN,TO BE COMPLTD	47802
IN 115	RESON PARAMS	EXPT-PROG	1. 0	5. 4	WASH1136 28 9/69	COL	CAMARDA+,NO DATA GIVEN,TO BE COMPLTD	47823
IN 115	STRNTH FNCTN	EXPT-PROG	1. 0	5. 4	WASH1136 28 9/69	COL	CAMARDA+,NO DATA GIVEN,TO BE COMPLTD	47843
IN 115	INELST GAMMA	EXPT-PROG	FISS		WASH1136 55 9/69	MTR	SCHUMAN+,ACTIVATION OF 4.5H ISOM,NDS	47928
IN 115	INELST GAMMA	EXPT-PROG	1.4 7		WASH1136 135 9/69	NEL	TEMPERLEY+,ACT,SIG TO IN115M GIVEN	48086
IN 115	NON REACTION	EXPT-PROG	1.4 7		WASH1136 135 9/69	NEL	TEMPERLEY+,ACT,SIG TO IN114M GIVEN	48087
IN 115	N,GAMMA	EXPT-PROG	1.4 7		WASH1136 135 9/69	NEL	TEMPERLEY+,ACT,SIG TO IN116M GIVEN	48085
IN 115	N,PROTON	EXPT-PROG	1.4 7		WASH1136 135 9/69	NEL	TEMPERLEY+,ACT,SIG TO CD115G GIVEN	48084
IN 115	N,ALPHA	EXPT-PROG	1.4 7		WASH1136 135 9/69	NEL	TEMPERLEY+,ACT,VALUE GIVEN	48083
SB	MONEL GAMMAS	EXPT-PROG	1.4 7		WASH1136 32 9/69	COL	STAMATELATOS+,GAMMA SPEC,NO DATA	47878
SB 121	N,GAMMA	EXPT-PROG	3		WASH1136 22 9/69	COL	ARBO+,TO BE DONE	47865
SB 123	N,GAMMA	EXPT-PROG	3		WASH1136 22 9/69	COL	ARBO+,TO BE DONE	47866
SB 123	N,GAMMA	EXPT-PROG	3		WASH1136 22 9/69	COL	ARBO+,TO BE DONE	47862
LA	TOTAL XSECT	EXPT-PROG	1. 0	5. 4	WASH1136 28 9/69	COL	CAMARDA+,NO DATA GIVEN,TO BE COMPLTD	47801
LA	RESON PARAMS	EXPT-PROG	1. 0	5. 4	WASH1136 28 9/69	COL	CAMARDA+,NO DATA GIVEN,TO BE COMPLTD	47822
LA	STRNTH FNCTN	EXPT-PROG	1. 0	5. 4	WASH1136 28 9/69	COL	CAMARDA+,NO DATA GIVEN,TO BE COMPLTD	47842
PR 141	RESON PARAMS	EXPT-PROG	3.2 1	2.4 2	WASH1136 19 9/69	BNL	CHRIEN+,PARTIAL WG DIST TO 13 STATES	47777
ND	N,GAMMA	EXPT-PROG	3.3-2	2.7-1	WASH1136 22 9/69	BNL	BRUNHART+,MONON-RAE DET,ANAL TBC	47786
ND 142	TOTAL XSECT	EXPT-PROG	3	5	WASH1136 208 9/69	DKE	PINEO+ ANALYSIS COMPLETED,NO DATA	48048
ND 144	TOTAL XSECT	EXPT-PROG	3	5	WASH1136 208 9/69	DKE	PINEO+ ANALYSIS COMPLETED,NO DATA	48047
ND 146	TOTAL XSECT	EXPT-PROG	3	5	WASH1136 208 9/69	DKE	PINEO+ ANALYSIS COMPLETED,NO DATA	48046
ND 148	TOTAL XSECT	EXPT-PROG	3	5	WASH1136 208 9/69	DKE	PINEO+ ANALYSIS COMPLETED,NO DATA	48045
PM 147	RESON PARAMS	EXPT-PROG	6.5 1	2.4 2	WASH1136 50 9/69	MTR	TROMP+,FAST CHOPPER,WN FOR 22RESON	47911
SM 147	TOTAL XSECT	EXPT-PROG	3	5	WASH1136 208 9/69	DKE	PINEO+ ANALYSIS COMPLETED,NO DATA	48044
SM 147	RESON PARAMS	EXPT-PROG	7.4 1	2.5 2	WASH1136 50 9/69	MTR	TROMP+,FAST CHOPPER,WN FOR 18RESON	47912
SM 148	TOTAL XSECT	EXPT-PROG	3	5	WASH1136 208 9/69	DKE	PINEO+ ANALYSIS COMPLETED,NO DATA	48043
SM 149	TOTAL XSECT	EXPT-PROG	3	5	WASH1136 208 9/69	DKE	PINEO+ ANALYSIS COMPLETED,NO DATA	48042
SM 152	TOTAL XSECT	EXPT-PROG	3	5	WASH1136 208 9/69	DKE	PINEO+ ANALYSIS COMPLETED,NO DATA	48041
SM 154	TOTAL XSECT	EXPT-PROG	3	5	WASH1136 208 9/69	DKE	PINEO+ ANALYSIS COMPLETED,NO DATA	48040
EU 151	TOTAL XSECT	EXPT-PROG	1. 0	5. 4	WASH1136 28 9/69	COL	CAMARDA+,NO DATA GIVEN,TO BE COMPLTD	47803
EU 151	RESON PARAMS	EXPT-PROG	1. 0	5. 4	WASH1136 28 9/69	COL	CAMARDA+,NO DATA GIVEN,TO BE COMPLTD	47824
EU 151	STRNTH FNCTN	EXPT-PROG	1. 0	5. 4	WASH1136 28 9/69	COL	CAMARDA+,NO DATA GIVEN,TO BE COMPLTD	47844
EU 153	TOTAL XSECT	EXPT-PROG	1. 0	5. 4	WASH1136 28 9/69	COL	CAMARDA+,NO DATA GIVEN,TO BE COMPLTD	47804
EU 153	RESON PARAMS	EXPT-PROG	1. 0	5. 4	WASH1136 28 9/69	COL	CAMARDA+,NO DATA GIVEN,TO BE COMPLTD	47825
EU 153	STRNTH FNCTN	EXPT-PROG	1. 0	5. 4	WASH1136 28 9/69	COL	CAMARDA+,NO DATA GIVEN,TO BE COMPLTD	47845
GD	RES INT ABS	EXPT-PROG	1. 0	4. 4	WASH1136 33 9/69	GA	FRIESENHAHN+,TOF,VALUE GIVEN	47887
GD 154	TOTAL XSECT	EXPT-PROG	1. 0	5. 4	WASH1136 28 9/69	COL	CAMARDA+,NO DATA GIVEN,TO BE COMPLTD	47805
GD 154	RESON PARAMS	EXPT-PROG	1. 0	5. 4	WASH1136 28 9/69	COL	CAMARDA+,NO DATA GIVEN,TO BE COMPLTD	47826
GD 154	STRNTH FNCTN	EXPT-PROG	1. 0	5. 4	WASH1136 28 9/69	COL	CAMARDA+,NO DATA GIVEN,TO BE COMPLTD	47846
GD 155	RESON PARAMS	EXPT-PROG	2. 0	2. 2	WASH1136 33 9/69	GA	FRIESENHAHN+,TOF,AVG W.,WN,D GIVEN	47889
GD 155	STRNTH FNCTN	EXPT-PROG	2. 0	2. 2	WASH1136 33 9/69	GA	FRIESENHAHN+,TOF,VALUE GIVEN	47892
GD 155	RES INT ABS	EXPT-PROG	1. 0	4. 4	WASH1136 33 9/69	GA	FRIESENHAHN+,TOF,VALUE GIVEN	47895

ELEMENT S A	QUANTITY	TYPE	ENERGY MIN	ENERGY MAX	DOCUMENTATION REF	VOL	PAGE	DATE	LAB	COMMENTS	SERIAL NO.
GD 155	N,GAMMA	EXPT-PROG	1. 0	4. 4	WASH1136	33		9/69	GA	FRIESENHAHN+,TOF,NO DATA GIVEN	47890
GD 157	RESON PARAMS	EXPT-PROG	2. 0	2. 2	WASH1136	33		9/69	GA	FRIESENHAHN+,TOF,AVG WG,WN,D GIVEN	47889
GD 157	STRNTH FNCTN	EXPT-PROG	2. 0	2. 2	WASH1136	33		9/69	GA	FRIESENHAHN+,TOF,VALUE GIVEN	47893
GD 157	RES INT ABS	EXPT-PROG	1. 0	4. 4	WASH1136	33		9/69	GA	FRIESENHAHN+,TOF,VALUE GIVEN	47896
GD 157	N,GAMMA	EXPT-PROG	1. 0	4. 4	WASH1136	33		9/69	GA	FRIESENHAHN+,TOF,NO DATA GIVEN	47891
GD 158	TOTAL XSECT	EXPT-PROG	1. 0	5. 4	WASH1136	28		9/69	COL	CAMARDA+,NO DATA GIVEN,TO BE COMPLTD	47805
GD 158	RESON PARAMS	EXPT-PROG	1. 0	5. 4	WASH1136	28		9/69	COL	CAMARDA+,NO DATA GIVEN,TO BE COMPLTD	47827
GD 158	STRNTH FNCTN	EXPT-PROG	1. 0	5. 4	WASH1136	28		9/69	COL	CAMARDA+,NO DATA GIVEN,TO BE COMPLTD	47847
TB 159	N,GAMMA	EXPT-PROG	3.3-2	2.7-1	WASH1136	22		9/69	BNL	BRUNHART+,MOXON-RAE DET,ANAL TBC	47784
HO 165	TOTAL XSECT	EXPT-PROG	1. 5	1.5 6	WASH1136	1		9/69	ANL	SMITH+,2KEV RESOL,NO STRUCTURE SEEN	47737
HO 165	RESON PARAMS	EXPT-PROG	NDG		WASH1136	11		9/69	ANL	POENITZ+,J FROM OCCUPATN PROB RATIOS	47765
HO 165	RESON PARAMS	EXPT-PROG	NDG		WASH1136	148		9/69	RPI	TATARCZUK+,J FROM CAPT SPEC,NDG,TBC	48001
HO 165	DIFF ELASTIC	EXPT-PROG	3. 5	1.5 6	WASH1136	1		9/69	ANL	SMITH+,ANAL TO BE COMPLETED,NO DATA	47739
HO 165	DIFF INELAST	EXPT-PROG	3. 5	1.5 6	WASH1136	1		9/69	ANL	SMITH+,ANAL TO BE COMPLETED,NO DATA	47739
HO 165	SPECT NGAMMA	EXPT-PROG	NDG		WASH1136	11		9/69	ANL	POENITZ+,NO DATA GIVEN	47762
HO 165	SPECT NGAMMA	EXPT-PROG	1. 1	7. 1	WASH1136	16		9/69	BNL	CHRIEN+,CAPT IN 11RESON,INTENS RATIO	47771
HO 165	SPECT NGAMMA	EXPT-PROG	NDG		WASH1136	148		9/69	RPI	TATARCZUK+,GE(LI) DET,NO DATA GIVEN	48044
EP	N,GAMMA	EXPT-PROG	3.3-2	2.7-1	WASH1136	22		9/69	BNL	BRUNHART+,MOXON-RAE DET,ANAL TBC	47785
EP 166	TOTAL XSECT	EXPT-PROG	1. 0	5. 4	WASH1136	28		9/69	COL	CAMARDA+,NO DATA GIVEN,TO BE COMPLTD	47807
EP 166	RESON PARAMS	EXPT-PROG	1. 0	5. 4	WASH1136	28		9/69	COL	CAMARDA+,NO DATA GIVEN,TO BE COMPLTD	47829
EP 166	STRNTH FNCTN	EXPT-PROG	1. 0	5. 4	WASH1136	28		9/69	COL	CAMARDA+,NO DATA GIVEN,TO BE COMPLTD	47848
EP 167	TOTAL XSECT	EXPT-PROG	1. 0	5. 4	WASH1136	28		9/69	COL	CAMARDA+,NO DATA GIVEN,TO BE COMPLTD	47809
EP 167	RESON PARAMS	EXPT-PROG	NDG		WASH1136	10		9/69	ANL	WETZEL+,J FROM CAPT MEASTS,NO DATA	47758
EP 167	RESON PARAMS	EXPT-PROG	1. 0	5. 4	WASH1136	28		9/69	COL	CAMARDA+,NO DATA GIVEN,TO BE COMPLTD	47829
EP 167	STRNTH FNCTN	EXPT-PROG	1. 0	5. 4	WASH1136	28		9/69	COL	CAMARDA+,NO DATA GIVEN,TO BE COMPLTD	47849
EP 168	TOTAL XSECT	EXPT-PROG	1. 0	5. 4	WASH1136	28		9/69	COL	CAMARDA+,NO DATA GIVEN,TO BE COMPLTD	47809
EP 168	RESON PARAMS	EXPT-PROG	1. 0	5. 4	WASH1136	28		9/69	COL	CAMARDA+,NO DATA GIVEN,TO BE COMPLTD	47830
EP 168	STRNTH FNCTN	EXPT-PROG	1. 0	5. 4	WASH1136	28		9/69	COL	CAMARDA+,NO DATA GIVEN,TO BE COMPLTD	47850
EP 170	TOTAL XSECT	EXPT-PROG	1. 0	5. 4	WASH1136	28		9/69	COL	CAMARDA+,NO DATA GIVEN,TO BE COMPLTD	47810
EP 170	RESON PARAMS	EXPT-PROG	1. 0	5. 4	WASH1136	28		9/69	COL	CAMARDA+,NO DATA GIVEN,TO BE COMPLTD	47831
EP 170	STRNTH FNCTN	EXPT-PROG	1. 0	5. 4	WASH1136	28		9/69	COL	CAMARDA+,NO DATA GIVEN,TO BE COMPLTD	47851
TM 169	RESON PARAMS	EXPT-PROG	1.4 1	1.2 2	WASH1136	16		9/69	BNL	CHRIEN+,J FOR 13RESON FROM CAPT SPEC	47773
TM 169	N,GAMMA	EXPT-PROG	3		WASH1136	30		9/69	COL	ARBO+,TO BE DONE	47863
TM 169	SPECT NGAMMA	EXPT-PROG	1.4 1	1.2 2	WASH1136	16		9/69	BNL	CHRIEN+,CAPT IN 13RESON,P-H SPECTRA	47772
TM 170	TOTAL XSECT	EXPT-PROG	1. 0	1. 2	WASH1136	44		9/69	MTR	STOKES+,FAST CHOPPER,TRANS,CURVES	47907
TM 170	RESON PARAMS	EXPT-PROG	2.8 0	9.0 1	WASH1136	44		9/69	MTR	STOKES+,WN+WG FOR 13RES FROM TOT SIG	47908
TM 170	STRNTH FNCTN	EXPT-PROG	2.8 0	9.0 1	WASH1136	44		9/69	MTR	STOKES+,VALUE GIVEN	47909
TM 170	RES INT ABS	EXPT-PROG	1. 0	1. 2	WASH1136	44		9/69	MTR	STOKES+,VALUE GIVEN	47910
YB 171	TOTAL XSECT	EXPT-PROG	1. 0	5. 4	WASH1136	28		9/69	COL	CAMARDA+,NO DATA GIVEN,TO BE COMPLTD	47811
YB 171	RESON PARAMS	EXPT-PROG	1. 0	5. 4	WASH1136	28		9/69	COL	CAMARDA+,NO DATA GIVEN,TO BE COMPLTD	47832
YB 171	STRNTH FNCTN	EXPT-PROG	1. 0	5. 4	WASH1136	28		9/69	COL	CAMARDA+,NO DATA GIVEN,TO BE COMPLTD	47852
YB 172	TOTAL XSECT	EXPT-PROG	1. 0	5. 4	WASH1136	28		9/69	COL	CAMARDA+,NO DATA GIVEN,TO BE COMPLTD	47812
YB 172	RESON PARAMS	EXPT-PROG	1. 0	5. 4	WASH1136	28		9/69	COL	CAMARDA+,NO DATA GIVEN,TO BE COMPLTD	47718
YB 172	STRNTH FNCTN	EXPT-PROG	1. 0	5. 4	WASH1136	28		9/69	COL	CAMARDA+,NO DATA GIVEN,TO BE COMPLTD	47853
YB 173	TOTAL XSECT	EXPT-PROG	1. 0	5. 4	WASH1136	28		9/69	COL	CAMARDA+,NO DATA GIVEN,TO BE COMPLTD	47813
YB 173	RESON PARAMS	EXPT-PROG	1. 0	5. 4	WASH1136	28		9/69	COL	CAMARDA+,NO DATA GIVEN,TO BE COMPLTD	47833
YB 173	STRNTH FNCTN	EXPT-PROG	1. 0	5. 4	WASH1136	28		9/69	COL	CAMARDA+,NO DATA GIVEN,TO BE COMPLTD	47854
LU 175	TOTAL XSECT	EXPT-PROG	1. 0	5. 4	WASH1136	28		9/69	COL	CAMARDA+,NO DATA GIVEN,TO BE COMPLTD	47814

ELEMENT S A	QUANTITY	TYPE	ENERGY MIN	ENERGY MAX	DOCUMENTATION REF	VOL	PAGE	DATE	LAB	COMMENTS	SERIAL NO.
LU 175	RESON PARAMS	EXPT-PROG	1. 0	5. 4	WASH1136	28		9/69	COL	CAMARDA+,NO DATA GIVEN,TO BE COMPLTD	47834
LU 175	STRNTH FNCTN	EXPT-PROG	1. 0	5. 4	WASH1136	28		9/69	COL	CAMARDA+,NO DATA GIVEN,TO BE COMPLTD	47855
LU 175	SPECT NGAMMA	EXPT-PROG	0	2	WASH1136	19		9/69	BNL	CHRIEN+,SPECTRUM FROM 18 RESON SHOWN	47778
LU 175	SPECT NGAMMA	EXPT-PROG	THR		WASH1136	123		9/69	LAS	MINOR+,GE(LI)+SI(LI) DET,LU176 LVLS	47980
LU 176	SPECT NGAMMA	EXPT-PROG	NDG		WASH1136	126		9/69	LAS	MINOR+,GE(LI)+SI(LI) DET,LU175 LVLS	48097
TA 181	TOTAL XSECT	EXPT-PROG	1. 0	5. 4	WASH1136	28		9/69	COL	CAMARDA+,NO DATA GIVEN,TO BE COMPLTD	47800
TA 181	RESON PARAMS	EXPT-PROG	NDG		WASH1136	11		9/69	ANL	POENITZ+ J FROM OCCUPATN PROB RATIOS	47770
TA 181	RESON PARAMS	EXPT-PROG	1. 0	5. 4	WASH1136	28		9/69	COL	CAMARDA+,NO DATA GIVEN,TO BE COMPLTD	47821
TA 181	RESON PARAMS	EXPT-PROG	NDG		WASH1136	148		9/69	RPI	TATARCZUK+,J FROM CAPT SPEC,NDG,TBC	48060
TA 181	STRNTH FNCTN	EXPT-PROG	1. 0	5. 4	WASH1136	28		9/69	COL	CAMARDA+,NO DATA GIVEN,TO BE COMPLTD	47841
TA 181	N,GAMMA	EXPT-PROG	1. 0	1. 3	WASH1136	33		9/69	GA	LOPEZ+,TOF,TO BE COMPLETED,NO DATA	47882
TA 181	SPECT NGAMMA	EXPT-PROG	NDG		WASH1136	11		9/69	ANL	POENITZ+,NO DATA GIVEN	47763
TA 181	SPECT NGAMMA	EXPT-PROG	NDG		WASH1136	148		9/69	RPI	TATARCZUK+,GE(LI) DET,NO DATA GIVEN	48063
W	INELST GAMMA	EXPT-PROG	4. 5	1.5 7	WASH1136	202		9/69	TNC	NELLIS+,3FS,GAMMA PRODUCTN SIGS GIVN	48109
W	INELST GAMMA	EXPT-PROG	5. 6	1.1 7	WASH1136	189		9/69	TNC	TUCKER+,SEE REPORT DASA-2333	48118
W	INELST GAMMA	EXPT-PROG	1.0 4		WASH1136	185		9/69	TNC	NELLIS+,LOW E GAMMAS+K X RAYS	48123
W	N,GAMMA	EXPT-PROG	3. 5		WASH1136	189		9/69	TNC	NELLIS+,TABLE OF GAMMA PROD SIGS GVN	47717
W 182	TOTAL XSECT	EXPT-PROG	1. 0	5. 4	WASH1136	28		9/69	COL	CAMARDA+,NO DATA GIVEN,TO BE COMPLTD	47815
W 182	RESON PARAMS	EXPT-PROG	1. 0	5. 4	WASH1136	28		9/69	COL	CAMARDA+,NO DATA GIVEN,TO BE COMPLTD	47835
W 182	STRNTH FNCTN	EXPT-PROG	1. 0	5. 4	WASH1136	28		9/69	COL	CAMARDA+,NO DATA GIVEN,TO BE COMPLTD	47856
W 183	RESON PARAMS	EXPT-PROG	NDG		WASH1136	11		9/69	ANL	POENITZ+ J FROM OCCUPATN PROB RATIOS	47768
W 183	RESON PARAMS	EXPT-PROG	NDG		WASH1136	148		9/69	RPI	TATARCZUK+,J FROM CAPT SPEC,NDG,TBC	48062
W 183	SPECT NGAMMA	EXPT-PROG	NDG		WASH1136	11		9/69	ANL	POENITZ+,NO DATA GIVEN	47761
W 183	SPECT NGAMMA	EXPT-PROG	NDG		WASH1136	148		9/69	RPI	TATARCZUK+,GE(LI) DET,NO DATA GIVEN	48065
W 184	TOTAL XSECT	EXPT-PROG	1. 0	5. 4	WASH1136	28		9/69	COL	CAMARDA+,NO DATA GIVEN,TO BE COMPLTD	47816
W 184	RESON PARAMS	EXPT-PROG	1. 0	5. 4	WASH1136	28		9/69	COL	CAMARDA+,NO DATA GIVEN,TO BE COMPLTD	47836
W 184	STRNTH FNCTN	EXPT-PROG	1. 0	5. 4	WASH1136	28		9/69	COL	CAMARDA+,NO DATA GIVEN,TO BE COMPLTD	47857
W 186	TOTAL XSECT	EXPT-PROG	1. 0	5. 4	WASH1136	28		9/69	COL	CAMARDA+,NO DATA GIVEN,TO BE COMPLTD	47817
W 186	RESON PARAMS	EXPT-PROG	1. 0	5. 4	WASH1136	28		9/69	COL	CAMARDA+,NO DATA GIVEN,TO BE COMPLTD	47837
W 186	STRNTH FNCTN	EXPT-PROG	1. 0	5. 4	WASH1136	28		9/69	COL	CAMARDA+,NO DATA GIVEN,TO BE COMPLTD	47858
OS 187	RESON PARAMS	EXPT-PROG	NDG		WASH1136	10		9/69	ANL	WETZEL+,J FROM CAPT MEASTS,NO DATA	47759
OS 189	RESON PARAMS	EXPT-PROG	NDG		WASH1136	10		9/69	ANL	WETZEL+,J FROM CAPT MEASTS,NO DATA	47760
OS 190	TOT INELASTC	EXPT-PROG	6		WASH1136	197		9/69	LOK	GRENCH+,TO ISOMER,TBC,XOKS H-F,NDG	49101
IR 191	N2N REACTION	EXPT-PROG	1.4 7		WASH1136	135		9/69	NEL	TEMPERLEY+,ACT,TO IR190M2,IR190M1+G	48087
IR 193	N2N REACTION	EXPT-PROG	1.4 7		WASH1136	135		9/69	NEL	TEMPERLEY+,ACT,SIG TO IR189M1+G GIVN	48081
AU 197	N2N REACTION	EXPT-PROG	FISS		WASH1136	55		9/69	MTR	SCHUMAN+,ACTIVATION,VALUE GIVEN	47934
AU 197	N,GAMMA	EXPT-PROG	1. 0	1. 3	WASH1136	33		9/69	GA	LOPEZ+,TOF,TO BE COMPLETED,NO DATA	47884
AU 197	N,GAMMA	EXPT-PROG	FISS		WASH1136	55		9/69	MTR	SCHUMAN+,ACTIVATION ONLY,NO DATA	47930
AU 197	N,GAMMA	EXPT-PROG	FISS		WASH1136	55		9/69	MTR	SCHUMAN+,ACTIVATION,VALUE GIVEN	47935
PB 206	N,GAMMA	EXPT-PROG			WASH1136	83		9/69	LRL	BOWMAN+,INVERSE REACT,DOORWAY STATE	47966
BI 209	TOTAL XSECT	EXPT-PROG	2. 5	1.4 6	WASH1136	2		9/69	ANL	SMITH+,STRUCTURE SEEN,DATA AVAILABLE	47740
BI 209	DIFF ELASTIC	EXPT-PROG	3. 5	1.5 6	WASH1136	2		9/69	ANL	SMITH+,20KEV RESOL,DATA AVAILABLE	47741
BI 209	DIFF INELAST	EXPT-PROG	3. 5	1.5 6	WASH1136	2		9/69	ANL	SMITH+,895+-2KEV STATE SEEN,NO DATA	47742
BI 209	SPECT NGAMMA	EXPT-PROG	THR		WASH1136	123		9/69	LAS	JURNEY,TABLE ENERGIES+INTENSITIES	47981
BI 209	SPECT NGAMMA	EXPT-PROG	THR		WASH1136	123		9/69	LAS	SHEPA,ANALYSIS TO BE COMPLETED,NDG	47982
TH 231	FISSION	EXPT-PROG	5. 5	2. 6	WASH1136	126		9/69	LAS	CRAMER+,SIG FROM(T,P+FISS)+H-F CALC	48096
TH 232	RESON PARAMS	EXPT-PROG	NDG		WASH1136	114		9/69	LAS	HARLOW+,PHYSICS -8 SHOT,ANAL TBC	47988
TH 232	N2N REACTION	EXPT-PROG	FISS		WASH1136	55		9/69	MTR	SCHUMAN+,ACTIVATION,VALUE GIVEN	47932

ELEMENT S A	QUANTITY	TYPE	ENERGY MIN	ENERGY MAX	DOCUMENTATION REF	VOL	PAGE	DATE	LAB	COMMENTS	SERIAL NO.
TH 232	N,GAMMA	EXPT-PROG	3		WASH1136	30		9/69	COL	ARBO+,TO BE DONE	47860
TH 232	N,GAMMA	EXPT-PROG	FISS		WASH1136	55		9/69	MTR	SCHUMAN+,ACTIVATION,VALUE GIVEN	47933
TH 232	SPECT NGAMMA	EXPT-PROG	NDG		WASH1136	114		9/69	LAS	HARLOW+,PHYSICS -8 SHOT,ANAL TBC	47987
TH 232	FISSION	EXPT-PROG	5. 5	2. 5	WASH1136	126		9/69	LAS	CRAMER+,SIG FROM(T,P+FISS)+H-F CALC	48095
U 232	ETA	EXPT-PROG	1. -1		WASH1136	65		9/69	MTR	SMITH+,MN BATH,TO BE COMPLETED	47961
U 232	FISS YIELD	EXPT-PROG	0	2	WASH1136	30		9/69	COL	FELVINCI+,YLD LONG-RANGE ALFAS,NDG	47871
U 232	FRAG SPECTRA	EXPT-PROG	0	2	WASH1136	30		9/69	COL	FELVINCI+,KE DIST VS. ALFA YLD,NDG	47870
U 232	N,GAMMA	EXPT-PROG	3		WASH1136	30		9/69	COL	ARBO+,TO BE DONE	47859
U 234	FISSION	EXPT-PROG	NDG		WASH1136	110		9/69	LAS	SILBERT+,PHYSICS-8 SHOT,ANAL TBC	47984
U 234	N,GAMMA	EXPT-PROG	NDG		WASH1136	110		9/69	LAS	SILBERT+,PHYSICS-8 SHOT,ANAL TBC	48006
U 235	TOTAL XSECT	EXPT-PROG	2. 3		WASH1136	59		9/69	MTR	SIMPSON+,TRANS,SIG VS.SAMPLE THICKNS	47953
U 235	RESON PARAMS	EXPT-PROG	6.4 0	2.3 1	WASH1136	145		9/69	PPI	REED+,J FOR 11 RESON FROM NU MEASTS	48067
U 235	RESON PARAMS	EXPT-PROG		1	WASH1136	93		9/69	LRL	BOWMAN+,J FROM N,G.ANAL TBC,NO DATA	48107
U 235	FISSION	EXPT-PROG	1.3 5	1.4 6	WASH1136	4		9/69	ANL	POENITZ,REL U238NG,PU239NF,TBP NSE	47751
U 235	FISSION	THEO-PROG	NDG		WASH1136	151		9/69	PPI	SHEA+,TIME-DEPENDNT MULTILVL EFFECTS	48057
U 235	NU	EXPT-PROG	1.2-2	2.5 1	WASH1136	145		9/69	PPI	REED+,CURVES	48068
U 235	SPECT FISS G	EXPT-PROG	THR		WASH1136	37		9/69	GA	VERBINSKI+,TOF,NAI DET,GAM YLDS GIVN	47900
U 235	SPECT FISS G	EXPT-PROG	THR		WASH1136	139		9/69	ORL	PFELLE+,CURV 0.3-7MEV GAMMAS,TBC	48077
U 235	FISS PROD GS	EXPT-PROG	NDG		WASH1136	107		9/69	LOK	IMHOF+,TBC,NDG,GROSS FISSION PRODUCT	48100
U 235	SPECT NGAMMA	EXPT-PROG		3. 3	WASH1136	93		9/69	LRL	BOWMAN+,MULTIPLICITY,ANAL TBC,NDG	47970
U 236	FISSION	EXPT-PROG	NDG		WASH1136	110		9/69	LAS	SILBERT+,PHYSICS-8 SHOT,ANAL TBC	48023
U 236	N,GAMMA	EXPT-PROG	NDG		WASH1136	110		9/69	LAS	SILBERT+,PHYSICS-8 SHOT,ANAL TBC	48005
U 237	FISSION	EXPT-PROG	5. 5	2. 6	WASH1136	126		9/69	LAS	CRAMER+,SIG FROM(T,P+FISS)+H-F CALC	48094
U 238	RESON PARAMS	THEO-PROG		2. 3	WASH1136	12		9/69	ANL	MOYAHAN+,LVL SPACING DISTR,OKS EXPT	47765
U 238	TOT INELASTIC	EXPT-PROG	5	1.6 6	WASH1136	2		9/69	ANL	SMITH+,2.6B MAXIMUM,TO BE COMPLETED	47743
U 238	INELST GAMMA	EXPT-PROG	1.0 6		WASH1136	185		9/69	TNC	NELLIS+,LOW E GAMMAS+K X RAYS	48122
U 238	FISSION	EXPT-PROG	NDG		WASH1136	110		9/69	LAS	SILBERT+,PHYSICS-8 SHOT,ANAL TBC	48022
U 238	N,GAMMA	EXPT-PROG	1.3 5	1.4 6	WASH1136	4		9/69	ANL	POENITZ,REL U235NF,PU239NF,TBP NSE	47752
U 238	N,GAMMA	EXPT-PROG	1. 0	1. 3	WASH1136	33		9/69	GA	LOPEZ+,TOF,TO BE COMPLETED,NO DATA	47883
U 238	N,GAMMA	EXPT-PROG	NDG		WASH1136	110		9/69	LAS	SILBERT+,PHYSICS-8 SHOT,ANAL TBC	48004
U 238	SPECT NGAMMA	EXPT-PROG	1.5-2	1. 5	WASH1136	34		9/69	GA	JOHN+,TOF,GE(LI)-NAI(TL) DET,PRELIM	47897
U 238	FISSION	EXPT-PROG	5. 5	2. 6	WASH1136	126		9/69	LAS	CRAMER+,SIG FROM(T,P+FISS)+H-F CALC	48093
NP 237	ELASTIC	EXPT-PROG	2.5 1	1. 5	WASH1136	114		9/69	LAS	HOFFMAN+,PHYSICS-8 SHOT,ANAL TBC	48027
NP 237	FISSION	EXPT-PROG	NDG		WASH1136	110		9/69	LAS	SILBERT+,PHYSICS-8 SHOT,ANAL TBC	48019
NP 237	N,GAMMA	EXPT-PROG	NDG		WASH1136	110		9/69	LAS	SILBERT+,PHYSICS-8 SHOT,ANAL TBC	48001
NP 237	N,GAMMA	EXPT-PROG	2.5 1	1. 5	WASH1136	114		9/69	LAS	HOFFMAN+,PHYSICS-8 SHOT,ANAL TBC	48026
PU	INELST GAMMA	EXPT-PROG	1.0 6		WASH1136	185		9/69	TNC	NELLIS+,LOW E GAMMAS+K X RAYS	48121
PU	N,GAMMA	EXPT-PROG	3. 5		WASH1136	189		9/69	TNC	NELLIS+,NO DATA GIVEN	48120
PU 239	TOTAL XSECT	EXPT-PROG	6. 5	1.5 6	WASH1136	3		9/69	ANL	SMITH+,TOF,NO STRUCTURE TO 1PC,NDG	47744
PU 239	TOTAL XSECT	EXPT-PROG	2. 3		WASH1136	59		9/69	MTR	SIMPSON+,TRANS,SIG VS.SAMPLE THICKNS	47954
PU 239	TOTAL XSECT	EXPT-PROG	2. 3		WASH1136	61		9/69	MTR	SIMPSON+,VALUE GIVEN	47955
PU 239	RESON PARAMS	EVAL-PROG	4.0 1	1.0 2	WASH1136	12		9/69	ANL	LAMBROPOULOS,ANALYSIS OF SACLAY DATA	47767
PU 239	ELASTIC	EXPT-PROG	3. 3		WASH1136	61		9/69	MTR	SIMPSON+,VALUE GIVEN	47956
PU 239	DIFF ELASTIC	EXPT-PROG	5	1.5 6	WASH1136	3		9/69	ANL	SMITH+,TOF,ANAL TO BE COMPLETED,NDG	47745
PU 239	NONELASTIC	EXPT-PROG	2. 3		WASH1136	61		9/69	MTR	SIMPSON+,VALUE GIVEN	47957
PU 239	DIFF INELAST	EXPT-PROG	5	1.5 6	WASH1136	3		9/69	ANL	SMITH+,TOF,TO BE COMPLETED,NO DATA	47746
PU 239	FISSION	EXPT-PROG	1.5 4	1.4 6	WASH1136	4		9/69	ANL	POENITZ,REL U238NG,U235NF,TBP NSE	47753
PU 239	FISSION	EVAL-PROG	4.0 1	1.0 2	WASH1136	12		9/69	ANL	LAMBROPOULOS,ANALYSIS OF SACLAY DATA	47766

ELEMENT S A	QUANTITY	TYPE	ENERGY MIN	ENERGY MAX	DOCUMENTATION REF VOL PAGE	DATE	LAB	COMMENTS	SERIAL NO.
PU 239	FISSION	EXPT-PROG	2. 3		WASH1136 61	9/69	MTR	SIMPSON+,VALUE GIVEN	47958
PU 239	FISSION	EXPT-PROG	2. -2	2. -1	WASH1136 74	9/69	MTR	SIMPSON+,CORRELATION CHOPPER,NO DATA	47965
PU 239	FISSION	EXPT-PROG	NDG		WASH1136 110	9/69	LAS	SILBERT+,PHYSICS-8 SHOT,ANAL TBC	48016
PU 239	ALPHA	EXPT-PROG	2. 3		WASH1136 61	9/69	MTR	SIMPSON+,VALUE GIVEN	47960
PU 239	ALPHA	EXPT-PROG	1. 2	3.4 4	WASH1136 97	9/69	LRL	CZIPR.21 ENERGY INTERVALS,TABLE,TBP	47971
PU 239	SPECT FISS N	EXPT-PROG	5	1.5 6	WASH1136 3	9/69	ANL	SMITH+,TOF,TO BE COMPLETED,NO DATA	47747
PU 239	SPECT FISS G	EXPT-PROG	THR		WASH1136 37	9/69	GA	VERBINSKI+,TOF,NAI DET,GAM YLDS GIVN	47901
PU 239	N,GAMMA	EXPT-PROG	2. 3		WASH1136 61	9/69	MTR	SIMPSON+,VALUE GIVEN	47959
PU 239	N,GAMMA	EXPT-PROG	NDG		WASH1136 110	9/69	LAS	SILBERT+,PHYSICS-8 SHOT,ANAL TBC	47998
PU 239	SPECT NGAMMA	EXPT-PROG	0	1	WASH1136 19	9/69	BNL	CHRIEN+,CAPT IN 7RESON,CURVS FOR 2	47774
PU 240	TOTAL XSECT	EXPT-PROG	7. 5	1.5 6	WASH1136 3	9/69	ANL	SMITH+,TO BE COMPLETED,NO DATA GIVEN	47749
PU 240	DIFF ELASTIC	EXPT-PROG	5. 5	1.5 6	WASH1136 3	9/69	ANL	SMITH+,TO BE COMPLETED,NO DATA GIVEN	47748
PU 240	DIFF INELAST	EXPT-PROG	5	6	WASH1136 3	9/69	ANL	SMITH+,TO BE COMPLETED,NO DATA GIVEN	47750
PU 240	FISSION	EXPT-PROG	6. 1	5. 4	WASH1136 143	9/69	RPI	HOCKENBURY+,ANALYSIS TO BE COMPLETED	48075
PU 240	N,GAMMA	EXPT-PROG	6. 1	5. 4	WASH1136 143	9/69	RPI	HOCKENBURY+,ANALYSIS TO BE COMPLETED	48076
PU 241	TOTAL XSECT	EXPT-PROG	5.1-4	1. -1	WASH1136 43	9/69	MTR	SMITH+,CRYST SPEC,TRANS,TABLE+CURVE	47906
PU 241	TOTAL XSECT	EVAL-PROG	1. 0	1.2 1	WASH1136 70	9/69	MTR	SMITH+,CURV FIT TO RESON PARAMS,TBC	47963
PU 241	RESON PARAMS	EVAL-PROG	-2.-1	5. 1	WASH1136 70	9/69	MTR	SMITH+,WN WG WF UP TO 10.2EV,TBC	47962
PU 241	FISSION	EVAL-PROG	1. 0	1.2 1	WASH1136 70	9/69	MTR	SMITH+,CURV FIT TO RESON PARAMS,TBC	47964
PU 242	FISSION	EXPT-PROG	NDG		WASH1136 110	9/69	LAS	SILBERT+,PHYSICS-8 SHOT,ANAL TBC	48021
PU 242	N,GAMMA	EXPT-PROG	NDG		WASH1136 110	9/69	LAS	SILBERT+,PHYSICS-8 SHOT,ANAL TBC	48003
PU 243	FISSION	EXPT-PROG	5. 5	2. 6	WASH1136 126	9/69	LAS	CRAMER+,SIG FROM(T,P+FISSI+H-F CALC	48092
PU 244	FISSION	EXPT-PROG	NDG		WASH1136 110	9/69	LAS	SILBERT+,PHYSICS-8 SHOT,ANAL TBC	48020
PU 244	FISSION	EXPT-PROG	1.5 1	2. 6	WASH1136 95	9/69	LRL	LOUGHEED+,PHYSICS-8 SHOT TBC,NO DATA	48106
PU 244	RES INT CAPT	EXPT-PROG	THR	5. -1	WASH1136 51	9/69	MTR	SCHUMAN,VALUE GIVN,THR AVG CD CUTOFF	47914
PU 244	N,GAMMA	EXPT-PROG	THR	5. -1	WASH1136 51	9/69	MTR	SCHUMAN,VALUE GIVN,THR AVG CD CUTOFF	47913
PU 244	N,GAMMA	EXPT-PROG	NDG		WASH1136 110	9/69	LAS	SILBERT+,PHYSICS-8 SHOT,ANAL TBC	48002
AM 241	RES INT CAPT	EXPT-PROG	5. -1	UP	WASH1136 53	9/69	MTR	SCHUMAN,TO 16HR AND 152YR AM242	47919
AM 242	RES INT ABS	EXPT-PROG	5. -1	UP	WASH1136 53	9/69	MTR	SCHUMAN,AM242M TARGET,VALUE GIVEN	47920
AM 243	FISSION	EXPT-PROG	NDG		WASH1136 110	9/69	LAS	SILBERT+,PHYSICS-8 SHOT,ANAL TBC	48018
AM 243	N,GAMMA	EXPT-PROG	NDG		WASH1136 110	9/69	LAS	SILBERT+,PHYSICS-8 SHOT,ANAL TBC	48000
CM 242	RES INT CAPT	EXPT-PROG	5. -1	UP	WASH1136 53	9/69	MTR	SCHUMAN,TO 32YR CM243,VALUE GIVEN	47921
CM 243	FISSION	EXPT-PROG	NDG		WASH1136 110	9/69	LAS	SILBERT+,PHYSICS-8 SHOT,ANAL TBC	48015
CM 243	FISSION	EXPT-PROG	1.5 1	2. 6	WASH1136 95	9/69	LRL	LOUGHEED+,PHYSICS-8 SHOT TBC,NO DATA	48105
CM 243	N,GAMMA	EXPT-PROG	NDG		WASH1136 110	9/69	LAS	SILBERT+,PHYSICS-8 SHOT,ANAL TBC	47997
CM 244	FISSION	EXPT-PROG	2. 1	2. 6	WASH1136 110	9/69	LAS	FULLWOOD+,TOF,BOMB SOURCE,CURVE	47973
CM 244	FISSION	EXPT-PROG	NDG		WASH1136 110	9/69	LAS	SILBERT+,PHYSICS-8 SHOT,ANAL TBC	48011
CM 244	RES INT CAPT	EXPT-PROG	5. -1	UP	WASH1136 54	9/69	MTR	SCHUMAN,VALUE GIVEN	47922
CM 244	N,GAMMA	EXPT-PROG	NDG		WASH1136 110	9/69	LAS	SILBERT+,PHYSICS-8 SHOT,ANAL TBC	47993
CM 245	FISSION	EXPT-PROG	NDG		WASH1136 110	9/69	LAS	SILBERT+,PHYSICS-8 SHOT,ANAL TBC	48014
CM 245	RES INT ABS	EXPT-PROG	5. -1	UP	WASH1136 54	9/69	MTR	SCHUMAN,VALUE GIVEN	47923
CM 245	N,GAMMA	EXPT-PROG	NDG		WASH1136 110	9/69	LAS	SILBERT+,PHYSICS-8 SHOT,ANAL TBC	47996
CM 246	FISSION	EXPT-PROG	NDG		WASH1136 110	9/69	LAS	SILBERT+,PHYSICS-8 SHOT,ANAL TBC	48010
CM 246	RES INT CAPT	EXPT-PROG	5. -1	UP	WASH1136 54	9/69	MTR	SCHUMAN,VALUE GIVEN	47924
CM 246	N,GAMMA	EXPT-PROG	NDG		WASH1136 110	9/69	LAS	SILBERT+,PHYSICS-8 SHOT,ANAL TBC	47992
CM 247	FISSION	EXPT-PROG	NDG		WASH1136 110	9/69	LAS	SILBERT+,PHYSICS-8 SHOT,ANAL TBC	48013
CM 247	N,GAMMA	EXPT-PROG	NDG		WASH1136 110	9/69	LAS	SILBERT+,PHYSICS-8 SHOT,ANAL TBC	47995
CM 249	FISSION	EXPT-PROG	NDG		WASH1136 110	9/69	LAS	SILBERT+,PHYSICS-8 SHOT,ANAL TBC	48009

ELEMENT S A	QUANTITY	TYPE	ENERGY MIN	ENERGY MAX	DOCUMENTATION REF	VOL	PAGE	DATE	LAB	COMMENTS	SERIAL NO.
CM 248	N,GAMMA	EXPT-PROG	NDG		WASH1136	110		9/69	LAS	SILBERT+,PHYSICS-8 SHOT,ANAL TBC	47991
BK 249	FISSION	EXPT-PROG	NDG		WASH1136	110		9/69	LAS	SILBERT+,PHYSICS-8 SHOT,ANAL TBC	48017
BK 249	FISSION	EXPT-PROG	1.5 1	2. 6	WASH1136	95		9/69	LRL	LOUGHEED+,PHYSICS-8 SHOT TBC,NO DATA	48104
BK 249	N,GAMMA	EXPT-PROG	NDG		WASH1136	110		9/69	LAS	SILBERT+,PHYSICS-8 SHOT,ANAL TBC	47999
CF 249	FISSION	EXPT-PROG	NDG		WASH1136	110		9/69	LAS	SILBERT+,PHYSICS-8 SHOT,ANAL TBC	48012
CF 249	FISSION	EXPT-PROG	1.5 1	2. 6	WASH1136	95		9/69	LRL	LOUGHEED+,PHYSICS-8 SHOT TBC,NO DATA	48103
CF 249	N,GAMMA	EXPT-PROG	NDG		WASH1136	110		9/69	LAS	SILBERT+,PHYSICS-8 SHOT,ANAL TBC	47994
CF 252	FISSION	EXPT-PROG	NDG		WASH1136	110		9/69	LAS	SILBERT+,PHYSICS-8 SHOT,ANAL TBC	48008
CF 252	SPECT FISS G	EXPT-PROG	SPON		WASH1136	37		9/69	GA	VERBINSKI+,TOF,NAI DET,GAM YLDS GIVN	47902
CF 252	SPECT FISS G	EXPT-PROG	SPON		WASH1136	93		9/69	LRL	JOHN+,GAMMA YLDS DELAYD UP TO 2MUSEC	48108
CF 252	N,GAMMA	EXPT-PROG	NDG		WASH1136	110		9/69	LAS	SILBERT+,PHYSICS-8 SHOT,ANAL TBC	47990
E 253	FISSION	EXPT-PROG	NDG		WASH1136	110		9/69	LAS	SILBERT+,PHYSICS-8 SHOT,ANAL TBC	48007
E 253	FISSION	EXPT-PROG	1.5 1	2. 6	WASH1136	95		9/69	LRL	LOUGHEED+,PHYSICS-8 SHOT TBC,NO DATA	48102
E 253	N,GAMMA	EXPT-PROG	NDG		WASH1136	110		9/69	LAS	SILBERT+,PHYSICS-8 SHOT,ANAL TBC	47989
MA NY	RESON PARAMS	THEO-PROG			WASH1136	12		9/69	ANL	MONAHAN+,METHOD FOR LVL SPACING DIST	47764
C2H2	TOTAL XSECT	EXPT-PROG	COLD		WASH1136	31		9/69	COL	MARKISZ+,DIMETHYLACETYLENE,NO DATA	47875
C2H6	TOTAL XSECT	EXPT-PROG	COLD		WASH1136	31		9/69	COL	MARKISZ+,ANAL TO BE COMPLETED,NDG	47874
CH4	TOTAL XSECT	EXPT-PROG	COLD		WASH1136	31		9/69	COL	MARKISZ+,ANAL TO BE COMPLETED,NDG	47873
NH4CL	TOTAL XSECT	EXPT-PROG	COLD		WASH1136	31		9/69	COL	MARKISZ+,METHYLAMMONIUM CHLORDE,NDG	47876
UC	TOTAL XSECT	EXPT-PROG	5. -3	4. 0	WASH1136	158		9/69	RPI	LAJEUNESSE+,NO DATA GIVEN	48055
UC	THRMLSCATLAW	THEO-PROG			WASH1136	42		9/69	GA	SLAGGIE,NO DATA,SEE GA-8675	47904
UC	THRMLSCATLAW	EXPT-PROG	9.0-2	1.6-1	WASH1136	158		9/69	RPI	LAJEUNESSE+,DOUBL DIFF INFL SIG,NDG	48055

ARGONNE NATIONAL LABORATORY

ACCELERATOR PROGRAMS

A. Fast Neutron Physics

1. Fast Neutron Scattering

a. Titanium
(A. Smith, J. Whalen, E. Barnard,* J. de Villiers* and D. Reitmann*)

Experimental studies of total, elastic scattering and inelastic scattering cross sections of natural titanium are complete. Numerical data is available on request covering the incident neutron energy range 0.1 to 1.5 MeV. Physical interpretation of the measured results is in progress and is proving particularly difficult due to the apparent mixture of compound-nucleus and intermediate resonance structure. (Pertinent to requests #76—77, WASH-1078)

b. Molybdenum-92, 94, 96, 98 and 100
(A. Smith, J. Whalen and J. Meadows)

Studies of differential elastic and inelastic scattering from isotopes has been completed to incident energies of ~1.5 MeV. The results must be corrected for a small oxygen content (3—5%) of the samples. Complementary total cross section measurements are partially complete. One sample (Mo-94) appears non-uniform and it may be difficult to obtain definitive total cross section values. Generally, the total cross section results show a great deal of partially resolved resonance structure. The objective of the work is an understanding of the shell dependence of the optical potential and the requisite interpretation is now in progress.

c. Holmium
(A. Smith, J. Whalen and J. Meadows)

Experimental studies of the total and scattering cross

---

*South African Atomic Energy Board, Pelindaba, Transvaal, Republic of South Africa.

sections of holmium have been completed. Good resolution (~2 keV) total cross sections from 0.1 to 1.5 MeV show no structure to an experimental accuracy of ~1%. Differential measurements define elastic and inelastic processes from 0.3 to 1.5 MeV. Cross sections for the inelastic neutron excitation of eleven states with $E_x \leq 1.2$ MeV were determined. The physical interpretation of the results in terms of a deformed potential model is in progress. The experimental data is available in tabular form on request.

d. Bismuth
(A. Smith, J. Whalen, E. Barnard, J. de Villiers and D. Reitmann)

The study of fast neutron interactions with bismuth has been completed. Total neutron cross sections of bismuth were measured with resolutions of ≥ 1 keV over the energy range 0.2 to 1.4 MeV. Differential elastic scattering cross sections were determined at intervals of <50 keV from 0.3 to 1.5 MeV with resolutions of ~20 keV. The inelastic neutron excitation of a state at 895 ± 2 keV was observed and the respective differential excitation cross sections determined with incident resolutions of ≥ 10 keV. Partially resolved resonance structure was evident in all the measured values. The experimental results were assayed for possible intermediate structure and were compared with the results of optical model and statistical calculations. The model calculations were cognizant of the fluctuation and correlation of compound-nucleus resonance widths and of the shell closure at N = 126.

A manuscript with numerical data is available on request.*

e. Uranium-238, revisited
(A. Smith, P. Lambropoulos)

Recent macroscopic measurement and calculation suggest that "accepted U-238 inelastic scatter cross sections** are 20 to 30%

---

*The numerical data resulting from this work has been transmitted to the National Neutron Cross Section Center, Brookhaven National Laboratory.

**Evaluated Neutron Data File-B, NNCSC-BNL.

larger than physical reality. This is particularly true from 1.0 to 2.0 MeV. For this reason the inelastic microscopic cross sections were experimentally re-examined to incident energies of 1.6 MeV. These recent results and previously reported values from this laboratory* are in good agreement and both support lower inelastic scattering cross sections of U-238 than found in widely used evaluated data sets.** Specifically, present results indicate that the total inelastic cross sections of U-238 nowhere exceeds ~2.6 barns (as contrasted to ~3.2 barns of some of the evaluated sets). The work is continuing in an effort to achieve better accuracies and is correlated with a detailed theoretical assay. (Pertinent to request #307, WASH-1078)

f. Plutonium-239
(A. Smith, J. Whalen, J. Meadows)

Some years ago elastic scattering from Pu-239 was studied in detail by this group. The results required correction for aluminum content of the sample. A high purity sample has been received recently and the previous work is being repeated and extended to include inelastic scattering and total cross sections up to incident energies of 1.5 MeV. Total cross sections have been determined from 0.6 to 1.5 MeV with accuracies of ~1%. Preliminary analysis of the scattering results indicate good agreement with previous elastic scattering values. Inelastic scattering cross sections and fission neutron spectral distributions are being derived from the measured time-of-flight distributions. (Pertinent to requests #330—332, WASH-1078)

g. Plutonium-240
(A. Smith, J. Whalen and J. Meadows)

A unique sample has been received from Los Alamos and initial scattering and total cross section measurements carried out. The sample has proven particularly "clean" without undue background from the natural activity. Tentative results have been obtained for; a) elastic scattering at incident energies of 0.5 to 1.5 MeV, b) inelastic scattering where $E_x \leq 0.5$ MeV, and c) total cross sections from 0.7 to 1.5 MeV. The reduction of the present data will soon be

---

*Nuclear Physics, 47, (1963) 633.

**Evaluated Neutron Data File-B, NNCSC-BNL.

completed and more measurements made to improve the definition and accuracy. The sample has been the key to what promises to be very good results. (Pertinent to request #355, WASH-1078)

2. Measurements of the Fast Neutron Cross Section Ratios of U-235(n,f), U-238(n,γ) and Pu-239(n,f) (W. P. Poenitz)

Measurements of the ratios σ_γ(U238)/σ_f(U235), σ_γ(U238)/σ_f(Pu239) and σ_f(Pu239)/σ_f(U235) in the energy range 130—1400 keV have been completed. The experimental techniques used in these measurements have been reported previously (Poenitz*). A paper is being prepared for submission to Nuclear Science and Engineering. The results are given in Table 1. (Pertinent to requests #343, 342, 341, 312, 309, 286, 287, WASH-1078)

*W. P. Poenitz, WASH-1127, page 3, (1969).

TABLE 1a. Results for the cross section ratio σ_γ(U238)/σ_f(U235).

E_n/keV	R	ΔR
130	.126	.006
150	.126	.006
250	.114	.004
300	.103	.003
400	.104	.003
500	.111	.003
600	.122	.004
700	.133	.004
900	.124	.004
1200	.097	.004
1250	.092	.004
1400	.074	.003

TABLE 1b. Results for the cross section ratio $\sigma_\gamma(U238)/\sigma_f(Pu239)$.

E_n/keV	R	ΔR
250	.095	.004
400	.082	.003
500	.082	.002
700	.087	.003
900	.086	.003
1400	.048	.002

TABLE 1c. Results for the ratio $\sigma_f(Pu239)/\sigma_f(U235)$.

E_n	R	R
150	0.969	.024
200	1.084	.031
250	1.093	.032
325	1.205	.030
500	1.335	.027
700	1.446	.026
850	1.478	.041
1000	1.372	.031
1200	1.437	.050
1300	1.435	.031
1400	1.463	.029

3. The Branching Ratios in the Decay of Be^7 and Zn^{65}
(W. P. Poenitz and A. de Volpi)

The branching ratios of Be^7 and Zn^{65} have been measured. These ratios are important for the use of the associated activity method for absolute neutron flux measurements. The neutron yields in the reactions $Li^7(p,n)Be^7$ and $Cr^{65}(p,n)Zn^{65}$ have been measured by means of the neutron flux integration method using a vanadium bath. The γ-activity from the targets has been measured with a calibrated NaI (Tℓ)-detector. The present results for the branching ratios are $R(Be^7) = 0.1051 \pm 0.0018$ and $R(Zn^{65}) = 0.485 \pm 0.011$. The former is in good agreement with a measurement by Taylor and Merritt* ($R = 0.1032 \pm 0.0016$), the latter is somewhat low compared with two accurate measurements reported by Spernol** ($R = 0.5065 \pm 0.0015$) and Taylor and Merritt† ($R = 0.507 \pm 0.005$).

4. The Thermal Neutron Absorption Cross Sections of ^6Li and ^{10}B
(J. W. Meadows and J. F. Whalen)

The thermal neutron absorption cross sections of ^6Li and ^{10}B were measured by the pulsed neutron method. Measurements were made on natural lithium and on separated isotopes and the 2200 m/sec cross sections listed below were calculated assuming a 1/v velocity dependence.

Isotope	^6Li			^{10}B
Atomic %	98.94	95.88	7.406	92.41
σ_a(2200 m/sec) in barns	936 ± 4	941 ± 5	924 ± 5	3855 ± 24

The σ_a for ^{10}B is in agreement with the results listed in BNL-325, supplement 2.

---

*J. G. V. Taylor and J. S. Merritt, Canadian J. of Physics, 40, 926 (1962).

**A. Spernol, priv. communication.

†J. G. V. Taylor and J. S. Merritt, Physics in Canada 19, 17 (1963).

The σ_a for ^{6}Li derived from the measurement with natural lithium is significantly lower than that obtained with separated isotopes. It seems probable that there is a systematic error in the mass spectrographic analysis which leads to a 1 to 2% error in the ^{7}Li/^{6}Li ratio. However, when the ^{6}Li content is greater than 90% the effect of such an error is negligible so the cross section obtained from measurements on the separated isotopes should be reliable.

5. Total Cross Section of Carbon
(J. Meadows and J. Whalen)

The measurement of the total cross section of carbon has been completed over the energy region 0.1 to 1.5 MeV with an energy resolution of ~2.5 keV. Measurements were made at 1.0 keV intervals below 0.65 MeV and at 2.0 keV intervals above that energy but the data was averaged over 10.0 keV intervals for analysis. A least squares fit to the data gives

$$\sigma_T = 4.8301 - 3.5580E + 1.5872E^2 - 0.3050E^3$$

$$s = \left(\frac{\sum d_i}{n - 4}\right)^{1/2} = 0.035$$

where σ_T is the total cross section in barns, E is the neutron energy in MeV, s is the standard deviation, d_i is the difference between the calculated and experimental values, and n is the number of data points. The fit is good. The statistical accuracy of the data required $s \geqslant 0.02$ and the inclusion of E^4 and E^5 terms gave no significant improvement.

6. Facilities Development (Reactor Physics Division)

The Fast Neutron Generator is being shipped to the ANL site and the components are being installed as they arrive. Specifications are for both tandem (8 MeV) and single ended (4 MeV) modes of operation. Pulsed and DC capability is available in both modes. In DC mode factory tests proton currents of ~200 microamps have been observed. Various large experimental facilities associated with the program at the new facility are under construction and installation; for example, time-of-flight collimators with flight paths to 7 meters at angles of +160° to -140°. Hopefully, Christmas will see full research operation.

7. Facilities Development (Physics Division)

The Argonne 4-MeV Dynamitron is now in operation. To date protons and deuterons have been accelerated and helium ions will be used in the immediate future. Until experience is obtained in handling large currents of energetic ions, most experiments will be designed to use currents less than a few hundred microamperes.

The energy resolution of the ion beam is at least as good as that of the old 4 MV Van de Graaff. The beam quality and positional stability is exceptionally good. At beam currents less than 100 μa a beam spot less than 3 mm is obtained both near to and at a considerable distance from the accelerator.

A new data room has been added to the facility. An on line computer is now operating. Provisions have been made for up to thirteen beam lines. A pulsed ion source including klystron bunching has been purchased and will be installed during the autumn.

B. Charged Particle Physics

1. Study of the $^{39}K(d,t)^{38}K$ Reaction at $E_d = 23$ MeV
(H. T. Fortune, N. G. Puttaswamy, and J. L. Yntema)

The $^{39}K(d,t)^{38}K$ reaction has been utilized to study states in ^{38}K below an excitation energy of 5 MeV. Spectroscopic factors have been extracted by comparing the data with distorted-wave calculations. For states for which both $\ell = 0$ and $\ell = 2$ transitions are allowed, attempts have been made to extract relative admixtures. Two positive-parity states, not previously reported in neutron-pickup experiments, have been observed at $E_x = 3.44$ and 3.99 MeV. Two weak negative-parity states have been observed at $E_x = 2.64$ MeV ($\ell = 1$) and 4.66 MeV ($\ell = 3$), indicating the admixture of core-excited configurations in the ground state wave function of ^{39}K.

2. Energy Levels in ^{33}P
(G. Hardie, R. E. Holland, L. Meyer-Schützmeister, F. T. Kuchnir, and H. Ohnuma)

The energies of many levels in ^{33}P were obtained by a magnetic spectrograph analysis of the protons from the $^{30}Si(\alpha,p)^{33}P$

reaction. Proton-gamma angular correlations were studied in the same reaction. Several gamma-decay branching ratios were determined. It was found that the 3.50-MeV state has a spin of $\frac{3}{2}$ or $\frac{5}{2}$, and the 3.63-MeV state has a spin of $\frac{7}{2}$. It is argued that the parity of the 3.63-MeV state is positive and that $\frac{7}{2}^-$ is the most likely assignment for the 4.23-MeV state. Mixing ratios of several transitions were also obtained.

3. Distorted-Wave Analysis of the $^{11}B(d,p)$ Reaction Leading to the Lowest Unbound Level in ^{12}B
(H. T. Fortune and C. M. Vincent)

The 3.39-MeV state of ^{12}B is 20 keV above the threshold for neutron decay, and has been seen both in $^{11}B(d,p)^{12}B$ and in $^{11}B(n,n)^{11}B$. We have carried out an analysis of $^{11}B(d,p)^{12}B$ by a new technique, and combined the stripping and elastic-scattering data to obtain the spin and parity of the state in question. The comparison of reaction and elastic scattering data yields an unambiguous assignment of negative parity. The spin assignment is not unique but combining all the available data for this state leads to $J^\pi = 3^-$ as the most likely assignment.

4. Study of the $Al^{27}(He^3,p)Si^{29}$ and $Al^{27}(He^3,p\gamma)Si^{29}$ Reactions
(L. Meyer-Schützmeister, D. S. Gemmell, R. E. Holland, F. T. Kuchnir, H. Ohnuma, and N. G. Puttaswamy)

The levels of Si^{29} have been studied by measuring angular distributions of the $Al^{27}(He^3,p)Si^{29}$ reaction. A few states, in particular the level at 8.310 MeV (the analog of the Al^{29} ground state), were strongly excited with an orbital angular-momentum transfer $L = 0$ leading to states with $J = \frac{3}{2}^+$, $\frac{5}{2}^+$, and possibly $\frac{7}{2}^+$. The γ decay of some of these levels has been studied by p-γ coincidences. They all showed a very similar γ decay, namely a preference to decay to those few positive-parity states that are also strongly populated in the (He^3,p) reaction. No transition to negative-parity states was seen.

5. (d,t) and (d,He^3) Reactions on the Calcium Isotopes
(J. L. Yntema)

The $Ca^{42}(d,t)Ca^{41}$, $Ca^{43}(d,t)Ca^{42}$, $Ca^{44}(d,t)Ca^{43}$, $Ca^{46}(d,t)Ca^{45}$, $Ca^{48}(d,t)Ca^{47}$, $Ca^{42}(d,He^3)K^{41}$, $Ca^{43}(d,He^3)K^{42}$, and $Ca^{44}(d,He^3)K^{43}$ reactions have been investigated at an incident deuteron energy of 22 MeV. The angular distributions have been compared with distorted-wave calculations and the spectroscopic strength has been

extracted. The larger fraction of the $d_{3/2}$ strength was found in the $\frac{3}{2}^+$ states at 2.02, 0.99, 1.04, and 2.60 MeV in Ca^{41}, Ca^{43}, Ca^{45}, and Ca^{47}, respectively. Strong s-wave transitions were observed to levels at 1.96, 1.90, and 2.00 MeV in Ca^{43}, Ca^{45}, and Ca^{47}, respectively. The $\frac{5}{2}^+$ hole state at 2.67 MeV in Ca^{41} was found to be less pure than the other strong s- and d-hole states. Similarly a pronounced fractionation of the s-hole configuration among the levels at 0.982, 1.273, 1.595, and 2.73 MeV was found in K^{41}—in contrast with the other even-parity hole states in K^{41} and K^{43} (including the $\frac{1}{2}^+$ level at 0.56 MeV) which are rather pure.

PILE NEUTRON PHYSICS

Since January 5 of this year the CP-5 Reactor has been shut down for extensive modification and rehabilitation. Current plans call for a return to full power in late 1969 or early 1970. Consquently, experiments associated with this facility have been discontinued and research activity limited to analysis of data obtained before the shutdown.

A. Average Resonance—Capture Measurements
(L. M. Bollinger, G. E. Thomas, D. J. Buss, and R. K. Smither)

Analysis is continuing on the data obtained for a large number of nuclei during the period preceeding the reactor shutdown. For details the reader is referred to the earlier report to NCSAC, WASH-1127, page 10.

B. Determination of Resonance Spins from Capture γ-ray Spectra
(K. J. Wetzel and G. E. Thomas)

A method has been explored for measuring the spin of s-wave neutron resonances in medium weight even-Z and odd-N target nuclei. Low-energy γ-ray spectra following resonance neutron capture were observed with a Ge(Li) detector system using the ANL fast chopper. For resonances of known spin the relative population of low lying 2^+, 4^+, and 6^+ levels was found to be directly correlated with the resonance spin value. The ratios of γ-ray intensities are in fact consistent with values predicted by a simple model of the γ-ray cascade process. Several even-Z odd-N target nuclei with resonances of known spins were studied as test cases, namely ^{183}W, ^{135}Ba, ^{105}Pd, ^{95}Mo, ^{167}Er, and ^{177}Hf. This method has also been used to obtain J for several unassigned

resonances in ^{167}Er and $^{187,189}Os$. A paper titled Method for Determining Spins of Neutron Resonances has been submitted to the Physical Review.

C. Determination of Resonance Spins By Measurements of Low Lying Level Occupation Probability Ratios
(W. P. Poenitz and J. R. Tatarczuk)

Previous studies of the low lying level occupation probability ratios (Poenitz*,**,†) has been continued with measurements of such ratios at the RPI Linac. For W^{183} and Ho^{165} the time-of-flight spectra of two γ-peak regions and of appropriate background ranges have been recorded in 1000 channels each. For Ta^{181} the γ-spectra in the range 50—500 keV have been measured in 23 resonances. These measurements will be used for checking the experimental technique of spin determination and, if applicable, for the determination of unknown spins, especially for tantalum resonances.

NUCLEAR THEORY AND ANALYSIS

A. Shell-Model and R-Matrix Calculations of Nuclear Reaction Cross Sections
(K. Takeuchi and P. A. Moldauer)

A simple and powerful method has been developed for the calculation of resonance cross sections. An R-matrix is obtained by a shell model calculation whose basis states are constructed from discrete single particle states in a Woods-Saxon potential and subject to R-matrix boundary conditions. This procedure permits the calculation of not only a finite set of R-matrix energies and the associated reduced partial widths, but it also yields the important background R-matrix associated with that finite set of states. From this R-matrix we calculate the S-matrix and total and reaction cross sections, which are independent of

---

*W. P. Poenitz, Thesis, Technical University Karlsruhe, 1966.

**W. P. Poenitz, Z. J. Physik 197, 262 (1966).

†W. P. Poenitz, Bull. Am. Phys. Soc. Vol. 13, 1389, B62 (1968).

the choice of R-matrix radii or boundary conditions and include the effects of wave function antisymmetrization. Sample calculations have been performed to confirm the insensitivity of the results to changes in the channel radii, to study the effects of antisymmetrization, and to study the way in which single particle states and particle-hole excitations are distributed among resonances.

B. Analysis of Nuclear Energy Level Spacing Distributions
(J. E. Monahan and N. Rosenzweig)

An empirical spacing distribution is always based on a finite, and usually a small number of observed levels. Thus, even if the random-matrix model were perfect the observed distribution would necessarily fluctuate about the theoretical mean. A statistic $\Lambda(n)$ has been defined which enables one to judge whether the magnitude of the observed fluctuations about the Gaudin-Mehta distributions is compatible with the random-matrix model. It is found that the correlation between spacings which are implied by the model tend to reduce the fluctuations significantly. The statistical properties of $\Lambda(n)$ are studied by means of a Monte-Carlo calculation with matrices of order 100 sampled from the Gaussian orthogonal ensemble. An illustrative analysis of the published neutron resonances observed in U^{238} reveals no obvious discrepancy between theory and experiment up to neutron kinetic energies of about 2 keV.

C. Multilevel Adler-Adler Parameters for the Pu-239 Fission Cross Section from 40 to 100 eV
(P. Lambropoulos)

The present analysis of the Saclay* fission data for Pu-239 was undertaken in an effort to determine a more reliable set of fission parameters. The experience gained in the analysis** of Petrel† data was useful in deciding on the resonance structure at the low lying valleys. Such structure in the Saclay data is masked by the relatively high

---

*G. DeSaussure et al. in Proceedings of the IAEA Symposium on the Physics and Chemistry of Fission, Salzburg, 1964 (International Atomic Energy Agency, Vienna, 1965), Vol I, p. 205.

**P. Lambropoulos et al., "Multi-level Analysis of the Pu-239 Fission Cross Section from 40 to 150 eV," Bull. Am. Phys. Soc. 13, 1409 (1968).

†E. R. Shunk et al, "Fission Cross Sections from Petrel," LA-3586, Sept. 1966; also, P. A. Sieger et al. Nucl. Phys. A96, 605 (1967).

background. On the other hand, the much superior resolution function of these data reveals more structure above the background level. This analysis seems to reveal a larger number of levels than reported heretofore. The existence of some of them, however, cannot be considered as conclusive until an analysis of the total or capture cross section of Pu-239 is performed and made compatible with the fission cross section. Such analysis was not undertaken in this work as the necessary experimental data were not available.

The fission cross section is described by four parameters: μ, ν, $G^{(F)}$ and $H^{(F)}$ for each resonance. The parameters obtained are given in Table 2. By comparing the present fits to the fits of reference 3 at well resolved resonances, it was found that the energy scale difference between the two sets of data was very small, if any. Thus it appears that, whatever differences exist in the positions of the poles between this analysis and that of reference 2 are not likely to be due to differences in the energy scale.

The present results seem to reveal 42 levels between 40 and 100 eV, while ENDF/B File 2 only 23 levels are listed. Compared to Farrell's* results with 28 levels between 40 and 90 eV, the present analysis reveals 34 levels in the same energy range. The angular momentum assignments, given in Table 1, have been made on the basis of level widths and level interference. These assignments, although not conclusive, are in general agreement with those of Farrell* with very few exceptions.

---

*J. A. Farrell, Phys. Rev. 165, 1371 (1968).

TABLE 2. Multi-level Fission Resonance Parameters for Pu-239 from 40 to 100 eV.

μ(eV)	ν(eV)	$G^{(F)}\ 10^{-4}\ (eV)^{1/2}$	$H^{(F)}\ 10^{-4}\ (eV)^{1/2}$	J
40.90	.400	- .1877 ± .049	.1483 ± .055	0
41.50	.075	2.2242 ± .062	- .0917 ± .038	1
42.50	.075	- .0336 ± .017	- .0213 ± .017	1
44.46	.015	1.1200 ± .039	.0640 ± .019	1
45.70	.140	.1049 ± .023	- .0428 ± .022	1
47.51	.115	3.0435 ± .076	- .2208 ± .039	0
49.60	.550	2.6238 ± .119	- .8530 ± .107	0
50.05	.020	1.2309 ± .065	.5594 ± .051	1
51.60	.040	.0174 ± .024	.0301 ± .023	1
52.50	.015	2.5341 ± .075	.0441 ± .033	1
54.40	.500	- .0286 ± .068	.3892 ± .065	0
55.50	.022	1.1082 ± .052	.1556 ± .034	1
57.50	.450	15.1709 ± .263	-2.2762 ± .174	0
59.05	.030	6.1212 ± .213	- .2586 ± .127	1
60.00	.800	1.6524 ± .283	- .8193 ± .329	0
63.05	.040	.7137 ± .078	.6976 ± .068	1
64.35	.400	-1.0708 ± .158	1.1020 ± .145	0
65.55	.036	11.3340 ± .313	1.7846 ± .176	1
66.25	.080	1.2239 ± .144	.1023 ± .136	1
67.00	.100	.4986 ± .102	.2157 ± .099	1
68.15	.500	.6069 ± .158	.7854 ± .153	0
71.00	1.000	- .2732 ± .226	1.4767 ± .209	0

TABLE 2. (Con't.)

μ(eV)	ν(eV)	$G^{(F)}$ $10^{-4}(eV)^{1/2}$	$H^{(F)}$ $10^{-4}(eV)^{1/2}$	J
73.35	.150	- .4606 ± .105	.2727 ± .109	1
74.25	.090	2.5335 ± .257	1.7349 ± .209	1
75.10	.070	17.5130 ± .665	- .1221 ± .288	1
76.20	.350	.6801 ± .246	- .4905 ± .220	1
77.50	.950	- .1556 ± .339	- .2204 ± .282	0
81.30	.995	3.1895 ± .234	-5.3270 ± .185	0
83.30	.053	1.3791 ± .103	- .3226 ± .092	1
84.80	.120	2.4018 ± .208	1.5482 ± .216	1
85.70	.085	8.0350 ± .364	5.0357 ± .330	1
86.30	.195	5.3621 ± .308	- .7772 ± .303	1
88.00	.750	5.4795 ± .304	3.9537 ± .264	0
89.60	.180	.6714 ± .082	.4432 ± .078	1
90.90	.030	3.1426 ± .099	.5829 ± .071	1
92.20	.210	1.2064 ± .128	.3705 ± .135	1
93.00	.180	.8190 ± .129	- .1816 ± .012	1
94.50	.800	2.3920 ± .381	- .4122 ± .381	0
95.50	.030	1.7169 ± .133	- .4193 ± .119	1
96.50	.100	1.7865 ± .177	- .5955 ± .168	1
97.60	.300	2.2886 ± .225	.8073 ± .196	1
99.00	1.100	1.5486 ± .412	- .8492 ± .306	0

BROOKHAVEN NATIONAL LABORATORY

A. NEUTRON PHYSICS

1. Fast Chopper (R. E. Chrien, O. A. Wasson, D. I. Garber*, M. R. Bhat*, S. F. Mughabghab*, R. G. Graves**, K. Rimawi+, M. Beer*, S. Bokharee+, and C. Zikides++

a. Instrumental

A program to measure the resonant neutron capture γ rays in the fissionable nuclei is under way. In order to distinguish the prompt fission γ rays from the capture γ rays, a special Ge(Li) detector, surrounded by an annulus of liquid scintillator, is under construction. The prompt fission γ rays in the Ge(Li) detector are in coincidence with the fast fission neutrons in the liquid scintillator. Since the scintillator is also sensitive to γ rays, pulse shape discrimination is used to differentiate neutrons from γ rays.

b. Experimental

1) Resonance spin assignments from low energy γ rays from neutron capture in Ho and Tm. Low energy (< 600 keV) γ rays from capture in the 11 resonances of Ho and 13 resonances of Tm were measured. A comparison of the spectra indicates that they fall into two groups corresponding to the two values of s-wave resonance spins. Measured ratios of the γ-ray intensities of the 116.8 keV ($3^- \rightarrow 2^-$) and 149.3 keV ($5^- \rightarrow 4^-$) for the 11 resonances in Ho are shown in Figure A-1 with the assigned spins as given in BNL-325. In Tm, the 144.5 keV ($3^+ \rightarrow 2^-$) and 149.7 keV ($0^- \rightarrow 1^-$) γ-ray intensities show variations from the 0^+ and 1^+ resonances. Typical spectra are shown in Figure A-2. The intensity variations could be accounted for qualitatively in terms of a two-step cascade of E-1 transitions populating these states. The resulting spin assignments, which agree with BNL 325, are shown in Table A-1.

---

* Department of Applied Science, BNL.

** State University of New York, Stony Brook.

\+ State University of New York, Albany.

++ Summer Student from Greece under BNL-Greek Cooperative Program.

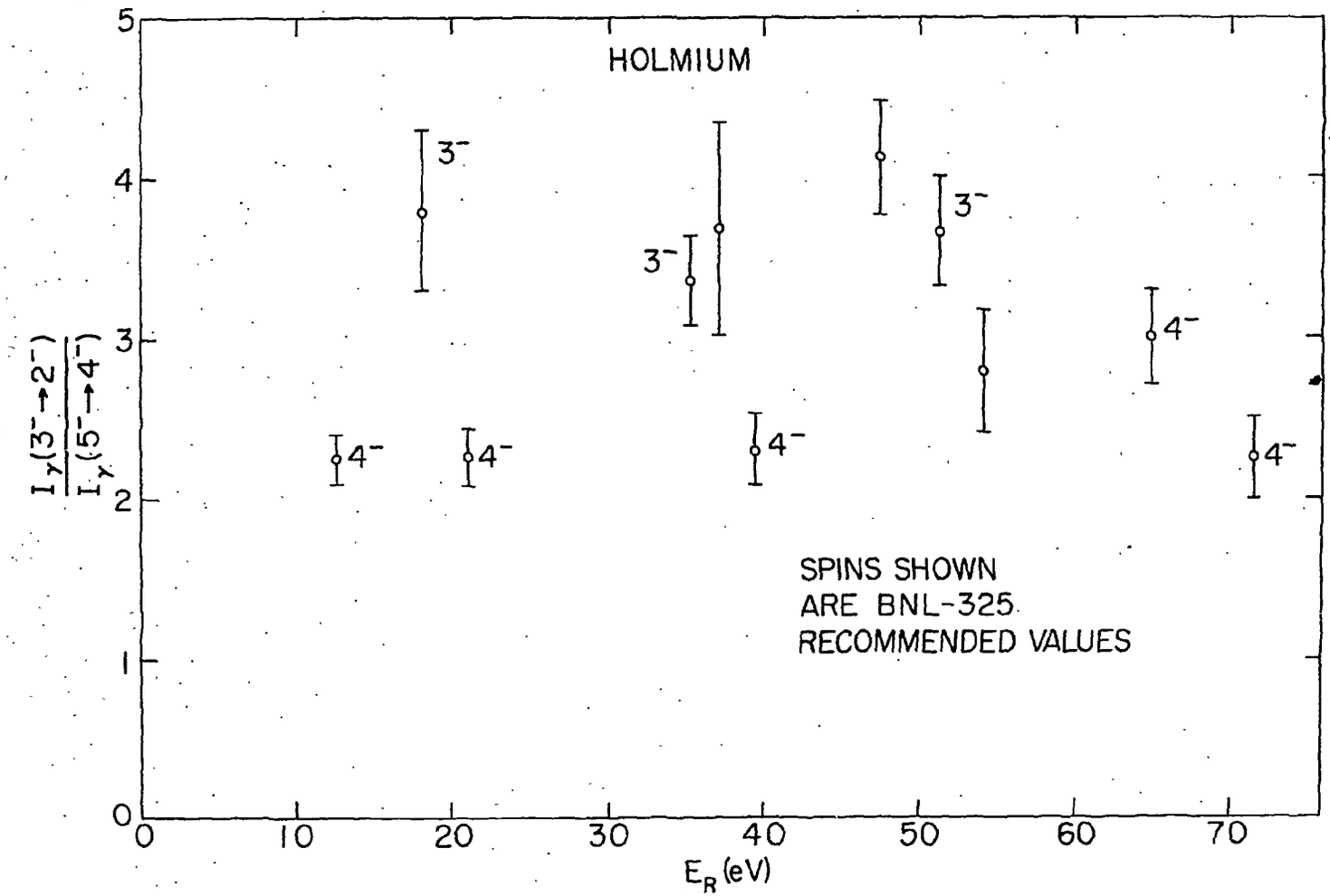

FIGURE A - 1

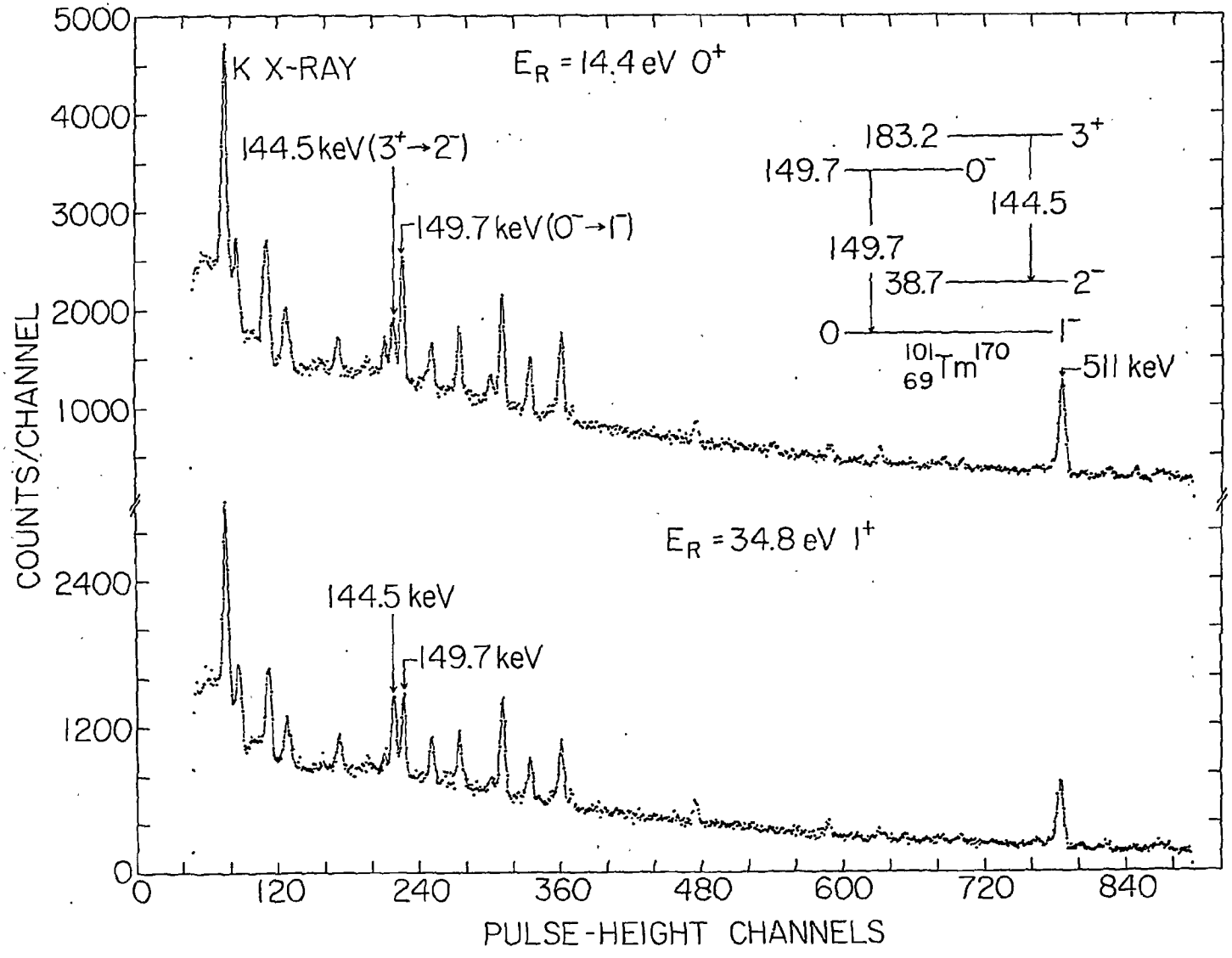

FIGURE A - 2

Table A-1

Tm Resonance Spin Assignments

E_R(eV)	J_R
14.4	0
17.5	0
29.1	1
34.8	1
38.0	not known, we assign 0^+
44.8	1
50.7	1
59.2	1
63.0	1
65.8	0
83.4	1
94.0	1
115.2	1

2) Plutonium Capture γ-Ray Measurements. The high energy γ rays ($E_\gamma > 3.6$MeV) from neutron capture in seven resonances in $Pu^{239}(n,\gamma)$ were measured. In contrast to U^{235}, a few strong γ rays are observed in the individual resonances as shown in Figure A-3.(Pertinent to Request 338)

3) $Mo^{92}(n,\gamma)$. Resonant neutron capture γ rays from a highly enriched sample of Mo^{92} have been studied. The resonance at 346 eV was determined to have spin and parity of $3/2^-$ and to result from p-wave capture. This is based on the observation of primary γ-ray transitions to a well-known $5/2^+$ final state. Evidence for an additional p-wave resonance between the 3.17 and 11.6 keV resonances is observed. The neutron separation energy of Mo^{93} is determined to be 8077 ± 3 keV.

4) The distribution of partial radiation widths in $Pr^{141}(n,\gamma)Pr^{142}$. The distribution of partial radiation for widths from the two 3^- resonances at 219 and 235 eV to 13 final states is fitted with a chi-squared distribution with $\nu = 3.4 {}^{+2.3}_{-1.3}$ degrees of freedom. This is inconsistent with the Porter-Thomas Distribution.

5) $Lu^{175}(n,\gamma)Lu^{176}$. Both high energy and low energy γ-ray spectra were obtained for 11 resolved resonances in the target nucleus Lu^{175}. The summed spectrum from the 18 lowest energy resonances is shown in Figure A-4. For $E_\gamma > 5.1$ MeV there are approximately 30% more γ rays observed in the resonance capture than in thermal capture. Assuming the highest energy γ ray to populate the 3^- state at 239.4 keV yields a neutron binding energy of 6294.6 ± 2.4 keV. For $E_\gamma < 5.1$ MeV few γ rays are resolved because of the complexity of the spectrum.

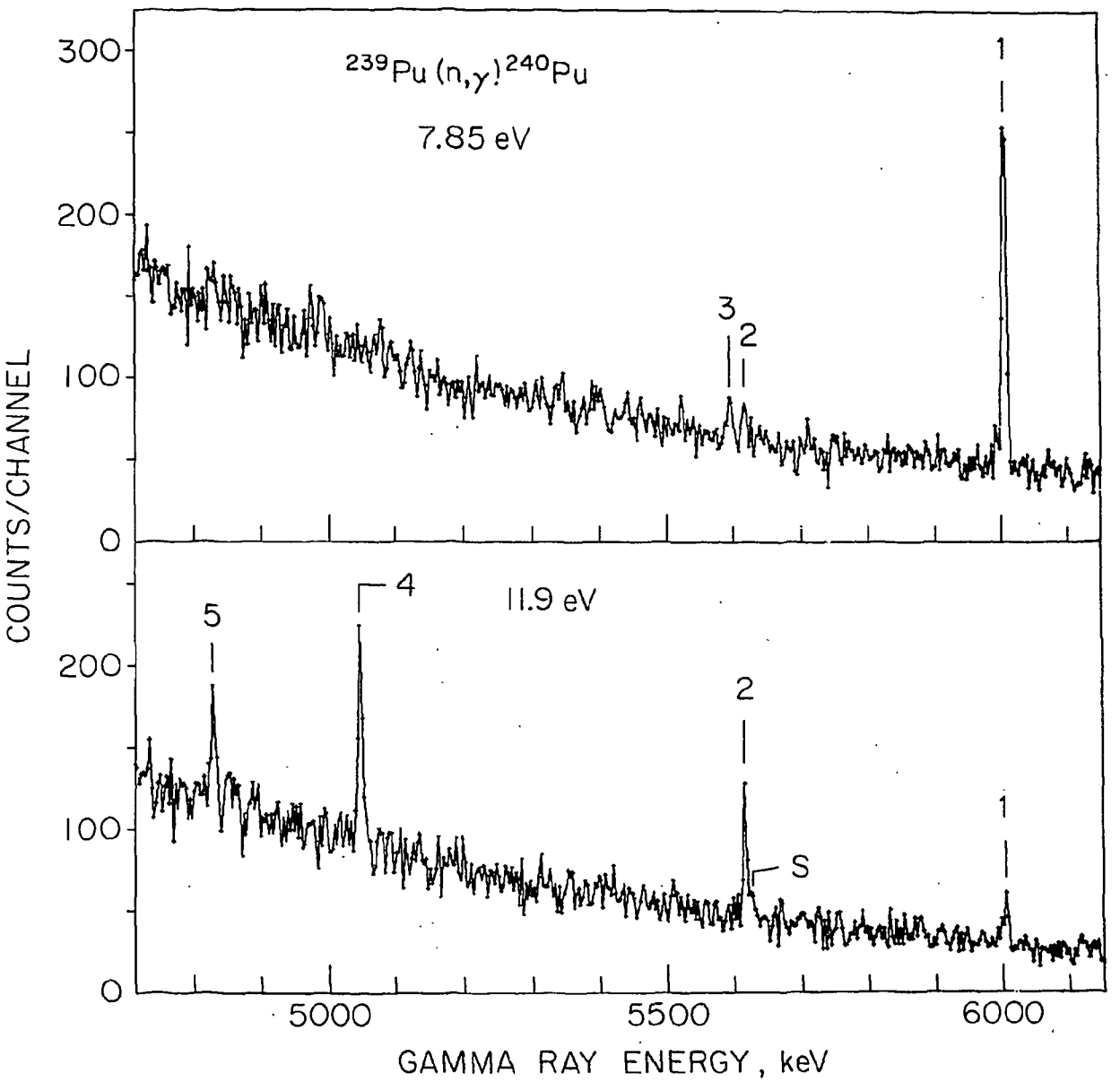

FIGURE A - 3

DATA NOT FOR QUOTATION

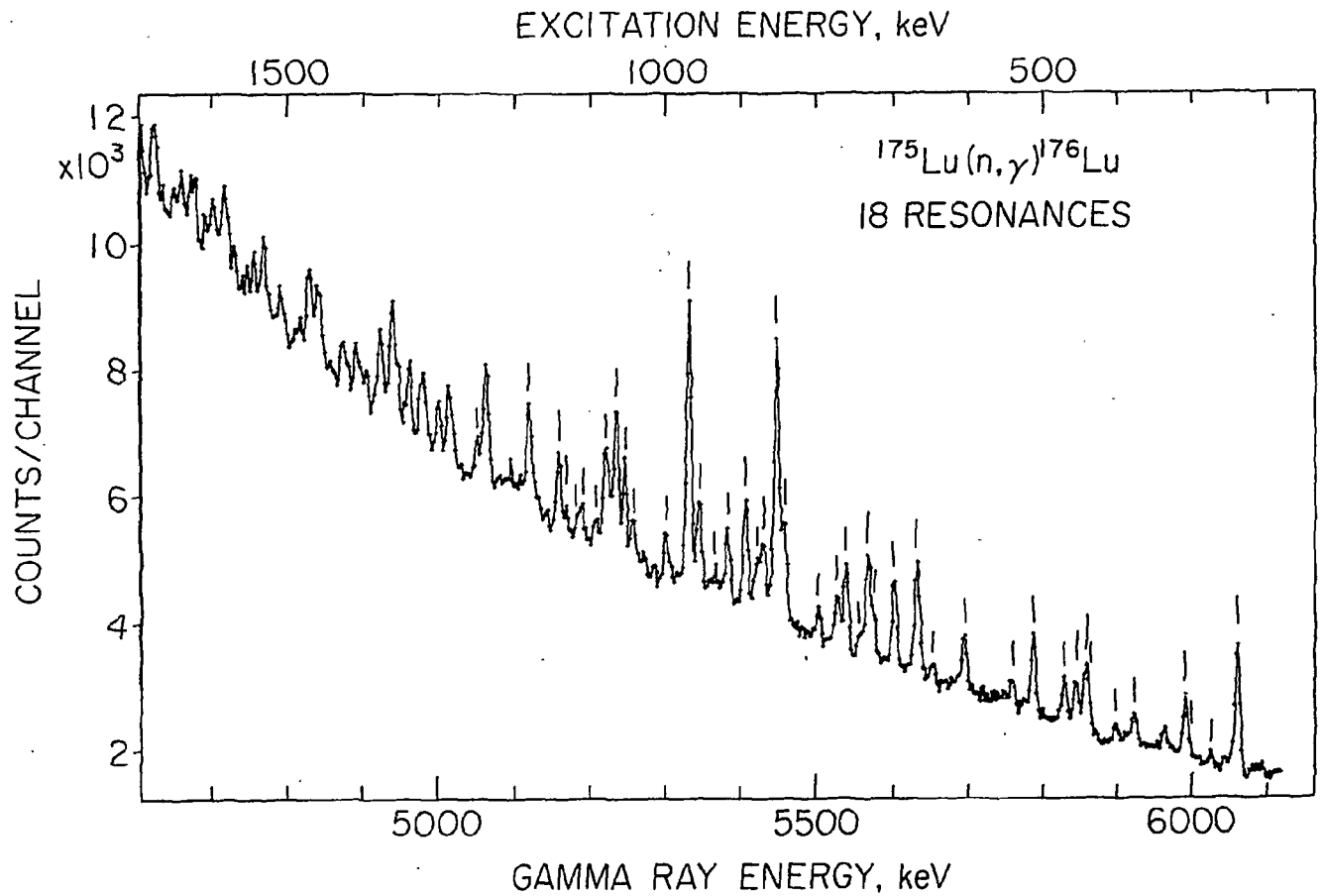

FIGURE A - 4

A statistical analysis of the distribution of partial radiation widths as well as the determination of the resonance spin assignments is in progress.

6) Evidence for Channel Resonance Capture in $Mn^{55}(n,\gamma)Mn^{56}$. The γ-ray intensities of 30 γ rays from neutron capture in the five lowest energy resonances were measured. In the capture process of Lane and Lynn, the internal resonance contribution to the partial radiation width is uncorrelated with the reduced neutron widths of both capturing and final states while the channel resonance contribution is proportional to the neutron widths. A correlation coefficient between the radiative widths and the product of the reduced neutron widths of the initial and final states was measured to be +0.4. The probability of observing a larger value for null correlation is less than 1%. Using a Monte Carlo technique to calculate the internal contribution requires the internal capture be about 5 times the channel capture for manganese.
(Pertinent to Request 91)

2. Nuclear Cryogenics - Measurements of the Low-Energy Absorption Cross Sections (G. Brunhart, S. S. Malik, F. J. Shore)

Absorption cross sections measurements for Zr, Ni, Cu, Tb, Er, and Nd were made at selected energies, 0.033, 0.075, 0.115, and 0.27 eV. The purpose of these measurements was to investigate systematic errors and to determine the ultimate precision that could be expected. The measurements were carried out with a Moxon-Rae type detector using carbon as converter. The linearity of the M-R detector as function of energy was checked by measuring the absorption cross sections of Al, Ta, Ag, and Rh using Au as a standard. The test showed that for these elements the cross sections behaved as 1/v. Checks were also made at lower gamma-ray energies with calibrated γ sources.

The results show that corrections involving the uniformity of sample thickness, multiple scattering, and γ-ray attenuation in the sample must be considered in detail to obtain reliable values of $\sigma_{n,\gamma}$. Test measurements for each of these effects were made with Au and Er samples. A computer program for making the necessary correction is being prepared.

B. NATIONAL NEUTRON CROSS SECTION CENTER (S. Pearlstein, M. Bhat, D. Cullen, D. Garber, M. D. Goldberg, T. J. Krieger, W. Kropp, B. Magurno, V. May, S. Mughabghab, A. Prince, U. Schulze, J. Stehn, T. Stephenson, L. Stromberg, and H. Bauman)

A list of definitions for neutron data specifications has been provided for 4-Center approval. This work is primarily an outgrowth of the

IAEA-sponsored Panel on Neutron Data Compilation. These definitions will be used as a basis for the various data libraries and bibliographic indexes, such as SCISRS and CINDA.

A PDP-10 computer was received by the NNCSC during July 1969 and is operating in a temporary location while awaiting construction of a permanent building. The SCISRS-II system developed on the CDC-6600 is being converted for PDP-10 operation. The purchase of interactive graphics equipment was delayed due to lack of AEC funds.

A revised version of the ENDF/B library will be issued in the fall of 1969. The fissile elements are being re-evaluated by a special task force comprised of experimenters and evaluators.

CASE WESTERN RESERVE UNIVERSITY

A. NEUTRON PHYSICS

1. Elastic and Inelastic Scattering of Neutrons (J. T. Lindow, P. Boschung and E. F. Shrader)

The program of measurements described in the last Reports to the NCSAC (Wash 1127) has been completed from which differential cross sections for elastic and inelastic neutron scattering from $^{54,56}Fe$, $^{58,60}Ni$ and elastic scattering from natural carbon are being extracted. Neutron energies of 4.0, 5.1 and 5.6 MeV and ten to twelve angles between 25° and 148° were studied.

Absolute cross sections are being obtained from the (n,p) cross section using scattering data from NE102 plastic scintillators placed in the same geometry as the other samples. The neutron time-of-flight spectrum was gated by the light output from the NE102 scintillator greatly reducing the number of events from carbon scattering and room background

Relative angular distributions have been extracted from the raw data. Work is in progress on modifications to MULCAT which is a computer program used to correct the data for finite source-sample geometry, neutron attenuation in the sample, and multiple scattering effects. The modifications will allow the code to handle the more complex situation presented by the NE102 scintillator-scatterer. MULCAT will calculate absolute cross sections corrected for all finite sample effects.

2. Neutron Polarization from the Reaction $C^{13}(d,n)$ at Incident Deuteron Energies of 1.6, 2.2 and 2.5 MeV (W. W. Lindstrom and E. F. Shrader)

Work is nearly complete on the computer calculation of polarimeter analyzing power to be used in the reduction of experimental data now on hand on the $C^{13}(d,n)$ reaction.

An existing proton recoil detector efficiency program[1] has been modified to include the effects of the 2.082 and 2.96 MeV resonances on C(n,n) elastic scattering cross sections and angular distributions. The statistical nature of photoelectron production and multiplication has also been simulated. The effects of the detector container and the incoming neutron spin have been neglected.

1) B. Gustafsson and O. Aspelund, Nucl. Instr. and Meth. 48 (1967) 77-86.

The results of this program will be used as input to a second existing program[2] which has been modified for our geometry.

3. Neutron Polarization from the $O^{16}(d,n_o)F^{17}$ Reaction. (B. Anderson and E. F. Shrader)

Targets to be used in an experiment to measure the neutron polarization in the reaction $O^{16}(d,n_o)F^{17}$ have been prepared. The oxygen targets, made by anodizing tantulum, range from approximately 30 KeV to 200 KeV thickness for 2.5 MeV deuterons. The He polarization analyzer has been set up and checked in the energy range to be studied by measuring the already measured[1] neutron polarization in the reaction $T(p,n)He^3$. Some possible modifications in the analyzing system are being contemplated.

2) G. M. Stinson, S. M. Tang and J. T. Sample, Nucl. Instr. and Meth. 62 (1968) 13-18.

1) R. L. Walter etal, Nuc. Phys. 30 (1962) 292-299

A Monte Carlo computer program, NOMCAR, has been written to simulate the experiment and calculate the inscattering for the geometry of the system. A feature of this program is that it simulates the pulsed beam by following the flight time in the scatterings and hence takes account of the finite electronic resolution of the time of flight detection system.

The cryostat for storage of the 5-foot long x 1 foot diameter liquid oxygen sample has been constructed and tested. The system has been designed to incorporate safety features, especially in the liquid oxygen transfer stages. The main sample vessel is in vacuum and is surrounded by a radiation shield maintained at liquid nitrogen temperature.

Further to the last report, essentially contained in the above paragraphs, several "dry" runs have been made to check out the various systems, prior to the actual use of the liquid oxygen absorber.

A time pick-off and beam burst display system has been designed and constructed. Installed in the control desk of the Van de Graaff, this system displays a crossover time pick-off (timing) signal and also a linear beam burst signal on a fast sampling oscilloscope. The accelerator can thus be tuned to give optimum (narrowest) beam burst and maintained thus throughout the experiment. Several independent 'runs' with this system have been observed on display, in agreement with estimates of pulsing performance based on observation of the C^{12} (He^3,n) O^{14}reaction described in the last report.

In observations of neutron time of flight with the $Li^7(p,n)Be^7$ reaction (to be used as the neutron source), the secondary neutron group to the Be^7 first excited state has been resolved from the primary (ground state) group, the neutron time resolution corresponding to 4.5 to 5 nsecs F.W.H.M. during that run.

Several sets of lithium targets on various backing materials have been tested for long term stability by observation of the Li^7 (p,n) threshold slope as a function of bombardment time.

A 2 foot long liquid nitrogen cold tube (through which the beam passes) is placed in front of the target and vacuum in the target region is maintained at approximately 10^{-6} Torr in an effort to eliminate carbon build-up on the targets with this system.

The pulse shape discrimination system, to distinguish between neutron and gamma-ray events in the liquid scintillator, has proved very satisfactory in these preliminary runs. A feature of the system provides rejection of low level and high level gamma-ray events in a high speed anticoincidence part of the circuit such that a window of (neutron) pulses can be selected for cross-over timing discrimination between neutrons and gamma rays.

Gamma rays whose production is time correlated with the beam burst, are thus effectively eliminated by the time of flight resolution and the background gamma rays are substantially reduced by the n-γ pulse shape discrimination.

The use of "tight" time resolution also assists in reducing the contribution of the neutron inscattering correction to the measured cross section.

As an independent study, n-γ discrimination has been investigated in a variety of liquid scintillators. As mentioned in the last report, the n-γ discrimination is observed to be poorer in large liquid scintillators and the general assumption that this effect is attributable to lower light collection efficiency is not wholly tenable since the pulse shape discrimination technique depends primarily on the analytical form of the light pulse rather than the intensity of the light flash.

A variety of these tests with various light pipes and light collection arrangements have indicated that the deterioration is not due merely to wide angle acceptance of light events from the scintillator.

Possible effects of transit time spread across the full (5 inch diameter) photocathode of a 58 AVP photo-tube have been investigated using a 5 nanosecond light flash from a pulsed light emitting diode (Ferranti XP-20). No significant effect was found, our preliminary measurements indicating the transit time spread is less than 2 nanoseconds and cannot account for the worsening of the n/γ events time separation.

The effect of pulse height uniformity across the photocathode is now being investigated in terms of n-γ discrimination properties of liquid scintillators with large (5") phototubes.

B. SLOW NEUTRON PHYSICS

1. Neutron Resonance Cross Section Measurements (H. Camarda, G. Macken, W.W. Havens, Jr., H. Liou, F. Rahn, J. Rainwater, M. Slagowitz and S. Wynchank)

Much attention has been given since the last report to the analysis of data obtained in the most recent run. Preliminary values of total cross sections, resonance parameters, reduced neutron widths, level spacings and strength functions are available for natural Na, Ar, Co, Ta and La and for the separated isotopes In^{115}, $Eu^{151,153}$, $Gd^{154,158}$, $Er^{166,167,168,170}$, $Yb^{171,172,173}$, Lu^{175} and $W^{182,184,186}$, in an energy range between 1 eV and 50 keV, and many new resonances have been found in the separated isotopes. Area analysis methods are being used in all cases to determine the resonance parameters, except for those of Na* and Co** for which an R matrix code has been employed. Six papers concerned with these results were presented at the Washington meeting in April, and two will be presented at the next meeting.

---

*A.B. Smith, WASH 1078, Data request No. 59, p. 12, June, 1967.

**Ibid., p. 23, Data request No. 107.

Preparation for the next run (winter 1969) has included a) improvements to the number and positioning of neutron flight paths through the cyclotron shielding wall, b) modifications to the proton beam deflection system, c) the addition of new detectors at the 200 meter station, d) the interface between detectors and the EMR 6130 computer, to be used for the first time in its data acquisition role in the next run and e) the writing of systems programs for data acquisition, display, plotting and some on line computation.

a. to make full use of the extended experimental area recently completed at the cyclotron and to use the largest number of parasitic experiments during a run of this group, two neutron channels 9" x 3" and two channels 2 1/2" x 2 1/2" will replace a single channel through the steel shielding wall. The other four channels will remain unchanged. Additional shielding and collimators will be employed to reduce backgrounds for the simultaneous experiments and to increase safety in the experimental area.

b. the proton beam deflection system is being modified. New types of thyratrons and transformer configurations are being tested to improve deflection rise time and amplitude. More efficient deflection is expected to help our resolution and counting rate. A cleaner neutron pulse should therefore result.

c. Eight assemblies each containing a 5" (diameter) x 1 1/2" NaI crystal and a fast (type XP1040) photomultiplier will be placed above the B^{10} slab at 200 meters. Together with the present 11" (diameter x 1" mosaic NaI assemblies below the B^{10} slab, more neutrons will be detected in the energy regions where the counting rate is low. Time permitting, the four crystals will be replaced by eight 5" crystals. This is being done to reduce dead time losses due to self blocking effects. In the time regio when all detectors are on they will give improved statistics in the energy region of greatest interest where the counting rate is low.

d. Data from several detectors are fed into a 50 MH_z time of flight analyzer (which in the future can operate at 100 MH_z). The time delay to the first channel and 32 independently variable channel widths, one for each block of 512 channels are selected with a pinboard. Channel widths can be 2^n x 20 nsec (n=0,1,2,4,.....64). A multi-level 16 word derandomizing buffer with a transfer dead time of 20 nsec is used to handle the peak data rates. Descriptor bits in the data words may be used to run up to four 4K histograms each one filled from an independent experiment or one 16K histogram with the ability to record two events each minimum channel width (currently 20 nsec). An adder is provided to allow flexibility of histogram storage. The time of flight analyzer empties 16 bit data words into the EMR 6130, (775 nsec cycle time) computer Internal gating is provided to allow the experimenters to turn detectors off at desired times.

e. Running programs are being written to allow data acquisition and pre-processing in a real-time environment. The computer will read, write, display, plot, print and reduce data, even though data may be simultaneously arriving each machine cycle.

2. Radiative Capture Cross Section Measurements in the Low keV Region (J. Arbo, C. Ho, J. Felvinci, F. Rahn, E. Melkonian, W.W. Havens, Jr., and J. Rainwater)

The run at the Nevis synchrocyclotron which had been planned for Summer, 1969, has now been rescheduled for mid-December, 1969.

Our earlier plans for capture measurements on U^{233}, Th^{232}, and Np^{237} remain unchanged. Since our last report, however, certian additional materials of intermediate mass number have tentatively been selected for study: Rh^{103}, Cs^{133}, Tm^{169}, Mn^{55}, $Sb^{121,123}$ and $Ag^{107,109}$. The previously planned measurement of the Fe cross section will now be done only if time permits.

The fast (20 nsec/channel) time-of-flight buffer has been delivered by Pegram Electronics Laboratories, and is currently being tested in combination with the PDP-8 computer and magnetic disk memory. Programs for data handling are being written.

3. Fission Fragment Mass Distributions from Correlated Energy and Time-of-Flight Measurements (M. Derengowski and E. Melkonian)

Further analysis of the neutron emission results has revealed a computer programming error which had affected the neutron number distributions from single fragments of fixed mass. The other results of the experiment, including mass distributions and average neutron emission, were not affected.

The corrected neutron number distributions show the following general characteristics. The light fragment distributions at fixed mass are peaked at one neutron or, in less than one-third of the cases, at two neutrons - not at zero, as had previously been reported. The distributions from heavy fragments at fixed mass were about equally divided between those that peaked at zero and those that peaked at one neutron, with very few cases in which the peak appeared at two neutrons.

4. Variation of Fission Fragment Kinetic Energy Distribution and Yield of Long Range Alpha Particles in the Resonance Neutron Induced Fission of U^{233} (J. Felvinci and E. Melkonian)

Further analyses on the U^{233} data have confirmed the earlier reported variations in the yield of the slow neutron resonances for different fission fragment kinetic energy groups. These statistically significant variations are especially striking at the 16.4 eV and 16.7 eV "doublet" and at the 20.8 eV and 22.1 eV "doublet". Other large variations are also noticeable at higher neutron energies (above 40 eV).

Quantitative results will be available in the near future, as soon as we can correlate these variations with better data taken from the gamma ray measurements (see next section).

5. Determination of the Spin of Slow Neutron Resonances in Fissionable Nuclei by Measuring the Yield of Gamma Rays (J. Felvinci and E. Melkonian)

No further results are obtained from the previous run which was only exploratory in nature. Preparations are under way to repeat this experiment with better statistics, better background discrimination and on several nuclei during the next run, scheduled to start in mid-December.

6. Precision Measurement of the 2200 m/sec Neutron-Proton Capture Cross Section (D. Cokinos, E. Melkonian and W.W. Havens, Jr.)

A precise determination of the neutron-proton capture cross section at the neutron laboratory velocity of 2200 m/sec has been made. The measurements were part of an extensive set of pulsed source experiments designed to measure diffusion and thermalization properties of neutrons in media poisoned with 1/v and non-1/v absorbers using the pulsed neutron beam of the powerful Columbia Nevis Synchrocyclotron, the exponential decay of the thermalized neutron population has been obtained for a set of water assemblies of rectangular geometries over a wide range in sites. The capture cross section has been determined by least square fitting the decan constants to the expression for λ obtained from the diffusion approximation to the neutron transport equation. Using the latest available physical constants our result for the hydrogen capture cross section at 0.025 ev is 332.7 ± 0.7 mb. This result is assigned a significantly smaller error than earlier measurements except for those of Cox et.al. [Nucl. Phys. 74, 497 (1965)] which appear somewhat high as they have not been corrected for neutron leakage. An estimated correction of 0.7% to their result reduces their value to 332.4 ± 0.5 bringing it to close agreement with ours.

7. Slow Neutron Scattering by Hydrogenous Compounds (J. Markisz, T.I. Taylor, P.S. Leung, and W.W. Havens, Jr.)

The Brookhaven Graphite Research Reactor is currently on standby status, so that no new measurements of total cross sections as a function of temperature and neutron wavelength have been made. The crystal monochromator has been transferred to Columbia for use with the TRIGA reactor. Further analysis of the data taken on methane, ethane, dimethylacetylene and methylammonium chloride is in progress.

During the preparation of the manuscript for the measurements on the rotation of large molecules such as camphor, 1,2 dichloroethane and 1,2 dibromoethane it was evident that inelastic scattering measurements at a few temperatures would aid significantly in the interpretation fo the results. These were obtained in collaboration with P.S. Leung at Union Carbide Nuclear. The torsional frequency of methyl groups in camphor at temperatures below the 244° transition is 230 20 Cm^{-1} corresponding in the motion of the CH_3 groups above the transition. A broad band at 53 cm was assigned to the torsional motion of the whole molecule. This broadens and merges into the quasielastic peak above the transition. Similar behavior was observed for the effect of rotation for both 1,2 dichloroethane and 1,2

dibromoethane. The results of both the total scattering cross section for these molecules will aid in the interpretation of the results for the molecular motions in polymers.

C. NEUTRON AND GAMMA-RAY PHYSICS

1. Sensitivity of Transport Calculation to Microscopic Cross Sections (H. Goldstein, W. Preeg, C. Weisbin, E. Troubetzkoy)

As indicated in the previous report (WASH)-1127, page 40, the investigations of cross sections minima on deep neutron penetration has been turned from consideration of isolated minima to the study of small scale fluctuations. The case of iron has been examined intensively, as highly detailed cross sections sets have recently become available from the name KARSRUHE and GULF General Atomic. About 1.5 MeV the measured total cross section exhibits fluctuations with a root mean square deviation of about 30%, decreasing to a few percent at 6 MeV. The calculations by the moments method show that in the region 1.5 to 2.0 MeV use of the actual cross section yields fluxes orders of magnitude higher than predicted by smooth ENDF/B cross sections at distances of 1 meter in iron. Even the (2) sets of cross section data, though nominally of nearly the same resolution, show highly significant differences in the predicted flux spectra. Preliminary results indicate that fluctuations in the shape of the elastic angular distributions, and in the inelastic cross section also have effects that cannot be neglected. As these cross section fluctuations are not likely to be accessible to experiment, an attempt is being made to construct a set of "mock-iron" data using statistically chosen level parameters in the framework of R-matrix theory.

2. Gamma-Ray Spectra from 14 Mev Neutron Interactions (M. Stamatelatos, B. Lawergren, and L.J. Lidofsky)

The coincidence-anticoincidence telescope-pair-spectrometer which was built and previously discussed has been used to measure gamma ray spectra (E_γ >8 Mev) produced by bombarding natural copper and antimony samples with 14 Mev neutrons. Currently, data is being collected from a zirconium sample. The low efficiency of the detector combined with neutron flux limitations due to radiation hazards and pile-up lead to running times of the order of 100 hours or more per element. The data, following unfolding, will be compared to the predictions of various models of gamma ray production.

GULF GENERAL ATOMIC INCORPORATED

SAN DIEGO, CALIFORNIA

A. NEUTRON CROSS SECTIONS

1. Fast Neutron Capture (W. M. Lopez, M. P. Fricke, A. D. Carlson and S. J. Friesenhahn)

The radiative capture cross sections for neutrons of energy 1-1000 keV are being measured for Mo, Rh, Ta and ^{238}U. These data are being obtained with time-of-flight techniques similar to those we used previously for Au, W, Re and Gd and reported in our contribution to NCSAC of October, 1968. In addition, further measurements have been made of the Au(n, γ) reaction with special emphasis on reducing the uncertainties of this important standard cross section. The capture cross sections measured for Rh, Ta and ^{238}U are expected to have total uncertainties of less than 10% and should provide a useful test of the conclusions[1] from a statistical-model analysis of our previous data. (Our present measurements are pertinent to request Nos. 161, 308 and 309 in WASH-1078.)

2. Resonance Parameters and Average Capture Cross Sections of Gadolinium (S. J. Friesenhahn, D. G. Costello, W. M. Lopez, M. P. Fricke and A. D. Carlson)

Resonance parameters of ^{155}Gd and ^{157}Gd have been determined between 2 eV and 200 eV using shape and area analysis of transmission, capture, and self-indication data taken at the 20-meter neutron flight path facility. Average capture cross sections of these two isotopes were also measured at this facility from 1 to 40 keV.

The calculated infinite dilution resonance integrals obtained from these data are 1341 ± 40 barns for ^{155}Gd and 763 ± 15 barns for ^{157}Gd. These values are in fair agreement with recent values reported by Mughabghab, et al.[2] who obtained 1417 barns for ^{155}Gd and 711 barns for ^{157}Gd. When our values are combined with the resonance parameters

---

[1] M. P. Fricke and W. M. Lopez, Physics Letters 29B, 393 (1969).

[2] S. F. Mughabghab and R. E. Chrien, BNL 13074 and private communication.

obtained by Karschavina, et al.[3] for the even-even gadolinium isotopes, a resonance integral of 361 barns is obtained for natural gadolinium.

The following average quantities were obtained from the resonance parameters after correcting for the effects of the finite number of resonances sampled:

Isotope	$\overline{\Gamma}_\gamma$ (meV)	$\overline{\Gamma}^o_n$ (meV)	D (eV)
^{155}Gd	106 ± 3	0.78 ± 0.12	2.0 ± 0.2
^{157}Gd	103 ± 2	2.5 ± 0.7	5.9 ± 0.8

The s-wave strength functions obtained from the resonance parameters are $2.17 \pm^{0.30}_{0.14} \times 10^{-4}$ for ^{155}Gd and $2.28 \pm^{0.92}_{0.53} \times 10^{-4}$ for ^{157}Gd. These values are in good agreement with those deduced from our measurements of the average capture cross sections. (This work is pertinent to request Nos. 207 and 209 in WASH-1078.)

3. Resonance Parameters of Rh (A. D. Carlson, S. J. Friesenhahn, W. M. Lopez and M. P. Fricke)

Work has begun on the determination of the resonance parameters and capture cross section of rhodium in order to define the infinite dilution resonance integral. From initial capture measurements, the values of $g\Gamma_n$ for the low lying s-wave resonances have been deduced. There is generally good agreement between these determinations and those reported in BNL-325. Self-indication measurements were recently completed which should allow determinations of radiation widths and spins for many of the strong levels. High resolution capture measurements are planned for the purpose of obtaining the radiation widths of weak p-wave levels. (This work is pertinent to request No. 161 in WASH-1078.)

4. Gamma Rays from Resonance Neutron Capture in ^{238}U (Joseph John, V. J. Orphan and C. G. Hoot)

The gamma-ray spectra resulting from the capture of neutrons by ^{238}U have been studied with a Ge(Li)-NaI(Tl) three-crystal pair

[3] E. N. Karschavina, et al., "Neutron Resonances of Gadolinium Isotopes," JINR P3 3882.

spectrometer and a 16-meter flight path facility.[4] Neutron energies from 0.015 eV to 100 keV have been covered in this experiment. The neutron energy resolution in this time-of-flight measurement was sufficient to resolve all resonances up to about 500 eV.

Preliminary gamma-ray spectra are shown for two neutron energy ranges in Fig. A-1. There is a distinct difference in the relative intensities of the two pairs of doublets (near 4-MeV gamma-ray energy) measured at thermal neutron energy and over the first resonance at 6.67 eV.

Analysis is in progress of the large amount of two-parameter (gamma-ray pulse height vs. neutron time of flight) data accumulated in this measurement in order to obtain the gamma-ray intensities as a function of incident neutron energy for ^{238}U. This effort includes the development of analytical spectral stripping techniques in order to accurately deduce the contribution from "continuum" gamma rays to the gamma-ray production cross section. A 6.129-MeV gamma-ray source (utilizing the activity from the $^{16}O(n,p)^{16}N^*$ reaction) has been constructed for measurement of the detector response for high energy gamma rays. These measurements will be used to define the detector response functions which are necessary for the unfolding of the gamma-ray spectral data. (This work is pertinent to request Nos. 310 and 311 in WASH-1078.)

5. Cross Sections for (n, xγ) Reactions in Fe and Al (C. G. Hoot, V. J. Orphan and Joseph John)

Gamma-ray production cross sections are under investigation from inelastic threshold energies to 16 MeV for Fe and Al using a 50-meter flight path facility. For this work a 70-cm^3 Ge(Li) DUODE detector is being used in order to obtain a higher peak to Compton ratio. The detection efficiency of this DUODE for 1.33-MeV gamma rays is the same as the 30-cm^3 Ge(Li) detector used in the N and O measurements of last year. Thus, we expect a considerable improvement in peak-to-background ratio with no sacrifice in count rates. This instrumental improvement, together with the development of spectrum stripping techniques, should facilitate the analysis of the Fe data in which a considerable portion of continuum gamma rays are expected. (This work is pertinent to request Nos. 65, 66, 101, 102 and 103 in WASH-1078.)

---

[4] V. J. Orphan, C. G. Hoot, A. D. Carlson, Joseph John and J. R. Beyster, to be published in Nuclear Instruments and Methods.

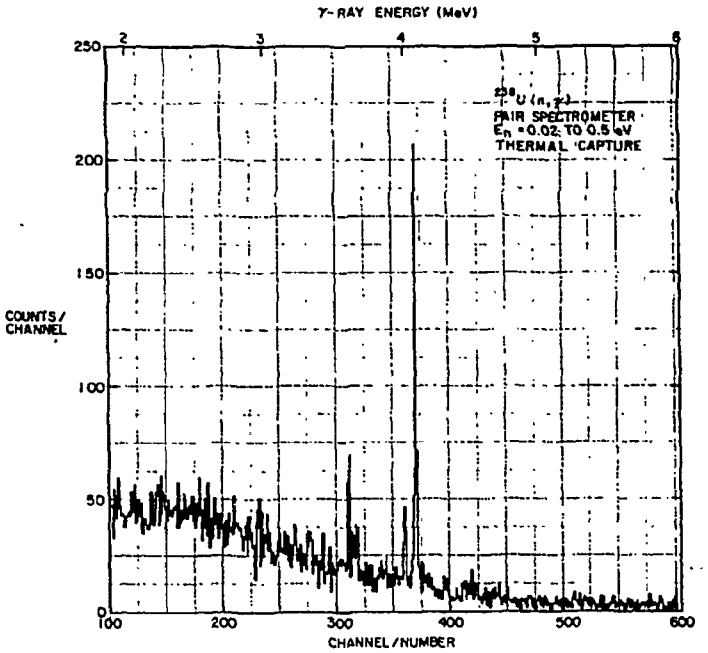

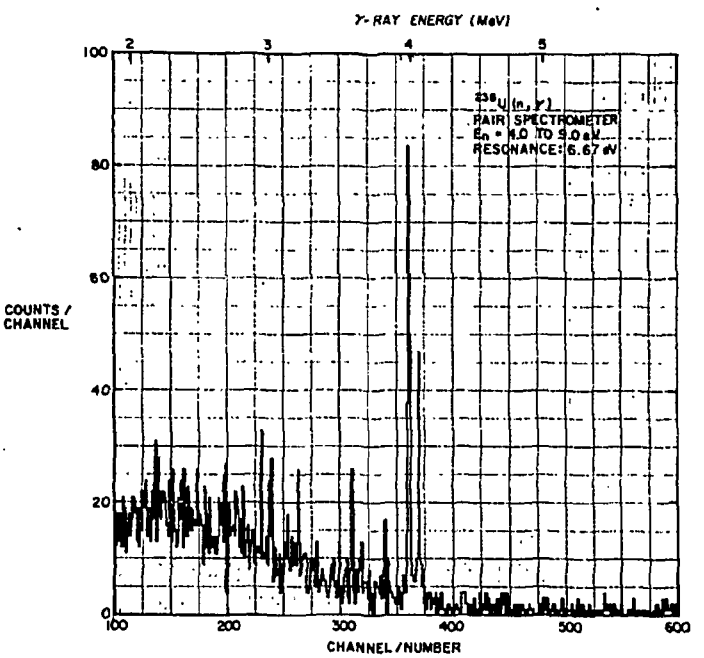

Figure A-1. Gamma-ray spectra resulting from the radiative capture of neutrons in ^{238}U. The upper spectrum was obtained from the capture of thermal (0.02 to 0.5 eV) neutrons and the lower spectrum corresponds to captures in the neutron energy range 4.0 to 9.0 eV. Both spectra were measured with the three-crystal pair spectrometer.

B. FISSION AND PHOTONUCLEAR MEASUREMENTS

1. Measurement of Prompt Gamma Rays from Thermal-Neutron Fission of ^{235}U and ^{239}Pu and from Spontaneous Fission of ^{252}Cf (V. V. Verbinski, H. Weber and R. E. Sund)

The absolute spectral intensity of prompt gamma rays associated with fission events was measured for thermal-neutron fission of ^{235}U and ^{239}Pu and spontaneous fission of ^{252}Cf. Time-of-flight separation of fast neutrons and gamma rays was employed. The gamma-ray spectrometer, a 2.3-in. diameter by 6-in. long NaI scintillator surrounded by an 8-in. diameter by 12-in. long NaI anti-Compton sheath, produced a simple Gaussian peak with a relatively weak tail over the entire energy range of 0.1 to 10 MeV. With this very localized response to monoenergetic gamma rays, the problems of obtaining an accurate gamma-ray spectrum from the pulse-height distribution were greatly reduced.

A surface-barrier detector was placed close to a thin layer of ^{235}U, ^{239}Pu, or ^{252}Cf. The gamma-ray detector was 70 cm away. With an over-all timing accuracy of 3.5 nsec FWHM (full width at half maximum) for both detectors, the counts due to fast neutrons from fission ($\sim$ 20%-25% of the gamma-ray counts) were almost complete rejected.

The gamma spectral yields are shown in Fig. B-1 for ^{235}U, ^{239}Pu, or ^{252}Cf. The respective values of integrated gamma-ray energy are 6.51, 6.82, and 6.84 MeV/fission with an average gamma-ray energy of 0.97, 0.94 and 0.88 MeV/fission for all gamma rays with energy greater than 0.14 MeV.

2. The $^{141}Pr(\gamma, n)$ Cross Section from Threshold to 24 MeV* (R. E. Sund, L. A. Kull, Hans Weber, and V. V. Verbinski)

The $^{141}Pr(\gamma, n)$ cross section was measured from threshold to 24 MeV with a photon beam produced by the in-flight annihilation of positrons. The gamma-ray resolution was determined during the course of the $Pr(\gamma, n)$ measurements by elastically scattering the gamma rays from the 15.1-MeV level in ^{12}C; the result of this measurement was a photon resolution of 1.2% full width at half maximum. The number of (γ, n) events was determined by counting the positron annihilation gamma rays from the ^{140}Pr decay.

*Research supported in part by the U. S. Office of Naval Research.

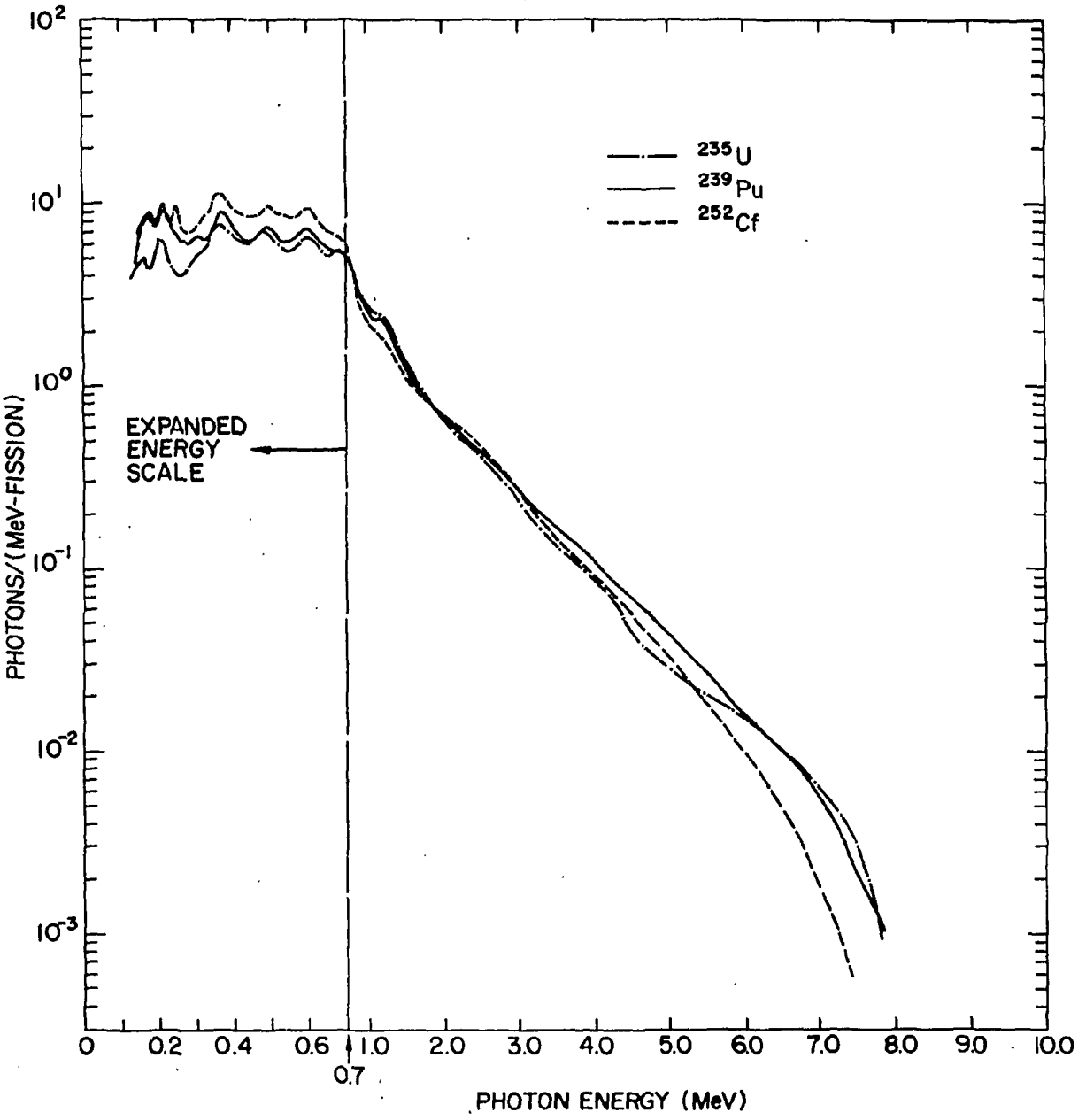

Figure B-1. Prompt gamma-ray yields for ^{235}U (n_{th}, f), ^{239}Pu (n_{th}, f) and ^{252}Cf (s. f).

DATA NOT FOR QUOTATION

The results of the present measurement are shown in Fig. B-2. The error bars shown in the figure include statistical uncertainties in the activation measurements and uncertainties in a small Faraday cup correction. Possible systematic errors amounting to ± 8% are mainly due to uncertainties in the photon flux, the efficiency of the NaI detectors, and the fraction of the ^{140}Pr nuclei which decay by positron emission. The electron subtraction procedure results in another smoothly changing uncertainty, which varies between essentially 0 mb at 16 MeV and ±8 mb at 24 MeV. Also shown in Fig. B-2 are two bremsstrahlung determinations[5, 6] of the ^{141}Pr(γ, n) cross section, each of which has been broadened by our photon resolution. It is clear from the figure that there is a strong disagreement between the present data and these previous bremsstrahlung cross sections. The present results agree well with the shape of the cross section reported by Bramblett, et al.[7] The results are of interest in whether structure exists in the giant El resonance of photonuclear cross sections for this mass region. Theoretical calculations based on the dynamic collection model[5, 8] indicate structure in the ^{141}Pr(γ, n) cross section; however, the widths of the levels are arbitrary in these calculations and the structure in the calculations disappears for wider widths than were used.[8]

C. NEUTRON THERMALIZATION STUDIES

1. Coherent Scattering Law for Polycrystalline Beryllium (G. M. Borgonovi)

A calculation of the scattering law for polycrystalline beryllium has been performed using the coherent one-phonon approximation. The scattering law has been calculated for $\beta < 3.5$ and $\alpha < 0.6$, using a model for the lattice vibrations which fits the measured dispersion relations. The superiority of this calculation over previous coherent calculations is in the limited dependence of the scattering law on the size of the mesh in reciprocal space. Figure C-1 shows the scattering law represented in histogram form for $\beta = 1.25$, the continuous line showing the prediction of the incoherent approximation. The experimental points

---

[5] P. H. Cannington, et al., Nucl. Phys. A109, 385 (1968).

[6] B. C. Cook, et al., Phys. Rev. 143, 730 (1966).

[7] R. L. Bramblett, et al., Phys. Rev. 148, 1198 (1966).

[8] Huber, et al., Phys. Rev. 155, 1073 (1967).

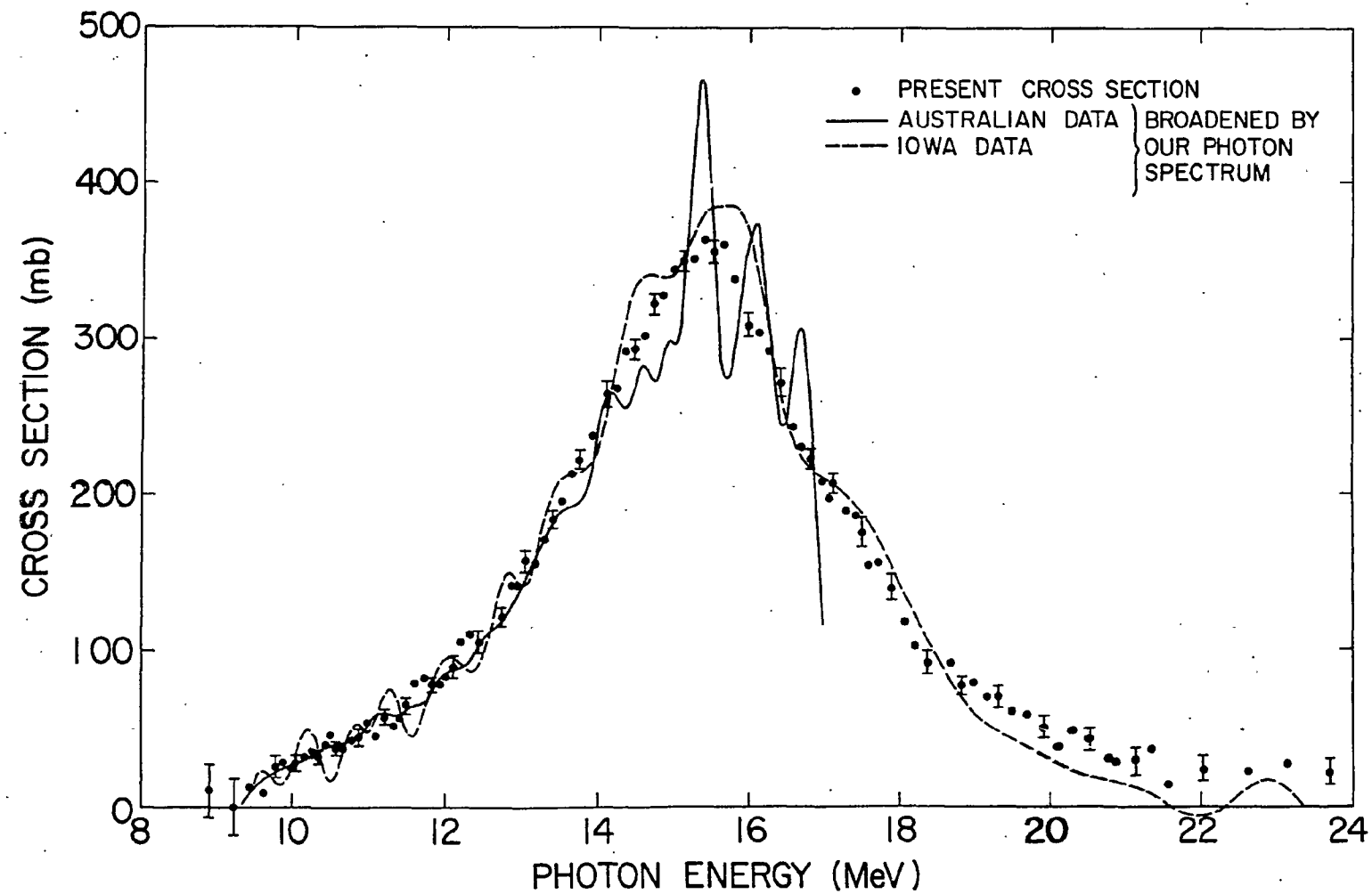

Figure B-2. The present $^{141}Pr(\gamma, n)$ cross section. Also shown are two bremsstrahlung determinations[5, 6] of the cross section, each of which has been broadened by our photon resolution.

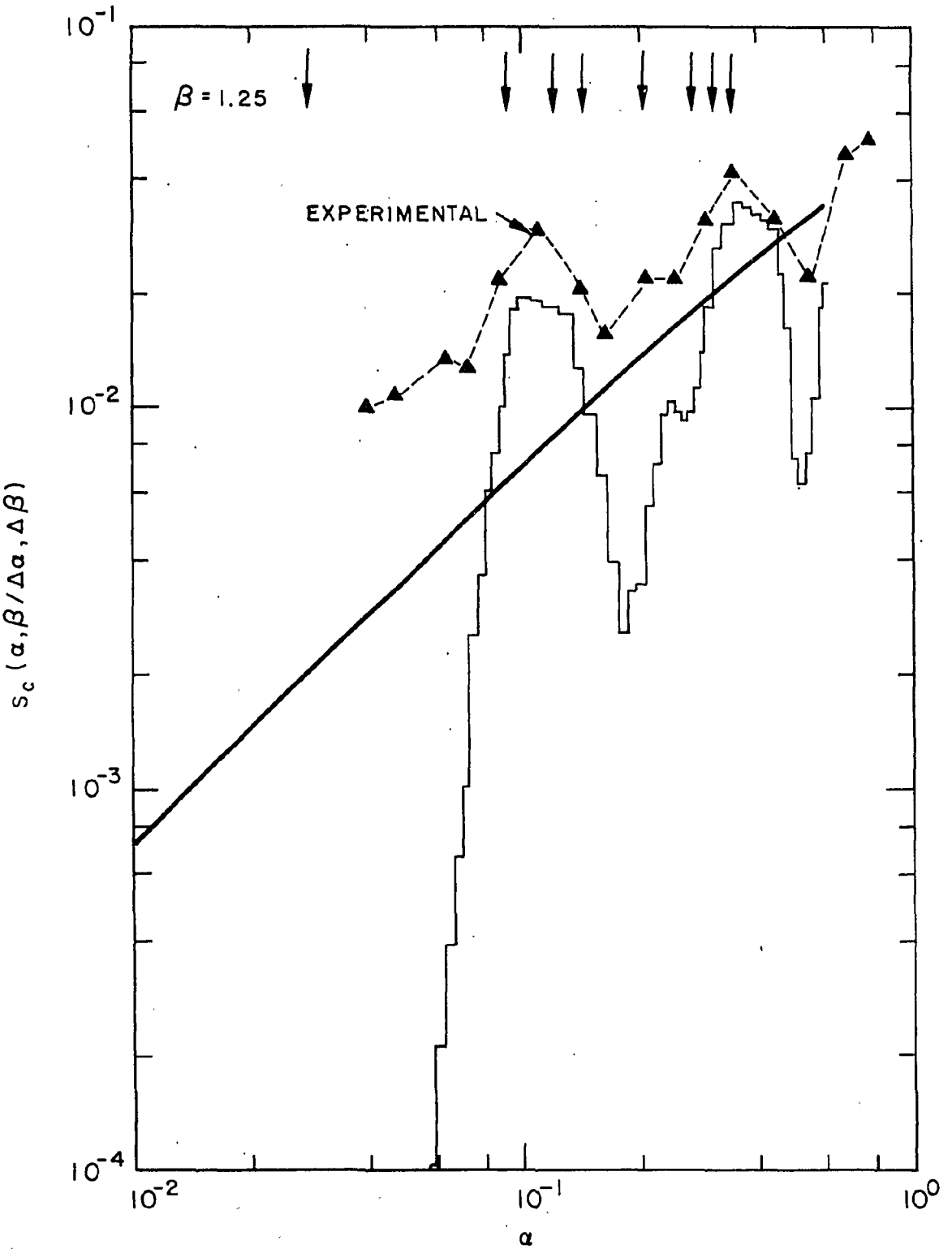

Figure C-1. Coherent scattering law for β = 1.25.

DATA NOT FOR QUOTATION

were measured by Schmunk.[9] A significant improvement over the incoherent approximation has also been obtained in the calculation of the total cross section below the Bragg cutoff. The calculation is reported in GA-9364.

2. Central Force Lattice Dynamical Model for Uranium Carbide (E. L. Slaggie)

The thermal neutron scattering law for uranium carbide has been calculated from weighted frequency distributions obtained from a next-nearest-neighbor central force model. The uranium carbon force constant was adjusted to give a peak in the normal mode frequency distribution at about 0.045 eV in accordance with neutron data.[10] The carbon-carbon force constant was selected to give a reasonable width to this peak. Finally, the uranium-uranium force constant was chosen to make possible a good fit to specific heat data. Details of the work are given in GA-8675.

3. Neutron Scattering from UO_2 (E. L. Slaggie)

A lattice dynamical model for uranium dioxide developed by Dolling, Cowley, and Woods[11] to fit dispersion curve measurements has been used as the basis of a calculation of the thermal neutron scattering law.[12] In addition to short-range core-core forces, the model includes shell-core, shell-shell, and long-range Coulomb interactions. Weighted frequency distributions were calculated from a dynamical matrix based on this model and used as input to the code GASKET[12] for calculation of the scattering law.[13]

---

[9] R. E. Schmunk, Phys. Rev. 136, A1303 (1964).

[10] S. N. Purohit, et al., "Inelastic Neutron Scattering in Metal Hydrides, UC and UO_2, and Applications of the Scattering Law," Proceedings of the IAEA Symposium on Neutron Thermalization, held July 1967 at the University of Michigan.

[11] G. Dolling, R. A. Cowley, and A. D. B. Woods, Can. J. Phys. 43, 1397 (1965).

[12] J. A. Young, "Neutron Scattering from Uranium Dioxide," USAEC Report GA-8760, Gulf General Atomic Incorporated, July 10, 1968.

[13] J. U. Koppel, J. R. Triplett, and Y. D. Naliboff, "GASKET, A Unified Code for Thermal Neutron Scattering," USAEC Report GA-7480, General Dynamics Corporation, General Atomic Division, November 1966.

IDAHO NUCLEAR CORPORATION

Most of the information that is presented in this NCSAC report can be found in greater detail in the FY 1969 Nuclear Technology Branch Annual Report which will be issued October 1. Reference will be made to this annual report describing additional experiments which have not been included in the following presentation.

A. CROSS SECTION MEASUREMENTS

1. Low Energy Total Neutron Cross Section of ^{241}Pu (J. R. Smith and T. E. Young)

The analytical fits[1] to the low energy absorption and fission data for ^{241}Pu gave the clearest picture then available of the behavior of these cross sections. This clarity is nevertheless far from adequate. The analytical fits indicate a very strong variation in eta. For example, they predict a variation in eta more than three times the variation observed in the manganese bath measurements at 0.0253 eV and 0.06 eV. Either the fission or the total cross section could be at fault.

Measurements of the total cross section of ^{241}Pu have been extended down in energy to 5.1×10^{-4} eV. The MTR crystal spectrometer used a mica crystal, in conjunction with a mechanical neutron filter, to achieve this low energy. Measurements were also made on the MTR fast chopper, the latter data extending down to 0.001 eV.

Four metal foils prepared for the manganese bath eta measurement were used in the measurements, and are the first metallic ^{241}Pu samples upon which total cross section measurements have been made. The use of metal foils eliminates the problems of water contamination and small angle scattering that are encountered in the use of oxide samples. On the other hand there is an uncertainty in the 1/N values of the foils due to irregularities in the scissors-trimmed, crack-infested contours of the foils. Weights and thicknesses of the samples were measured before the foils were sealed in their aluminum containers, but an area or density determination is also needed for determination of cross sections from sample transmissions. The samples were x-rayed, and area measurements made upon the images.

Transmission measurements were made using all four samples on the crystal spectrometer and samples 1 and 2 only on the fast chopper. Below 0.01 eV only the thinnest sample (2) was used. On both instruments measurements were made several months apart as a check on the accuracy of the ^{241}Am contaminant correction. The corrected cross sections agreed within statistical errors.

---

[1] R. G. Fluharty, N. H. Marshall and O. D. Simpson, Conf. on Neutron Cross Section Technology, CONF-660303, 2, 985 (1966).

The ^{241}Pu total cross section including data from both spectrometers is shown in Figure A-1. Table A-1 shows the determination of the 0.0253 eV value. For each data run made on each instrument using each sample, the value of $\sigma_{nT}\sqrt{E}$ was averaged over 9 to 16 data points centered on 0.0253 eV. The average of the determinations yields 1389 ± 15 barns.

The shape of the total cross section is very close to that indicated by the analytical fit,[1] so the low energy anomaly in ^{241}Pu persists. Additional measurements of σ_{nT} and eta as a function of energy will be required to eliminate the discrepancy.

Table A-1

Summary of σ_{nT} Values for ^{241}Pu at 0.0253 eV

	Crystal Spectrometer			Fast Chopper	
Sample and Transmission	Crystal Planes	1967	1968	1967	1968
1	Be(10$\bar{1}$1)	1379		1378	
0.21	Be(0002)	1375	1377		
2	Be(10$\bar{1}$1)	1405		1394	1400
0.58	Be(0002)	1409	1413		
3	Be(0002)	1368	1374		
0.015					
4	Be(0002)		1399		
0.35					

Average Value: 1389 ± 15 b.

2. The Total Neutron Cross Section of Thulium-170 in the Resonance Region* (G. E. Stokes, R. P. Schuman and F. B. Simpson)

The total neutron cross section of ^{170}Tm from 1 to 100 eV has been measured on the Materials Testing Reactor (MTR) fast chopper.

The ^{169}Tm metal foil was cut into strips 0.13 cm x 0.0025 cm and these strips were placed around a spool to allow a uniform irradiation of the sample. The spool was slipped in a stainless steel container and the container was sealed for irradiation in the Engineering Test Reactor (ETR). The capsule was irradiated in the ETR at a flux of $\sim 4 \times 10^{14}$ neutrons/cm^{2}sec for 56 days. At the end of the irradiation the foils were removed from the capsule and prepared for a sample to be used on the MTR fast chopper. The irradiation converted approximately 8.2% of the ^{169}Tm to ^{170}Tm.

*These data supply information for the request in WASH-1078, 1967, (^{170}Tm NG, Th-1 keV, priority 1).

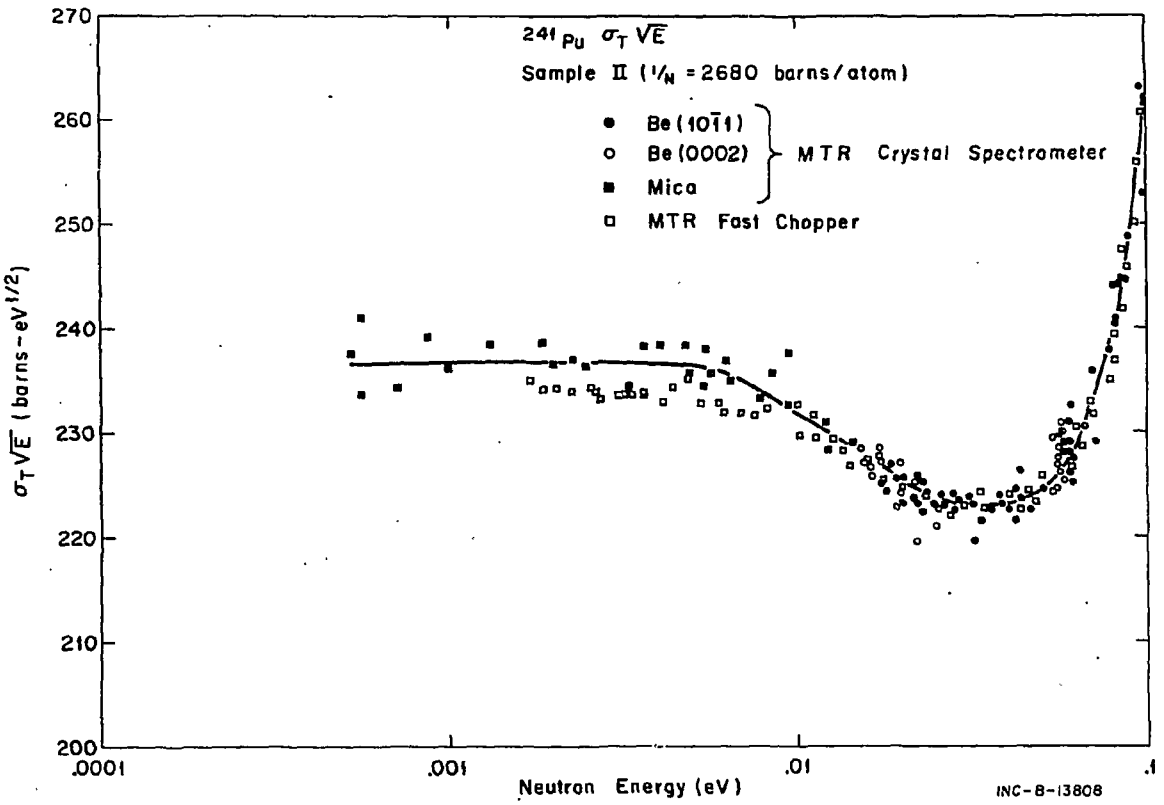

Figure A-1. Total neutron cross section of ^{241}Pu below 0.1 eV, as measured by the crystal spectrometer and fast chopper using the thinnest sample only. The thickness of this sample (Foil 2) was 2680 barns/atom.

The data were analyzed using the Breit-Wigner single level equation in conjunction with shape-fitting and area analysis. Transmission plots of data taken soon after irradiation and data taken after nearly one half-life of decay are shown in Figures A-2 and A-3. The solid line represents a theoretical fit to the data obtained from the Breit-Wigner equation. The fit to the data of the run after 111 days of decay was generated using the parameters derived from the early run. This comparison is shown to illustrate the consistency in the identification and quantities of the various isotopes derived from the analysis of the data. There are a number of places where large ^{169}Tm resonances in the open have removed all the neutrons from the beam. These places are left blank in the data plot.

The parameters derived from the analysis are given in Table A-2. A cross-section curve was generated from the derived parameters and is shown in Figure A-4. This cross section was calculated using the Breit-Wigner single level equation and Doppler broadened for a temperature of 300°K.

Table A-2

^{170}Tm Resonance Parameters

E_o(eV)	Γ_n^o(meV)	Γ_γ(meV)
2.82 ± 0.015	0.13 ± 0.02	104 ± 11
9.44 ± 0.02	0.32 ± 0.03	105 ± 10
12.38 ± 0.02	4.1 ± 0.5	110 ± 12
17.51 ± 0.05	2.6 ± 0.6	210 ± 60
20.38 ± 0.05	0.21 ± 0.03	80 ± 15
21.4 ± 0.1	0.62 ± 0.07	100*
25.5 ± 0.1	0.30 ± 0.04	100*
57.2 ± 0.2	2.0 ± 0.3	100*
70.9 ± 0.3	0.63 ± 0.07	100*
75.2 ± 0.3	1.5 ± 0.2	100*
78.9 ± 0.3	4.5 ± 0.5	100*
85.3 ± 0.4	5.1 ± 0.6	100*
89.6 ± 0.4	1.1 ± 0.2	100*

*Assumed values.

Using an average Γ_n^o obtained from the analyzed resonances and calculating an average level spacing per spin state D from the observed resonances the neutron strength function $\overline{\Gamma}_n^o/D = (1.5 \pm 0.2) \times 10^{-4}$. A resonance absorption integral was calculated using the measured parameters below 100 eV and average parameters for the higher energies. The value for the resonance absorption integral obtained from these data is 460 ± 50 barns.

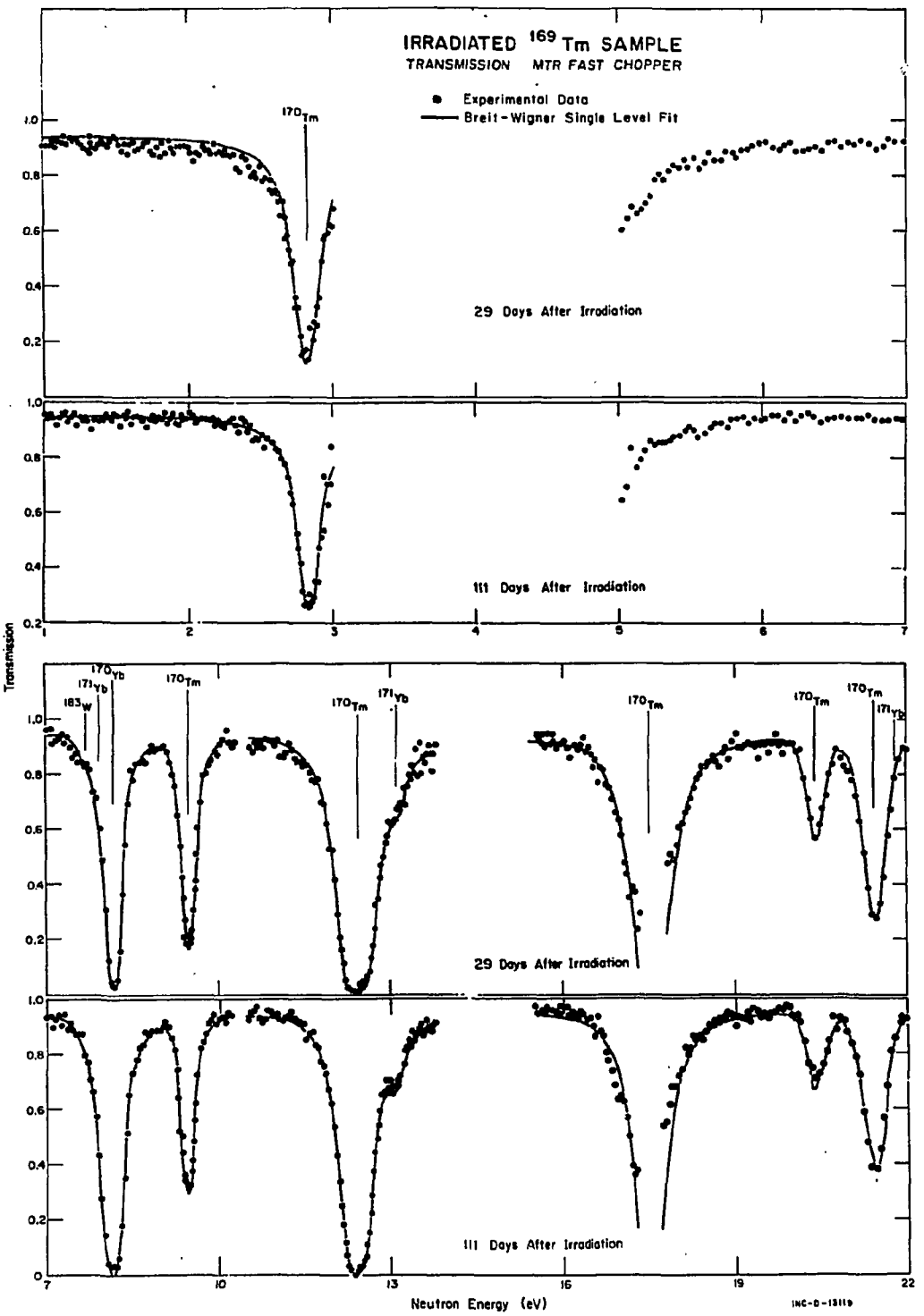

Figure A-2. A transmission versus neutron energy curve from 1 to 22 eV. A comparison is shown between a fit at t = 29 days and t = 111 days.

DATA NOT FOR QUOTATION

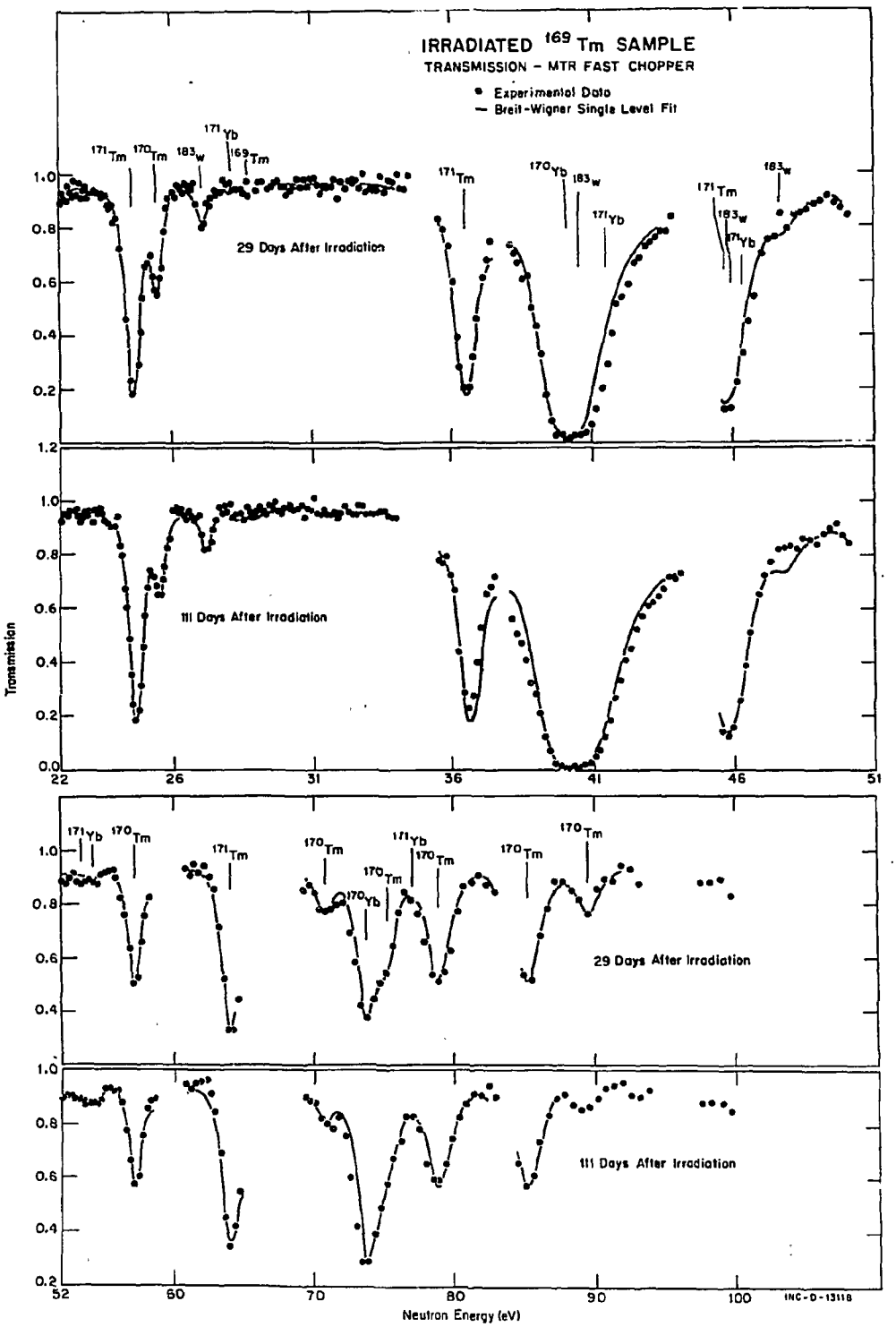

Figure A-3. A transmission versus neutron energy curve from 22 to 105 eV. A comparison is shown between a fit at t = 29 days and t = 111 days.

DATA NOT FOR QUOTATION

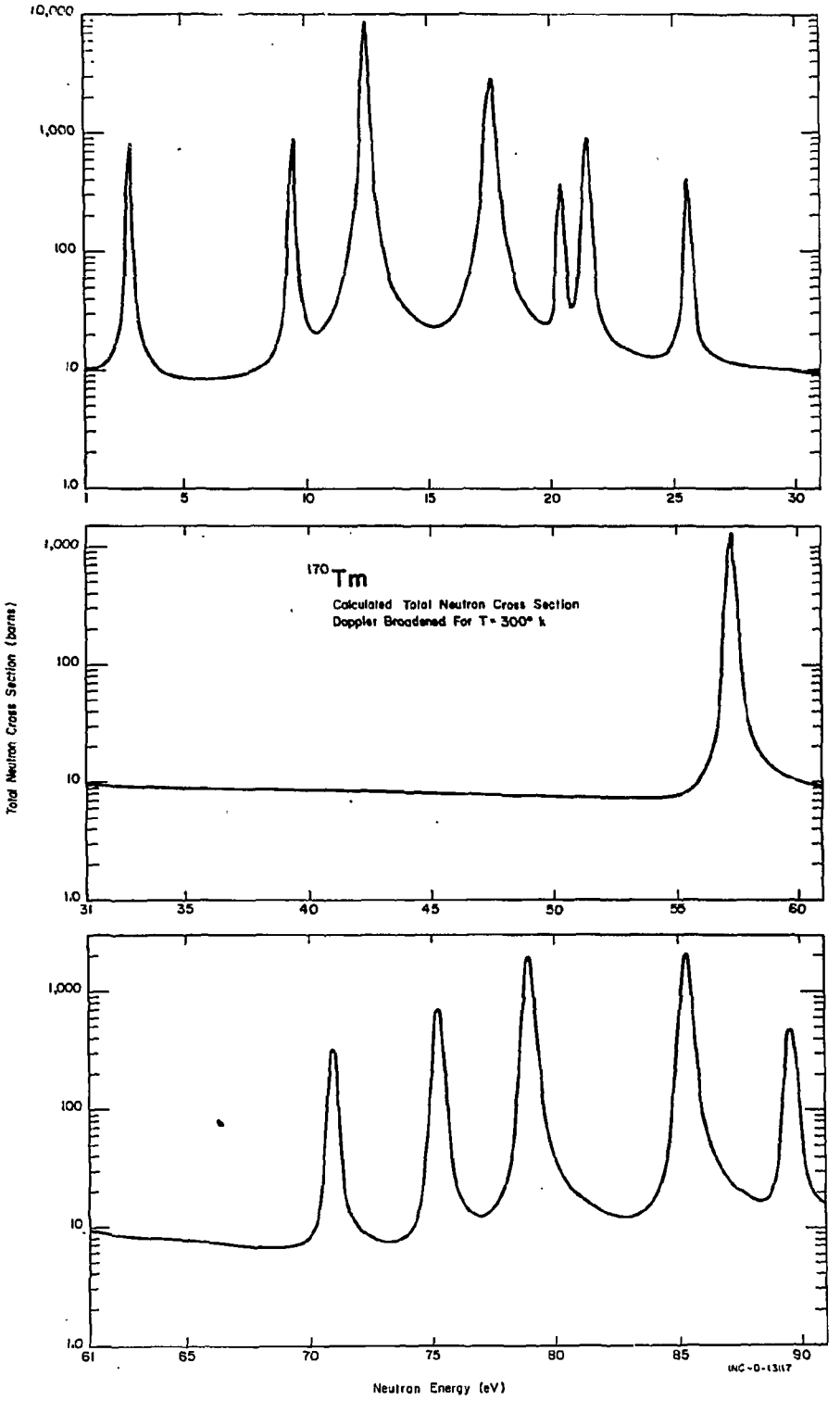

Figure A-4. The total neutron cross section of ^{170}Tm from 1 to 90 eV. This curve was generated from the descriptive parameters of the isotope.

DATA NOT FOR QUOTATION

3. Resonance Energy and Parameter Assignments for ^{147}Pm and ^{147}Sm*
(R. L. Tromp, J. W. Codding and F. B. Simpson)

Neutron resonance parameter determinations for ^{147}Pm (and decay product ^{147}Sm) have been extended to cover the range between 60 eV and 250 eV. Details of sample preparation, MTR fast chopper operation and data analysis of the lower energy range, were described previously.[1]

Inclusion and consideration of ^{147}Sm in the ^{147}Pm resonance analysis (which is of principal interest) was necessary due to the finite amount of this daughter present at even the earliest chopper runs, and thus, also, to the sketchy ^{147}Sm resonance data for this energy region available in the literature.

The resonance parameters were obtained using an area analysis program. In some instances it was impossible to separate the ^{147}Pm resonances from the ^{147}Sm levels. The fact that Sm grew into the Pm sample as a function of time complicated the analyses. However, since the concentration of Sm was known as a function of time it was possible to obtain a consistent set of resonance parameters that would describe the various sets of measured cross sections.

The Γ_n^o values listed in Table A-3, below, have a confidence level ranging between $\pm$ 10% at lowest energies and $\pm$ 50% at the highest. The 65.5 eV ^{147}Pm resonance is believed, from shape-fit analysis, to be a doublet separated by 0.4 eV; this is unresolvable in area analysis, thus the Γ_n^o value obtained is without exact physical meaning.

Table A-3

Resonance Assignments and Parameters, 60 eV to 250 eV;
45 Meter Area Analysis

(Assumed Γ_γ: ^{147}Pm = 80 meV, ^{147}Sm = 65 meV)

E_o(eV)	Isotope	Γ_n^o(meV)	E_o(eV)	Isotope	Γ_n^o(meV)
65.5	^{147}Pm (doublet)	(9)	80.1	^{147}Sm	0.3
76.4	^{147}Sm	2	82.6	^{147}Pm	3.5

*These data supply information for the request in WASH-1078, 1967, (^{147}Pm, NG, 0-1 eV, priority 1); the resonance parameters in the eV region will make theoretical prediction of the capture cross section below 1 eV more accurate.

[1]Codding, Tromp and Simpson, USAEC Report, IN-1218, 31 (1968).

Table A-3 (Continued)

E_o(eV)	Isotope	Γ_n^o(meV)	E_o(eV)	Isotope	Γ_n^o(meV)
83.9	^{147}Sm	6	148.5	^{147}Pm	8
85.5	^{147}Pm	4	152.2	^{147}Sm	8
89.8	^{147}Pm	0.12	154.3	^{147}Pm	4
91.5	^{147}Pm	0.10	161.4	^{147}Sm	4.5
95.4	^{147}Pm	2.7	164.5	^{147}Sm	7
99.8	{ ^{147}Pm	3.0	174.0	^{147}Pm	20
	{ ^{147}Sm	24	179.1	^{147}Pm	0.9
103.1	^{147}Sm	10	185.3	^{147}Sm	15
107.4	^{147}Sm	4	190.3	^{147}Pm	8
115.2	^{147}Pm	5	193.1	^{147}Pm	9
117.7	^{147}Pm	0.24	208.9	^{147}Sm	20
124.6	^{147}Sm	15	211.1	^{147}Pm	4
131.5	^{147}Pm	15	222.1	{ ^{147}Pm	3
140.1	{ ^{147}Pm	0.27		{ ^{147}Sm	4.5
	{ ^{147}Sm	64	224.0	^{147}Sm	7
145.1	^{147}Pm	3	231.7	^{147}Pm	2.5
			241.2	^{147}Pm	12
			249.0	^{147}Sm	10

4. Thermal (Subcadmium) Capture Cross Section and Resonance Integral of ^{244}Pu (R. P. Schuman)

Because of its very long half life, $(8.28 \pm 0.10) \times 10^7$ years, ^{244}Pu is an extremely valuable isotope for chemical studies (essentially no radiolysis or radiation damage) and biological studies (chemical toxicity probably greater than radioactive). Small amounts of enriched ^{244}Pu have been produced by electromagnetic enrichment of highly irradiated transuranium program plutonium, and a production of gram quantities is feasible. The buildup of ^{244}Pu depends strongly upon its cross section; consequently, a determination was made of the thermal (subcadmium) capture cross section and resonance capture integral. Previously, only "pile" cross sections had been measured. The enriched plutonium (Pu-244-239A) was obtained from Oak Ridge National Laboratory and has been mass analyzed by them. It contained: ^{238}Pu < 0.006%, ^{239}Pu 0.018%, ^{240}Pu 0.007%, ^{241}Pu 0.002%, ^{242}Pu 0.904% and ^{244}Pu 99.06%.

The cross sections were measured by irradiation of ~200 μg samples of highly enriched ^{244}Pu. The fluxes of the irradiation positions were determined from the thin Au-Al alloy monitors assuming that the thermal capture cross section of ^{197}Au is 98.8 barns and the resonance capture integral 1558 b. The amount of ^{198}Au was determined by absolute Ge(Li) gamma counting assuming an abundance of 96% for the 412 keV gamma ray.

The thermal (subcadmium) activation cross section of ^{244}Pu was measured as 1.6 ± 0.3 barns and the resonance integral as 35 ± 7

barns. The uncertainty in the gamma abundances is the largest contributor to the errors. The counting and experimental errors are about ±10%. The values can be compared with "pile" cross sections of 2.1 ± 0.3 barns[1] and 1.4 ± 0.5 barns[2] previously measured.

5. Thermal Cross Sections and Resonance Integrals of ^{93}Nb and ^{94}Nb* (R. P. Schuman)

The resonance integral and thermal capture cross section of niobium, 100% ^{93}Nb, were measured by irradiating ∿1 mg samples of niobium metal, both inside a 2 mm thick Cd shield and unshielded, in the core of the MTR. The 20,300 year ^{94}Nb formed was determined by absolute gamma counting of the 871.1 keV (100% abundant) gamma ray of ^{94}Nb on a standardized NaI(Tl) scintillation spectrometer using the counting efficiencies given by Heath.[3] The resonance and thermal fluxes were determined by 0.5% Co-Al activation monitors assuming σ_{th} of ^{59}Co = 38 b and R.I. of ^{59}Co = 74.6 b.[4] The cross sections obtained for ^{93}Nb are: thermal (subcadmium) cross section, 1.0 ± 0.1 b and resonance integral (including 1/v contribution), 8.5 ± 0.5 b.

Since the long term irradiation of Nb also produced ^{95}Nb by second order capture, samples of niobium metal that had been irradiated to an nvt of 1.2 x 10^{22} n/cm^2 in the MTR and which had stood long enough for all the 35.3 d ^{95}Nb to decay were re-irradiated, along with dilute Au-Al flux monitors, for one hour, both unshielded and in a 1 mm thick cadmium shield, in a pneumatic rabbit in the MTR. The irradiated samples were counted, after ^{95m}Nb had decayed, with a standardized Ge(Li) gamma spectrometer and the cross section determined assuming the 765 keV gamma ray is 100% abundant. The thermal (subcadmium) cross section of ^{94}Nb is 13.6 ± 1.5 b and the resonance integral, 125 ± 8 b, assuming gold = 98.8 b thermal and 1558 b resonance integral.[5] Our values can be compared with ^{93}Nb, σ_{th} = 1.1 ± 0.1 b, R.I. = 9.2 ± 0.5 b and ^{94}Nb, σ_{th} = 16.8 ± 1.5 b, R.I. = 122 ± 10 b.[6]

---

*These data supply the resonance integrals requested in WASH-1078, (Nb-94, priority 11).

[1]Butler, Eastwood, Collins, Jones, Rourke and Schuman, "Half-Lives and Neutron Capture Cross Sections of the Heavy Plutonium Isotopes", Phys. Rev. 103, 634 (1956).

[2]Fields, Studier, Friedman, Diamond, Sjoblom and Sellers, J. Inorg. Nucl. Chem., 1, 262 (1955).

[3]R. L. Heath, "Scintillation Spectrometry Gamma-Ray Spectrum Catalogue", IDO-16408 (1957) and IDO-16880 (1964).

[4]R. P. Schuman and J. R. Berreth, "Resonance Integral Measurements", IN-1296 (1969).

[5]R. L. Macklin and H. S. Pomerance, "Resonance Capture Integrals", Progress in Nuclear Energy Ser. 1, 187 (1956).

[6]R. E. Druschel and J. Halperin, "Chem. Division Progress Report", ORNL-4306 (1968).

6. Resonance Integrals from the Cadmium Shielded Irradiation of ^{241}Am (R. P. Schuman)

In order to investigate the possibility of producing a higher enrichment ^{242m}Am cross-section sample, two samples of pure ^{241}Am were irradiated in high flux ETR core positions to different integrated fluxes in 3 mm and 7 mm thick cadmium shields, respectively.

The resonance flux of the irradiations was determined assuming a ^{59}Co resonance integral of 74.6 barns.[1] The resonance integrals of ^{241}Am, ^{242m}Am and ^{242}Cm were obtained by assuming values of resonance integrals and calculating isotopic ratios using Bateman equations, and then taking the values that give the best fit. The calculations were made on a PDP-8 computer using the ESI language. The resonance integrals given in Table A-4 are the values measured and are not corrected for variable Cd shield thickness. The second resonance (at 0.576 eV)[2] in ^{241}Am occurs at the cadmium cut off energy and, as expected, the measured ^{241}Am resonance integral was less (810 barns to 16 hr ^{242}Am) for the thicker shield (initially 7 mm) than (875 barns to 16 hr ^{242}Am) for the thinner shield (initially 3 mm). The ^{241}Am resonance integral was calculated assuming that the total resonance integral of 16 hr ^{242}Am is <20,000 b. The ^{242}Cm resonance capture integral was calculated assuming the total resonance integral of ^{243}Cm is <3000 b.

The purified curium fraction from the irradiated Am was counted with a standardized lithium-drifted germanium gamma spectrometer, and the photon abundances of the ^{242}Cm and ^{243}Cm gamma rays determined by comparing gamma intensities with alpha counting rates. The results of the gamma intensity measurements are given in Table A-5.

Table A-4

Resonance Integrals of ^{241}Am, ^{242m}Am and ^{242}Cm

Target Nucleus	Product Nucleus	Resonance Integrals (barns)
458 yr ^{241}Am	16 hr ^{242}Am	850 ± 60 b
458 yr ^{241}Am	152 yr ^{242m}Am	250 ± 40 b
152 yr ^{242m}Am	total destruction	7000 ± 2000 b
162.5 d ^{242}Cm	32 yr ^{243}Cm	150 ± 40 b

[1] R. P. Schuman and J. R. Berreth, "Resonance Integral Measurements", IN-1296 (1969).

[2] Stehn, Goldberg, Wiener-Chasman, Mughabghab, Mugurno and May, "Neutron Cross Sections, Vol. III, Z = 88 to 98", BNL-325, 2nd Ed. Suppl. #2 (Feb. 1965).

Table A-5

Photon Intensities of ^{242}Cm and ^{243}Cm Gamma Rays

Nuclide	Gamma-Ray Energy (keV)	Photon Intensity (%)
162.5 d ^{242}Cm	44.1	0.027
	102.0	0.0023
	157.7	0.00155
32 yr ^{243}Cm	209.9	3.5
	228.4	11.8
	277.8	16.6

7. Resonance Integrals from the Cadmium Shielded Irradiation of ^{244}Cm (R. P. Schuman)

In order to investigate the possibility of producing curium with much higher percentages of ^{245}Cm by resonance flux irradiation, a ∿1 μg sample of ^{244}Cm was included with the Am sample during the second high integrated flux irradiation in an ETR core position. The irradiation resulted in an even greater buildup of ^{245}Cm than expected. The resonance flux was determined using a 0.5% Co-Al flux monitor and assuming a resonance integral of 74.6 barns for ^{59}Co.[1] The resonance integrals of a number of curium isotopes were estimated by assuming resonance integral values and calculating abundances using Bateman equations. The calculations were made using a PDP-8 computer and the ESI language. Since only one sample was irradiated, and abundances depend upon a number of cross sections, only approximate values of resonance integrals could be obtained. The values that give the best fit and seem most likely are listed in Table A-6. Resonance integrals of ^{244}Cm and ^{246}Cm were also estimated from resonance parameters and are also given in Table A-6.

The purified curium fraction was counted with a standardized lithium-drifted germanium gamma spectrometer and photon abundances and energies of the major ^{244}Cm and ^{245}Cm gamma rays determined (see Table A-7). Alpha spectrum measurements on the purified curium showed the major alpha group of ^{245}Cm, but the uncertainty in the abundance measurement was quite large.

---

[1] R. P. Schuman and J. R. Berreth, "Resonance Integral Measurements", IN-1296 (May 1969).

[2] Stehn, Goldberg, Wiener-Chasman, Mughabghab, Mugurno and May, "Neutron Cross Sections, Vol. III, Z = 88 to 98", BNL-325, 2nd Ed., Suppl. #2 (February 1965).

Table A-6

Resonance Integrals of Cm Isotopes
7 mm Cd Shield Initially

Target Nucleus	Product Nucleus	Resonance Integral-Barns*	Notes
^{244}Cm	^{245}Cm	650 ± 50 b	Also calculated 650 b from resonance parameters[1]
^{245}Cm	Total Destruction	680 ± 300 b	Assume R.I. ^{244}Cm = 650 b. MTR fast chopper resonance parameters[2] 800 ± 100
^{246}Cm	^{247}Cm	110 ± 40 b	Assume ^{247}Cm, R.I. < 2500 b. Estimated R.I. = 140 b from resonance parameters.[1] 110 ± 20 fast chopper data.[3]

*Values as measured; no correction made for the effects of resonances near cadmium cut off.

Table A-7

Energies and Photon Intensities of ^{244}Cm and ^{245}Cm Gamma Rays

Nuclide	Gamma-Ray Energy (keV)	Photon Intensity (%)
18.0 yr ^{244}Cm	42.85	0.018%
	152.6	0.0012%
9300 yr ^{245}Cm	133.0	2.6%
	175.1	9.7%

8. Fast Neutron Activation Cross Sections (R. P. Schuman and D. K. Oestreich)

In order to check the feasibility of using a spontaneous fission neutron source for measuring fission spectrum threshold reaction cross sections, samples of aluminum, iron, indium and gold were placed next to a 2 g ^{244}Cm source (2.2×10^7 n/sec). Activation products due to Al(n,α) Al(n,p), Fe(n,p), In(n,n') as well as In(n,γ) and Au(n,γ) were detected. The activation was then repeated using a 50 μg ^{252}Cf

[1]Stehn, Goldberg, Wiener-Chasman, Maghabghab, Mugurno and May, "Neutron Cross Sections, Vol. III, Z = 88 to 98", BNL-325, 2nd Ed., Suppl. #2, (February 1965).

[2]J. R. Berreth, private communication

[3]F. B. Simpson, private communication.

($\sim$1.2 x 10^8 n/sec) fast neutron source. The californium was stored in a moderating environment so the samples were wrapped in 0.5 mm Cd to minimize thermal neutron capture. The following threshold reaction activities were produced in sufficient yield to detect easily by Ge(Li) and NaI(Tl) counting: 14.96 hr ^{24}Na and 9.46 min ^{27}Mg from Al, 3.43 d ^{47}Sc from Ti, 713. d ^{58}Co from Ni, 4.50 hr ^{115m}In from In and 6.18 d ^{196}Au from Au. These preliminary experiments showed that a large, $\sim$1 mg, ^{252}Cf source, emitting 2.4 x 10^9 n/sec, and placed in an environment where scatters tailored the proper flux, could be used to determine typical fast reactor activation cross sections.

In order to obtain some quantitative cross sections, a number of targets were irradiated for one hour in the Argonne AFSR reactor operating at 500 watts. Titanium, nickel, zinc, gold, thorium and aluminum were irradiated and the aluminum used as the fast flux monitor. The irradiated foils were counted with standardized Ge(Li) and NaI(Tl) counters. The cross sections determined, based on absolute gamma counting with standardized lithium-drifted germanium and scintillation counters and on the gamma abundances listed in the Table of Isotopes[1] are given in Table A-8. The errors given are the estimated errors assuming the gamma abundances and ^{27}Al(n,α)^{24}Na cross section are correct. If more than one gamma ray was used, the errors include any relative error in the gamma abundances The thorium fission cross-section determinations showed that the fission yields in the Reactor Handbook[2] are in error for several fission products. The cross sections determined are those for the AFSR glory hole and the n,γ cross sections will vary considerably from those for other fast reactors; the threshold cross section will vary less.

Table A-8

Fast Activation Cross Sections in the AFSR Glory Hole Flux

Target	Product	Gamma Counted	Cross Section (Millibarns)
Aluminum (n,α)	^{24}Na	1369 (100%) 2754 (100%)	0.767 (standard)[3]
Thorium (n,2n)	^{131}Th	84 (7.4%)	$\sim$10
(n,f)	^{140}Ba	537 (27%)	

[1] C. M. Lederer, J. M. Hollander and I. Perlman, "Table of Isotopes", John Wiley and Sons, Inc., New York (1967).

[2] C. R. Tipton, Jr., Editor, "Reactor Handbook", Interscience Publications, Inc., New York (1960).

[3] W. N. McElroy, S. Berg and T. B. Crockett, "Measurement of Neutron Flux Spectra by a Multiple-Foil Activation Interative Method and Comparison with Reactor Physics Calculations and Spectrometer Measurements", Trans. Amer. Nuc. Soc. 10, 577 (November 1967); also CONF-671102.

Table A-8 (Continued)

Target		Product	Gamma Counted	Cross Section (Millibarns)	
Thorium	(n,γ)	^{233}Pa	311 (34%)	262	±15
Gold	(n,2n)	^{196}Au	356 (94%) 333 (25%)	3.14	± 0.2
	(n,γ)	^{198}Au	412 (96%)	250	±15
Zinc	(n,γ)	^{65}Zn	1115 (49%)	40	± 2
	(n,p)	^{64}Cu	511 (38%)	32	± 2
	(n,p)	^{67}Cu	184 (40%)	1.11	± 0.08
	(n,α)	^{65}Ni	1481 (25%)	0.077	± 0.01
	(n,α)	^{71m}Zn	385 (94%) 495 (75%)	4.0	± 0.8
	(n,γ)	^{69m}Zn	439 (95%)	3.6	± 0.3
Nickel	(n,p)	^{58}Co	810 (99%)	114	± 7
	(n,p)	^{61}Co	67 (89%)	1.3	± 0.1
	(n,γ)	^{65}Ni	1481 (25%)	3.3	± 0.2
Titanaium	(n,p)	^{46}Sc	1120 (100%)	10.9	± 0.7
	(n,p)	^{47}Sc	150 (73%)	19.8	± 1.2
	(n,p)	^{48}Sc	1314 (100%)	0.334	± 0.02
	(n,2n)	^{45}Ti	511 (170%)	0.0087	± 0.001
	(n,γ)	^{51}Ti	320 (95%)	2.6	± 0.4

9. Total Neutron Cross Section of ^{94}Nb and ^{95}Nb* (T. E. Young and M. R. Serpa)

Data acquisition for total neutron cross section determinations of ^{94}Nb and ^{95}Nb has been completed. The thickest sample used had an inverse sample thickness of 185 b/atom for ^{94}Nb and 7400 b/atom for ^{95}Nb. Preliminary resonance parameters for ^{94}Nb are given in Table A-9. No resonances were observed in ^{95}Nb below 50 eV.

Table A-9

Preliminary Resonance Parameters for ^{94}Nb

E_o(eV)	Γ_n^o(meV)	Γ_γ(meV)
11.63	1.72	162
22.79	0.20	213

*These data supply information as requested in WASH-1078, 1967, (^{94}Nb and ^{95}Nb, priority 11, the resonance parameters can be used to calculate the capture cross section).

B. FILTERED NEUTRON BEAMS

1. 2 keV Scandium Filtered Beam Facility (O. D. Simpson, L. G. Miller and D. R. Staples)

The 2 keV beam facility[1] has not been changed during the past year. An interface has been designed and built for the PDP-8/S data acquisition machine that will automatically control and change the temperature of a furnace. This interface will make it possible to investigate the variation in cross sections as a function of temperature at 2 keV. The facility has been used extensively and many of the beam characteristics have been investigated. The following experiments have been carried out during the past year using the 2 keV beam and are reported in the annual report.

1. Proton-Recoil Measurements in the MTR 2 keV Neutron Beam, J. W. Rogers and O. D. Simpson.

2. Proton-Recoil Calibration Studies in the MTR Neutron Beams with Hydrogen and Methane Detectors, J. W. Rogers.

3. Biological Research in the 2 keV and 25 keV Beam, R. M. Brugger and L. G. Miller.

4. Eta Measurements of ^{239}Pu and ^{235}U at 2 keV, J. R. Smith and S. D. Reeder.

5. ^{239}Pu Partial Cross Section and Alpha Measurements at 2 keV, O. D. Simpson and L. G. Miller.

6. The Total Neutron Cross Section of ^{235}U and ^{239}Pu at 2 keV as a Function of Sample Thickness, O. D. Simpson and L. G. Miller.

7. Filtered Beams as a Neutron Source for Seed Irradiation Studies, J. R. Berreth.

8. Activation Cross-Section Measurements Using the 2 keV Sc Filtered and 25 keV Fe Filtered Neutron Beams, R. P. Schuman and R. L. Tromp.

9. Levels in ^{182}Ta, R. G. Helmer, R. C. Greenwood and C. W. Reich.

10. Excited $K^{\pi} = 0^{+}$ Bands in ^{172}Yb, R. C. Greenwood, C. W. Reich and R. A. Harlan.

11. Levels in ^{156}Gd from ^{155}Gd (n,γ), R. C. Greenwood, and C. W. Reich.

12. Neutron Capture Gamma-Ray Measurements with a 2 keV Reactor Produced Neutron Beam, R. C. Greenwood, R. A. Harlan, R. G. Helmer and C. W. Reich.

[1] O. D. Simpson and L. G. Miller, "Scandium Beam Experiments", Nuclear Technology Branch Yearly Progress Report for Period Ending June 30, 1968, p. 3.

13. Measurement of Fast Neutron Capture Gamma-Ray Spectra for Fast Reactor Shielding Calculations, R. C. Greenwood, R. A. Harlan and C. W. Reich.

2. 144 keV Silicon Filtered Beam Facility (O. D. Simpson, J. W. Rogers and H. G. Miller)

A third neutron filtering material that has been tested is silicon. The resonance at 200 keV in silicon has a strong interference dip in the cross sectior at 144 keV. This interference dip indicated that silicon would produce a 144 keV beam much in the same manner as scandium and iron produced the 2 and 25 keV beams. For preliminary studies, forty inches of silicon (99.999% purity) were purchased.

A proton-recoil spectrometer using a hydrogen filled proportional counter was used to examine the spectrum between 50 keV and 300 keV. These measurements show the major transmission "window" at 144 $\pm$ 2 keV and a secondary "window" at approximately 55 keV as depicted in Figure B-1. Titanium has a large cross section in the region of 55 keV and was therefore used to remove the peak which was observed at 55 keV with no detectable distortion in the primary beam. The measurements were not extended to lower energies due to the high gamma background but gamma discrimination measurements will be made following beam modifications. Higher energy measurements were not necessary since no flux could be detected above the 144 keV "window". The gamma intensity was measured in the direct beam and was found to be approximately 8 R/hr.

Because of a Bragg cutoff at 0.002 eV in silicon a strong low energy neutron component was present in the beam and was detected by the $^{14}N(n,p)^{14}C$ reaction from the nitrogen in the counter. This was easily removed by a boron-10 filter with no significant spectrum distortion.

A study was made as to the best way of removing the strong gamma component in the beam, and it was concluded that the thickness of silicon needs to be increased. Therefore, an additional 24 inches of silicon has been ordered. It is expected that by increasing the filter thickness by 24 inches that the gamma background will be reduced to the order of a few hundred mR/hr. The optimization of the 144 keV beam will be accomplished by investigating the beam intensity for various thicknesses of silicon, titanium and cadmium or ^{10}B.

C. NEUTRON INTERACTIONS WITH FISSILE NUCLEI

1. The Total Neutron Cross Section of ^{235}U and ^{239}Pu at 2 keV as a Function of Sample Thickness (O. D. Simpson and L. G. Miller)

It is of interest to know how the self-shielding of neutron resonances effects the cross sections of ^{239}Pu and ^{235}U in the low keV unresolved resonance region. The total cross section was calculated

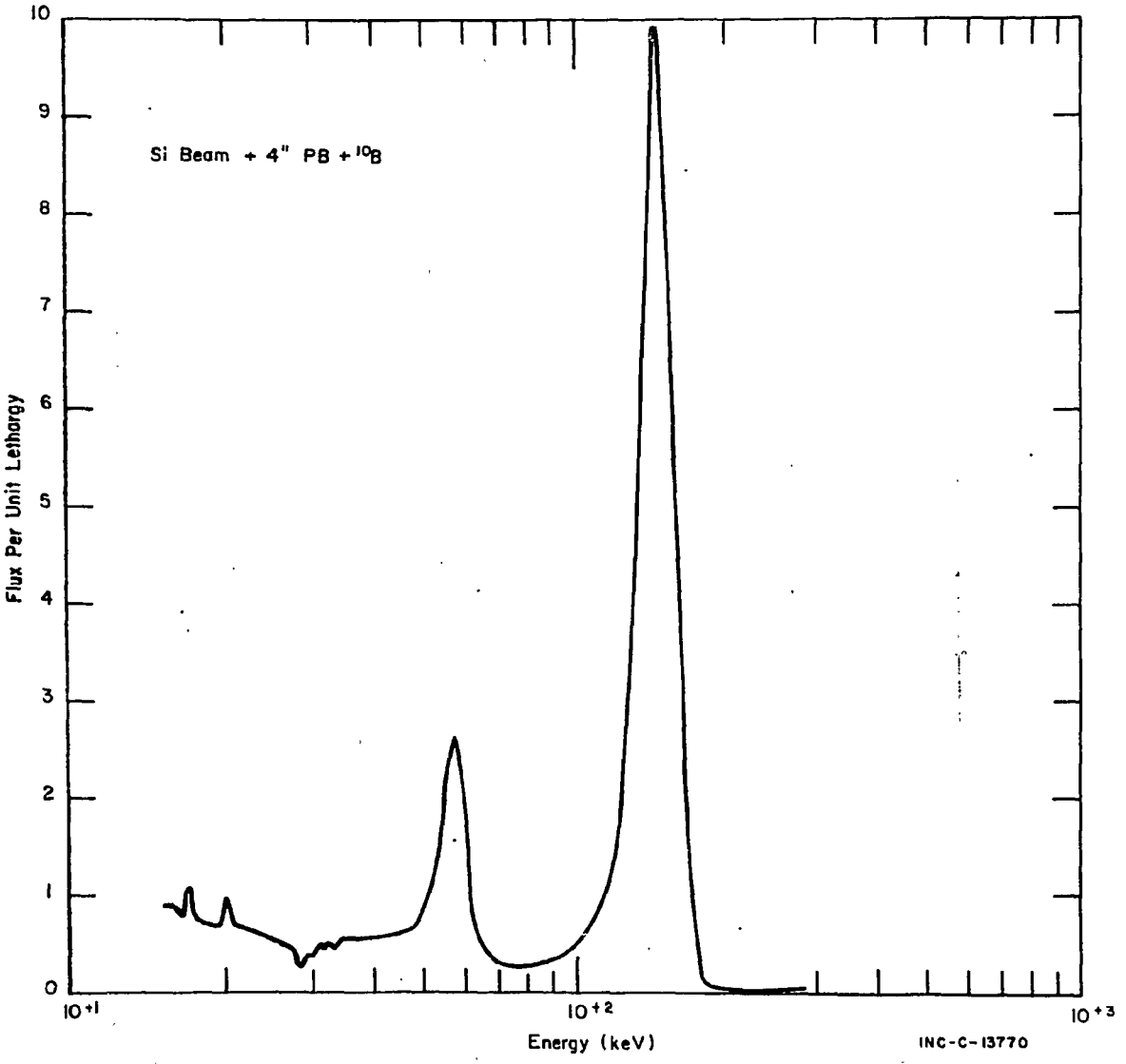

Figure B-1. The spectrum from 50-300 keV through 42" of silicon. The data were obtained with a proton-recoil spectrometer using a hydrogen filled proportional counter.

from transmission data which were determined using the sample-in sample-out technique. The data were taken using the 2 keV filtered beam facility. The total cross sections for ^{235}U and ^{239}Pu are shown in Figure C-1. The error bars are standard deviations due to counting statistics only. For sample thicknesses greater than 0.100 in. the counting statistics are smaller than the experimental data points. It is interesting to note that the variation in cross sections as a function of sample thickness for ^{239}Pu is more pronounced than for ^{235}U. This is expected because the reduced neutron scattering widths on the average are much larger for ^{239}Pu than ^{235}U. It is the reduced neutron scattering width (Γ_n^o) that determines the strength of a resonance which reflects directly into the self-shielding problem.

For reactor calculation it is important to know the cross section for infinitely thin samples. Most total cross section measurements are not made with these type of samples and should therefore be corrected for sample thickness effects. Future plans are scheduled to not only measure partial cross sections as a function of sample thickness but to also see how they vary as a function of sample temperature.

2. ^{239}Pu Partial Cross Sections and Alpha at 2 keV (O. D. Simpson, L. G. Miller, J. R. Smith and S. D. Reeder)

A set of pilot experiments have been performed to study the feasibility of making partial cross section measurements in the 2 keV scandium-filtered beam. From this experiment preliminary values of the partial cross sections and alpha for ^{239}Pu have been derived. Alpha has been determined using two different techniques: (1) from partial cross section measurements $\alpha = \sigma_{n\gamma}/\sigma_{nf}$, and (2) measuring eta directly and calculating alpha by $\alpha = \bar{\nu}/\eta - 1$.

Table C-1 lists the partial cross sections and describes how each value was determined.

The other method of measuring eta directly was done by using three special detectors: (1) a total detector BF_3 counter, which records the number of neutrons that were removed from the beam by the fissile sample. (2) A scattering detector which determines the number of neutrons that were scattered by the sample. This detector was calibrated relative to the scattering cross section of Pb. (3) A fission detector which records the number of fission neutrons. This detector was calibrated using a ^{252}Cf neutron source. The efficiencies of the scattering detector to fission neutrons and the fission detector to scattered neutrons were also determined.

The absolute value of eta could not be determined because the flux of the 2 keV beam was not known accurately enough. Therefore, alpha for ^{239}Pu was determined relative to an assumed alpha value of 0.42 for ^{235}U. Table C-2 lists the measured value of alpha for ^{239}Pu relative to ^{235}U.

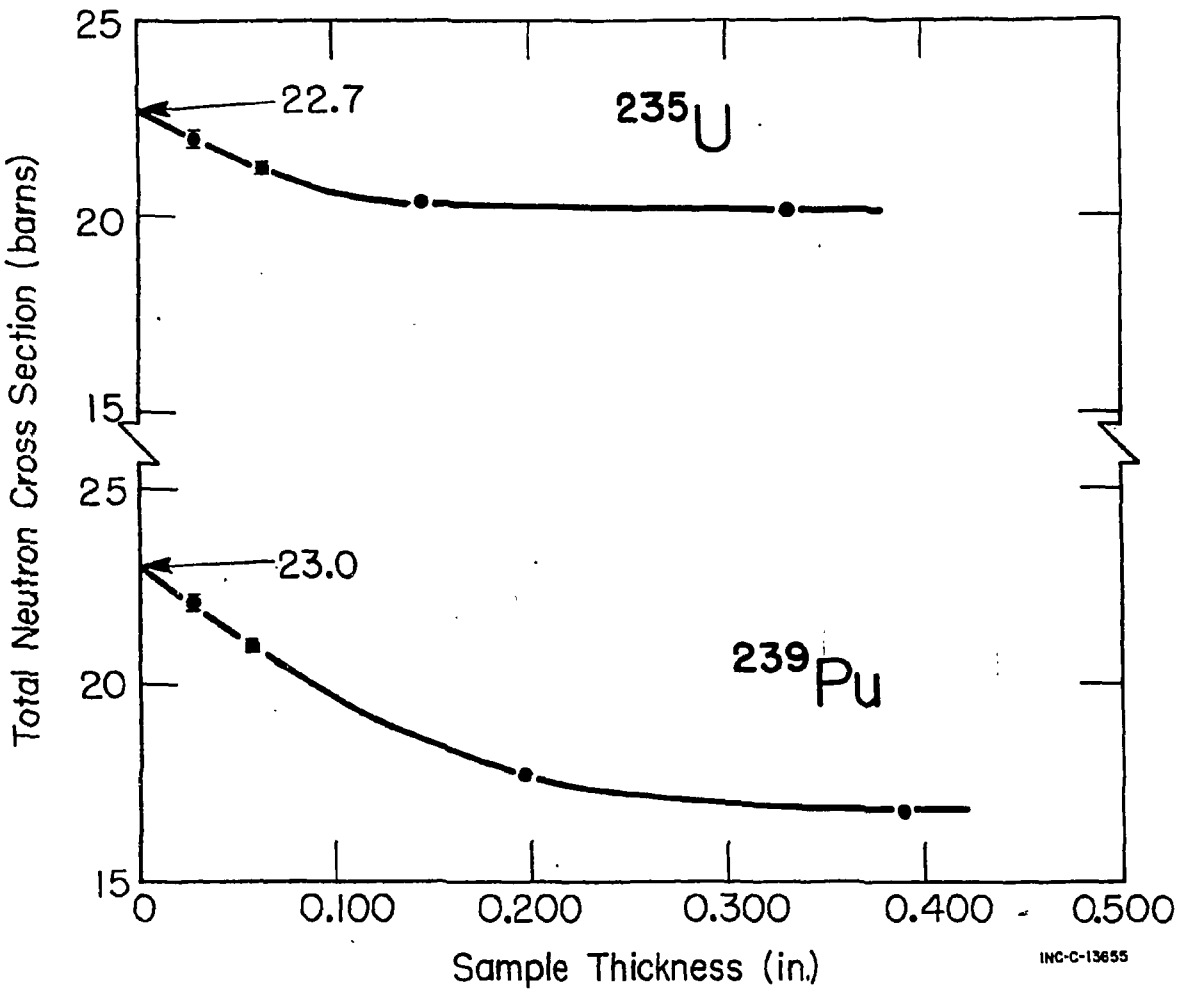

Figure C-1. The total neutron cross-section of ^{235}U and ^{239}Pu as a function of sample thickness at 2 keV.

For means of comparison the values of alpha for ^{239}Pu as quoted in the NCSAC report for the period of October 1968 to March 1969, are shown with those of the present experiment in Figure C-2.

Table C-1

Partial Cross Sections and Alpha for ^{239}Pu at 2 keV

$\sigma_{nT} = 23.0 \pm 0.5$ b	Determined from the ^{239}Pu total cross section measurements as a function of sample thickness, extrapolated to zero thickness.
$\sigma_{nn} = 15.1 \pm 0.8$	Measured relative to the scattering cross section of lead.
$\sigma_{nx} = 7.9 \pm 0.9$	$\sigma_{nx} = \sigma_{nT} - \sigma_{nn}$.
$\sigma_{nf} = 3.5 \pm 0.5$	Measured with a fission chamber in the 2 keV beam relative to a fission cross section of 6.4* barns for ^{235}U. The ^{239}Pu and ^{235}U fission chambers had been previously calibrated at 0.0025 on the MTR crystal spectrometer.
$\sigma_{n\gamma} = 4.4 \pm 1.0$	$\sigma_{n\gamma} = \sigma_{nx} - \sigma_{nf}$.
$\alpha = 1.26 \pm 0.33$	$\alpha = \sigma_{n\gamma}/\sigma_{nf}$.

*This number was obtained from the evaluation of ^{235}U as measured by several laboratories. The values below were obtained by weighting the differential fission cross sections with the 2 keV beam spectrum.

W. K. Brown, Nuclear Explosions (1966)	6.26
ENDF/B (1967)	6.24
Wang-Shi-De (1966)	6.36
Yeater (1966)	6.64
Parker (1966)	6.48
Michaudon (1966)	6.31
Average	6.4

Table C-2

Alpha for ^{239}Pu Relative to an Alpha of 0.42 for ^{235}U at 2 keV

Sample Thickness Inches	Alpha
0.020	1.46
0.040	1.20

Errors have not been determined for the above values but are probably of the order of $\pm$ 25%.

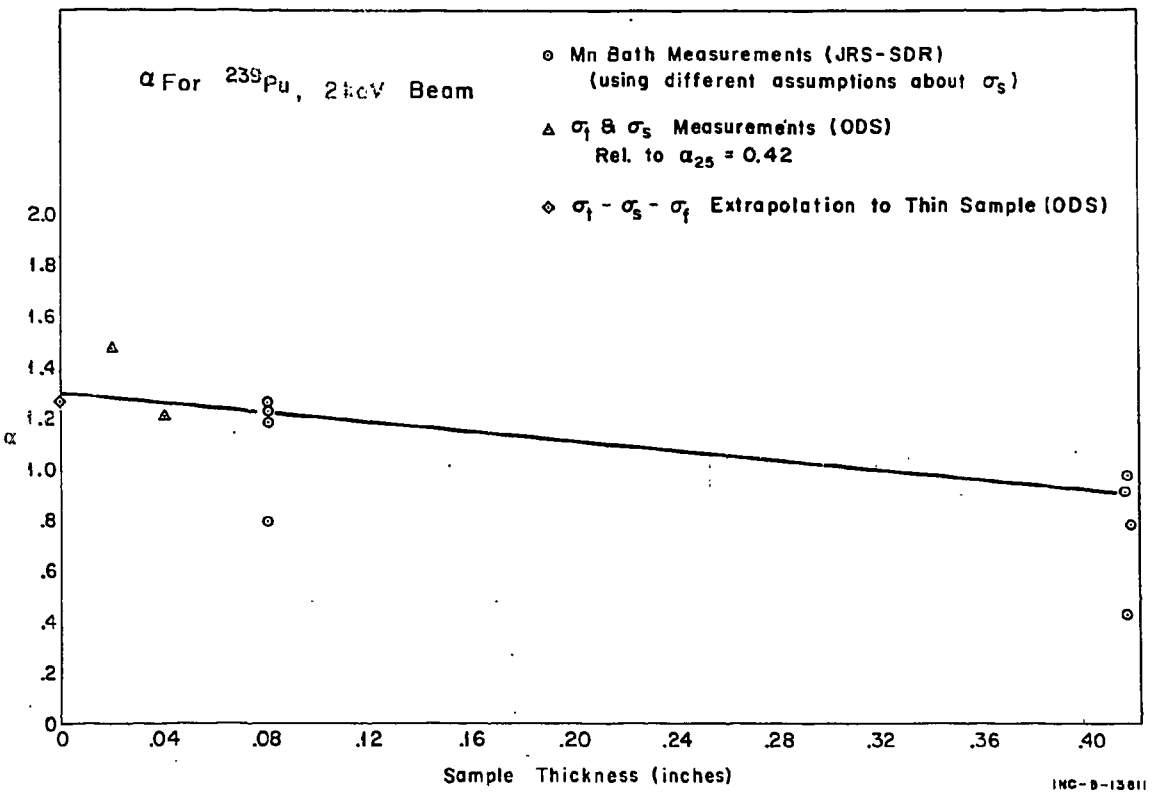

Figure C-2. Alpha for ^{239}Pu as a function of sample thickness at 2 keV.

3. Eta Measurements of ^{233}U at 0.1 eV (J. R. Smith and S. D. Reeder)

The importance of eta for ^{233}U is such that concern was expressed over even the small discrepancies between the old MTR crystal spectrometer data and the newer data of Weston et al.[1] Figure C-3, showing a comparison of the data, is from the Weston report. It was felt that the best way to shed further light on the problem would be to make a series of manganese bath measurements of eta in the region of interest. The corrections to this type of experiment vary much more slowly with energy than do those for the direct neutron counting experiment. For example, the counting efficiency is constant for the Mn bath, both the low energy and fission neutrons are absorbed in thick absorbers and counted with essentially the same efficiency, and the effects of second order in the Bragg beam are less troublesome.

Two problems faced the use of the Mn bath for these higher energy measurements. The beam strength falls off as the energy increases and the background would become unbearable if the tank were to get into the path of the main beam. To minimize these problems we decided to make relative measurements with the small (21" dia.) Mn bath tank, normalizing these to the previous results using the large tank.

There was time for measurement of only one energy point in addition to a 0.06 eV normalization point, before the long reactor shutdown prior to the Phoenix experiment. Accordingly, data were taken at 0.06 and 0.095 eV, each set consisting of three runs each of sample and open beam data, and two background determinations. The mechanical neutron filter was not used, partly because its mount for use on the short arm was not ready, but mainly because second order measurements and calculations indicated that the second order fraction in both these points was low enough to have negligible effect on

The results of the measurement showed that eta at 0.095 eV is about half a per cent lower than it is at 0.060 eV. This includes a correction for the difference in sample transmission between the two points. The error on this relative measurement is about 0.4%, evaluated at a 75% confidence level.

D. NEUTRON TRANSMISSION MEASUREMENTS FOR SHIELDING (J. W. Rogers, R. M. Brugger and O. D. Simpson)

It is well known that an accurate description of the deep penetration of neutrons is vital to design and optimization of reactor shielding. These neutron effects are evident in radiation damage, energy deposition and biological exposure. Such descriptions depend on an accurate knowledge of the cross sections, particularly for those cross sections (called windows) that are minimal. The measurements of these minimal

[1]Weston, et al., "Neutron Fission and Capture Cross Section Measurements for ^{233}U in the Energy Region 0.02 to 1 eV", ORNL-TM-2353, Feb. 1, 1969.

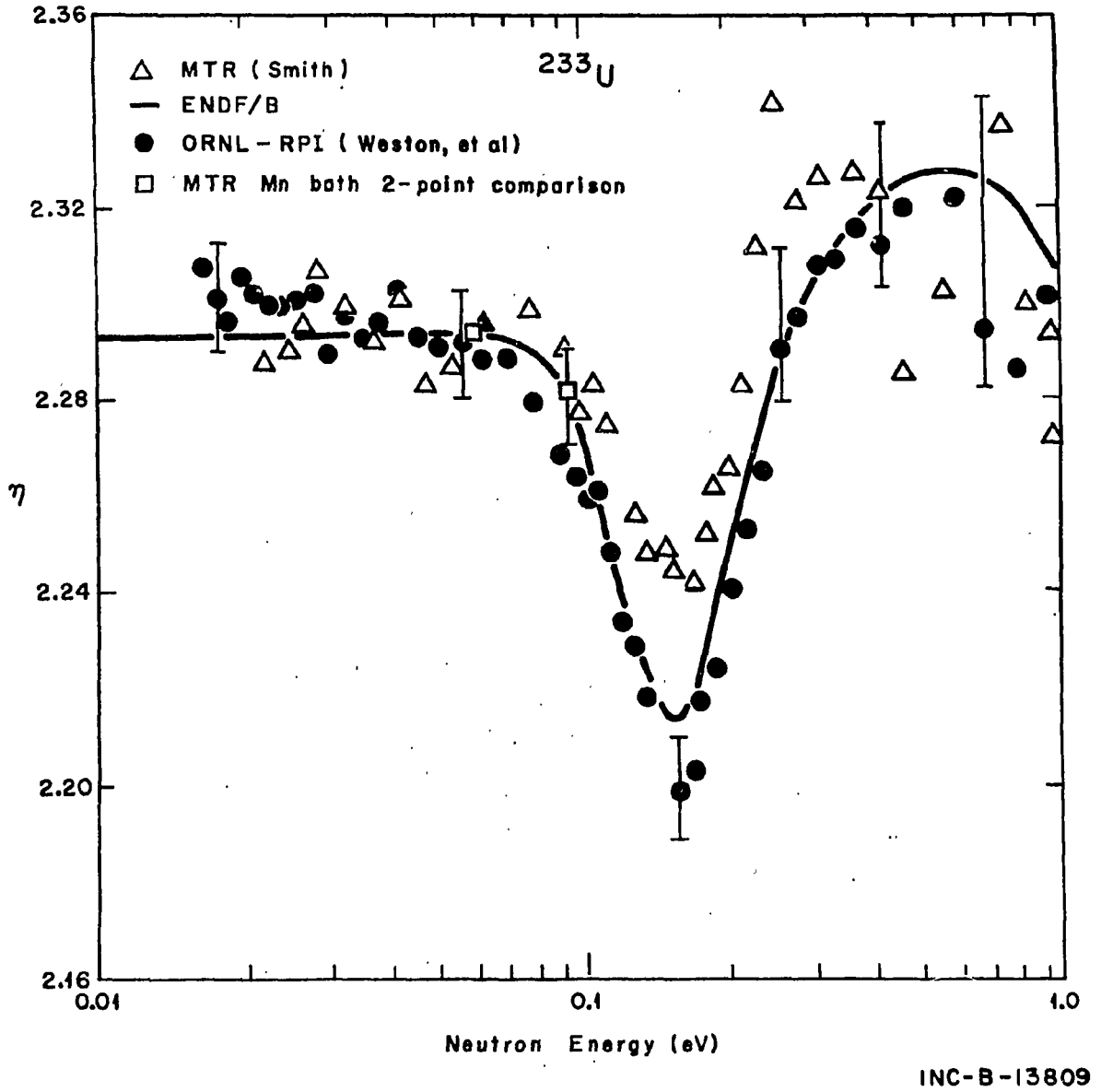

Figure C-3. Eta for ^{233}U as a function of neutron energy. The figure is from Weston, showing the comparison of the MTR and ORNL data. The square points represent the recent measurements of eta at 0.06 eV and 0.095 eV.

cross sections are the most difficult to make by the conventional transmission methods.

While developing the iron filtered beam[1] it was realized that the measurements of the spectra passed by the filters are closely related to cross section measurements of these windows. In fact, the proton recoil measurements of the spectra passed by the windows has the potential for determining the "parameters" of the window much more precise than does a conventional transmission measurement. Exploratory runs were started to develop this capability.

Neutron spectra from thicknesses ranging between 7.98 and 40.62 inches of iron were measured. Two proton recoil detectors of different sensitivities were used because of the increase in intensity as the filter thickness was reduced. A spherical methane filled (200 cm Hg) detector was used for Fe thicknesses ranging from 40.62" to 18.62" and a small cylindrical hydrogen filled (380 cm Hg) detector was used for Fe thicknesses ranging from 23.94" to 7.98". The spectra obtained from these measurements are shown in Figures D-1 and D-2.

The measurements were made by placing the detectors in the beam and adjusting the gas amplification of each detector to the energy range between 100 keV and 400 keV. In this energy range the detectors are insensitive to gamma rays; neutron windows at 6 discrete and resolvable energies (136, 167, 218, 271, 307 and 350 keV)[2] were observed.

The relative change of magnitude of the transmission peaks as the thickness of the filter was changed indicates that each window has a different minimum cross section and window width. An area analysis routine similar to that used in the "area analysis" of resonances is being developed to determine these parameters. Once these parameters have been measured, measurements of inelastic scattering[3] in the last few inches of the iron will also be measured.

E. THE BETA-DECAY HALF LIFE OF ^{241}Pu (R. G. Nisle and I. E. Stepan)

Reported values for the beta-decay half life of ^{241}Pu have varied over a disturbingly large range. Early variations in these values were attributed to erroneous values of the half life of ^{241}Am. Later results showed discrepancies that could not be attributed to uncertainties in ^{241}Am half life. To get an accurate value we measured the ^{241}Pu content of a sample by a reactivity method over a period of about two and one-half years.

---

[1] B. W. Howes, R. M. Brugger, J. W. Rogers, R. P. Schuman and O. D. Simpson, "MTR 25 keV Neutron Beam", Trans. Am. Nuc. Soc. (June 1969).

[2] J. Rainwater, private communication (April 1969).

[3] W. E. Preeg and H. Goldstein, "Effects of Cross-Section Minima on Deep Penetration of Neutrons", Trans. Am. Nuc. Soc. (June 1969).

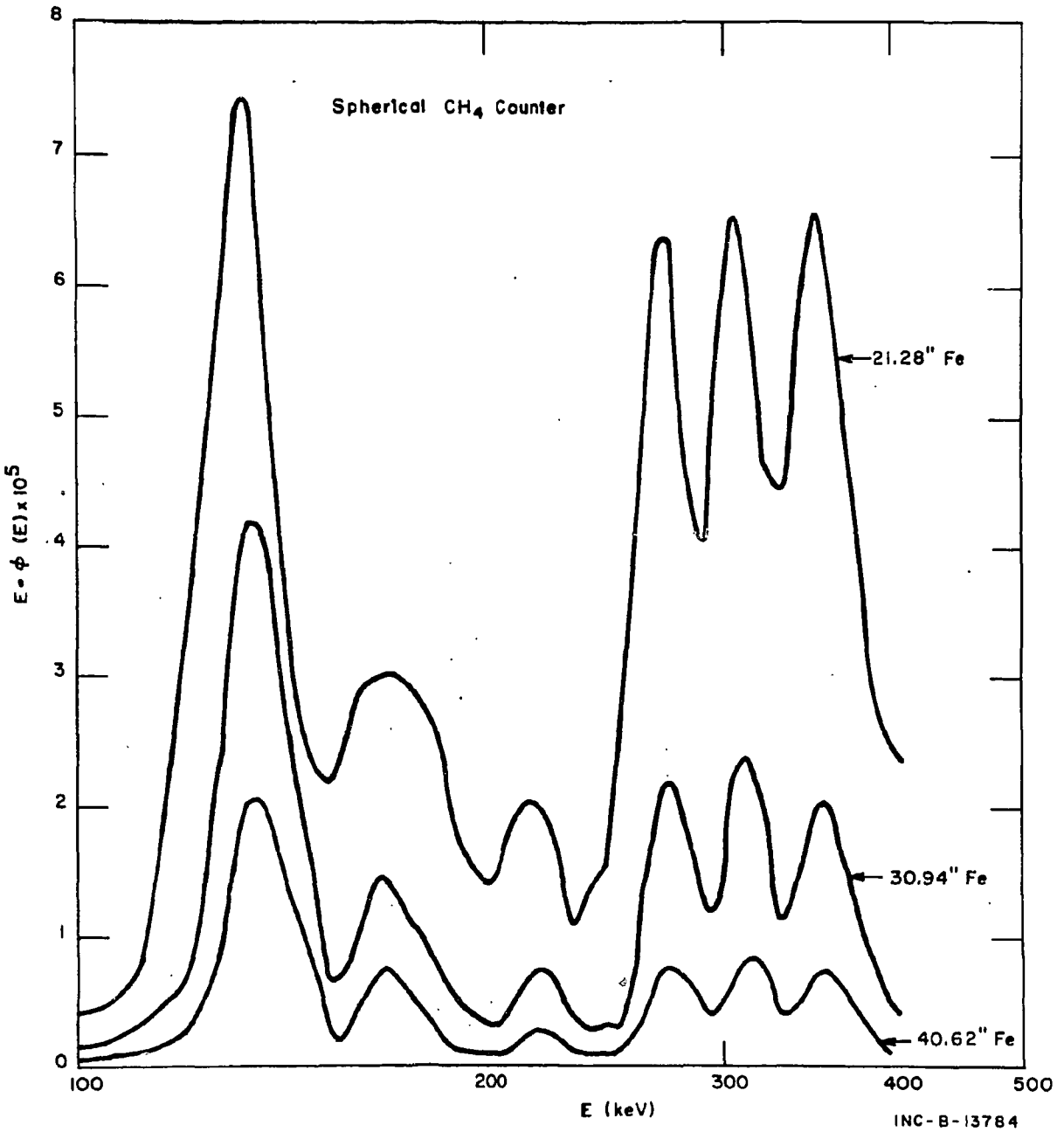

Figure D-1. The neutron spectra through various thicknesses of iron as a function of neutron energy. The data were taken using a proton-recoil spectrometer with a methane spherical (200 cm Hg) detector.

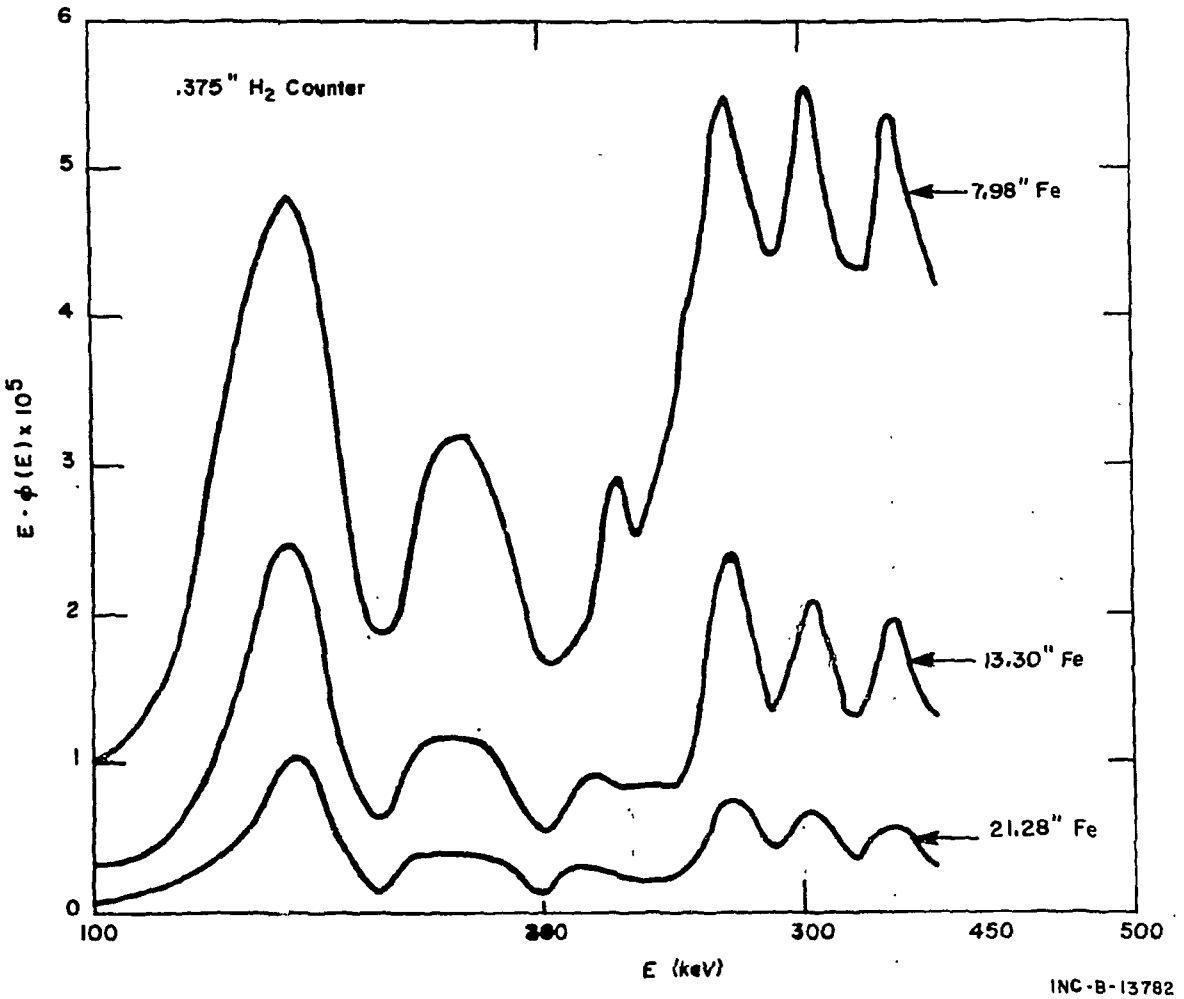

Figure D-2. The neutron spectra through various thicknesses of iron as a function of neutron energy. The data were taken using a proton-recoil spectrometer with a small cylindrical hydrogen filled (380 cm Hg) detector.

Figure E-1 shows the results of these experiments in which the reactivity measurements have been converted to ^{241}Pu content. The dashed line shown in this figure is the expected decay curve obtained by fitting the usual decay equation to the last ten points. The resulting half life is 14.56 ± 0.56 years. The standard deviation of the experimental points was found to be ± 0.16 mg whereas the deviation of the data from the expected decay curve is about + 1.2 mg at early times. Furthermore, the data deviate from the expected curve in a systematic manner. Such behavior is typical of a multicomponent system. Consequently, a two-component equation was fitted to the data; and the resulting fit is shown as a solid line in Figure E-1. The standard deviation of the points from the fitted curve is ± 0.17 mg which agrees well with the uncertainty quoted above for the individual points. The decay curve of Figure E-1 indicates the existence of two components. One, having a half life of 14.63 ± 0.27 years, is recognized as the normal ^{241}Pu. The second, having a half life of 0.34 ± 0.11 years, is postulated to be an isomeric state in ^{241}Pu.

F. EVALUATIONS

1. Automatic Cross Section Analysis Program (ACSAP) (O. D. Simpson and N. H. Marshall)

The Automatic Cross Section Analysis Program (ACSAP) has been improved during the past six months. The code has been used quite extensively in the analysis of fast chopper data. A few of the changes are as follows: (1) convolution techniques have been speeded up by a factor of 10 in the region below 2 eV. (2) the code will now do "wing" fitting. Wing fitting is needed when the peak cross section of a resonance cannot be defined. This happens when the transmission of a sample approaches zero. (3) the code now produces a difference table. This table is valuable in the analysis of the data and is obtained from the difference between the theoretical and experimental data.

ACSAP is now being used as a tool at the MTR to assist in data evaluation for the ENDF/B data file. The SCORE program is still in the process of being combined with ACSAP and will supply the much needed interactive graphics.

2. ^{241}Pu Data Evaluation for ENDF/B (J. R. Smith and O. D. Simpson)

The Automatic Cross Section Analysis Program (ACSAP) is being used to obtain a set of single-level resonance parameters for ^{241}Pu. These parameters will be used in a revised ENDF/B data file for the fissile and fertile materials. The current ENDF/B does not contain resonance parameters for ^{241}Pu.

The basis of the resonance portion of the file will be total cross section measurements made on the MTR fast chopper and fission cross section measurements made on both the RPI linear accelerator and the Petrel nuclear explosion. The first step is to obtain a single set of multilevel parameters to describe both the MTR total

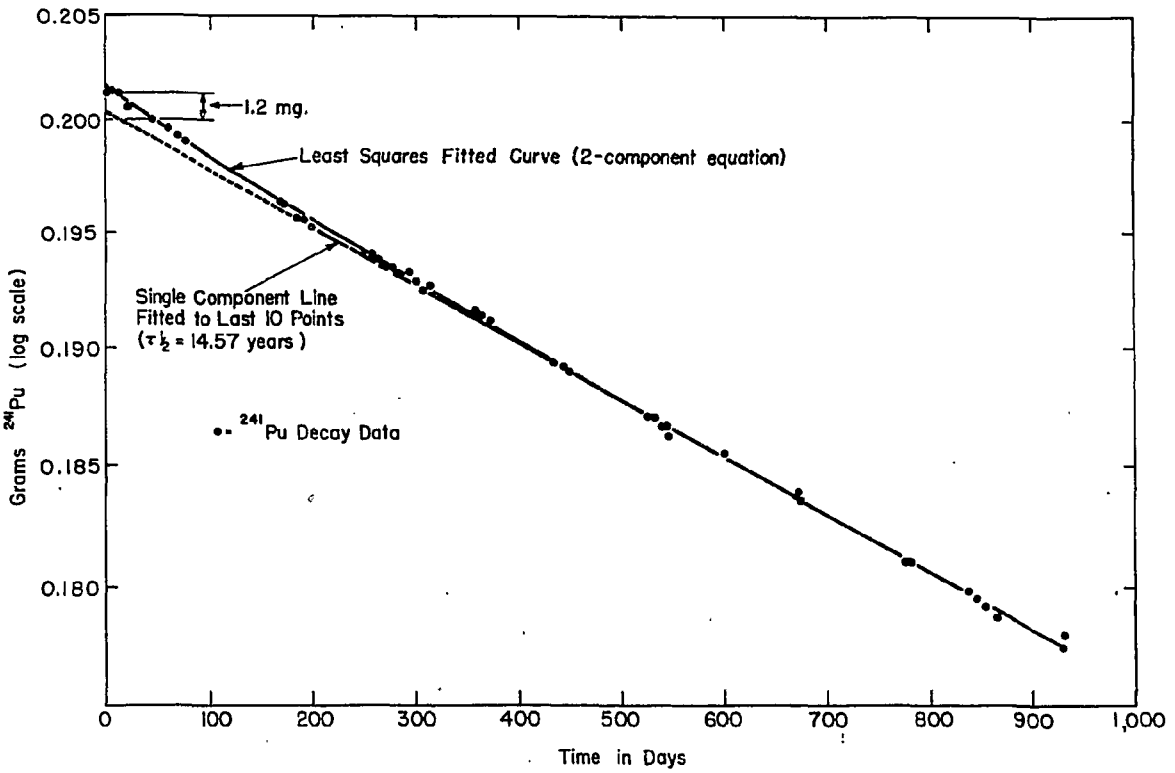

Figure E-1. Decay data on the ^{241}Pu sample. The time of the first reactivity measurements is taken as t = 0, and the ^{241}Pu content is plotted on a logarithmic scale. The standard deviation of the measured values of the ^{241}Pu content of the sample is $\pm$ 0.17 mg. This value is comparable to the size of the data points shown.

cross section and the RPI fission cross section data in the energy region 1-12 eV. A provisional fit to these data is shown in Figure F-1. The resonance parameters used are shown in Table F-1. To obtain this fit, it has been necessary to use values of Γ_γ in the vicinity of 29 meV. Previous fits of total and fission cross sections separately assumed Γ_γ = 40 meV. The lower values for Γ_γ will lead to lower values of alpha in the resonance region.

The second step in the evaluation will be to obtain a single-level fit to the data. The evaluation is in the process of being extended up to 50 eV.

Table F-1

Multilevel Resonance Parameters for ^{241}Pu

E_o (eV)	Γ_n^o (meV)	Γ_γ (meV)	Γ_{f_1} (meV)	Γ_{f_2} (meV)
-0.160*	0.0725	40	0	60
0.264*	0.101	40	0	- 72
4.278	0.270	35	0	42
4.560	0.191	29†	- 190	0
5.910	1.02	29†	-1350	0
6.922	0.235	18	0	-123
8.600	0.285	34	0	80
9.50	0.045	29†	0	-100
10.20	0.453	29†	1000	0

*Resonance parameters assumed from previous analysis.

†Assumed.

NOTE: The fission widths are always positive; the sign is used to define the type of interference. Resonances having fission widths of the same sign interfere destructively between resonances while resonances with opposite signs interfere constructively.

G. DIFFERENTIAL FLUX MEASUREMENTS (D. A. Pearson and C. H. Hogg)

A critical need exists in the fast reactor development program for an accurate simple differential flux monitor. Recent research at the MTR has been encouraging toward meeting this need.

The McElroy foil technique is being tested, but with accurate comparisons against proton recoil counter flux measurements. A stack of selected foils are activated in a fast flux, then the foil activation is counted. A computer program which contains the best available differential activation cross section data is used to predict the measured activations. If the initially selected flux does not

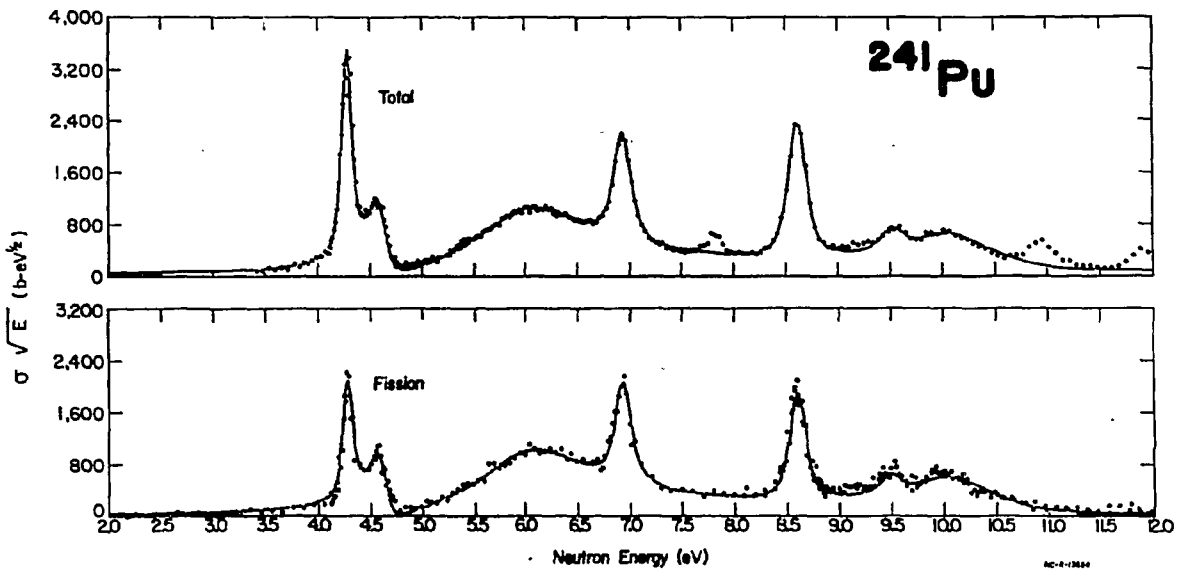

Figure F-1. The total fission cross section of ^{241}Pu from 1-12 eV. The solid curves were calculated using the multilevel parameters listed in Table F-1.

yield the activations within the prescribed error, the flux distribution is adjusted till agreement is achieved. The final flux obtained from foil activation is compared to the flux measured with a proton recoil counter. (The proton recoil counters were calibrated in the MTR filtered beams.) Figure G-1 is an example of the agreement. Note that this flux is peaked in the keV region, the most difficult for the foil technique.

The following possible sources of errors are being considered in this development:

1. accuracy of the differential activation cross sections.
2. self absorption.
3. uniqueness of adjusting flux.
4. reliability of measured structure.
5. resolution and accuracy.
6. graphic flux adjustment.

H. USE OF A CORRELATION CHOPPER FOR MEASURING PARTIAL CROSS SECTIONS

(F. B. Simpson, T. Watanabe, W. R. Myers and P. D. Randolph

Fission cross section measurements have been made on ^{239}Pu with a correlation chopper from 0.02 to 0.2 eV. These data were taken with a 1.6 to 1.0 signal-to-noise ratio in order to determine the feasibility and advantages of using such a device to measure fission events in the presence of a high spontaneous fission rate. This experiment has demonstrated the feasibility and some of the advantages in using this technique for making partial cross section measurements which inherently have a low signal-to-noise ratio.

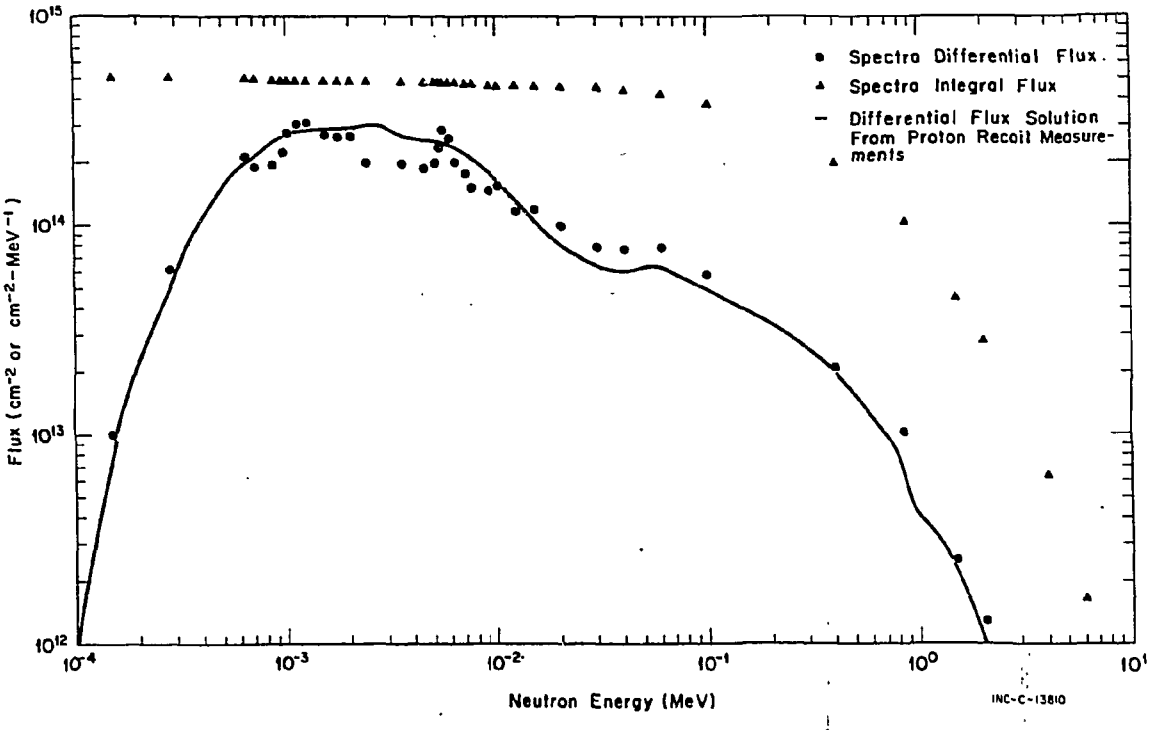

Figure G-1. The neutron flux in the Coupled Fast Reactivity Measurement Facility as measured by the foil technique and by using a proton-recoil spectrometer.

LAWRENCE RADIATION LABORATORY

A. NEW FACILITIES

1. The Livermore Electron Accelerator Facility (S. C. Fultz, C. D. Bowman)

The new electron accelerator being installed at the Lawrence Radiation Laboratory, Livermore, consists initially of five S-band sections with room and provision to expand to seven sections. The first five sections are powered by R. F. modulators constructed by Applied Radiation Company, and the last two will be modified forms of the SLAC design. The accelerator installation has been completed and the accelerator sections are being tested under R. F. power. The first beam is expected October 1.

The accelerator will be operated in a choice of three modes. These are as follows:

a. The Steady State Mode: Pulse lengths ranging from 5 nsec to 3 μsec are available, with a duty cycle of 10^{-3}. The energy for five sections is to be continuously variable from 10 to 80 MeV at a full peak load current of 700 ma.

b. The Transient Mode: For this mode the accelerator will be loaded with currents from 10 to 15 amps. The pulse width will be approximately 5 nsec or less, with a pulse repetition rate as high as 1800 pps. Maximum power with 5 sections is 55 KW.

c. Positron Accelerator: The positrons are to be created at the end of the third section (at approximately 60 MeV) and accelerated in the fourth, fifth, and subsequent sections. Initially positrons of energy ranging from 10 to 80 MeV, will be available. With future expansion the energy will reach 170 MeV. By placing a converter at the end of the first section the positron energy will be extended to 250 MeV, with considerable loss of intensity. The peak current will be approximately 1 ma with an average current of 1μA.

Further characteristics of the five-section accelerator are given in Table A-1.

TABLE A1

	Energy (MeV)	Peak Current (Amp.)	Max. Pulse Width (μSec.)	Max. Pulse Rep. Rate (p.p.s.)	Mode
I	10-80	0.700	0.10	660	Steady State
	" "	"	1.0	420	" "
	" "	"	3.0	300	" "
II	10-140	10.0-15.0	0.005	1800	Transient
III	10-100	0.100	0.10	1800	Peak R. F. Power reduced to half
	" "	"	1.00	840	
	" "	"	3.00	600	
IV	10-80	0.001	3.0	300	Positron mode Full R. F. average power

Beam Transport System: This will consist initially of six beam lines expandable to a maximum of nine. The six beam lines will be realized through the use of 14 bending magnets eight quadrupole pairs and about five singlet lenses. A power slit will be located after the first 22.5° bend, which will make available momentum spread for photonuclear experiments as small as 0.05%. Two large experimental caves are constructed to the north and south of a magnet room. High electron beam currents will not be permitted in these caves in order to avoid activation of the walls and beam transport equipment.

Two of the beam lines are required to pass a momentum spread of ±15%. These lines go to neutron producing targets and must have a high transmission for electron beams with a high momentum spread. Because of aberrations, second order corrections to the quadrupole fields must be calculated to retain the achromatic features and small focal spots at the targets.

Target Cooling: All high power targets will be cooled by a closed loop system containing a heat exchanger, ion exchange column and hydrogen recombiner. It will be possible to switch these units from one target to another without the necessity of their being duplicated.

Time-of-Flight Facilities: The accelerator may be used as a pulsed neutron source both below ground and above ground. Below ground there are six neutron drift tubes with maximum lengths of 20m, and a minimum length of 4m. There will be two target positions below ground for the production of neutrons. The neutron yield will be approximately 10^{14} neutrons/sec. Above ground the flight tubes will have lengths of 15m, 66m and 240m. About half of the accelerator time will be devoted to neutron time-of-flight experiments.

B. NEUTRON PHYSICS

1. Detection of Direct Neutron Capture in Pb^{207} by Threshold Photoneutron Measurements on Pb^{208} (C. D. Bowman, R. J. Baglan and B. L. Berman)

At least two sources of direct neutron capture have been discussed in the literature. Lane and Lynn[1] proposed a direct capture mechanism in which an incoming neutron in an s-wave single particle orbit falls directly into a bound p-wave orbit, bypassing the formation of the compound nucleus and emitting a single gamma ray. A semi-direct reaction was proposed by Brown[2] in which the particle first excites the giant dipole state and is then captured into a bound orbit with the emission of a single gamma ray. The capture is therefore delayed by the lifetime of the dipole state, whence comes the description as a semi-direct process. If an appreciable part of the giant dipole state decays to the ground state of the residual nucleus, that portion, when extrapolated by means of the Lorentz formula from the giant resonance region down to the excitation energy excited by slow neutron capture, might be larger than Lane and Lynn's direct term.

Nuclei near magic numbers appear to be the most likely places for the detection of the semi-direct reaction. We carried out a threshold photoneutron experiment on Pb^{208} since the (γ,n) experiment is easier than the corresponding (n,γ) experiment on Pb^{207}. The results are shown in Fig.B1 where cross section in mb/sr is plotted against neutron energy for natural lead. The measurements were also made on separated isotopes of Pb so that all peaks could be assigned to the proper isotope. Peaks not belonging to Pb^{208} are shown by the vertical arrows. There are three 1^- states in this spectrum, located at 41, 257 and 319 keV. The spins of these states were determined by comparing measurements taken at 90° and 135°. The attention here is focused particularly on the peak at 41 keV which is a well-known state seen in both neutron capture and total cross section measurements on Pb^{207}.

The points of Fig.B1 are replotted in Fig.B2 on a wider scale. The peak at 37.5 keV has a total width much narrower than the resolution function of the experimental apparatus, so it serves to measure the resolution in the experiment. The peak at 41 keV, which shows the marked asymmetry, is a few times wider than the resolution so determined and it therefore is completely resolved.

The data points have been fitted with an expression which can be written for neutron capture as

$$\sigma_{n\gamma} = \frac{\pi}{k_n^2} g_n \left| a - \frac{(\bar{\Gamma}_\gamma \bar{\Gamma}_n)^{1/2}}{(E_n+B-\bar{E})+i\Gamma/2} + \frac{ie^{-i\phi}(\Gamma\,\Gamma_{\gamma o})^{1/2}}{(E_n-E_o)+i\Gamma/2} \right|^2 . \qquad (1)$$

By reciprocity, $\sigma_{n\gamma} = \sigma_{\gamma n}\,(k_\gamma^2 g_n / k_n^2 g_\gamma)$. The first term in Eq. (1) is the direct term described by Lane and Lynn,[1] and the second term is the semi-direct capture discussed by Longo and Saporetti,[3] who extended Brown's work. In the second term, B is the separation energy of the neutron, $\bar{\Gamma}$ is the total width of the giant dipole resonance, and $\bar{\Gamma}_n \bar{\Gamma}_\gamma$ is proportional to that portion of the giant dipole resonance (GDR) decaying to the ground state of the residual nucleus. $\bar{E}$ is the energy of the GDR; all three of these parameters can be obtained by a fit to the GDR. The last term in the equation is the compound-nucleus Breit-Wigner expression as written by Lane and Lynn. In general a, $\bar{\Gamma}_\gamma^{1/2}$ and $\Gamma_{\gamma o}^{1/2}$ are complex quantities. Equation (1) can be rewritten in the following form:

$$\sigma_{n\gamma} = \frac{\pi}{k_n k_n^o} \frac{2J+1}{2(2I+1)} \left\{ d^{o^2} + \frac{4d^o(\Gamma_n^o \Gamma_{\gamma o}/\Gamma^2)^{1/2}}{1+X^2} (X \sin(\nu)+\cos(\nu) + \frac{4\Gamma_r^o \Gamma_{\gamma o}/\Gamma^2}{1+X^2} \right. \qquad (2)$$

where k_n^o, d^o, Γ_n^o represent these quantities evaluated at 1 eV and $x = 2(E_n-E_o)/\Gamma$. The phase angle ν is a complicated function of the magnitude and phases of all three terms of Eq. (1).

The 41 keV peak has been fitted with Eq. (2) as shown by the line through the points. Two solutions are possible. The direct cross section required is 1.2 mb/sr and Γ_n = 1520 eV. For $\nu = 130^\circ$, $\Gamma_{\gamma o}$ = 4.18 eV, while for $\nu = 207^\circ$, $\Gamma_{\gamma o}$ = 6.44 eV. The direct cross section is more than an order of magnitude larger than the value predicted by Lane and Lynn's model but is consistent with Brown's model. Since the momentum of a 7 MeV γ-ray and a 40 keV neutron are roughly equal, those measurements imply a non-resonant neutron capture cross section in Pb^{207} at 40 keV of about 10 mb.

References

[1] A. M. Lane and J. E. Lynn, Nuc. Phys. 17, 563 (1960), Nuc. Phys. 17, 586 (1960).

[2] G. E. Brown, Nuc. Phys. 57, 339 (1964). Also C. F. Clement, A. M. Lane and J. R. Rook, Nuc. Phys. 66, 273 (1965).

[3] G. Longo and F. Saporetti, Nuovo Cimento LV1, 264 (1968).

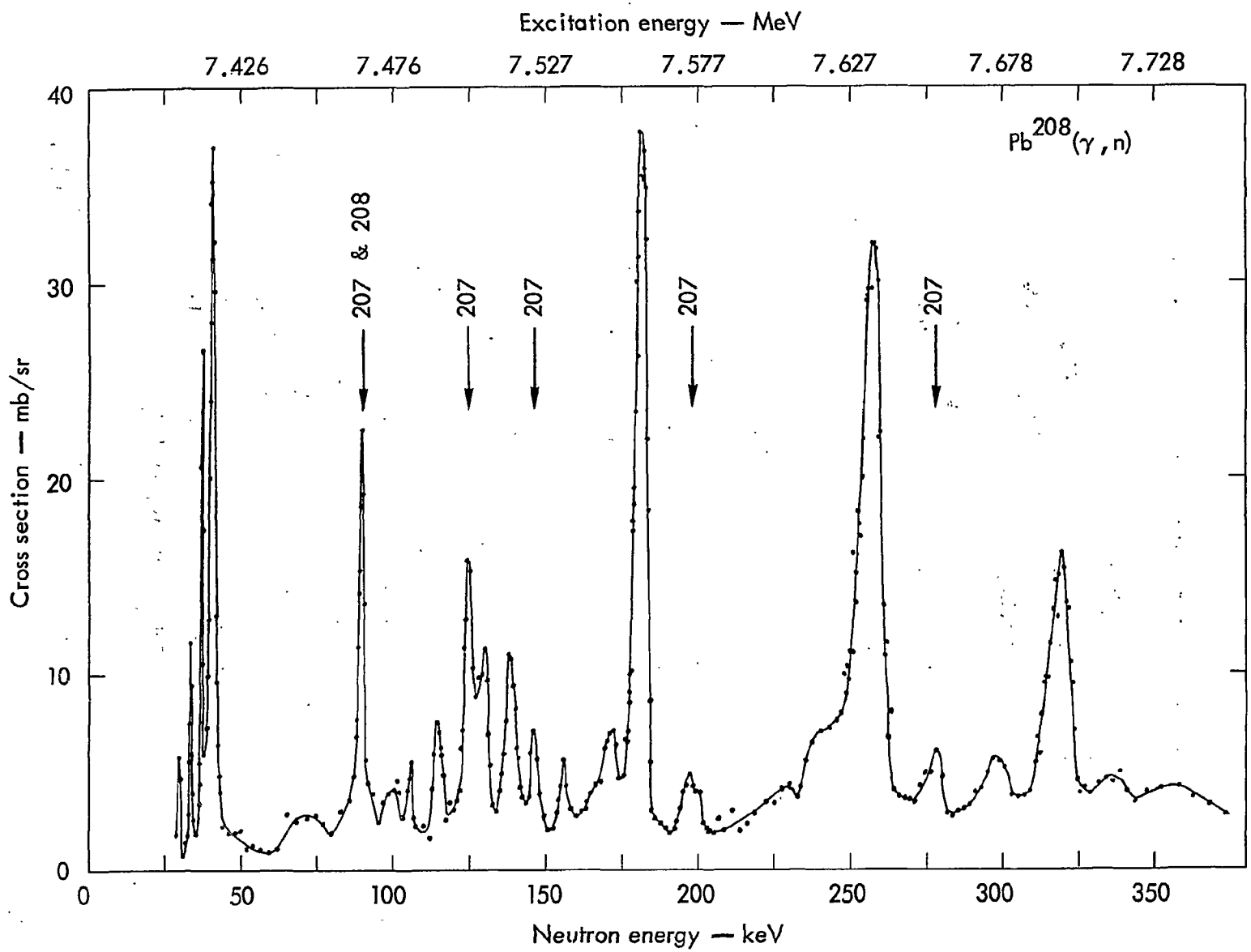

Fig. B1

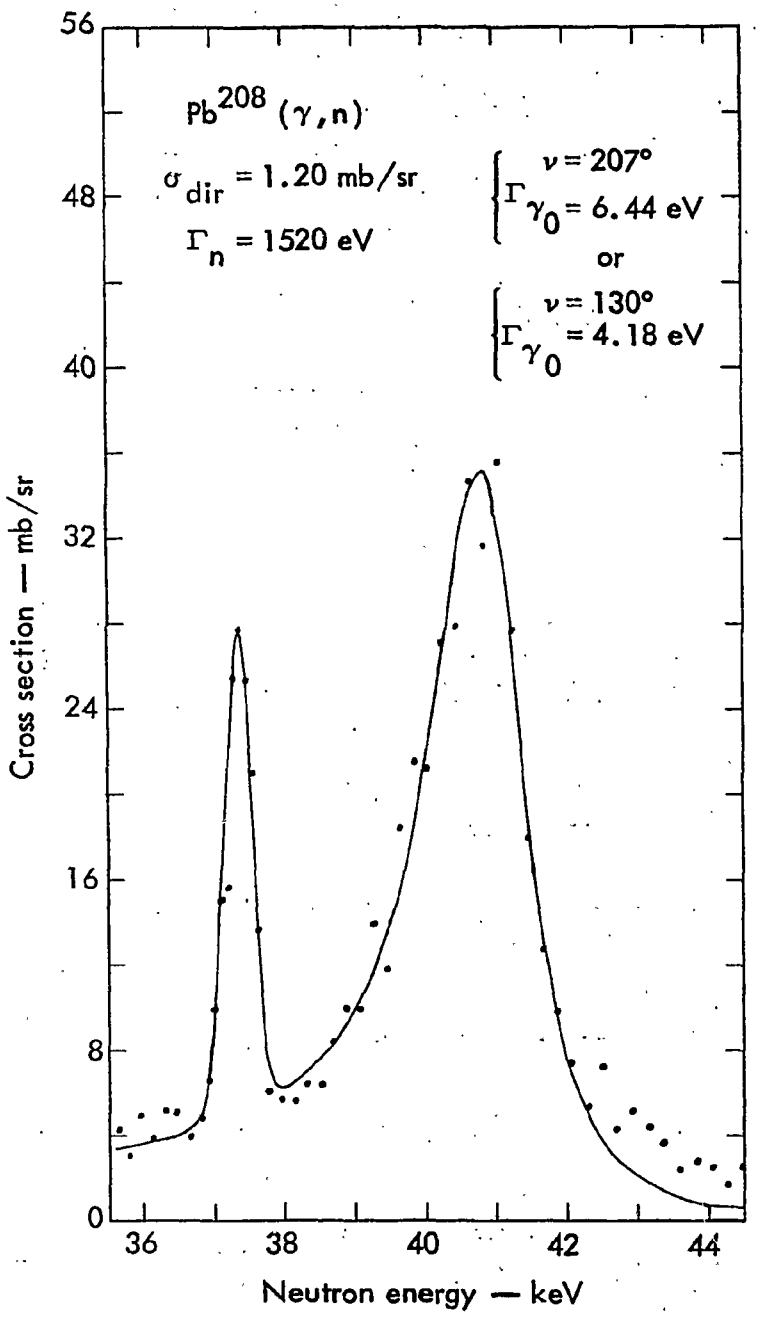

Fig. B2

2. Gamma Ray Decay of the Doorway State in Pb^{206}+n from Threshold Photoneutron Measurements on Pb^{207} (C. D. Bowman, R. J. Baglan and B. L. Berman)

Probably the best example of a doorway state, excited by neutron absorption, was discovered by Farrell et al[1] in the neutron total cross section of Pb^{206} at 500 keV. In this measurement we attempted to obtain more information about the nature of the doorway state by studying its radiative decay. Since the final state is well known and the initial (doorway) state is a relatively simple configuration, a measurement of the ground state gamma-ray decay width $\Gamma_{\gamma o}$ of the state could yield information about the nature of the doorway state.

Such information could be obtained by studying the ground state gamma radiation following neutron capture in Pb^{206}. However, the threshold photoneutron reaction, (γ,n) on Pb^{207}, was used since the photonuclear experiment is easier to perform. The results for Pb^{207} (γ,n) are shown in Fig.B3 where cross section in mb/sr is plotted against the energy of the emitted neutron. The measurements were carried out with a 140 gram sample of isotopic composition 92.36% Pb^{207}, 5.48% Pb^{208} and 2.16% Pb^{206}. Isotopic contamination from Pb^{208} introduced spurious peaks at 181, 255 and 318 keV. There strength was about 1/20 of that in Pb^{208} in rough accordance with the abundance ratio (1:17).

Below 600 keV the positions of $1/2^+$ states could be assigned from neutron total cross section measurements on Pb^{206} and the position of these states is shown by the verticle arrows. Clearly there is additional structure besides that with spin $1/2^+$. In fact the observation of additional structure is expected since E1 photon absorption by the 1/2-Pb^{207} ground state will excite both $1/2^+$ and $3/2^+$ states. As long as $\Gamma_n >> \Gamma_{\gamma o}$, the $3/2^+$ states will be detected as easily as the $1/2^+$ states even though they must decay by d-wave neutron emission.

According to the neutron experiments there is concentration of neutron strength near 500 keV with spin $1/2^+$ which apparently is a "doorway" state. In this experiment an attempt has been made to find a similar broad peak in the (γ,n) curve and hence in $\Gamma_{\gamma o}$. Indeed there appears to be a peak in this energy region bounded by regions of rather low cross section above 800 keV and between 150 and 300 keV.

Another view of the region including the $1/2^+$ strength is given in Fig. B4. When the (γ,n) cross section of Fig. B3 has been integrated in 50 keV intervals and the area plotted as a function of neutron energy. The verticle bars show the position and magnitude of the reduced neutron widths Γ_n^o for the known 1/2+ states. Keeping in mind the fact that the peak in the curve near 100 keV is known not to be

associated with $1/2^+$ states since only one of the many states in this region is known to be $1/2^+$, the evidence for a peak near 500 keV is rather strong.

The gamma-ray strength of the doorway state must be concentrated between 200 and 700 keV as the neutron strength is, so that the cross section in that interval can be integrated to give a value for decay of the doorway state to the ground state by gamma-ray emission, $\Gamma_{\gamma o}^{ds}$. The value is $\Gamma_{\gamma o}^{ds} = 260$ eV $^{+60}_{-100}$ which is the same as the E1 single particle width.

The spin and the neutron width of the doorway is known from the neutron experiment and the width for radiative decay to the ground state is determined from the present experiment. In addition, the ground state configuration of Pb^{207} is well known. All this information taken together implies a "doorway" state configuration consisting of the p1/2 neutron hole coupled either to a 1^- proton or neutron particle-hole state, or to a coherent sum of such states. This picture, in fact, is essentially that suggested earlier by Farrell[1] et al when the doorway state was discovered.

---

[1] J. A. Farrell, G. C. Kyker, Jr., E. G. Bilpuch and H. W. Newson, Phys. Letters 17, 286 (1965).

FIGURE CAPTIONS

Fig. B3 The (γ,n) cross section of Pb^{207} measured at 135°. The positions of $1/2^+$ states determined from neutron total cross section measurements[1] on Pb^{206} are indicated by the verticle arrows.

Fig. B4 The (γ,n) area as a function of neutron energy. The data of Fig. B3 has been integrated in 50 keV intervals and the resulting areas plotted as a function of neutron energy. The values for the reduced neutron width Γ_n^o are given at the resonance energy by the verticle lines.

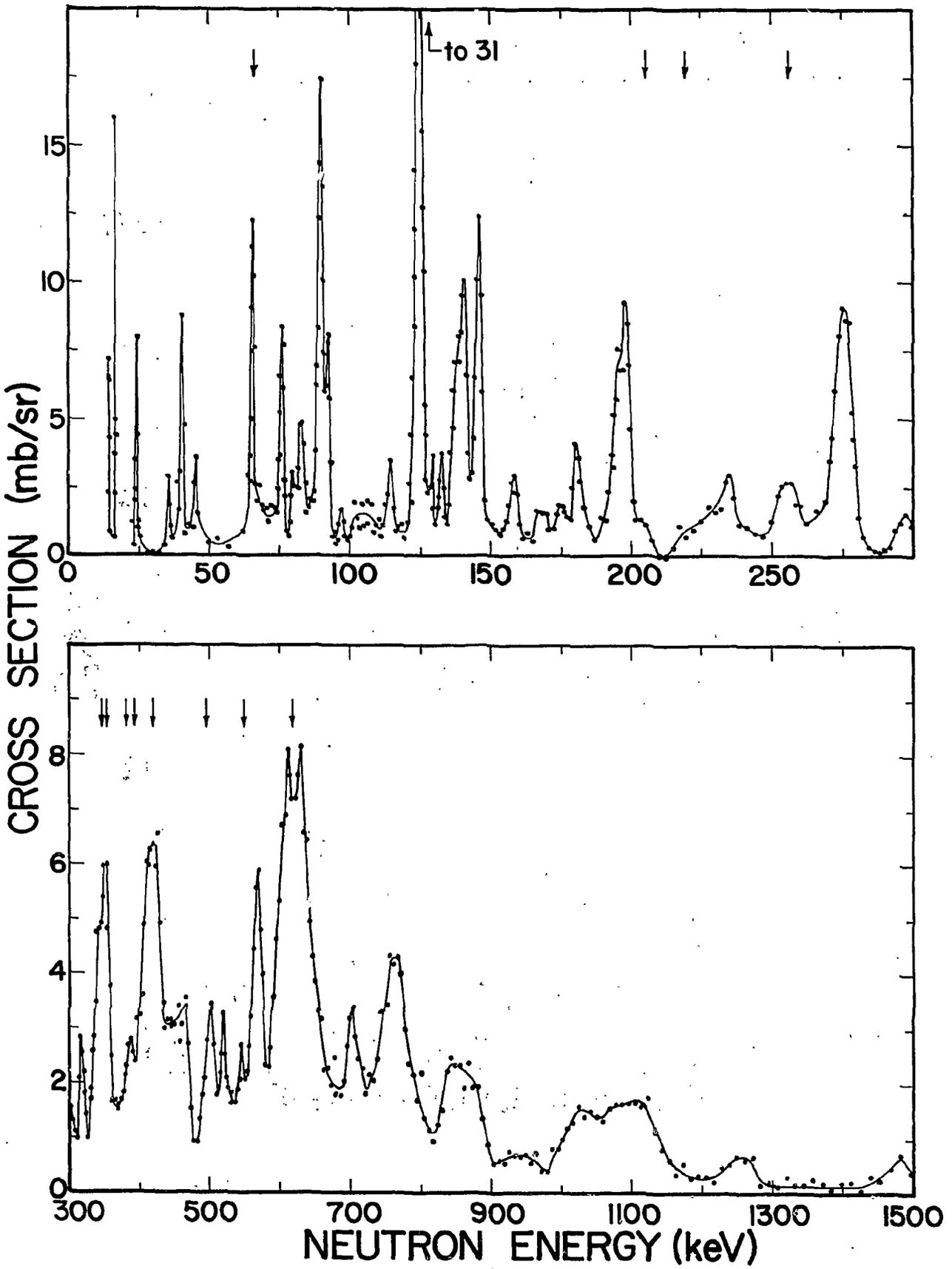

Fig. B3

DATA NOT FOR QUOTATION

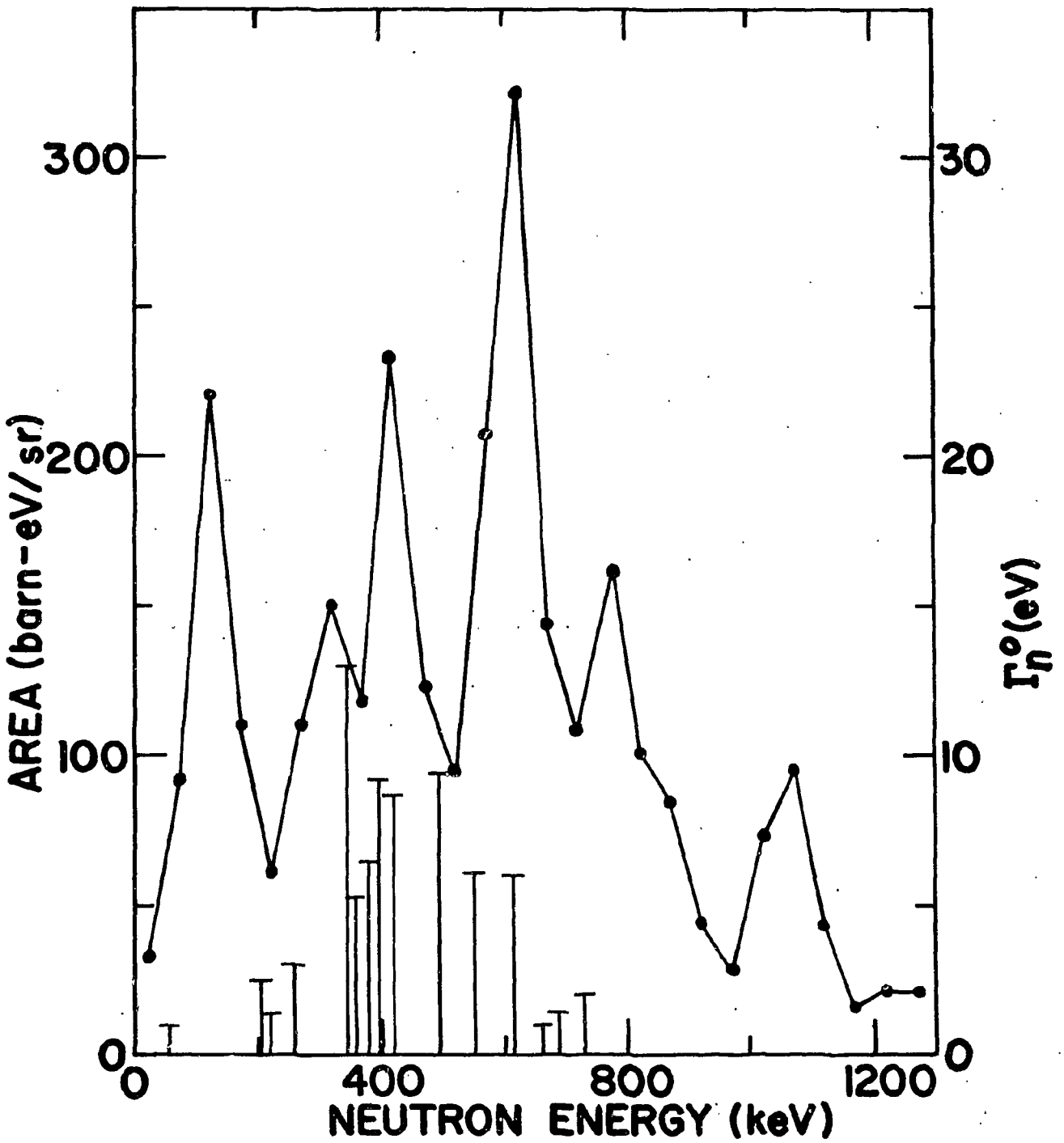

Fig. B4

DATA NOT FOR QUOTATION

3. Radiative Capture of Fast Neutrons on He^3 from the Photoneutron Cross Section for He^4 (B. L. Berman, S. C. Fultz, and M. A. Kelly*)

The photoneutron cross section for He^4 has been measured with monoenergetic photons from the annihilation-in-flight of fast positrons at the Livermore electron linear accelerator. The gamma-ray energy range for which the measurement was performed is from threshold to 31 MeV (neutron energy from 0 to 8 MeV): the energy resolution was less than 400 keV.

The (γ,n) cross section was transformed to an (n,γ) cross section by detailed balance:

$$\sigma(n,\gamma) = \sigma(\gamma,n) \left(\frac{\lambda\!\!\!^{-}_n}{\lambda\!\!\!^{-}_\gamma}\right)^2 \left[\frac{2\ I(He^4) + 1}{2\ I(He^3) + 1}\right]$$

$$= \sigma(\gamma,n) \frac{E_\gamma^{\ 2}}{4E_n\ M_n C^2} = \frac{\sigma(\gamma,n)\ E_\gamma^{\ 2}}{3758\ E_n}$$

where

$$E_n = 3(E_\gamma - 20.578)/4.$$

The results are shown on Fig. B5.

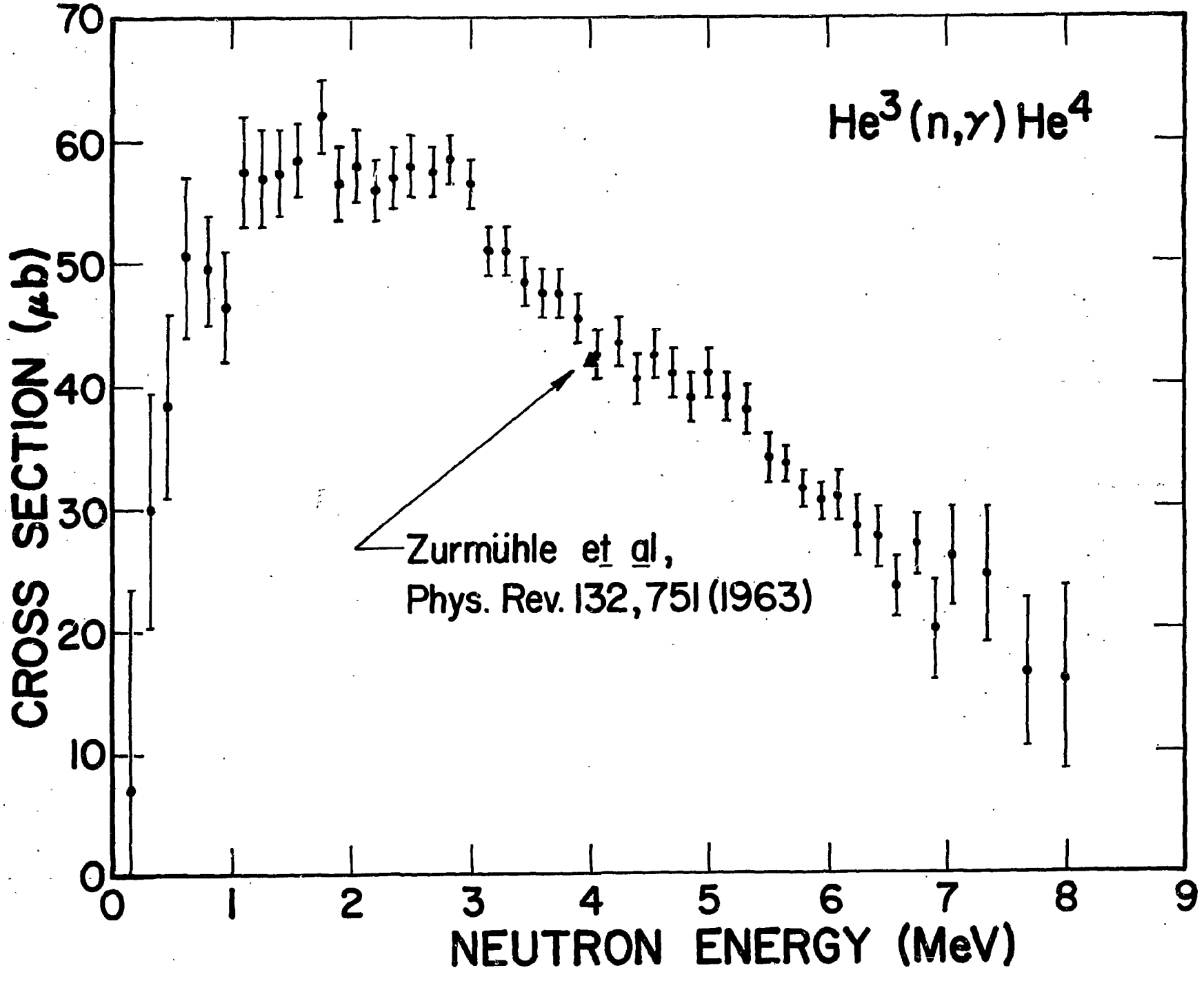

DATA NOT FOR QUOTATION

Fig. B5

4. Structure in (n,α) Reactions Induced by 14-MeV Neutrons
(M. A. Warnock and D. G. Gardner)

We have recently begun a program to look for intermediate structure in certain (n,α) reactions induced by 14-MeV neutrons. In many cases, particularly for medium weight and heavy nuclei, the number of α particles emitted exceeds that expected from statistical evaporation by one or more orders of magnitude. It is tempting, therefore, to think of α-particle clusters that become directly involved with doorway states.

Neutrons from the $T(d,n)^4He$ reactions were obtained from the ICT facility at Livermore, with an intensity of about $2x10^{12}$ neutrons/sec. The neutron energy was varied by placing samples on the surface of a sphere at different angles with respect to the deuteron beam. Corrections were made for the anisotropy of the neutron emission, and in some cases for scattering in the target.

The daughter product radioactivity was observed, summing over all possible final states. The neutron energy resolution is about 150 keV for most of the available energy range. FigureB6 shows the results of our cross section measurements on Al. Error limits are standard deviations from mean value, the average deviation being 0.93%. Autocorrelation function analyses have been made, and the results are consistent with Ericson fluctuation theory. However, the peak around 14.1-MeV appears to be too narrow to be consistent with the calculated resolution function and additional experimental measurements are planned to recheck the energy regions from 14.0 to 14.2 MeV.

The reaction $^{75}As(n,\alpha)^{72}Ga$ was studied next. Here the coherence energy is so small that Ericson fluctuations would not be observed in this work. Any structure observed in the excitation function would require some other explanation. The results are shown in Figure B7. The results appear rather structureless, although the quality of the data is not as good as in the Al case. However, additional measurements were made using much better targets, and these results appear in Figure B8. With these samples the variance was improved by a factor of 100. Additional experimental measurements are planned to try to confirm the structure appearing in Figure B8.

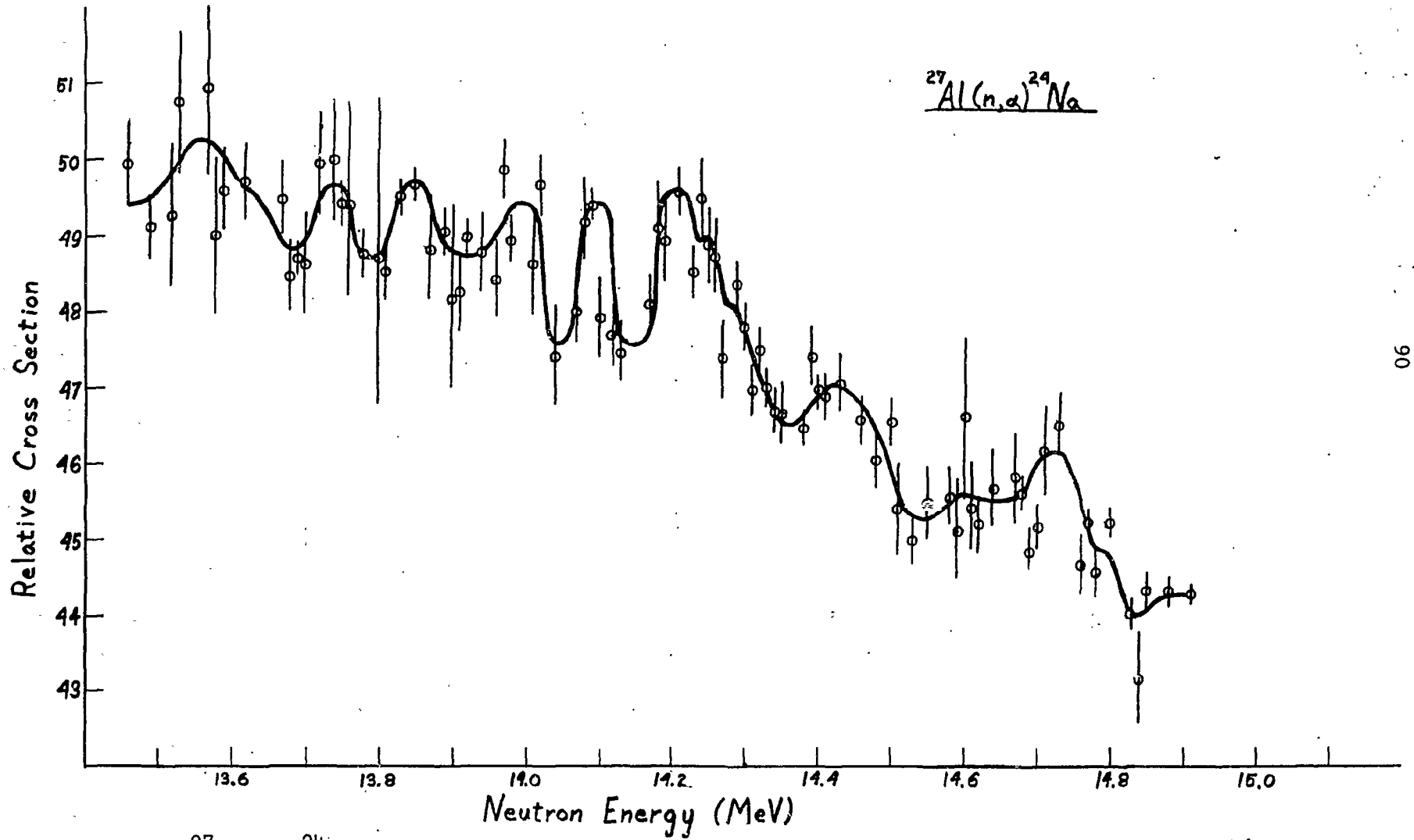

$^{27}Al(n,\alpha)^{24}Na$ Excitation Function

Fig. B6

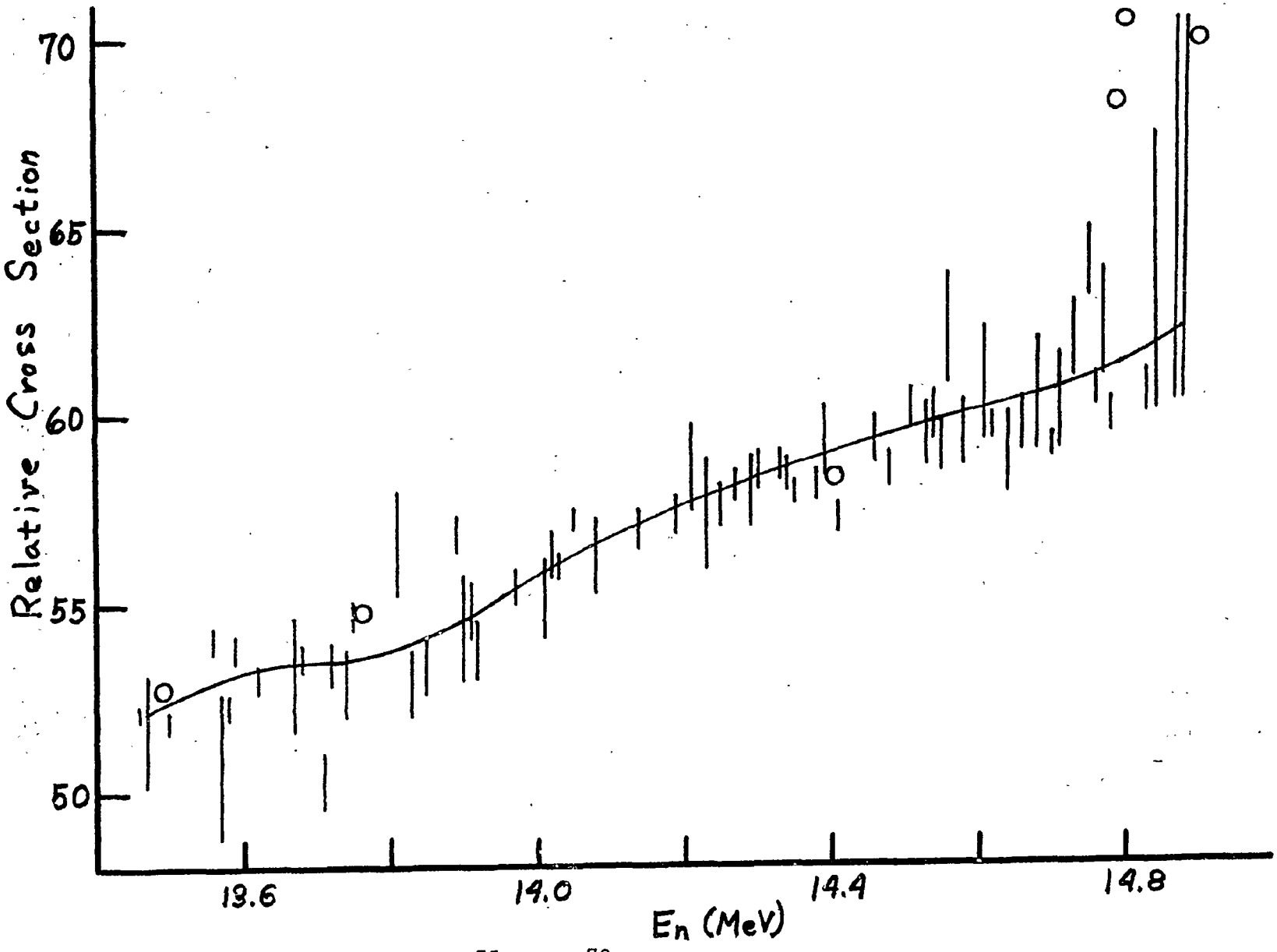

Excitation Function for the $^{75}As(n,\alpha)^{72}Ga$ Reaction (o - indicates single measurement).

Fig.B7

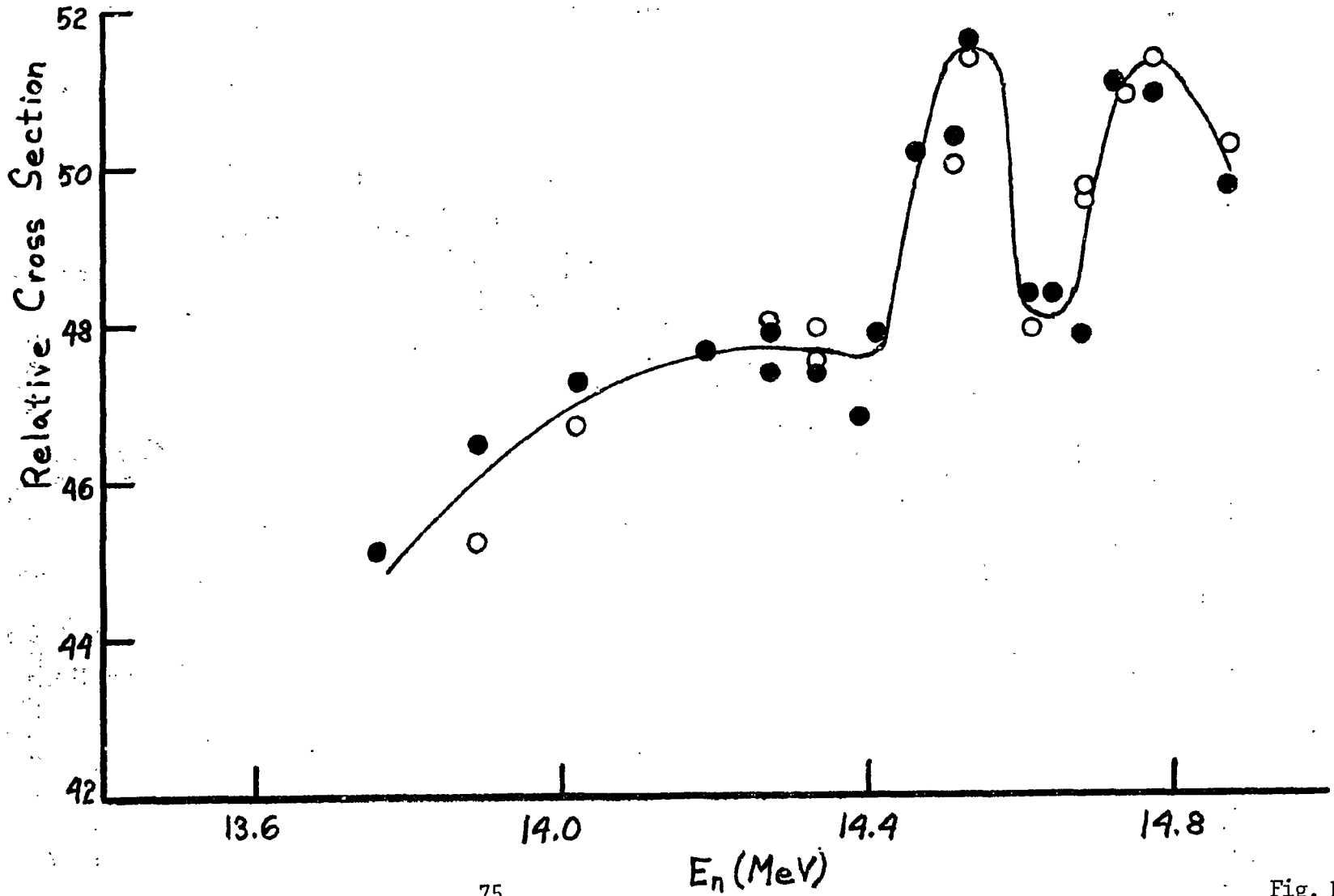

Fig. B8

Excitation Function for the $^{75}As(n,\alpha)72Ga$ Reaction (Data obtained from arsenic metal samples only).

C. FISSION PHYSICS

1. Measurements of Delayed Gamma Rays from Spontaneous Fission of ^{252}Cf (W. John, J. J. Wesolowski, F. Guy and R. Jewell)

Relatively little is known about the delayed gamma rays from fission. In order to study the gamma spectra for particular fission fragments it is necessary to make multiparameter measurements. In the present work, the kinetic energies of both fission fragments from the spontaneous fission of ^{252}Cf were measured with Si detectors. The energies of the gamma rays emitted by the fragments which had stopped on one of the Si detectors were measured with a Ge (Li) detector. In addition, the time delay was measured with a time-to-amplitude converter which started on the fission fragment signal and stopped on the gamma ray signal. The time interval extended from 5 ns to 2 μs. For each event the four pulse heights were recorded on magnetic tape.

The data from 10^7 events were analyzed on a computer. For each event the mass of the gamma-emitting fragment was calculated from the fragment energies. The data were then sorted to produce well-resolved gamma ray spectra for each mass. The decay curve for each gamma ray could also be obtained.

The total yield of delayed gamma rays was found to exhibit considerable structure as a function of fragment mass. The yield vs mass also changes with time. Data for three major time intervals were compiled and are shown in Fig. C1.

References to Other Recent Work:

[1] "Systematics of Fission Product X-Ray Intensities", W. John, R. Massey and B. G. Saunders, Phys. Letters 24B (1967) 336.

[2] "High-resolution Studies of Fission X-Rays and Gamma Rays", Arkiv for Fysik 36 (1967) 287.

2. Attempts to Measure Spins of Resonances and Intermediate Structure in U^{235} (C. D. Bowman, B. L. Berman, R. J. Baglan and G. D. Sauter)

Neutron capture gamma-ray multiplicity measurements for determining the spin of resonances in U^{235}, which were reported in the last NCSAC report, have been repeated. The measurements also were extended to 3 keV in an attempt to locate intermediate structure in U^{235}. Analysis of the new data should be completed by October 1969.

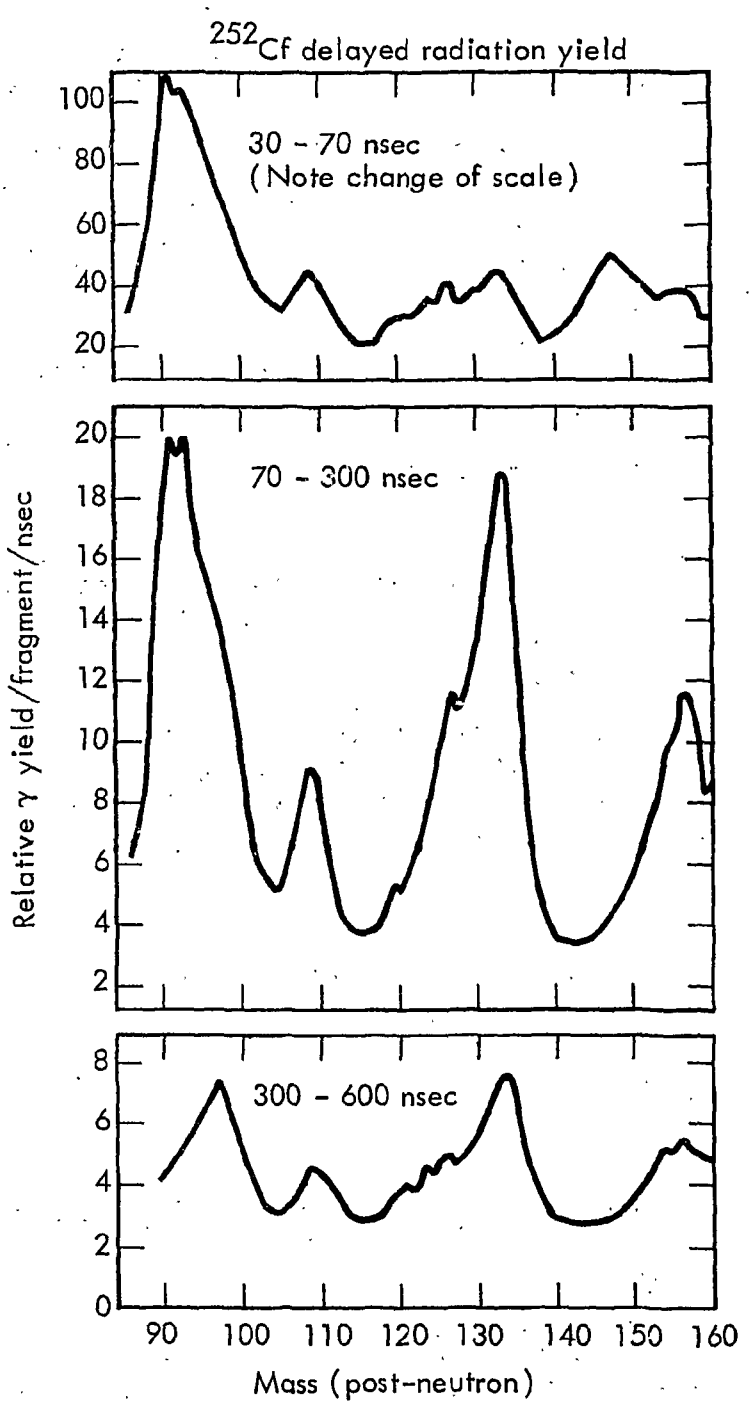

Fig. C1

3. Sample Preparation for the Physics VIII Experiment
(R. W. Lougheed, M. S. Coops, J. E. Evans, and R. W. Hoff)

This report summarizes part of a cooperative effort between members of the LRL Radiochemistry Division and LASL physicists to measure fission cross sections in the range 15 eV to 2 MeV for certain heavy nuclides. The measurements are made with a nuclear explosion as a neutron source, a technique which has been described in detail previously. The nuclides chosen for study, ^{244}Pu, ^{243}Cm, ^{249}Bk, ^{249}Cf, and ^{253}Es are available only in limited quantities and, for the most part, exhibit high levels of alpha radioactivity. Except for an earlier experiment with ^{243}Cm, no detailed measurements of $\sigma_{n,f}$ as a function of neutron energy have been made for these nuclides although values for thermal neutrons are known for ^{249}Cf and ^{243}Cm.

All samples were purified chemically, in some cases just prior to the experiment to reduce the amount of radioactive decay daughter(s) present. A uniform deposit was produced by electroplating on to 0.00014-inch thick stainless steel from a solution of dilute nitric acid and isopropyl alcohol. The amount of material in each sample was assayed directly by alpha counting in a low-geometry counter.

The samples prepared for study are listed in Table C1.

The ^{244}Pu was produced in long-term neutron irradiation of ordinary plutonium followed by isotopic enrichment in a calutron at ORNL.

The ^{243}Cm is a product of low exposure neutron irradiations of ^{241}Am where the 162-day ^{242}Cm originally present decayed to ^{238}Pu which was then removed. An earlier measurement of ^{243}Cm $\sigma_{n,f}$ in the Pommard event was less than optimum due to problems in the data recording system.

The ^{249}Bk and ^{249}Cf are products of long-term neutron irradiation of ^{242}Pu and ^{244}Cm in the High Flux Isotope Reactor. The measurement of $\sigma_{n,f}$ for these nuclides is of significance relative to the use of a resonance reactor for production of ^{252}Cf.

The ^{253}Es is the most intensely alpha active material whose $\sigma_{n,f}$ measurement has been attempted by use of this technique. The total amount of Es, 4 μg, is lower than we had desired due to problems of scheduling the HFIR neutron irradiation of californium relative to the date of the explosion.

Early indications following the explosion were that satisfactory data were obtained for each of these samples.

Table C-1

Samples prepared for $\sigma_{n,f}$ measurement in the Physics VIII Experiment

Nuclide	Amount	Half-life	Activity level	Isotopic purity	Previous $\sigma_{n,f}$ measurements
^{244}Pu	500 μg	8×10^7 yr	4.4×10^5 α dpm	99.06% 244	None
				0.904% 242	
				0.002% 241	
				0.007% 240	
				0.018% 239	
				0.00002% 238	
^{243}Cm	250 μg	32 yr	2.5×10^{10} α dpm	0. 040% 242	Pommard:
				89.00% 243	thermal: 690±50
				10.89% 244	
				0.057% 245	
				0.013% 246	
^{249}Bk	100 μg	314 da	3.7×10^{11} β dpm	100% ^{249}Bk	Thermal: < 6 b
			2.5×10^7 α dpm		
			(^{249}Bk α + ^{249}Cf α)		
^{249}Cf	100 μg	360 yr	9.2×10^8 α dpm	Essentially	Thermal: 1735±7
				100% 249	
^{253}Es	4 μg	20 da	2.3×10^{11} α dpm	Essentially	Thermal: < 60 b
				100% 253	

page 97 follows after page 266

4. A Measurement of ^{239}Pu Capture and Fission Cross Sections (J. B. Czirr)

The previously reported measurement of α for ^{239}Pu has been repeated in an effort to extend the energy range to 30 keV and to confirm the normalization procedure. The experimental techniques are unchanged from that reported in Ref. 1.

Table C2 lists the results of this later measurement, including the effects of the improved normalization.

The effects of any further corrections to the data (such as variations in $\bar{\nu}$ with energy) will probably be small. The combined results of both measurements will be submitted for publication in final form in the early fall.

---

[1] J. B. Czirr, Nucl. Inst. and Methods 72, (1969) 23.

Table C-2

Neutron Energy (keV) Min.	Max.	$\langle\sigma_C\rangle/\langle\sigma_F\rangle$
20.6	33.5	0.37
10.1	20.6	0.42
9.0	10.1	0.62
8.0	9.0	0.58
6.9	8.0	0.60
6.0	6.9	0.89
5.0	6.0	0.88
3.9	5.0	0.81
3.0	3.9	0.89
2.0	3.0	1.03
1.0	2.0	0.86
0.90	1.0	0.71
0.80	0.90	0.65
0.70	0.80	0.92
0.60	0.70	1.62
0.50	0.60	0.66
0.40	0.50	0.46
0.30	0.40	1.13
0.20	0.30	0.87
0.10	0.20	0.79
0.10	10.1	0.81

D. EVALUATION AND BULK EXPERIMENTS

1. Neutron and Photon Transport Calculational Constants (R. J. Howerton, S. T. Perkins, R. Doyas, V. Hampel, and C. P. Altamirano)

A new package for production of neutron and photon transport calculational constants, which are derived from evaluated microscopic cross sections, has been developed for use on the CDC 6600 and 7600 computers. The package is in two parts. First is a new form for the LRL Evaluated Cross Section Library. The main features of this format are: 1) allowance for evaluated data for individual reactions rather than requiring complete evaluations for an isotope or element; 2) inclusion of photon and charged particle induced reactions; 3) allowance for more detail of partial reactions than had previously been possible. The second part is a new processing code (CLYDE) which manipulates the data of the new evaluated library into appropriate calculational constants. CLYDE will handle neutron, photon, and charged particle induced reactions. The main features are: 1) unlimited number of groups; 2) unlimited P_ℓ representations.

2. Spherical Critical Assembly Calculations (R. J. Howerton, S. T. Perkins, R. Doyas, V. Hampel, and C. P. Altamirano)

In preparation for an extensive neutron cross section reevaluation program, baseline calculations, using current LRL evaluated cross sections and the SORS Monte Carlo neutronics code, have been made for over two-hundred spherical critical assemblies.

3. Pulsed Sphere Program (L. F. Hansen, J. D. Anderson, E. Goldberg, J. Kammerdeiner, E. F. Plechaty and C. Wong)

Using the sphere transmission and time-of-flight techniques, the neutron spectra emitted from 0.58, 1.06 and 3.0 mean free path radius spheres of nitrogen have been measured for a nominal 14 MeV neutrons. The analysis of the data has been done using the Livermore Monte Carlo Neutron Transport Program (SORS) with the revised cross sections obtained from the analysis of the 1 mfp nitrogen[1]. The overall shape of the calculated spectrum for the 3 mfp was in good agreement with the measurements; however, the magnitude of the calculated neutron flux at the highest neutron energies was 20% lower than the measured value. This result indicated that the total cross section used in the calculation was too large. To raise the calculated spectrum in the region of 14-13 MeV the magitude of the total cross section had to be reduced to 1550 mb. At this time the revised (n,xγ) cross sections in

nitrogen between 5.8 and 8.6 MeV measured by Dickens and Perey[2] became available. Since their initial values had been used to infer the n,n'γ cross sections up to 14 MeV[1] a complete revision of the cross sections used in SORS was carried out. It immediately became evident that it was not possible to reconcile the values of the total cross sections obtained by Foster and Glasgow[3] with the sum of values of the elastic cross sections measured by Bauer et al[4] and the non-elastic cross sections reported by Dickens and Perey[2]. Since all three measurements appear reliable, it was impossible to justify any change in the measured cross sections. Therefore two extreme cases were considered for the neutron-cross-section library to be used in SORS:

a. in "Library A" it was assumed that the measured elastic cross sections[4] were too low, and they were raised accordingly to give the value of σ_{total};

b. in "Library B" the assumption was made that the measured inelastic cross sections[2] were low and they were raised to give the value of σ_{total}.

In both cases, σ_{total} was reduced below the values of Ref. 3 with 1550 mb at 14 MeV.

Figs. D1 and D2 show the SORS calculations with these two libraries for 1.06 and 3.0 mfp of nitrogen. Libraries A and B are given in Tables D1 and D2. In Table D3 are given the (n,n') cross sections assigned to the 3.95-, 5.10-, 5.75-, 7.07 and 7.95 MeV levels as a function of energy.

---

[1] L. F. Hansen, J. D. Anderson, E. Goldberg, E. F. Plechaty, M. L. Stelts and C. Wong, Nucl. Sci. and Eng. 35, 227 (1969).

[2] J. K. Dickens and F. G. Perey, Nucl. Sci. and Eng. 36, 280 (1969).

[3] Foster and Glasgow (Private communication 1963).

[4] R. W. Bauer, J. D. Anderson and L. J. Christensen, Nucl. Phys. 47, 241 (1963).

Table D-1

Nitrogen Neutron Library A

Group	$E_{initial}$	σ_{total}	$\sigma_{elastic}$	σ_{n-e}	$\sigma(n,n')$ Levels	$\sigma(n,n')$ Continuum	$\sigma(n,2n)$	$\sigma(n,x_1)$*	$\sigma(n,x_2)$*
32	1.602	1988	1921	67				22	45
33	1.791	1745	1647	98				13	85
34	1.989	1558	1479	79				20	59
35	2.198	1428	1282	146				36	110
36	2.418	1409	1274	135				30	105
37	2.648	1390	1234	156				21	135
38	2.889	1618	1329	289	2			42	245
39	3.140	1600	1237	363	4			34	325
40	3.401	1723	1298	425	8			47	370
41	3.673	1797	1418	379	10			59	310
42	3.955	2065	1575	490	15			75	400
43	4.248	1696	1286	410	18			52	340
44	4.551	1218	844	374	24			50	300
45	4.865	1275	920	355	31			49	275
46	5.189	1459	1197	262	44			48	170
47	5.524	1382	1106	276	60			46	170

Group	$E_{initial}$	σ_{total}	$\sigma_{elastic}$	σ_{n-e}	$\sigma(n,n')$ Levels	$\sigma(n,n')$ Continuum	$\sigma(n,2n)$	$\sigma(n,x_1)$*	$\sigma(n,x_2)$*
48	5.869	1421	1119	302	85			42	175
49	6.224	1307	995	312	112			40	160
50	6.590	1208	893	315	138			37	140
51	6.967	1428	1054	374	165			34	175
52	7.354	1437	1043	394	180			34	180
53	7.751	1375	959	416	181			35	200
54	8.159	1220	802	418	182			36	200
55	8.577	1278	884	394	183	25		36	150
56	9.006	1282	878	404	183	45		36	140
57	9.445	1363	943	420	183	70		37	130
58	9.894	1437	1002	435	183	96		36	120
59	10.35	1417	968	449	183	121		35	110
60	10.83	1402	940	462	182	149		31	100
61	11.31	1468	977	491	180	184		27	100
62	11.80	1542	982	560	180	249		26	105
63	12.56	1516	961	555	170	280	2	23	80
64	13.33	1526	983	543	142	300	4	22	75
65	13.87	1550	989	561	138	330	6	22	65
66	14.41 14.60	1550	980	570	135	345	8	22	60

*x_1 and x_2 stand for single and double charged particles respectively

Table D-2

Nitrogen Neutron Library B

Group	$E_{initial}$	σ_{total}	$\sigma_{elastic}$	σ_{n-e}	$\sigma(n,n')$ Levels	$\sigma(n,n')$ Continuum	$\sigma(n,2n)$	$\sigma(n,x_1)$*	$\sigma(n,x_2)$*
32	1.602	1988	1921	67				22	45
33	1.791	1745	1647	98				13	85
34	1.989	1558	1479	79				20	59
35	2.198	1428	1282	146				36	110
36	2.418	1409	1274	135				30	105
37	2.648	1390	1234	156				21	135
38	2.889	1618	1328	290	3			42	245
39	3.140	1600	1231	369	10			34	325
40	3.401	1723	1286	437	20			47	370
41	3.673	1797	1392	405	36			59	310
42	3.955	2065	1540	525	50			75	400
43	4.248	1696	1239	457	65			52	340
44	4.551	1218	798	420	70			50	300
45	4.865	1275	863	412	88			49	275
46	5.189	1459	1125	334	116			48	170
47	5.524	1382	1020	362	146			46	170

Group	$E_{initial}$	σ_{total}	$\sigma_{elastic}$	σ_{n-e}	$\sigma(n,n')$ Levels	$\sigma(n,n')$ Continuum	$\sigma(n,2n)$	$\sigma(n,x_1)$*	$\sigma(n,x_2)$*
48	5.869	1421	1026	395	178			42	175
49	6.224	1307	884	423	220			40	180
50	6.590	1189	750	439	240			37	162
51	6.967	1428	870	558	272			34	252
52	7.354	1437	910	527	242			34	251
53	7.751	1375	897	478	240			35	203
54	8.159	1220	782	438	240			36	162
55	8.577	1278	750	528	240	25		36	207
56	9.006	1282	792	490	230	45		36	179
57	9.445	1363	836	527	220	70		37	200
58	9.894	1437	858	579	210	96		36	237
59	10.35	1417	831	586	200	127		35	224
60	10.83	1402	787	615	200	166		3.	218
61	11.31	1468	820	648	180	204		27	237
62	11.80	1542	880	660	177	254	1	26	202
63	12.56	1516	920	596	170	280	2	23	121
64	13.33	1525	950	575	142	300	4	22	97
65	13.87	1550	955	595	138	330	6	22	99
66	14.41	1550	960	590	135	355	8	22	70

Table D-3

Probability Distribution of the (n,n') Cross Section
Assigned to the Levels as Function of Energy

E_{Lab} (MeV)	Excited levels in N included in SORS (MeV)				
	3.95	5.10	5.75	7.07	7.95
4.0	1.0	---	---	---	---
6.25	.90	.10	---	---	---
7.0	.604	.244	.152	---	---
8.0	.373	.245	.336	.046	---
10.0	.300	.205	.310	.127	.058
12.0	.265	.190	.310	.157	.078
14.1	.254	.173	.309	.178	.086

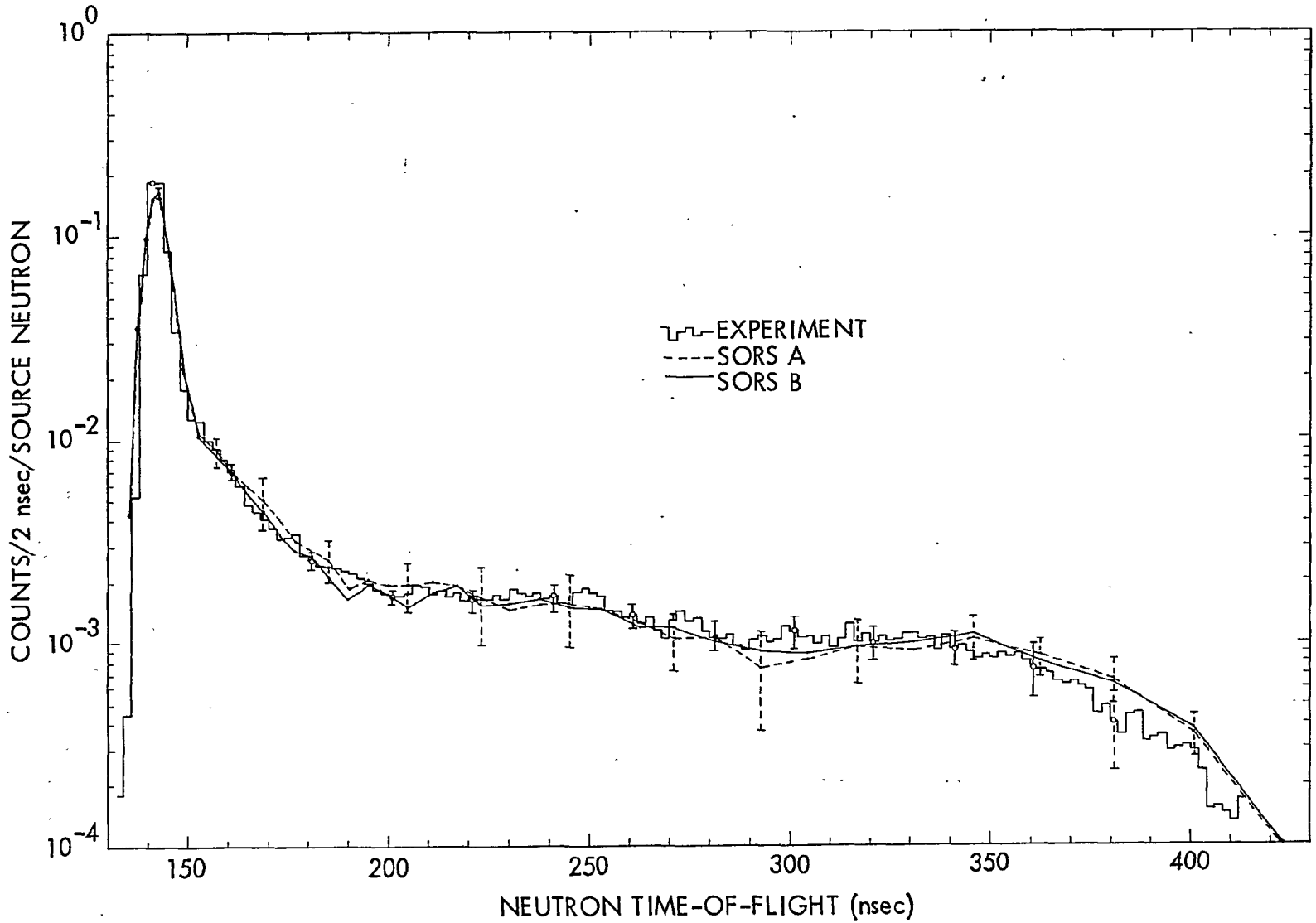

Figure D1

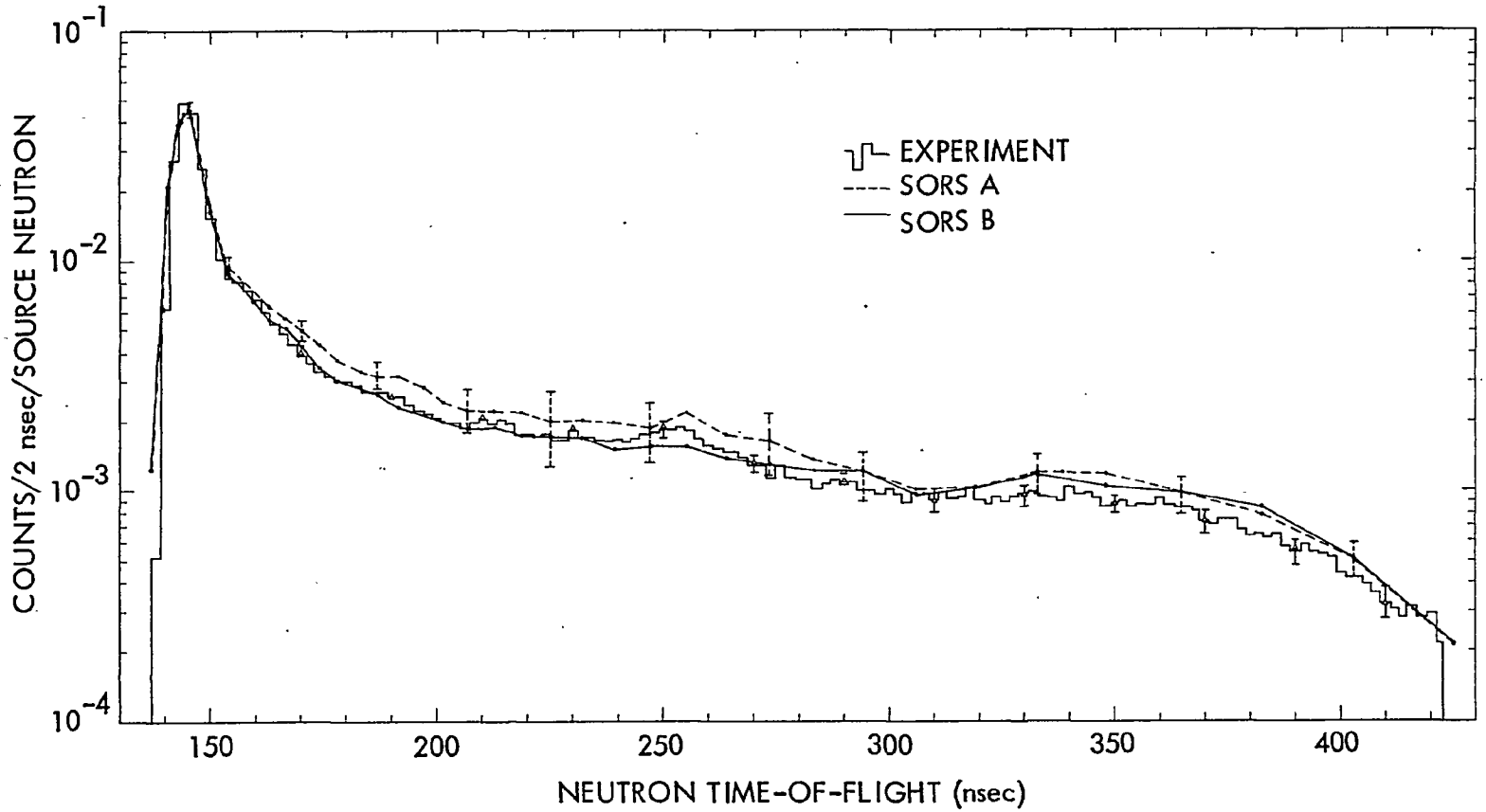

Figure D2

LOCKHEED PALO ALTO RESEARCH LABORATORY

A. NEUTRON PHYSICS

1. The $^{64}Ni(n,p)^{64}Co$ Reaction (H. A. Grench, K. E. Bender, and F. J. Vaughn)

A computer-controlled rapid-transfer system has been built for the irradiation-count cycle needed in studying the possible 0.5-min ^{64}Co activity formed via the $^{64}Ni(n,p)^{64}Co$ reaction.[1]

2. The $^{190}Os(n,n')^{190m}Os$ Reaction (H. A. Grench, K. E. Bender, and F. J. Vaughn)

A preliminary measurement has been made of the $^{190}Os(n,n')^{190m}Os$ activation cross section.[1] This work has demonstrated the feasibility of pursuing the experiment. In particular, activity due to the $^{189}Os(n,\gamma)^{190m}Os$ reaction can be separated from the primary reaction by the simultaneous irradiation of enriched ^{189}Os and ^{190}Os samples. The cross section obtained from the preliminary work, done at an average neutron energy of about 1.9 MeV, is at least an order of magnitude higher than a theoretical value based on Hauser-Feshbach theory. Further experiments at neutron energies closer to threshold and with improved energy resolution will be carried out, and more detailed theoretical calculations will be made.

3. Gross-Fission-Product Gamma-Ray Spectroscopy (W. L. Imhof, L. F. Chase, Jr., R. A. Chalmers, and F. J. Vaughn)

The procedures and equipment used for the investigation of gamma-ray spectral dependence on neutron energy, fissionable isotope, and time after fission have undergone modification. A 30 cm^3 Ge(Li) detector has been obtained, and both gain- and zero-level stabilization employed in its use yielding a measured resolution at 1 MeV of 2.15 keV. Preliminary runs attempting to compare ^{235}U spectra with those of ^{238}U proved unsuccessful due to the presence of too much ^{24}Na activity in the activated ^{235}U targets. Continuing improvements in the machine analysis of the data are being made.

---

[1]Reports to the AEC Nuclear Cross Sections Advisory Committee, WASH-1127.

4. Polarized ^{59}Co Target for Fast-Neutron Total-Cross-Section Measurements (T. R. Fisher, J. McCarthy*, and D. Healey*)

In our last report,[1] experimental work on the total cross section for fast neutrons on oriented ^{165}Ho was described, and the possibility of extending the measurements to other nuclei was mentioned. The achievement of nuclear orientation in a target suitable for fast-neutron experiments generally requires lower temperatures than were necessary in the especially favorable case of ^{165}Ho. For operation at these temperatures the recently developed ^{3}He-^{4}He dilution refrigerator offers significant advantages over more conventional techniques of adiabatic demagnetization. We have therefore designed and built such a refrigerator to be used in producing a polarized ^{59}Co target. The lowest temperature measured for the refrigerator itself is about 0.030°K. The ^{59}Co sample (32 g of polycrystalline Co metal) has been cooled to 0.034°K in the 7 kOe field of a superconducting solenoid. Under these conditions, the nuclear polarization is 40%. The ^{59}Co sample was activated prior to the test run, and the anisotropy of the γ rays from ^{60}Co was used to determine the final temperature achieved. The target will first be used, together with neutrons from the $^{7}Li(p,n)^{7}Be$ reaction, to study the structure in the ^{59}Co total neutron cross section below 1 MeV.

B. CHARGED-PARTICLE REACTIONS

1. The β Decay of ^{25}Na and ^{29}Al (A. D. W. Jones, J. A. Becker R. E. McDonald, and A. R. Poletti)

The β-decay modes of these nuclides deduced from the observed delayed γ-ray spectra are being compared with predictions of the Nilsson model. In addition, measured $\Delta T = 1$ γ-ray strengths for M1 transitions are being compared with the observed β-decay strengths.

2. The β Decay of ^{33}Cl and ^{25}Al (T. T. Bardin, J. A Becker, and R. E. McDonald)

Several previously unreported γ rays following β decay of ^{33}Cl have been observed; β branches to the 0.84-, 1.97-, and 2.84-MeV levels have been deduced from the γ spectrum. For ^{25}Al, we find a 0.8% branch to the ^{25}Mg 1.61-MeV level.

*Stanford University, Stanford, California.

3. Studies of ^{24}Na (J. A. Becker, R. E. McDonald, and R. W. Nightingale)

A level scheme is being deduced for ^{24}Na based on p-γ coincident pulse-height-distribution measurements. Doppler-shift attenuations are also being extracted from these data.

4. Studies of ^{25}Na (J. A. Becker, R. E. McDonald, L. F. Chase, Jr., and D. Kohler)

Gamma decays for levels in ^{25}Na with $E_x < 4.1$ MeV have been observed at $\theta_\gamma = 90°$. Precise level energies (in agreement with earlier work) have been extracted from these data, as well as intensity ratios of ground-state vs. first-excited-state γ decays.

5. Lifetime Measurements in ^{29}Al (A. D. W. Jones, R. E. McDonald, J. A. Becker, and A. R. Poletti)

The measurement of lifetimes of levels in ^{29}Al using the Doppler shift attenuation method has been repeated in order to obtain better statistics and confirm our earlier results. The results are now being analyzed.

6. DSAM Studies in ^{29}Si (A. D W. Jones, T. T. Bardin, T. R. Fisher, J. A. Becker, R. E. McDonald, and R. W. Nightingale)

Lifetimes in ^{29}Si are being measured using the $^{26}Mg(\alpha,n)^{29}Si$ reaction to excite the desired levels. The Stanford FN Van de Graaff accelerator is being employed to produce the ^{4}He beam.

7. The ^{10}B 1.74-MeV Level (T. R. Fisher, A. D. W. Jones, and T. T. Bardin)

The $^{7}Li(\alpha,n)^{10}B$ reaction is being used to study the lifetime of the 1.74-MeV level in ^{10}B. Preliminary measurements indicate that the desired level is copiously populated by this reaction.

8. Magnet Installation (R. E. McDonald)

Installation of a 7-port magnet for momentum analysis and beam switching has been completed. New electrostatic lenses have also been installed. The beam quality is much improved.

LOS ALAMOS SCIENTIFIC LABORATORY

A. TIME OF FLIGHT WITH NUCLEAR EXPLOSIONS

1. Fission Cross Section of ^{244}Cm (R. R. Fullwood, J. H. McNally, and E. R. Shunk)

The neutron induced fission cross section of ^{244}Cm was measured on the Persimmon event (Physics 6) with a 304.2-m flight path. The fission fragments were detected by silicon solid state detectors located at laboratory angles of 55° or 90° and recorded on independent systems. The results of the two measurements cover the neutron energy range 20 eV to 2 MeV and agree within the experimental error as shown in Fig. A-1. For energies above 0.6 MeV there is a systematic deviation (the higher values correspond to 55°). The threshold for fission is observed to occur at 0.71 MeV. The cross section from 100 keV to 4 keV is less than 0.01 b.

The observed fission cross section exhibits clusters of very sharp resonances below 5 keV with the cross section becoming very small between clusters. In many instances the cross sections between resonances within a cluster become very small, but there are several exceptions to this tendency. As an example a "glob" is observed at 3.5 keV of about 1 keV width and 0.15 b cross section. These "globs" may result from longer lived fission isomers which tend to wash out the resolution in a time-of-flight experiment. Structure in the cross section is also observed just below the threshold. For instance, there is a resonance at 0.107 MeV of about 0.2 b.

These phenomena are interpreted as evidence of a second maximum in the fission barrier. It had been thought that nuclei as heavy as A = 244 might not exhibit this effect because of a general tendency to suppress the second maximum with large A. This appears not to be the case.

2. Fission and Capture Measurements on Physics-8 (Groups P-3 and W-8*)

Data films obtained on the Physics-8 experiment have been inspected and almost all measurements appear to have been made successfully. A plate-camera trace of the observed neutron intensity is shown as Fig. A-2. Casual inspection of the low resolution (streak) film indicates that the following results may obtain:

^{234}U, ^{236}U, ^{238}U, ^{242}Pu, ^{244}Pu. In all cases except ^{238}U, a moderately large number of fission resonances (10 to 20) is observed,

*Contributors include M. Anaya, G. Auchampaugh, D. Bergen, B. Diven, A. Ellis, M. Ennis, J. Farrell, R. Fullwood, A. Hemmendinger, M. Moore, D. Peterson, E Robinson, R. Rosul, P. Seeger, E. Shunk, M. Silbert, M. Coops (LRL), R. Hoff (LRL), and F. Simpson (INC).

Fig. A-1. The fission cross section of ^{244}Cm, as determined by time of flight with the Persimmon event (Physics-6). Two detectors were used, at 55° and 90° to the neutron beam. Where the data deviate from one another, the higher values correspond to the 55° detector. Large solid circles are data obtained by D. M. Barton and P. G. Koontz (private communication).

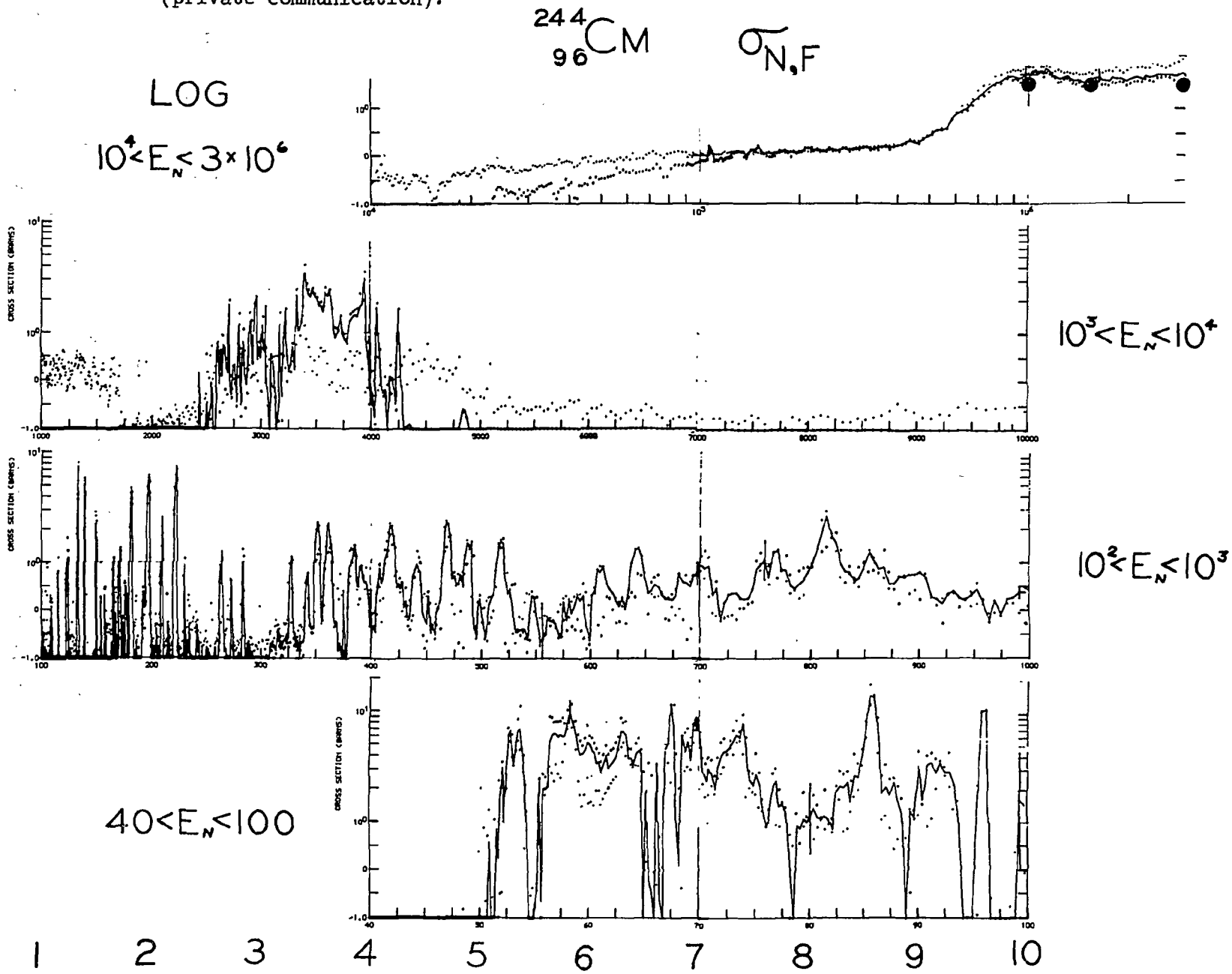

DATA NOT FOR QUOTATION

Fig. A-2. Neutron time-of-flight spectrum observed for a 1/v detector in the Physics-8 event. The flight path was 240 m; each major division corresponds to 500 μsec flight time. The 1/E spectrum extends to about 300 eV, the observed peak of the maxwellian is at 80 eV, and the neutron reaction rate falls below the rate in the 1/E spectrum at 25 eV. The neutron intensity in the beam is estimated at 6×10^{15} n/cm^2/sec at 1 keV, and 1.5×10^{16} n/cm^2/sec at 80 eV.

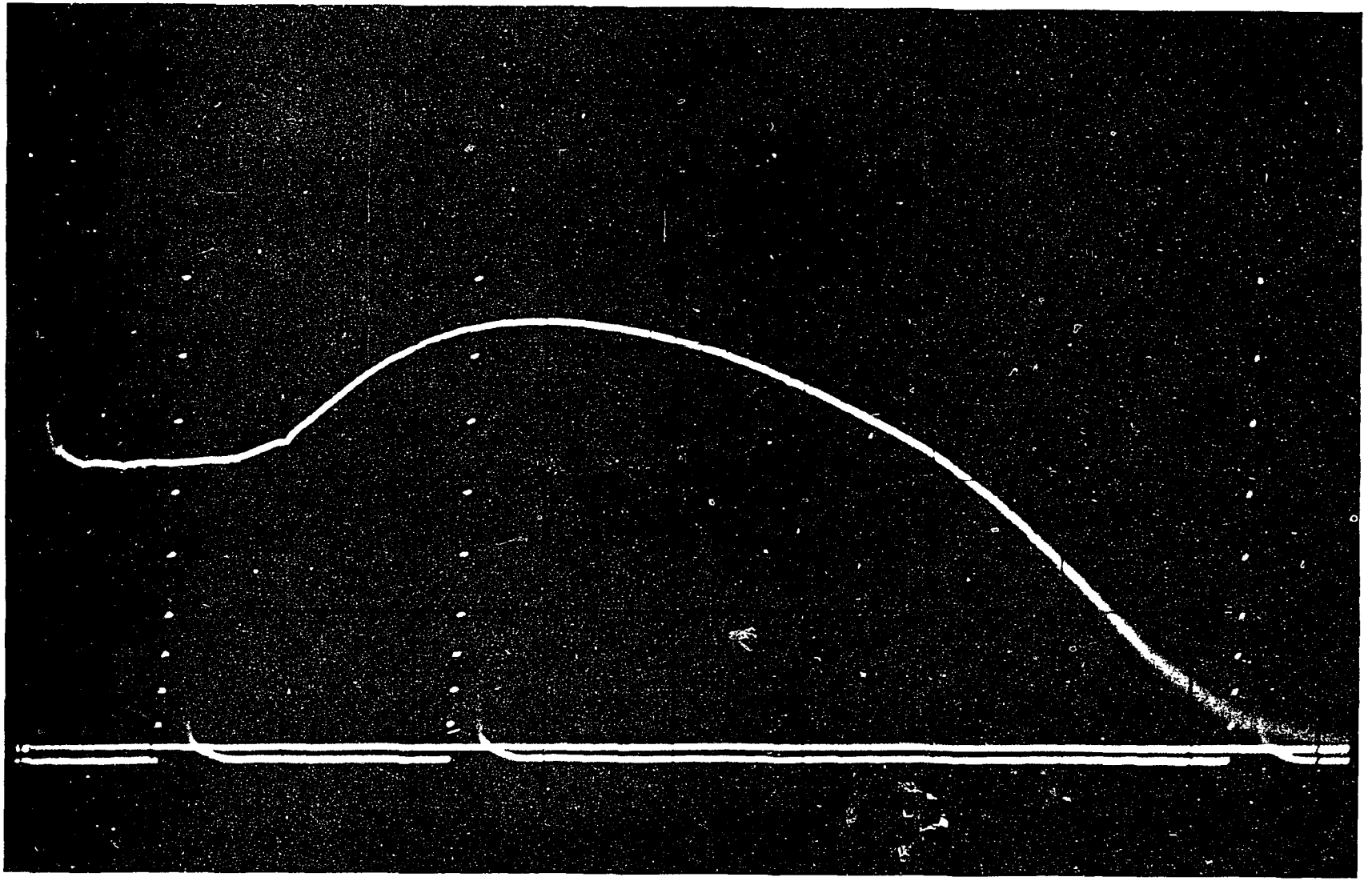

Fig. A-1. The fission cross section of ^{244}Cm, as determined by time of flight with the Persimmon event (Physics-6). Two detectors were used, at 55° and 90° to the neutron beam. Where the data deviate from one another, the higher values correspond to the 55° detector. Large solid circles are data obtained by D. M. Barton and P. G. Koontz (private communication).

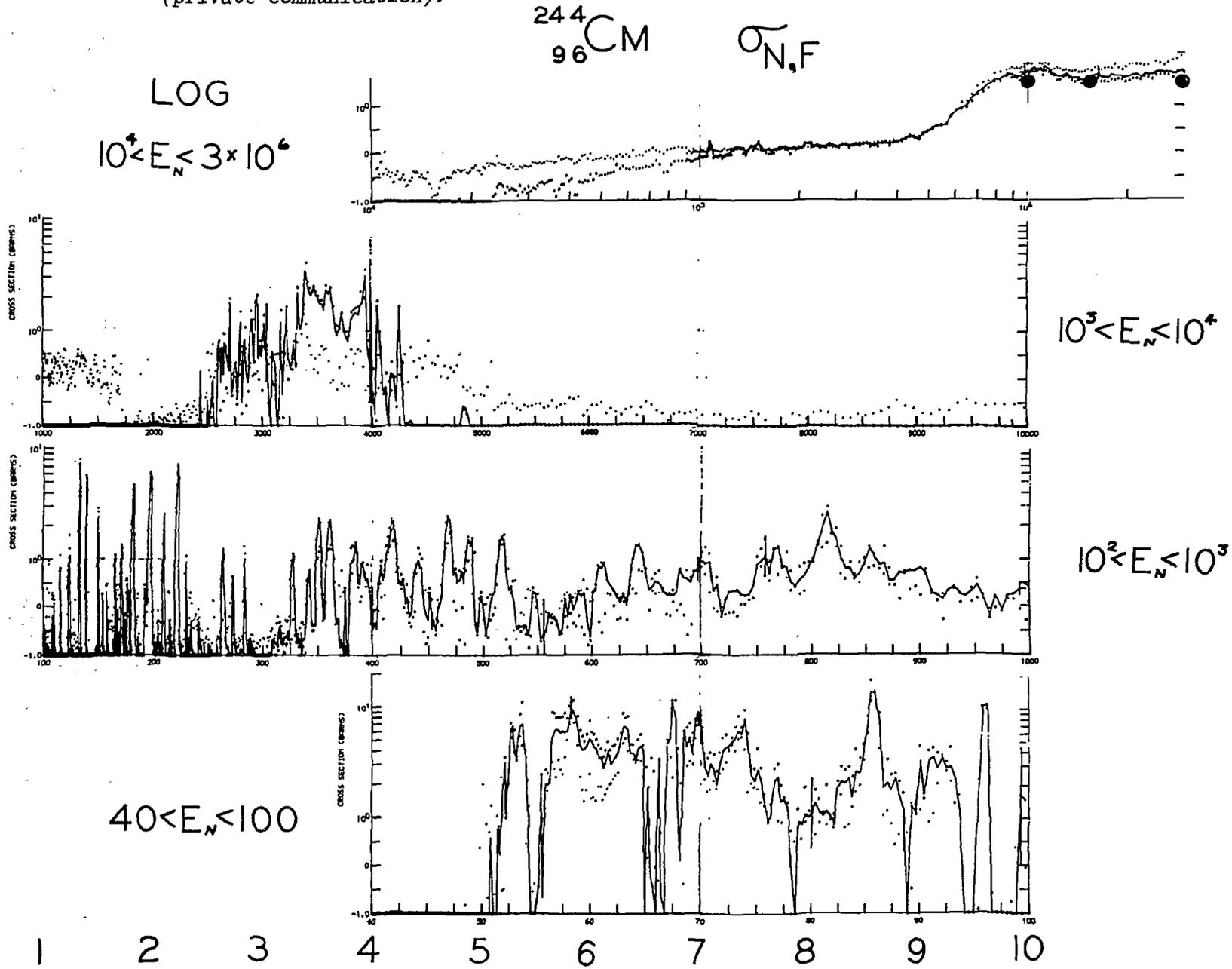

DATA NOT FOR QUOTATION

Fig. A-2. Neutron time-of-flight spectrum observed for a 1/v detector in the *Physics-8 event*. The flight path was 240 m; each major division corresponds to 500 μsec flight time. The 1/E spectrum extends to about 300 eV, the observed peak of the maxwellian is at 80 eV, and the neutron reaction rate falls below the rate in the 1/E spectrum at 25 eV. The neutron intensity in the beam is estimated at 6×10^{15} n/cm^2/sec at 1 keV, and 1.5×10^{16} n/cm^2/sec at 80 eV.

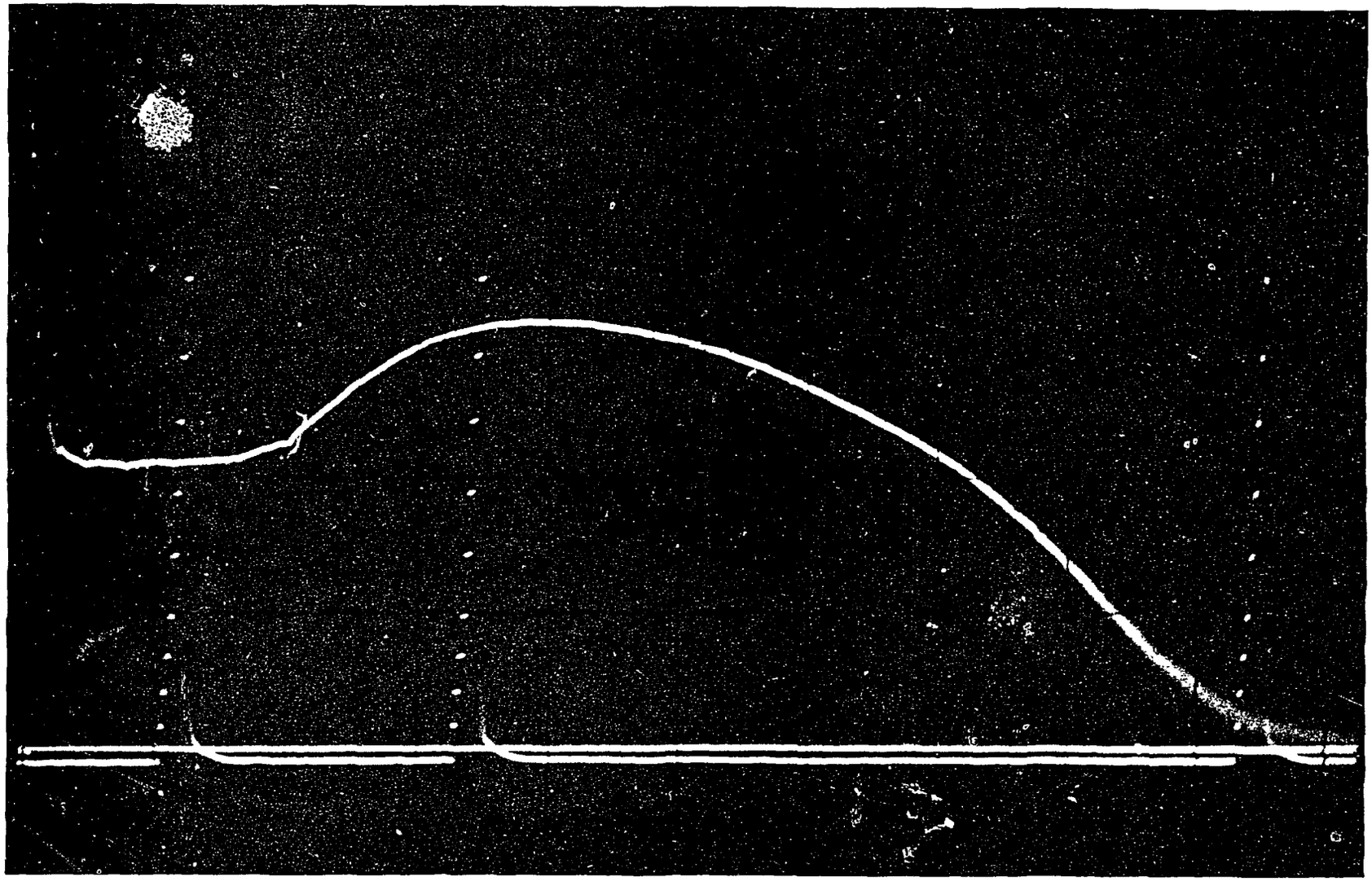

presumably corresponding to sub-barrier fission in these even-even non-fissile targets. Weak structure is also observed in the ^{238}U data, but there is a strong likelihood that the peaks are due primarily to neutron capture in the fission foil. The Moxon-Rae signal for the ^{238}U-^{197}Au wheel shows promise that the calibration of the Moxon-Rae detector against the absolute activity of the wheel can be accomplished for ^{238}U.

^{237}Np, ^{243}Am, ^{249}Bk. A large number of sub-barrier fission resonances can be observed in these odd-even non-fissile targets.

^{239}Pu. Fission, capture, and differential flux signals look reasonably good. It is not possible to evaluate the signals from the scattering detectors by casual inspection. Signals from the blank do show some evidence of "cross-talk," or slight sensitivity of a given detector to a large sample located elsewhere in the stack.

^{243}Cm, ^{245}Cm, ^{247}Cm, ^{249}Cf. Very large signals were observed, with a resonance spacing resembling ^{233}U for these fissile targets.

^{244}Cm, ^{246}Cm, ^{248}Cm, ^{252}Cf. All appear to show sub-barrier fission in 10-30 resonances. The $^{244}Cm/^{246}Cm$ capture signal shows some 20-30 large resonances. It is also expected that reasonably adequate total cross sections can be extracted from flux monitors above and below the sample.

^{253}Es. The small size of the sample (~ 5 μg) and of the signal make conclusions drawn from casual inspection highly speculative. Structure can be observed, and may be due to the ^{253}Es target material. However, 3 of 5 stainless steel blanks in the fission stacks also show weak structure in the low resonance region.

3. Polarization of the Neutron Beam on Physics-8 (G. Keyworth, J. Lemley, G. Ohlsen, J. Jackson, J. Hill)

Prior to actually attempting experiments utilizing polarized targets in conjunction with a polarized neutron beam, it was decided to determine the feasibility of polarizing the intense neutron beam from an underground nuclear explosion.

The method used was to pass the neutron beam through a sample of polarized protons. The protons are in the water of hydration in single crystals of $La_2Mg_3(NO_3)_{12}\cdot 24H_2O$. Below ~50 keV neutron energy, the polarization of the transmitted neutron beam is very close in magnitude to that of the proton polarizer. This is due to the great difference in the singlet and triplet cross sections for formation of the compound system.

The protons were polarized by the solid effect or by dynamic

nuclear polarization. This technique involves inducing the simultaneous spin flip of an electron in the paramagnetic crystal and a proton. In our case, this was achieved by the application of 77 GHz power in a magnetic field of 20.3 kG. The entire sample is maintained at 1°K, at which temperature the proton relaxation time is ~1 hour. Proton polarizations on the order of 60% or greater are readily obtained with this technique. Although the crystals undergo a significant temperature increase from the intense neutron beam, it was predicted that the proton relaxation time would remain long compared to the few millisecond duration of the neutron burst.

The beam polarization system has now been tested, on the Physics 8 event, and, as far as is discernable from preliminary results, was entirely successful as a means of polarizing the neutron beam.

4. Radiative Capture Experiments on Physics-8 (M. V. Harlow, N. W. Glass, A. D Schelberg, J. H. Warren)

Gamma-ray yields from neutron capture in natural niobium and thorium were measured on the most recent nuclear explosion physics event, Physics-8. Three samples of thorium, two of niobium, beam monitor foils, and background samples were placed in the neutron beam ~248 m from the moderated source. Gamma-ray yields were measured by Moxon-Rae detectors placed near each of the capture samples. A preliminary look at all of the film records shows that the quality of the resonance capture data for both elements are probably as good as those taken for ^{238}U on the Petrel event (Physics-5). For example, resonances in niobium between 3 and 4 keV were clearly resolved.

5. Neutron Scattering and Capture Measurements on Physics-8 (M. M. Hoffman, W. L. Baird, G. B. Barber, G. J. Berzins, W. A. Biggers, J. H. Calligan III, M. R. Cates, R. E. Dorsey, and D. D. Phillips)

Neutron interactions with ^{103}Rh and ^{197}Au targets were measured by J-12 during the recent physics event at NTS. Our data analysis will yield (n,n) and (n,γ) cross sections from approximately 25 eV up to 100 keV. In addition, the (n,n), (n,γ), and (n,f) cross sections were measured for a ^{237}Np target. The beam was monitored via the $^{6}Li(n,\gamma)$ reaction and by ^{3}He neutron detectors.

6. MULTI, A Fortran Code for Least Square Fitting All Four Partial Cross Sections Simultaneously Using the Reich-Moore Multilevel Formalism (G. F. Auchampaugh)

MULTI[1] is a Fortran code which uses the Reich-Moore multilevel formalism[2] to extract the best set of resonance parameters from a weighted

[1] G. Auchampaugh, "Multilevel Code for Analyzing Cross-Section Data for Resonance Parameters Using a CDC 6600 Computer," WASH-1071 (1966).

[2] C. W. Reich and M. S. Moore, Phys. Rev. 111, 929 (1958).

least square fit to several sets of different partial cross-section data, such as fission and capture data. In the present version of MULTI all four partial cross sections can be handled simultaneously with very little increase in running time over that required for a fit to one set of partial cross-section data. This version also allows an arbitrary shaped resolution function, which can vary with energy, to be folded into the data.

Considerable effort has been spent in the last year to reduce the size and running time of the code and to improve the least square search routine. It is now possible to fit a fairly good size problem (200 data points with weights, 50 resonances, and 60 parameters) into less than 32K.

An example of a two fission-channel fit to some mock fission and total cross-section data is shown in Fig. A-3. The upper two plots represent the 0th iteration conditions. The bottom plots represent the conditions after 5 iterations. Running time was less than 4 minutes. Initial estimates of the parameters and the final parameters are summarized in Table A-1. The capture widths of the resonances were not iterated on. Notice that it is not necessary to apriori divide the total fission widths up into components nor to choose the relative signs of the products $(\Gamma_{n_\lambda}{}^{0}\Gamma_{f_i\lambda})^{1/2}$. The values of the partial fission components are not unique. What appears to be unique is the total fission width of each resonance.

TABLE A-1

	E_0(eV)	Γ_γ(mV)	$\Gamma_n{}^0$(mV)	Γ_{f_1}(mV)	Γ_{f_2}(mV)	Γ_f(mV)
Parameters used to generate "mock" data:						
	128.06	40	1.70	201	171	372
	131.39	40	0.19	-2.1	317	319
	141.73	40	2.14	265	13.9	279
	149.16	40	0.16	35.9	221	257
Initial guess parameters for zeroth iteration:						
	128.06	40	0.70	320	0	320
	131.39	40	0.09	200	0	200
	141.73	40	1.10	200	0	200
	149.16	40	0.20	300	0	300
Parameters after 5th iteration:						
	128.06	40	1.70	369	2	371
	131.39	40	0.19	216	102	318
	141.23	40	2.14	198	81	279
	149.16	40	0.16	25	231	256

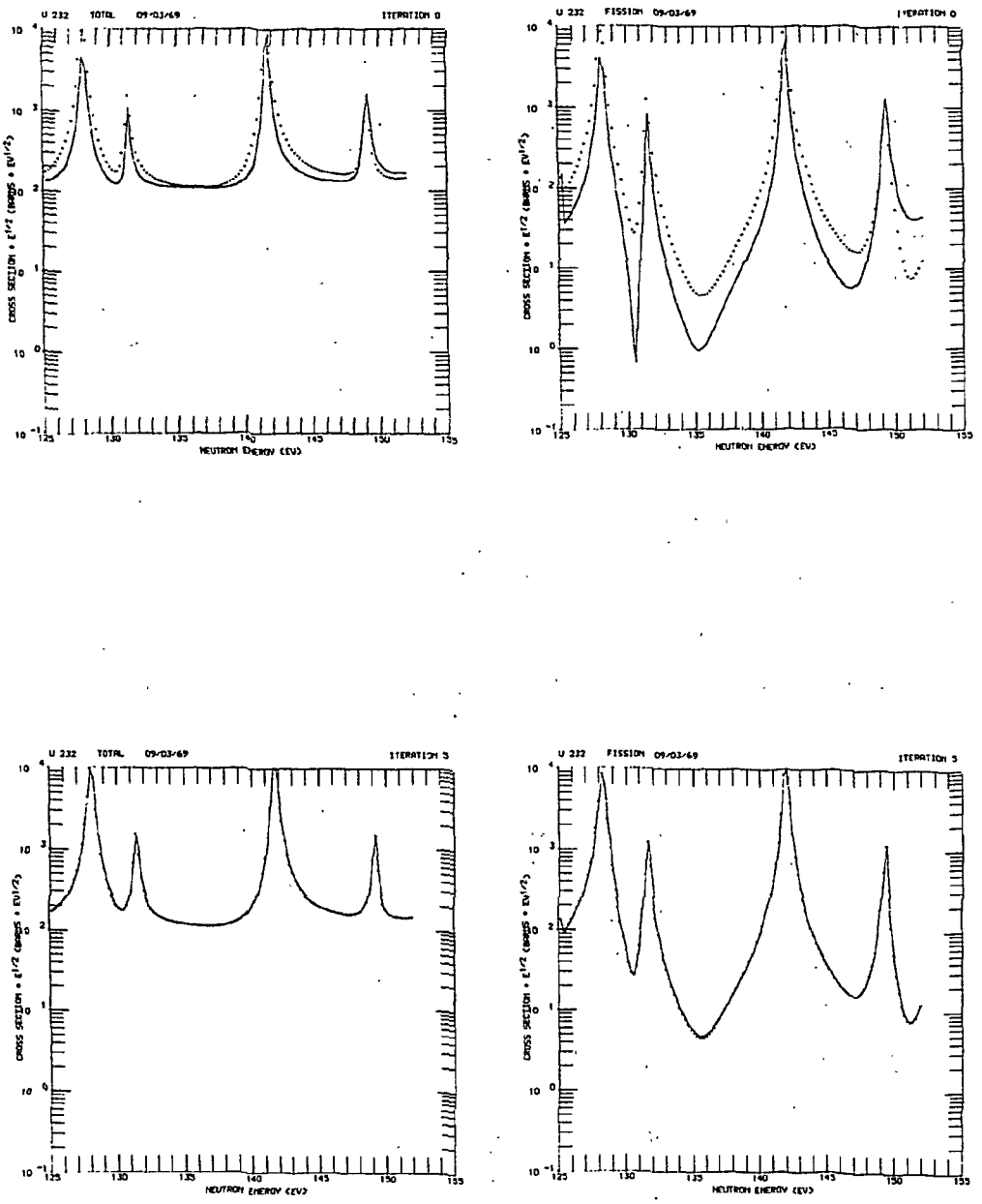

Fig. A-3. Comparison of zeroth iteration (top row) and fifth iteration (bottom row) results of the R-matrix least-squares fitting code MULTI. While only total and fission cross sections for four resonances were fitted in this test, the code is capable of simultaneously fitting up to four partial cross sections.

7. Magnetic Disc Recording on Physics-8 (A. P. Furnish, W. K. Brown, H. D. Arlowe,* and R. McAvoy*)

A small portion of the data obtained from LASL shot Physics-8 was recorded in magnetic form. This is a novel way of recording data, and a considerable departure from the conventional oscilloscope and moving photographic film method. This experiment was a proof of the magnetic recording method; no new or unusual data were to be recorded.

Frequency-modulation recording was used, with a rotating hard-surface magnetic disc as the recording medium. The disc turns at 3600 rpm and will record rf signals up to 6 or 7 MHz. The FM electronics used have a center frequency of 4.5 MHz and a deviation of ±33%. Signal-to-noise ratio of the overall system is about 100/1. Recording was done simultaneously on 5 tracks--3 data and 2 clock tracks. Signals from ^{235}U, ^{6}Li, and a blank foil were recorded on the data tracks. Amplitude stair-step calibrations were put on the signal channels milliseconds after the event.

Figure A-4 is a plot of a portion of the data from the ^{235}U detector. The plot was made by using a display converter that samples the data on the disc once/revolution. The data will also be sampled in this manner, then fed through a relatively low speed A-D converter, and put on magnetic tape in digital form, eliminating the tedious film reading process used with conventional photographic film methods.

No unusual background signal was noted from the blank foil, and no magnetic effects were observed. The experiment appears to have been a complete success. It is hoped that this type of equipment may eventually replace our oscilloscope-camera system. Recorders are now available with signal/noise ratios of 300/1, bandwidth of D-C to 3 MHz, and at a cost of about $1500/channel.

B. VAN DE GRAAFF NEUTRON STUDIES

1. Polarization Measurements of Neutrons Elastically Scattered from Deuterium and Tritium (J. C. Hopkins, E. C. Kerr, J. T. Martin, A. Niiler, J. D. Seagrave, R. H. Sherman, and R. K. Walter†)

Collection of data in the experiment was completed in April, 1969. Twenty-two-MeV polarized neutrons from the $T(d,n)^{4}He$ reaction were scattered from approximately one mole of liquid tritium and from liquid

*The experiment was done jointly with Sandia Laboratory in Albuquerque. H. D. Arlowe and R. McAvoy from Sandia provided the recorder and necessary technical support, and W. K. Brown and A. P. Furnish of LASL set up and provided the balance of the data-gathering and timing system.

†Associated Western Universities.

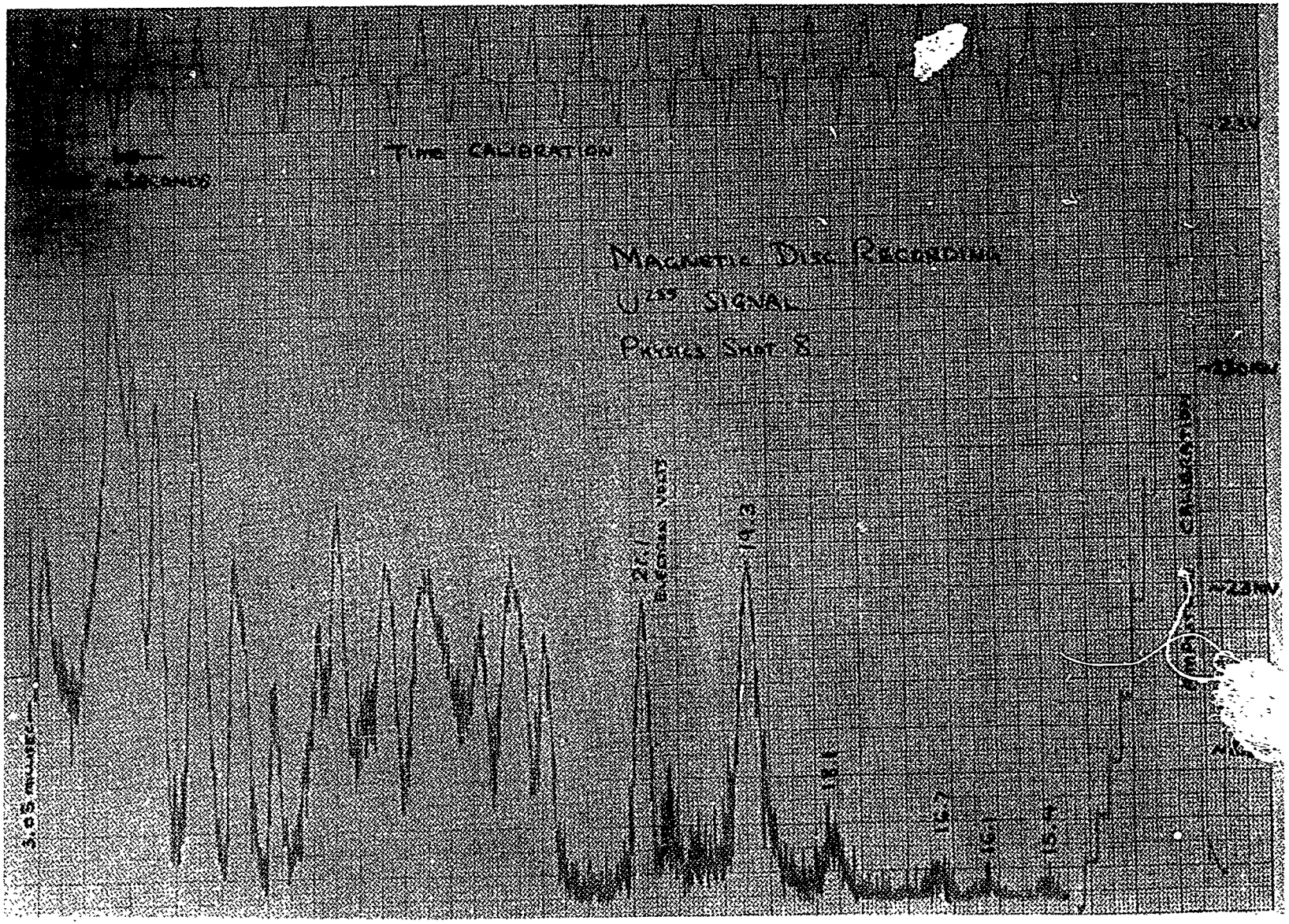

Fig. A-4. Read-out of magnetic disc record of ^{235}U fission rate observed on the Physics-8 event, from 3- to 5-msec flight time. Time calibration, amplitude calibration, and the energies of several prominent resonances in ^{235}U are indicated.

deuterium. The time-of-flight method and neutron-gamma-ray discrimination in a two-detector system were used to measure the asymmetry for laboratory angles from 40° to 118.5°.

Analysis of the data and errors has proceeded since that time with the use of two computer codes written specifically for that purpose. FLZEIT is a data reduction code incorporating subroutines to provide options for handling left and right detectors separately if desired, linear or logarithmic plotting, etc. The program calculates for any number of foreground, background run pairs, the number of counts in channel I, the standard deviation, and the summations of counts and squares of deviations. DSCHNIT is a short program for integrating by the trapezoidal method,

$$\mathrm{DSNIT} = \int_a^b f(x)\,dx \Big/ \int_a^b g(x)\,dx,$$

for any functions f(x) and g(x). This program was used to determine the effective angular position of the scattering sample.

For tritium the measured asymmetry is negative for angles forward of 95° (lab) and large and positive for angles larger than $\sim 100^{\circ}$ (lab). The extrema of the n-T polarization based on the incident neutron polarization of 40% are -59% at 85° (lab) and +90% at 110° (lab). For deuterium the measured asymmetry is negative for laboratory angles between 40° and 73° and is positive at 105°.

2. Neutron-Alpha Particle Elastic Scattering Cross Sections (A. Niiler, K. Walter, J. T. Martin, J. C. Hopkins, J. D. Seagrave, G. Kerr, and R. Sherman)

Angular distributions of neutrons elastically scattered from alpha particles are being measured for incident neutron energies of 17.7, 20.9, and ~23 MeV in the range of laboratory angles $20^{\circ} < \theta_L < 140^{\circ}$. Scattered neutron times of flight are measured by two similar detector assemblies used in previous cross sections and polarization work. Approximately one mole of liquid ^{4}He is used as the scattering sample. This work is carried on at the buncher facility of the vertical accelerator at P-9.

These measurements are intended to check the accuracy of the forward angle cross section extrapolations of earlier n-α scattering data in which the recoil α particles' energy distribution is recorded.

3. The Elastic Channel in Nucleon-Deuteron Scattering (J. D. Seagrave)

A report is available* in which the final n-D scattering lengths are given as $^4a = 6.13 \pm 0.04$ fm and $^2a = 0.15 \pm 0.05$ fm; the experimental bases for these results are described. The difficulty of extracting the s-wave phase shifts at low energies is illustrated, and preliminary error limits at 0.1 and 0.2 MeV are given. Cubic spline data fitting is outlined mathematically and illustrated graphically, and applied to the representation of n-P and n-D total cross sections for energy up to 1 GeV; the n-n difference between the n-D and n-P spline fits is also presented. Tables of the spline representation of the n-D total cross section, the numerical data, and of p-D total cross sections at high energy are provided. The present status of phase-shift analysis is found unsatisfactory, though both experiment and theory appear adequate; an energy-dependent analysis is called for. The suggestion that there may be undetected fluctuations in the n-P and n-D total cross sections is examined in detail, with negative results.

Ninety-three sets of differential cross sections between 0.1 and 2000 MeV are presented in a uniform, computer-generated, graphical compilation, using cubic spline fitting. The spline fits are represented in oblique three-parameter displays in five logarithmic decades of energy. The 100-1000 MeV decade is found wanting of adequate experimental coverage. New Los Alamos n-D data at 5.55, 7, 8, 9, 18.55, 20.5, and 23 MeV are presented, and the extensive unpublished p-D data between 1 and 11.5 MeV from Rice and Wisconsin are included in the compilation. Unpublished or inaccessible high-energy small-angle or isolated cross sections are also tabulated. New Los Alamos results for n-T polarization at 22 MeV are presented, and the development of a superconducting solenoid for neutron spin precession, and of "supercollimation" of negative ion beams are illustrated.

4. Gamma-Production Cross Sections (D. M. Drake and J. C. Hopkins)

Gamma-production cross sections for aluminum at 4, 6, and 7.5 MeV are listed in Tables B1 to B3. This is the last element of the gamma-production measurements and a LA report which includes all the previously analyzed data is being prepared. Measurement of the cross section for fast-neutron excitation of the 4.44-MeV level of ^{12}C has been extended to 14 MeV.

---

*Invited paper presented at the International Conference on the Three-Body Problem in Nuclear and Particle Physics, 8-10 July 1969, Univ. of Birmingham, England.

TABLE B-1

Aluminum

Separable Gamma-Ray Energies (MeV)	4.0-MeV Neutrons ($d\sigma/d\Omega$) $\theta=55^{\circ}$
0.84	7.1
1.01	16.3
1.72	8.7
2.21	12.9
2.73	1.6
3.00	12.8
3.67	0.6

TABLE B-2

Aluminum

Gamma-Ray Energy Interval (MeV)	$d\sigma/d\Omega dE$(mb/sr MeV) Neutron Energy = 6.0 MeV			
	$\theta=39^{\circ}$	$\theta=55^{\circ}$	$\theta=72^{\circ}$	$\theta=90^{\circ}$
0.50-0.75	21	18	17	9
0.75-1.00	56	49	62	39
1.00-1.25	79	78	77	79
1.25-1.50	15	9	14	9
1.50-1.75	35	35	35	32
1.75-2.00	20	14	13	13
2.00-2.25	83	85	78	80
2.25-2.50	20	7	16	10
2.50-2.75	11	14	12	10
2.75-3.00	24	12	15	17
3.00-3.25	68	61	63	64
3.25-3.50	14	14	14	11
3.50-3.75	8	7	8	7
3.75-4.00	7	7	7	7
4.00-4.25	6	6	5	5
4.25-4.50				
4.50-4.75				

Separable Gamma-Ray Energies (MeV)	$d\sigma/d\Omega$ (mb/sr)			
	$\theta=39^{\circ}$	$\theta=55^{\circ}$	$\theta=72^{\circ}$	$\theta=90^{\circ}$
0.845	9.6	10.4	10.1	9.1
1.01	20.2	20.8	21.0	19.8
1.72	10.2	10.1	10.2	9.5
2.21	21.4	22.1	22.0	18.6
2.73	4.0	2.9	3.3	
3.00	20.3	19.5	17.7	18.1

TABLE B-3

Aluminum

Gamma-Ray Energy Interval (MeV)	$d\sigma/d\Omega dE$(mb/sr MeV) Neutron Energy = 7.5 MeV			
	$\theta=39^\circ$	$\theta=55^\circ$	$\theta=72^\circ$	$\theta=90^\circ$
0.50-0.75	30	27	22	14
0.75-1.00	51	57	49	50
1.00-1.25	78	82	75	74
1.25-1.50	18	13	11	9
1.50-1.75	26	29	25	25
1.75-2.00	24	24	22	23
2.00-2.25	52	58	51	54
2.25-2.50	48	49	46	43
2.50-2.75	20	23	16	19
2.75-3.00	22	26	26	25
3.00-3.25	59	61	58	59
3.25-3.50	15	18	15	14
3.50-3.75	15	12	10	11
3.75-4.00	16	18	16	16
4.00-4.25	12	14	16	15
4.25-4.50	10	12	10	10

Separable Gamma-Ray Energies (MeV)	$d\sigma/d\Omega$ (mb/sr)			
	$\theta=39^\circ$	$\theta=55^\circ$	$\theta=72^\circ$	$\theta=90^\circ$
0.84	9.9	10.2	8.7	8.7
1.01	20.3	19.5	18.5	18.7
1.72	10.2	9.9	9.0	9.6
2.21	22.9	21.9	18.7	19.5
2.73	3.5	3.4	3.7	4.1
3.00	18.9	16.8	15.4	15.1
3.15	4.3	4.7	4.2	4.0

C. THERMAL NEUTRON CAPTURE GAMMA-RAY STUDIES

1. Energy Levels of ^{175}Lu (M. M. Minor,* R. K. Sheline,* E. B. Shera, and E. T. Jurney

The gamma-ray spectrum from thermal-neutron capture in enriched targets of ^{175}Lu has been studied in four energy intervals using Ge(Li) and Si(Li) detectors. Twenty transitions in the energy region between 5.3 and 6.0 MeV have been observed in ^{175}Lu with a Ge(Li) detector operated in conjunction with a large NaI detector as a two-quantum escape spectrometer. Low-energy gamma radiation has been measured from 20-1000 keV in both singles and gamma-gamma coincidence experiments. Data from the reaction ^{175}Lu(d,d') have been analyzed. The combination of results of these experiments with those previously reported in the literature, lead to the level scheme shown in Fig. C-1, which involves the following spectroscopic assignments (denoted by band head energy in keV, K^{π}, and Nilsson configuration): ground state, $7^-[404 + 514]$; 126.5, I = 1, $0^-[404 - 514]$; 198.0, $1^+[404 - 624]$; 390.2, $1^-[404 - 512]$; 662.0, $3^-[404 - 510]$; and 791.5, $4^-[404 + 510]$. The neutron separation energy of ^{175}Lu is determined to be 6293 ± 4 keV.

2. ^{209}Bi(n,γ)^{210}Bi (E. T. Jurney)

The capture gamma-ray spectrum from Bi has been completely redone, since our older data were badly contaminated by gamma rays from target impurities. Table C-1 lists the observed primary transitions, the corresponding level excitation energies, photon intensities, the levels observed in the charged-particle experiments of Erskine[1] and J assignments proposed by Erskine, and by Kim and Rasmussen.[2]

3. Coincidence Study of the ^{209}Bi(n,γ)^{210}Bi Reaction (E. B. Shera)

During the past quarter coincidence data from the ^{209}Bi(n,γ)^{210}Bi reaction has been collected. Analysis of this data is still in progress. However, preliminary results suggest either that the presently accepted spin sequence in ^{210}Bi arising from the $g_{9/2}h_{9/2}$ configuration is seriously in error, or that the most intense primary transition in the high energy capture spectrum has E2 multipolarity. We hope that new data now being collected using thermal (E. T. Jurney) and 2-keV neutrons (R. C. Greenwood, Idaho Nuclear Corp.) will resolve this dilemma.

---

*Florida State University.

[1] J. R. Erskine, W. W. Buechner, and H. A. Enge, Phys. Rev. 128, 720 (1962).

[2] Y. E. Kim and J. O. Rasmussen, Nucl. Phys. 47, 184 (1963).

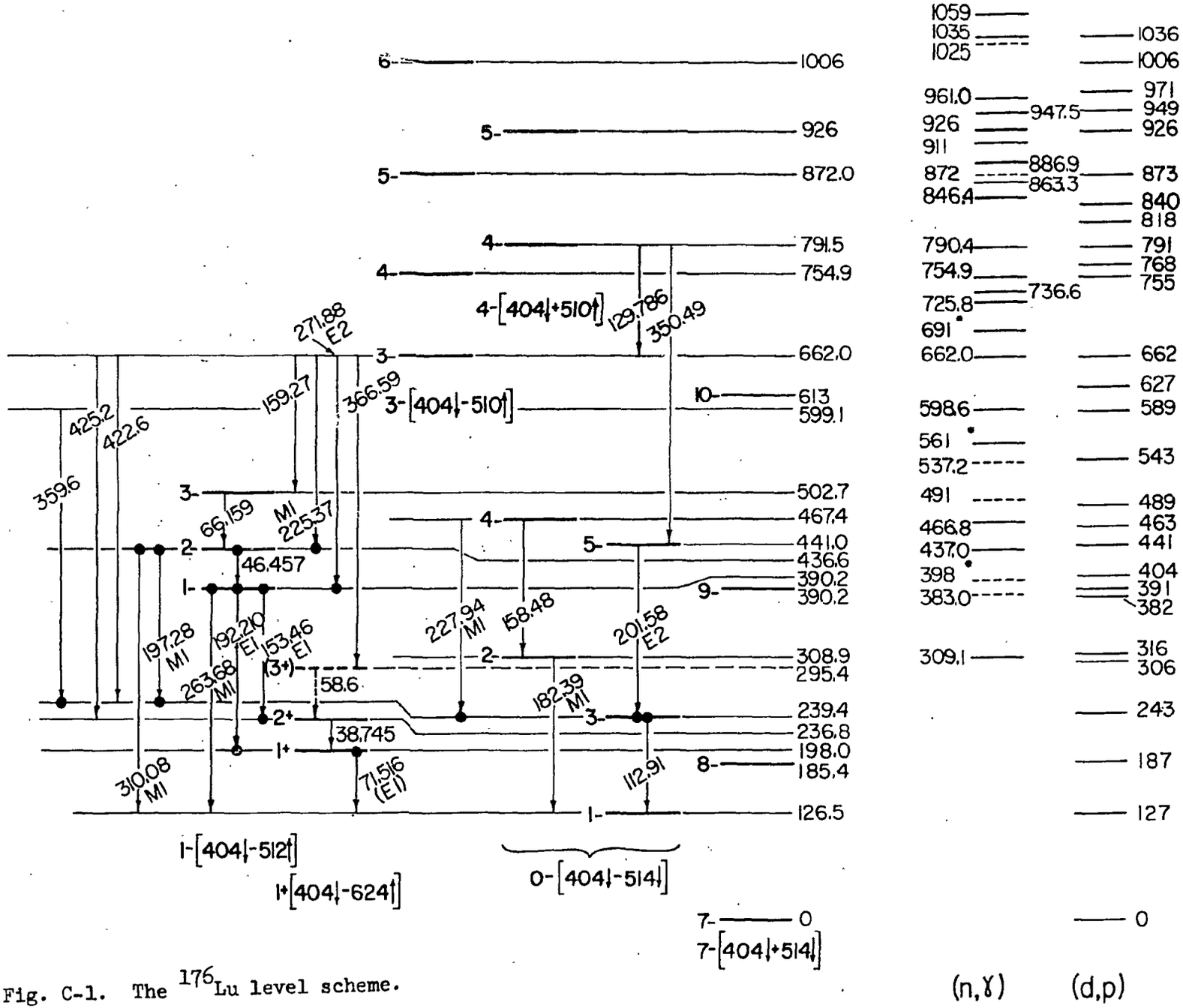

Fig. C-1. The ^{176}Lu level scheme.

TABLE C-1

E_γ(keV)	E_{ex}(keV)	$I_\gamma(\gamma/10^2 n)$	$E_{(d,p)}$(keV)	J
			0	1
			47	0
			268	9
4284.9	319.7	0.7	320	2
4256.8	347.9	4.6	347	3
4171.1	433.5	34.6	433	5,7
4165.5	439.2	4.4		
4101.8	502.8	17.2	501	4
4054.5	550.1	28.7	546	6
			581	8
			672	
			912	
3632.8	971.8	2.8		
3610.6	994.1	0.4		
3429.4	1175.2	0.4	1172	
3407.9	1196.7	0.5		
3396.0	1208.6	3.6		
3356.5	1248.1	3.7		
			1325	
3268.8	1335.8	0.6		
3230.7	1373.8	0.7	1372	
3214.5	1390.1	1.4		
3141.5	1463.2	0.7	1460	
3081.3	1523.4	1.8	1517	
			1577	2
2898.2	1706.5	1.8		
2828.3	1776.3	4.3		
			1916	
2624.4	1980.3	3.6	1972	
2598.2	2006.5	3.5		
2570.6	2034.1	0.7	2027	
			2075	
2505.2	2099.4	4.7		
			2102	
			2138	
			2173	
			2235	
			2517	4
			2572	5

4. Nuclear Levels in ^{177}Lu and ^{175}Lu (M. M. Minor,* R. K. Sheline,* and E. T. Jurney)

One- and three-quasi particle states have been investigated in ^{175}Lu and ^{177}Lu using (d,p), (d,t), and (n,γ) reactions on isotope-separated targets of ^{176}Lu. The (d,p) and (d,t) studies utilized 12-MeV deuterons and a broad range magnetic spectrograph; the (n,γ) studies used Ge(Li) and Si(Li) spectrometers. The ground state one-quasiparticle band $7/2^+[404]$ through the $17/2^+$ member and 4 tentative three-quasiparticle bands are observed in ^{175}Lu. Members of the following one-quasiparticle bands are observed in ^{177}Lu: $7/2^+[404]$ ground state, $9/2^-[514]$, $5/2^+[402]$, and $1/2^+[411]$; in addition the following three-quasiparticle bands are observed in ^{177}Lu: $23/2^-[p404 + n514 + n624]$, $11/2^+[p514 + n624 + n514]$, $13/2^+$ and $15/2^+[p404 + n514 \pm n510]$, K + 2 gamma vibration built on the $7/2^+[404]$ ground state, tentatively $17/2^+[p404 + n514 + n512]$ and tentatively $13/2^+$ and $15/2^+[p404 + n514 \pm n521]$. The neutron separation energy of ^{177}Lu has been measured as 7072.7 ± 2.0 keV and the Q value for the reaction ^{176}Lu(d,t)^{175}Lu as -25 ± 15 keV. Identification of differential cross-section patterns to various members of three-quasiparticle rotational bands in both the (d,p) and (d,t) reactions indicates that this spectroscopic tool is also valuable for three-quasiparticle states. A sum rule is suggested and experimentally evaluated for the total differential cross sections in the (d,p) reaction to rotational members of the two different bands resulting from parallel and antiparallel coupling of the last neutron.

D. CHARGED-PARTICLE STUDIES

1. Cross Sections for Several (n,f) Reactions from (t,pf) Experiments (J. D. Cramer and H. C. Britt)

Experimental fission probabilities determined from direct-reaction-fission data can be used along with a Hauser-Feshbach calculation to determine the neutron induced fission cross section for various short-lived target nuclei. Specifically, the di-neutron transfer in the (t,pf) reaction on relatively stable even-even targets allows one to measure fission probabilities of neutron rich even-even nuclei which could not be obtained by neutron-induced fission experiments. The lifetimes of the corresponding neutron targets are far too short for the presently available experimental techniques.

It is assumed that in the limited region of energy from 0.5 to 2.0 MeV the formation cross section σ_n of the compound nucleus by neutron capture can be determined using a Hauser-Feshbach calculation with the appropriate optical model transmissions. With the measured fission probability P_f from (t,pf) results the computed (n,f) cross section $\sigma_{n,f}$

*Florida State University.

can be written as

$$\sigma_{n,f} = \sigma_n \times P_f.$$

This very simple picture assumes that similar angular momentum states are populated by both fast neutrons and the (t,p) reaction which is true only for neutron energies in excess of ~ 1.5 MeV.

A reasonable test of this method for determining (n,f) cross sections can be performed by comparing the computed values from (t,p) results with the measured values where they exist. The results of this comparison for $^{235}U(n,f)$ and $^{241}Pu(n,f)$ are shown in Table D-1 for several incident neutron energies E_n.

The remaining cross sections determined by this technique and for which no (n,f) data are available are listed in Table D-2.

TABLE D-1

Comparison to Experimental Data

E_n(MeV)	$\sigma(n,f)$*	$^{235}U(n,f)$ $\sigma_n \times P_f$†	Ratio	$\sigma(n,f)$**	$^{241}Pu(n,f)$ $\sigma_n \times P_f$††	Ratio
0.5	1.175	1.75	1.49	1.60	1.91	1.12
0.6	1.157	1.65	1.43	1.58	1.77	1.12
0.8	1.20	1.51	1.26	1.60	1.67	1.04
1.0	1.22	1.42	1.16	1.65	1.60	0.97
1.25	1.24	1.32	1.06	1.70	1.68	0.99
1.5	1.26	1.26	1.00	1.80	1.61	0.89
1.75	1.28	1.26	0.98	1.80	1.48	0.92
2.00	1.29	1.23	0.95	1.80	1.45	0.81

*B. C. Diven, EANDC(US)-96 "L" (February 1, 1967).

†H. C. Britt et al., Phys. Rev. 175, 1525 (1968).

**BNL-325.

††J. D. Cramer, Los Alamos Scientific Laboratory Report, LA-4198 (1969).

TABLE D-2

Fission Cross Sections for (n,f) Reactions

Cross Sections (barns) for Listed Targets

E_n(MeV)	^{231}Th	^{233}Th	^{237}U	^{239}U	^{243}Pu
0.5	0.82	0.22	0.90	0.78	1.78
0.6	0.41	0.23	0.89	0.73	1.65
0.8	0.30	0.16	0.78	0.67	1.42
1.0	0.25	0.14	0.69	0.58	1.36
1.25	0.23	0.12	0.64	0.57	1.38
1.50	0.20	0.11	0.60	0.50	1.35
1.75	0.18	0.11	0.60	0.50	1.25
2.00	0.19	0.11	0.60	0.47	1.19

2. Fission Isomer Studies (H. C. Britt, S. C. Burnett, B. H. Erkkila, and W. E. Stein)

The first data obtained from the experiment designed to study short-lived fission isomers by observing their decay between beam pulses on the cyclotron have been analyzed. The decay of Pu fission isomers formed by (α,2n) reactions on ^{233}U, ^{234}U, ^{235}U, ^{236}U, and ^{238}U targets and the (α,3n) reaction on ^{238}U have been observed. Table D-3 summarizes information concerning the reactions studied. Reading from left to right, there are tabulated the target, the energy of the incident alpha particle, the isomer formed through the (α,2n) reaction, an estimate of the excitation energy left in the isomeric compound nucleus after the emission of

TABLE D-3

Target	α Energy (MeV)	Isomer Formed (α,2n)	E* (MeV)	Prob. of Evaporating 2n	Isomer Formed (α,3n)	E* (MeV)	Prob. of Evaporating 3n
U-233	23.5	Pu-235	2.14	.02			
U-234	23.5	Pu-236	2.66	.04			
U-235	23.5	Pu-237	3.20	.06			
U-236	23.5	Pu-238	3.67	.11			
U-238	23.5	Pu-240	4.57	.28			
U-233	28.4	Pu-235	7.04	.02	Pu-234	-.19	.002
U-234	28.4	Pu-236	7.56	.04	Pu-235	-.80	.004
U-235	28.4	Pu-237	8.10	.06	Pu-236	1.25	.01
U-236	28.4	Pu-238	8.57	.11	Pu-237	.57	.02
U-238	28.4	Pu-240	9.47	.28	Pu-239	1.95	.11

2 neutrons, an estimate of the probability of evaporating 2 neutrons from the compound nucleus, and similar information about the $(\alpha, 3n)$ reaction.

The value of E^* was calculated by subtracting from the incident alpha energy corrected for kinematics, the Q-value of the reaction, the binding energy of 2 or 3 neutrons, and an estimate of the kinetic energy carried away by the evaporated neutron (~1 MeV/neutron). The probability of evaporating x neutrons strongly influences the production of the isomeric state. Estimates of the probability are based on published values of Γ_n/Γ_f derived from photofission and spallation data.

If the isomeric well is 2-3 MeV above the ground state, these calculations would indicate that for an alpha energy of 23.5 MeV, the reactions on all five U targets are $(\alpha, 2n)$. At an alpha energy of 28.4 MeV, the reactions still appear to be $(\alpha, 2n)$ except for the ^{238}U target where there may be enough energy available to form the ^{239}U isomer through the $(\alpha, 3n)$ reaction.

In Table D-4, a summary of preliminary results is presented. The first column is a best guess of the isomer formed for a given target and alpha energy. The second column is an estimate of the number of isomeric compound nuclei produced which decay by fission. Care was taken to assure that the isomer fission data were not contaminated with events that occurred due to a beam tail or from neutron background. An estimate of the error in the N_{isomer} is less than 20% in all cases except perhaps in the ^{240}Pu case where a short isomer half-life (~4.6 nsec) has been observed. Since the number of isomers formed per unit channel (time) in this case increases rapidly as the prompt peak is approached, a small error in the determination of the position of the beam in time could produce a large error in the calculation of N_{isomer}.

Column 3 is a tabulation of the number of prompt fission events (accurate to ~10%) for which both fragments were detected. In the next column is the ratio of fission isomers to prompt fission, σ_I/σ_{pf} $(x10^{-6})$. Of primary importance is σ_I/σ_{2n}, the ratio of fission isomers to the production of the ground state through the evaporation of 2 neutrons. We have a measure of σ_I/σ_{pf} but no direct knowledge of σ_{2n}. If σ_c is the cross section for the formation of a compound nucleus in the alpha bombardment, then:

$$\sigma_{2n} = \sigma_c \left(\frac{\Gamma_n}{\Gamma_f + \Gamma_n}\right)_{1n} \left(\frac{\Gamma_n}{\Gamma_f + \Gamma_n}\right)_{2n} \cdots\cdots = P\sigma_c \qquad (1)$$

P is the probability of evaporating 1, 2, or 3 neutrons and is tabulated in Table D-3. Since

TABLE D-4

	Isomer Formed	N_{isomer}, Fission Isomers Produced	pf, Prompt Fissions Produced ($x10^6$)	N_{isomer}/pf ($x10^{-6}$)	σ_I/σ_{2n} ($x10^{-4}$)	σ_I/σ_{3n} ($x10^{-4}$)	Half-Life (nsec)
23.5 MeV	^{235}Pu	120	58	2.1	1.0	--	--
	^{236}Pu	120	183	.7	.2	--	--
	^{237}Pu	2500	187	13.4	2.1	--	80 ± 15
	^{238}Pu	890	257	3.5	.3	--	25 ± 10
	^{240}Pu	5500	302	18.2	.5	--	4.6 ± .3
28.4 MeV	^{235}Pu	230	277	.8	.4	--	--
	^{236}Pu	200	508	.4	.1	--	--
	^{237}Pu	590	257	2.3	.4	--	50 ± 20
	^{238}Pu	430	451	1.0	.1	--	--
	^{239}Pu	4000	319	12.5	--	1.0	>100

$$\sigma_{2n} = P\sigma_c = \sigma_c - \sigma_{pf}, \tag{2}$$

we can write

$$\frac{\sigma_I}{\sigma_{2n}} \simeq \frac{\sigma_I}{\sigma_{pf}} \left(\frac{1 - P}{P}\right). \tag{3}$$

The fission isomer half-lives which can be measured with some statistical reliability, are listed in the last column of Table D-4. There are two determinations of the half-life of ^{237}Pu for which the errors overlap.

E. INSTRUMENTATION AND METHODS

1. Neutron Monochromator Crystals (R. G. Wenzel)

In order to obtain a reasonable compromise between beam intensity and spatial and energy resolution in a 3 axis neutron spectrometer, it is necessary to use collimators which transmit a slightly divergent neutron beam. A typical divergence is of the order of 0.5°. To obtain the maximum possible beam intensity for a given resolution, it is necessary to use a monochromator with a mosaic distribution which matches the beam divergence. In the past we have specified acceptable mosaic distributions as part of the specifications in requests for bids when we were trying to purchase monochromator crystals. These specifications had to be very tolerant, as suppliers had no means for controlling mosaic distributions of crystals produced. We were, in effect, trying to choose the best of what was available.

Recently there have been several successful attempts to broaden the mosaics of selected crystals. Following Brockhouse[1] we have broadened the mosaic of a copper single crystal from 0.09° to 0.43°. The technique involves successive bending and flattening on a press at about 10,000 psi. This has resulted in an increase of 68% in beam intensity, in the spectrometer configuration as used in the argon-36 experiment.

Work is currently in progress to broaden the mosaic distribution of a test germanium crystal, using a technique described by Dolling[2] in which the crystal is compressed approximately 1% at 775°C. The mosaic has been increased from 0.03° to 0.14° so far.

---

[1] B. N. Brockhouse, G. A. deWit, and E. D. Hallman, Neutron Inelastic Scattering (IAEA Symposium, 1968) Vol. II, 259.

[2] G. Dolling and H. Nieman, Nucl. Instr. and Meth. 49, 117 (1967).

Another variable influencing the efficiency of neutron monochromators is the thickness. The optimum thickness is dependent upon the mosaic distribution. Using criteria developed by Popovici[3] for thickness and mosaic spread, a single crystal of magnesium has been ordered. The techniques developed in broadening the mosaics of copper and germanium are expected to be of help in obtaining an optimum mosaic for magnesium.

2. Capture Gamma-Ray Coincidence Experiment (E. B. Shera)

Uncertainty in the correspondence between energy and channel address of the pulse-height analysis system presents a major obstacle in the precise determination of gamma-ray energies with Ge(Li) detectors. In the past we have tried to calibrate this correspondence function by recording the response of the analysis system to a series of equally spaced pulse amplitudes derived from a precision pulser. With this method, values of the response function are obtained for only a few discrete input pulse amplitudes and an estimate of the response to all other amplitudes must be derived from these values. Recently, a design for a highly linear ($<0.005\%$) sliding pulser has become available.[4] Such a sliding pulser permits determination of the system response for all values of input pulse amplitude. Preliminary results using this new technique indicate that gamma-ray energies can now be routinely determined with an uncertainty less than 50 eV at 500 keV and 200 eV at 5 MeV. This represents a factor of 2-5 improvement over previous methods and should make the interpretation of capture gamma-ray data, which frequently relies on precise energy loops, considerably easier.

3. Liquid Fuel High Intensity Neutron Sources (L. D. P. King)

In the category of disposable core fast burst reactors work on a small scale is continuing to demonstrate the feasibility of using uranyl sulfate fuel under the operating conditions computed possible in the LEPR (Liquid Excursion Pulsed Reactor) concept. Experiments with energy depositions of a megajoule per liter using a laser beam have shown no visible fuel changes. Present plans call for subjecting a 0.1-ml fuel sample to a maximum energy deposition of 2×10^{15} fissions per gram of ^{235}U in the Livermore Super Kukla burst facility.

In the category of a continuous neutron source, static critical measurements for the Kinetic Intense Neutron Generator (KING) reactor concept are in progress. All components for the dynamic criticals are on order or have been received. Present estimates are that hydraulic testing can begin in October.

---

[3] M. Popovici, Z. Gheorghui, and D. Gelberg, Nucl. Instr. and Meth. 69, 125 (1969).

[4] M. G. Strauss, private communication.

NATIONAL BUREAU OF STANDARDS

A. NEUTRON PHYSICS

1. Hydrogen (R. B. Schwartz, R. A. Schrack, and H. T. Heaton II)

The hydrogen cross section was measured primarily to check a recent suggestion[1] that this cross section may not be smooth, but may have some structure. The hydrogen sample was a thick piece of polyethylene (CH_2) containing 1.44 x 10^{24} atoms/cm^2 of hydrogen. The "open" beam was filtered through graphite whose thickness was carefully chosen to contain the same number of atoms/cm^2 of carbon as was contained in the polyethelene. In this way, the carbon exactly cancels and it was not necessary to correct for it. The measurements were made over the range 1.5 to 15 MeV. No statistically significant fluctuations from a smooth curve could be seen in these data.

To make any fluctuations in the data more apparent, the original 1500 data points were averaged in groups of 8, with consequent improvement in statistical precision. Our averaged experimental points were then subtracted from a (smooth) theoretical curve, with the results shown in Fig. A-1. The points are our data, treated as indicated above. The solid line is the curve given in Ref. 1. A careful analysis of our data shows that it is consistent with either a straight line, or with fluctuations whose amplitude is only about 6 mb, or 10% of that given in Ref. 1.

We also note that the absolute values of our (averaged) data were between 1/2% and 1% of the current best theoretical values.

2. Iron (R. B. Schwartz, R. A. Schrack, and H. T. Heaton II)

The iron cross section was measured over the range 0.5 to 15 MeV, with a resolution between 0.08 and 0.12 nsec/m. In the lower half of the energy range, where there is much fine structure, we are in reasonable agreement with the recent GGA results. In this region, however, it is difficult to make a very quantitative comparison since our resolution is not adequate to show all the structure found by the GGA group. Above 7 MeV, there is good agreement among our data and the GGA, Carlson and Barschall, and Karlsruhe results, with only about 2% (or less) discrepancies. At 7 MeV, however, GGA seems to be about 4% lower than the other three sets of data, which, in turn, are within <1% of each other.

---

[1] Gy. Hrehuss and T. Czibók, Phys. Letters 28B, 585 (1969).

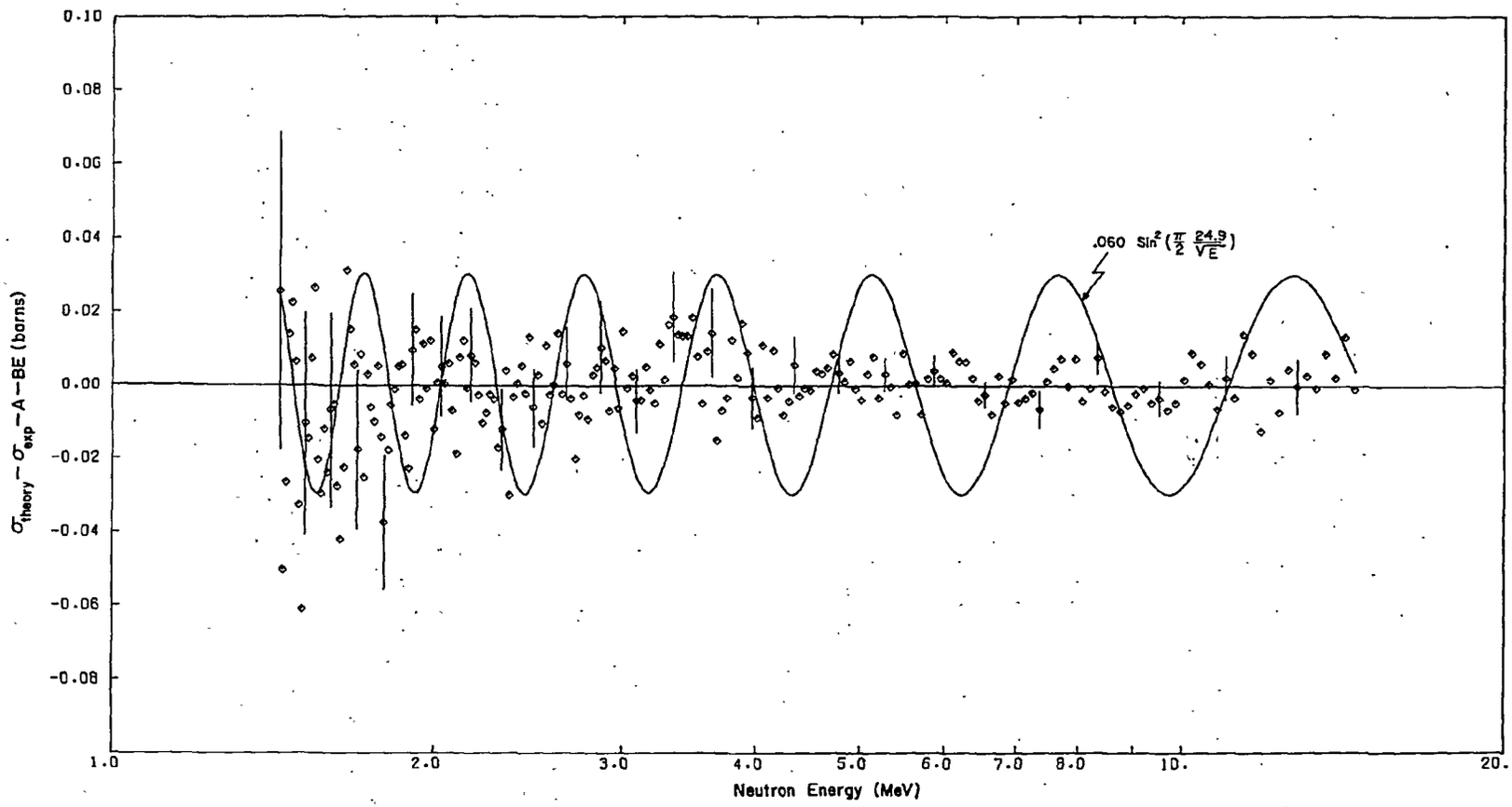

Figure A-1. The quantity $\sigma_{theory} - \sigma_{exp} - .021 + 0012E$ plotted vs neutron energy. The cross sections, σ, are in barns, and the neutron energy, E, is in MeV. (The third and fourth term simply account for this 1/2% to 1% systematic error in our experiment.) The solid line is the curve suggested in Ref. 1: $.06 \sin^3(\frac{\pi}{2}\frac{24.9}{\sqrt{E}}$ barns. This curve has been shifted to make it symmetric about zero.

NUCLEAR EFFECTS LABORATORY, U. S. ARMY

A. GENERAL INFORMATION

The FN Tandem Accelerator has been accepted and is now fully operational. An HVEC beam pulsing and bunching system to be used for neutron time-of-flight studies has been tested and accepted. The direct-extraction diode source used with the pulsing system routinely produces 125 μa of H^- ions, and on occasion as much as 300 μa of H^- ions has been extracted from this source. Proton pulse widths of less than one nanosecond have been obtained on target in the neutron room for proton energies from 9 to 15 MeV. Peak currents attainable are of the order of 1 ma. The basic pulser frequency is 2 MHz with countdown capabilities (by factors of 2) to a minimum pulsing frequency of 1/64 of the primary.

A tritium gas-target facility to permit use of the p-t reaction as a neutron source is planned for the future. For the first year or so of operation, the d-d reaction will be used as a neutron source.

B. NEUTRON ACTIVATION CROSS SECTIONS AT 14.1 MeV

(J. K. Temperley and D. E. Barnes)

Fast-neutron activation cross sections for indium and iridium isotopes have been measured relative to the $^{56}Fe(n,p)\,^{56}Mn$ cross section. Powdered metallic samples of natural-isotopic-abundance In and Ir were irradiated with 14.1 ± 0.5-MeV neutrons. The activites produced were determined by observing the gamma radiation with a Ge(Li) detector. The cross sections measured are listed in the following table:

Reaction	σ(mb)
$^{113}In(n,2n)^{112g}In$	220 ± 30
$^{113}In(n,2n)^{112m}In$	1210 ± 140
$^{113}In(n,n'\gamma)^{113m}In$	63 ± 7
$^{115}In(n,2n)\,^{114m}In$	1210 ± 140
$^{115}In(n,n'\gamma)^{115m}In$	73 ± 8
$^{115}In(n,\gamma)^{116m}In$	11 ± 2
$^{115}In(n,p)^{115g}Cd$	4 ± 2
$^{115}In(n,\alpha)^{112}Ag$	2.5 ± 0.4
$^{191}Ir(n,2n)^{190m2}Ir$	141 ± 16
$^{191}Ir(n,2n)^{190m1+g}Ir$	1830 ± 210
$^{193}Ir(n,2n)^{192m_1+g}Ir$	2090 ± 230

OAK RIDGE NATIONAL LABORATORY

1. Oak Ridge Electron Linear Accelerator (ORELA) (J. A. Harvey and F. C. Maienschein)

On August 25, 1969, the electron linear accelerator was accepted by ORNL and experiments were officially started. The accelerator has met or exceeded all its performance specifications (except the peak current at 2.5 nsec was 13.2 A) which were:

140 MeV average energy

15 amperes peak current 2.3 to 24 nseconds

2.3 to 1000 nanosecond pulse

50 joules/pulse

1000 pps

50 kilowatts

< 10 μamp dark current during rf burst

The reliability runs were modified in order not to further delay the use of the accelerator for neutron cross-section measurements. The accelerator was operated the first week at a reduced repetition rate since the first experiments could not tolerate a high repetition rate. During the first week the accelerator operated 44.3 hours out of a scheduled 45 hours and produced 17.5 amp pulses at 28 nanoseconds at 100 pps and 75 joules/pulse at 30 pps. A new electron gun was installed in the accelerator on August 22 since the emission of the old gun (which had been used for 8 months) had dropped by a factor of two.

The data-acquisition system (two SEL-computers) and peripheral equipment are operating reliably and data can be accumulated into the memory of the computer. It is estimated that the software to store data into the 800,000 and 400,000 word disks will be completed by the end of September. Four bids for the immediate analysis computer were received in August and are being evaluated.

Experiments which are in progress, being de-bugged, or being installed on the linac include:

(a) η of ^{233}U from thermal to 10 eV,

(b) capture cross section of ^{238}U up to several keV using an 800-gallon liquid scintillator,

(c) high-resolution transmission measurements up to 100 keV; total cross-section measurements on transplutonium isotopes up to a few keV in cooperation with Savannah River Laboratory,

(d) gamma-ray spectra measurements from neutron capture in individual resonances using a Ge(Li) detector,

(e) capture cross-section measurements from 5 to 500 keV,

(f) fission measurements with aligned nuclei and transmission and fission measurements with polarized neutrons and polarized nuclei.

2. Neutron Differential Scattering from ^{16}O at the 1.833 MeV Resonance (J. L. Fowler and C. H. Johnson)

At the Dubna Conference in 1968 we[1] assigned J = 3/2 to the 1.833 MeV resonance on the basis of the observed peak total cross section. We also tentatively assigned even parity on the basis of the observed interference dip before the resonance. Such a dip is expected because the $d_{3/2}$ phase shift[2] is about -12° at this energy. We have now confirmed this parity assignment by measurements of differential scattering cross sections. The state has $J^{\pi} = 3/2^{+}$.

3. The $^{16}O(n,x\gamma)$ Reaction for $6.7 \leq E_n \leq 11.0$ MeV (J. K. Dickens and F. G. Perey)

Below is the abstract of a paper submitted for publication in Nuclear Science and Engineering.

> We have obtained gamma-ray spectra for the reactions $^{16}O(n,n'\gamma)^{16}O$ and $^{16}O(n,\alpha\gamma)^{13}C$ for incident mean neutron energies E_n = between 6.7 and 11.0 MeV. The gamma rays were detected using a 30 cm^3 coaxial Ge(Li) detector placed at 55° and 90° with respect to the incident neutron direction. Time-of-flight electronics was used with the gamma-ray detector to discriminate against unwanted pulses due to neutrons and background gamma radiation. Two samples of 75 and 31 gm of BeO in the form of right circular cylinders were used. The incident neutron beam was produced by

[1] J. L. Fowler, C. H. Johnson, and F. X. Haas, Proc. International Symposium on Nuclear Structure, p. 1 (Dubna, USSR, July 1968).

[2] C. H. Johnson and J. L. Fowler, Phys. Rev. 162, 890 (1967).

bombarding a deuterium-filled gas cell with a pulsed deuteron beam of appropriate energy; for $E_n \leq 8.5$ MeV the deuteron beam was obtained from the ORNL 6-MV Van de Graaff, and for $E_n \leq 8.6$ MeV it was obtained from the ORNL Tandem Van de Graaff. These data have been reduced to differential cross sections for production of gamma rays from ^{16}O. The cross sections have been compared, where possible, with previously measured values with reasonable agreement. However, there are several important differences, and these are discussed. Summing the partial cross sections yields values for the total nonelastic cross section which are in good agreement with values for the nonelastic cross section obtained from the difference between the total cross section and the total elastic cross section.
(Work pertinent to requests #50, 54, WASH-1078)

4. Alpha and Proton Radiative Capture Cross Section Measurements at Low Energies (R. J. Jaszczak, D. Chittenden, J. H. Gibbons, and R. L. Macklin)

Radiative alpha and proton capture cross section measurements are being made with emphasis on reactions of interest in stellar evolution reaction rates. Two methods have been used. If the compound nucleus is a positron emitter (such as the $^{14}N(\alpha,\gamma)^{18}F$ reaction), then the annihilation radiation is measured. A shielded coincidence counting system consisting of two face-to-face 5 in. by 5 in. NaI(Tl) detectors is used. Preliminary cross-section measurements for the $^{14}N(\alpha,\gamma)^{18}F$ reaction have been made at alpha-particle bombarding energies of 1.10, 1.16, 1.38, 1.54, and 1.63 MeV. This method will also be used to study certain proton capture reactions (yielding a positron emitter) at low energies thereby minimizing complications due to decay schemes.

The $^{12}C(\alpha,\gamma)^{16}O$ reaction cross section for $1.8 \leq E_\alpha \leq 3.2$ MeV has been measured using isotopically enriched ^{12}C targets, a pulsed $^4He^+$ beam from the ORNL 5.5-MV Van de Graaff, a 9 in. by 12 in. NaI(Tl) detector, and time-of-flight techniques for event discrimination. Results of the experiment indicate the following values for the $^{12}C(\alpha,\gamma)^{16}O$ cross section:

E_α (MeV)	α(* 10^{-9} barn)
1.80	0.40 ± 0.09
2.02	1.5 ± 0.4
2.22	2.9 ± 0.6
2.42	4.7 ± 0.6
2.62	6.7 ± 0.7
2.83	19 ± 2
3.20	40 ± 3

These measurements will be extended to lower energies using a pulsed $^4He^+$ beam from the ORNL 3-MV Van de Graaff accelerator.

5. Proton Strength Functions for Isotopes of Sn (C. H. Johnson, J. K. Bair, and C. M. Jones)

Earlier measurements[3] of strength functions for protons with energies less than 5.4 MeV indicated that the p-wave size resonance peaks near 5.4 MeV for ^{124}Sn and at progressively higher energies for the lighter isotopes of Sn. We have confirmed this expected behavior by measurements up to about 6.5 MeV. These results are preliminary because the target deposits were non-uniform. Nevertheless, the measurements do show the expected behavior and, in particular, they show a well-defined maximum near 5.5 MeV for ^{124}Sn. We plan to repeat the measurements with uniform targets.

6. Spectrum of Prompt Gamma Rays from Thermal Fission of ^{235}U (R. W. Peelle, W. Zobel, and F. C. Maienschein)

The energy spectrum of gamma rays from the fission of ^{235}U must be used as input data for reactor shielding and heating calculations. The data generally used for this purpose were obtained from a preliminary evaluation in 1958 of partial results from an experiment which used a multiple-crystal scintillation spectrometer operated in ~ 60 nsec coincidence with a fission chamber exposed to thermal neutrons from the ORNL BSF thermal column.[4,5] Since that preliminary publication, additional fission data were accumulated, extensive spectrometer calibrations were performed, more detailed background corrections were made, and the effects of non-unique spectrometer response have been unfolded properly using the FERD system of W. R. Burrus.[6] The resulting data presented here should be used in preference to those of Ref. 4.

---

[3] C. H. Johnson and R. L. Kernell, Phys. Rev. 23, 20 (1969).

[4] F. C. Maienschein et al., Proc. U. N. International Conference on Peaceful Uses of Atomic Energy, Second Geneva Conference 15, 366 (1958).

[5] R. W. Peelle et al., Pile Neutron Research in Physics, International Atomic Energy Agency, Vienna, p. 273, 1962.

[6] W. R. Burrus, Utilization of A Priori Information by Means of Mathematical Programming in the Statistical Interpretation of Measured Distributions, Oak Ridge National Laboratory Report, ORNL-3743, 1965; W. R. Burrus et al., Neutron Physics Division Annual Progress Report, Oak Ridge National Laboratory Report, ORNL-3973, Vol. 1, p. 61, 1966.

Figure 1 illustrates the spectrum for the energy region from 0.3 to 7 MeV, with the upper and lower 2/3 confidence limit shown by the two lines (straight lines join the points output by the unfolding procedure). Some of the data from Ref. 4 are shown as points for comparison, and indicate that in some energy regions the earlier analysis had systematic difficulties causing errors in the range 10-20%. Table I lists the numbers of photons observed in various broad energy intervals. In the figure and table the spacing between the upper and lower confidence limits includes propagated "counting statistics" as well as uncertainties inherent in the unfolding process, but does not include systematic uncertainties amounting to ~ 6%. The resolution associated with the plotted data is ~ 1.5 times larger than the interval between the vertices on the lines representing the confidence limits. Examination of the raw pulse-height spectra with its narrower resolution did not reveal more structure.

Work is continuing to clarify the uncertainties and to derive spectral results from additional data covering the range from .01 to .1 MeV.[5,7]

7. POLLA, A Fortran Program to Convert R-Matrix-Type Multilevel Resonance Parameters for Fissile Nuclei Into Equivalent Kapur-Peierls-Type Parameters (G. de Saussure and R. B. Perez)

Below is the abstract of an Oak Ridge National Laboratory Report, ORNL-TM-2599.

> The program POLLA converts a set of R-matrix resonance parameters for fissile nuclei into an equivalent set of Kapur-Peierls parameters. The program utilizes the multilevel formalism developed by Reich and Moore and avoids the diagonalization of the level matrix, hence, it is particularly useful where many levels and few fission channels are involved. Some applications of the program are given and a FORTRAN listing is given in an appendix.

[7] T. A. Love, F. C. Maienschein, and R. W. Peelle, Neutron Physics Division Annual Progress Report, Oak Ridge National Laboratory Report, ORNL-2842, p. 93, 1959.

ORNL DWG. 69-6225

FISSION GAMMA-RAY INTENSITIES IN BROAD ENERGY GROUPS[a]

Energy Range (MeV)	Photon/Fission	MeV/Fission
0.1 - 0.3	1.22 ± 0.03	0.236 ± 0.005
0.3 - 1.0	4.0 ± 0.1	2.43 ± 0.07
1.0 - 1.5	1.18 ± 0.05	1.44 ± 0.06
1.5 - 2.0	0.47 ± 0.05	0.83 ± 0.08
2.0 - 2.5	0.314 ± 0.017	0.70 ± 0.04
2.5 - 3.0	0.194 ± 0.009	0.531 ± 0.026
3.0 - 4.0	0.161 ± 0.005	0.554 ± 0.015
4.0 - 5.0	0.0586 ± 0.0023	0.256 ± 0.010
5.0 - 6.0	0.0197 ± 0.0023	0.107 ± 0.012
6.0 - 7.2	0.0093 ± 0.0020	0.060 ± 0.012
7.2 - 10.5	0.0007 ± 0.001	0.006 ± 0.009
0.1 - 10.5	7.7 ± 0.2	7.2 ± 0.1

[a]Listed uncertainties do not include systematic effects of perhaps 6%.

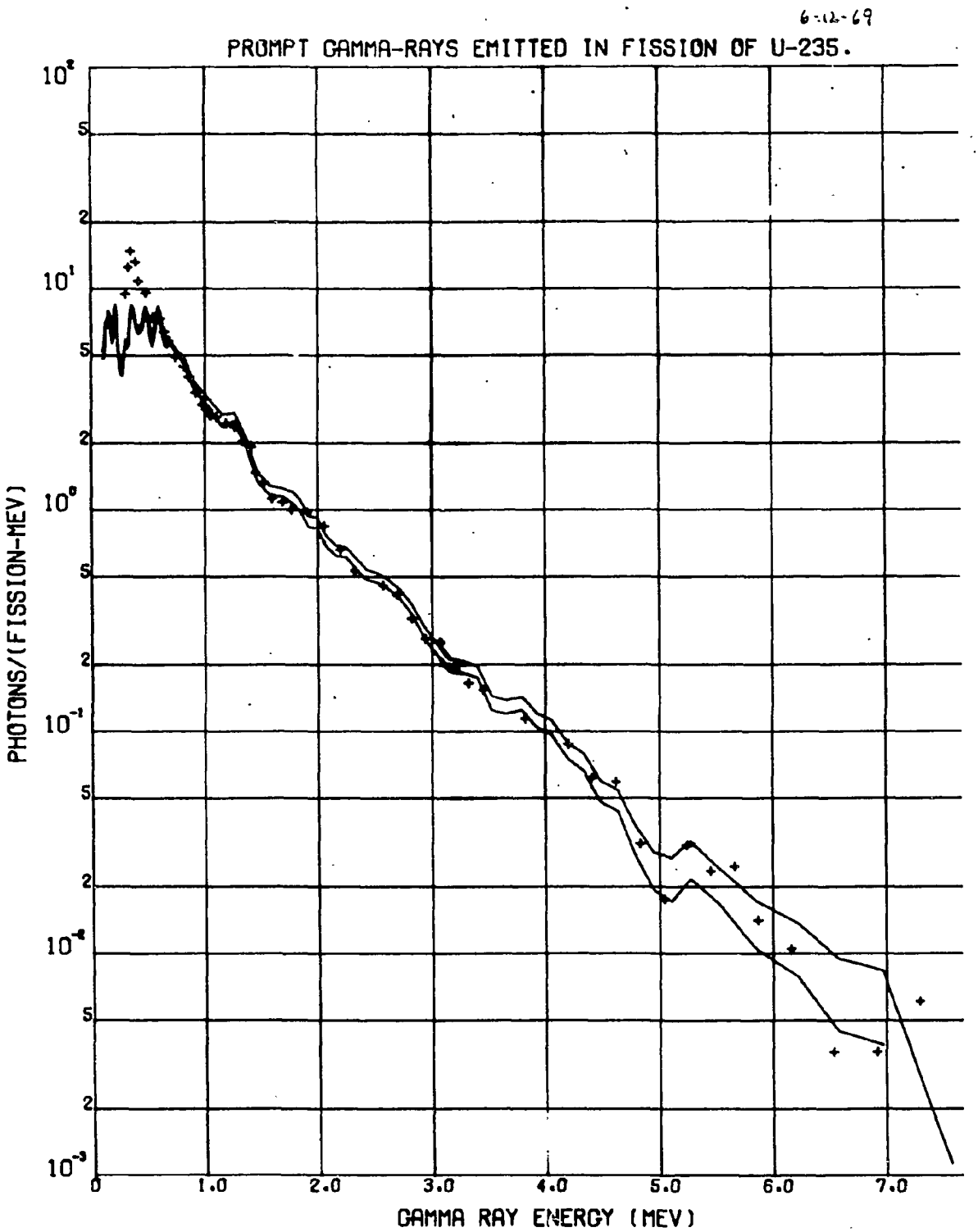

DATA NOT FOR QUOTATION

RENSSELAER POLYTECHNIC INSTITUTE

A. CROSS SECTION MEASUREMENTS

1. KeV Neutron Capture Measurements on ^{240}Pu*

(R. W. Hockenbury, J. D. Boice, W. R. Moyer and R. C. Block)

Neutron absorption measurements have now been made on ^{240}Pu using the 1.25 meter diameter capture detector at a 25 meter flight path. The experiment was designed to emphasize the keV region; however, data were taken over the entire range from 60 eV to 90 keV. Since Al and Na filters were used to determine the time-dependent background, there are gaps in the data near 2.8, 35, and 88 keV. The ^{240}Pu samples weighed a total of 24.5 grams and were on loan from the Los Alamos Scientific Laboratory.

A routing system was used such that all detector pulses between a "low" bias and a "high" bias were stored in the first region and all those above the "high" bias were stored in the second region. This "low-high" bias method[1] should permit the fission component to be separated from the total absorption, thus giving the capture cross section. A sample of the data for the keV region is shown in Figure A-1. The background due to sample activity has been subtracted from these data. There is an apparent difference in resonance structure between the "low" and "high" bias data since the fraction of detector events above the "high" bias is greater for fission than for capture. Figure A-2 shows data in another energy region with many resolved resonances. The structure due to sub-threshold fission[2]

---

* Work pertinent to requests # 357, 358, WASH-1078.

[1] R. Gwin, G. de Saussure, L. Weston, E. Haddad and W. Lopez, ORNL 3499, Vol. I (1963).

[2] E. Migneco and J. P. Theobald, Nuclear Physics A112 (1968) 603.

is easily seen in the "high" bias data; whereas, in the "low" bias data, the resonances with significant fission components are indistinguishable from the predominantly capture resonances.

In order to determine the detector efficiency, a series of time-of-flight runs were made with the capture detector discriminator set at different biases. The output from a second discriminator, set to a fixed bias, was used in each run for normalization. This method gives the detector pulse-height spectra as a function of neutron energy for capture and fission without suffering from extreme counting rate losses.

The data are now being analyzed to determine detector efficiency and capture and fission cross sections.

2. Neutron Capture and Transmission Measurements in Vanadium and the Separated Isotopes of ^{60}Ni, ^{50}Cr, ^{52}Cr, ^{53}Cr and ^{54}Cr* (R. G. Stieglitz, R. W. Hockenbury and R. C. Block)

Neutron capture measurements have been completed on V, ^{60}Ni, ^{50}Cr, ^{52}Cr, ^{53}Cr and ^{54}Cr samples using both intermediate (2.5 nsec/m) and high (0.6 nsec/m) resolution covering the energy range from several eV to about one MeV. Transmission measurements have also been completed for the V and ^{60}Ni samples. The capture data for these six nuclides all have similar resonance structure. They exhibit a few very broad and often interfering s-wave resonances with many narrow peaks superimposed (see Fig. A-1). These narrow resonances are suspected to be due to interactions of higher angular momenta neutrons. A new program utilizing the R-matrix multilevel formalism is being written to analyze these data for resonance parameters (see section B. 1.)

* Work pertinent to requests # 84, 87, WASH-1078.

Preliminary results indicate that resonances will be resolved to nearly 125 keV for vanadium and ^{53}Cr, to about 200 keV for ^{50}Cr and ^{60}Ni and higher still for the isotopes of ^{52}Cr and ^{54}Cr.

3. Fission Neutron Multiplicity Measurements in ^{235}U
(R. Reed, S. Weinstein and R. C. Block)

Fission multiplicity data were taken for ^{235}U over the thermal energy region and in the resonance region up to 25 eV. The thermal results are plotted in Fig. A-4. There is an apparent variation of $\bar{\nu}$ over the thermal region for this nuclide, with a multiplicity reduction of about 0.6% from the 0.3 eV resonance to 0.012 eV. Variations of this magnitude must be looked upon with suspicion because of possible systematic biases and statistical fluctuations. However this measurement was repeated with a different set of experimental conditions and the same variation observed. From a careful consideration of possible systematic effects, a $\bar{\nu}$ variation of this magnitude cannot be attributed to any time-of-flight dependent bias. We thus conclude that the observed thermal variation is a true reflection of a change in $\bar{\nu}$.

The resonance region $\bar{\nu}$ results are plotted in Fig. A-5. The data for the resonance region have not been completely analyzed and the results for the 13 resolved resonances shown in Fig. A-5 have been arbitrarily normalized. The resonance $\bar{\nu}$ values appear to fall into two groups, a high group containing the 8.79 eV level and a low group containing the 19.3 eV level. If the same method of assignning compound nuclear spins is applied to these results as was applied to the ^{239}Pu results, then the resonances with high values of $\bar{\nu}$ can be assigned to $J = 3^-$ and the resonances with low values to $J = 4^-$. Spin assignments for these 13 levels are shown in the Table I along

with assignments by Asghar[1] and Weigmann et al.[2] based on capture gamma ray spectra measurements. The agreement among the three sets of assignments is seen to be quite good. However, it is likely that there is a $\bar{\nu}$ -group corresponding to each available fission channel, implying that ambiguities in the assignments would exist if more than one channel were open for a given spin state.

TABLE I ^{235}U RESONANCE SPIN (J) ASSIGNMENTS

Resonance Energy (eV)	Present Work	Asghar[1]	Weigmann et al.[2]
6.39	4	4	4
7.08	3	3	3
8.79	3	3	
11.67	4	4	
12.39	4	4	4
15.45	U*	3	3
16.10	4	(4)	3
16.67	4	3	3
18.05	4	3	
19.30	4	4	4
21.10	3		3
22.95	3	3	3
23.65	U		4

* U = Unassigned

[1] Asghar, M., Michaudon, A., and Paya, D., Phys. Letters 26B, 664 (1964).

[2] Weigmann, H., Winter, J., and Heske, M., Private Communication.

4. Thick-Sample Transmission Measurements of the 229 eV Resonance in ^{65}Cu (N. Yamamuro and R. C. Block)

Neutron capture spectra measurements upon copper by Stein et al.[1] have shown that either the spin and parity of the 229 eV resonance of ^{65}Cu is 2^- if the resonance is caused by s-wave neutrons or that the spin is 2 or 3 if higher angular momenta neutrons are involved. In order to resolve this question we have carried out a thick-sample transmission measurement upon copper to look for the characteristic asymmetric line shape resulting from s-wave resonance-potential interference. A 2.54 cm thick metallic copper sample was used, and the transmission data are shown in Fig. A-6. The data were analyzed with the Harvey-Atta area program[2] assuming a symmetric Gaussian neutron resolution function. The two curves in Fig. A-6 represent fits to the data for a total width of 0.26 eV, as reported by Julien et al.,[3] and a sample thickness of 0.215 atom/barn. The $\ell = o$ curve is determined for a potential scattering radius of 7.5f, while the $\ell \neq o$ curve represents a potential scattering radius of o f. The area analysis results in a value of $2 g\Gamma n$ of (26 ± 4) meV for $\ell = o$ and (24 ± 4) meV for $\ell \neq o$, as compared to the Julien et al. value of (20 ± 1) meV. Although both s-wave and non s-wave determinations of $2 g\Gamma n$

---

[1] W. E. Stein, B. W. Thomas and E. R. Rae, Bull. Am. Phys, Soc. Series II 14, 513 (1969).

[2] S. Atta and J. Harvey, Journal Soc. Appl. Math. 10, 617 (1962).

[3] J. Julien, S. deBarros, P. L. Chevillon, V. D. Huynh, G. LePoittevin, J. Morgenstern, F. Netter and C. Samour, Int'l. Conf. on the Study of Nuclear Structure with Neutrons, Antwerp, paper 80 (1965).

are in reasonable agreement with Julien et al., the asymmetric $\ell = o$ curve in Fig. A-6 fits the data considerably better than the $\ell \neq o$ curve. If one also considers that the neutron resolution function for such a moderator source of neutrons is asymmetric and tends to decrease the low energy asymmetry of the s-wave line shape, then the only interpretation of Fig. A-6 is that indeed the 229 eV resonance of ^{65}Cu is s-wave. Hence the spin and parity of this resonance is 2^-.

5. Resonance Spin Determination From Low Level Occupation Ratios (J. R. Tatarczuk, J. D. Boice and W. P. Poenitz*)

Neutron capture gamma ray spectra have been measured for samples of ^{183}W, holmium, and tantalum in the resonance region with a 25 cc Ge(Li) detector at the 12.65 meter station. Data for gamma rays between 40 and 400 keV were stored in the on-line PDP-7 computer by two different methods. One program stores time-of-flight spectra for selected pulse-height regions, while the second program stores the entire pulse-height spectra for selected time-of-flight regions. The measurement of the occupation ratios of low-lying states should allow the determination of resonance spins.[1] Since most of the spins of ^{183}W resonances have been previously determined, these data should serve as a good check of the method. Completion of the data analysis should result in the determination of spin values for 15 resonances in Ta and remove the uncertainty of some of the values reported for ^{165}Ho.

---

* Argonne National Laboratory, Argonne, Illinois.

[1] W. P. Poenitz, Bull. Am. Phy. Soc. 13, 1389 (1968).

6. High Energy Total Cross Section Measurements (P. Stoler, P. F. Yergin, D. Mann, J. Clement and J. F. Lewis)

Preparations have been initiated to carry out MeV neutron total cross-section measurements at the 250 meter flight station. With an electron burst width of 10 nanoseconds and a fast proton-recoil detector at 250 meters the time-of-flight resolution should be $\sim$ 0.04 nsec/meter. Previous experience at Rensselaer indicates that transmission data should be obtainable to 20 MeV or possibly higher at the 250 meter flight path with small samples of pure isotopes and with adequate counting statistics. The first experiment planned is a measurement of the neutron total cross section of ^{1}H between approximately 1 MeV and 20 MeV.

B. THEORY AND ANALYSIS

1. Application of Multilevel Formalism to the Analysis of Cross-Section Data (M. Lubert, N. C. Francis and R. C. Block)

The interactive graphics and physics capabilities of the multilevel program MULTLVL, previously described,[1] have been extended. The initial cross-section calculation utilizes an R-matrix theory which is valid for interactions in which $\Gamma_n \gg \Gamma_\gamma$. This has been verified by comparison with the OPTIC[2] program. The Adler-Adler formalism has

---

[1] Linear Accelerator Project Progress Report, Jan. - March 1969, (RPI-328-160).

[2] OPTIC - A program for the calculation of nuclear cross sections and Legrende moments using the optical model, KAPL-3085.

been added to the MULTLVL program and is currently being debugged. The interactive graphics programming is complete, and it is now possible to visually fit either experimental total cross section or transmission data. The analysis of the Columbia ^{51}V total cross section data[3] shown in Fig. B-1 was performed using the MULTLVL program in an interactive mode. The parameters obtained were:

E_0 (keV)	Γ_n (keV)	J
4.17	0.50	4
6.85	1.28	3
11.81	5.58	3
16.26	0.35	4
17.00	0.35	4

The program MULTLVL has a resolution broadening function which is used in the calculation of neutron transmission. This accounts for the neutron energy resolution uncertainty introduced by both the initial accelerator burst width and the polyethylene moderator. An expression for the energy distribution of neutrons emitted from the polyethylene has been derived by Laplace transforming the time-dependent Boltzmann equation. For a delta function (in time) source of neutrons at high energy, an infinite medium, and no angular dependence, the relation for the time dependence of the neutrons leaving the polyethylene is given by:

$$g(v) = (v \Sigma_s t)^2 e^{-v \Sigma_s t}$$

where v is the exit neutron velocity, t is the time at which the neutron leaves the moderator, and Σ_s is the macroscopic scattering cross section for polyethylene. Greenwold and Groendijk[4] have previously obtained this expression. This relation has been convoluted with an

[3] J. D. Garg (private communication).

[4] Greenwold, H. J., and Groendijk, H., Physica 13, 141 (1947).

accelerator burst width which may have either a triangular or trapezoidal shape (in time). The energy resolution functions for several neutron energies with a typical accelerator burst width of 30 nsec (FWHM) and 10 nsec rise and falltimes, a 25 meter flight path, and a 2.54 cm thick CH_2 moderator are shown in Fig. B-2. The asymmetry of the resolution function is quite marked for neutron energies $\lesssim$ 1 keV.

The Monte Carlo multiple scattering program[5] currently being used to interpret capture yields has also been added to MULTLVL. The total and scattering cross sections required by the Monte Carlo program are obtained from the multilevel cross section calculations, enabling capture yields to be analyzed for resonance parameters when multilevel effects are encountered in the keV energy region.

2. Temperature Dependent, Multi-Level Effects on Neutron Resonance Cross Sections (T. E. Shea, S. N. Purohit and R. C. Block)

A quasi-resonance, temperature-dependent, multi-level, multi-channel neutron reaction cross section formalism has been developed based on the Wigner-Eisenbud R-Matrix theory of nuclear reactions. Mathematical expressions for neutron reaction cross sections are obtained through a partial fraction expansion of the square of the collision matrix in terms of its complex energy poles. The expansion terms are grouped by complex conjugates. The resulting expression for a multi-level, multi-channel neutron reaction cross section is a sum over quasi-resonance levels of terms that are similar to the Breit-Wigner formula.

To account for the thermal motion of the nucleus, the quasi-resonance multi-level, multi-channel reaction cross section expressions are folded with the temperature dependent scattering law of the medium in which the nucleus

[5] J. G. Sullivan, G. G. Warner, R. C. Block and R. W. Hockenbury, "A Monte Carlo Code for Neutron Capture Experiments" RPI-328-155 (1969).

is bound. In the final expressions, each quasi-resonance contribution to the cross section is characterized by a symmetric and an asymmetric part, given in terms of the standard ψ and χ Doppler-broadening line-shape functions.

One immediate advantage of the present work is that the quasi-resonance parameters are obtained directly from R-Matrix resonance parameters. The statistical properties of R-Matrix parameters are well understood; therefore, the range of applicability of the quasi-resonance formalism can be extended to the unresolved resonance region by generating quasi-resonance parameters from R-Matrix parameters, which have been obtained from the appropriate statistical distributions.

Progress to date on the development of the formalism has been limited to the cases of two and three interfering levels in the multi-level, multi-channel temperature-dependent fission cross section. A code (TRIPLET) is being developed to compare cross sections calculated with single-level, two-level, and three-level schemes.

To date, application of the quasi-resonance cross section formalism has been limited to the study of the temperature-dependent behavior of two and three interfering levels in the fission cross section of ^{235}U. Preliminary numerical results on a few resonances have been obtained, thereby extending the work of Lynn and of Garrison. Several alternative schemes are being investigated to generate the temperature-dependent, multi-level ^{235}U fission cross section from few-level quasi-resonance sequences.

C. NEUTRON SPECTRA MEASUREMENTS

1. Fast Reactor Physics Studies (E. R. Gaerttner, M. Golay, N. N. Kaushal and B. K. Malaviya)

In the last quarter, time-of-flight studies of fast neutron spectra in a large aluminum assembly have been started; these measurements are continuing. Measurements have also been made to investigate the feasibility of observing the effect of temperature on fast neutron spectra in aluminum. As part of the new fast kinetic studies, a ^{3}He semiconductor detector has been employed to observe the time-dependence of the fast neutron flux and preliminary results for a depleted uranium assembly have been reported.[1] Such measurements are being continued. Work is also in progress on the design of a large sodium system for fast neutron "integral" experiments.

The analysis of these measurements involves comparison with calculated spectra based on transport-theory codes using different cross-section sets. The evaluation of ENDF/B and other available data for Fe, U and Al on this basis is underway.

D. PHOTONUCLEAR REACTIONS

1. (γ,xn) Reactions in ^{169}Tm* (J. C. Leader, H. A. Medicus, E. J. Winhold, P. F. Yergin and S. J. Mecca)

^{169}Tm (γ,xn) $^{169-x}Tm$ reactions were studied for $1 \leq x \leq 6$ using bremsstrahlung with endpoints from 20 MeV to 75 MeV. Cross sections were obtained by Penfold-Leiss

---

[1] N. N. Kaushal, B. K. Malaviya and E. R. Gaerttner, "Kinetic Studies in a Depleted-Uranium Assembly," Trans. Am. Nucl. Soc., 12 (1), 223 (June 1969).

* Supported by the National Science Foundation.

analysis of yield rates calculated from the activities induced in thulium measured with a Ge(Li) detector. Neutron energy spectra, obtained by time-of-flight measurements, were also obtained from thulium at several bremsstrahlung energies and angles. Analysis of these energy spectra data provided lower limits on the differential cross sections for neutrons arising from (γ,n) and (γ,2n) reactions.

The activation experiment gave 2.07 $\pm$ 0.12 MeV-b and 0.27 $\pm$ 0.04 MeV-b for the (γ,n) and (γ,2n) reactions. It, furthermore, provided information on the cross sections of the (γ,3n) and (γ,4n) and (γ,5n) reactions and one yield value at 75 MeV for the (γ,6n) reaction. (Figs. D-1 and D-2). The (γ,3n) and (γ,4n) cross sections reach peaks of 13 mb and 7 mb at 38 MeV and 50 MeV respectively after rising from threshold. The (γ,3n) cross section decreases to 0 mb at 57 MeV, rising again to approximately 9 mb at 70 MeV. The (γ,4n) cross section also falls after peaking to about 3 mb at 57 MeV and increases again to approximately 8 mb at 70 MeV. The (γ,5n) measurements indicated that this cross section peaks at about .7 mb at an energy of 52 MeV, after rising from threshold; it then decreases until 75 MeV (the highest measured energy). The (γ,6n) reaction could only be detected in the measurement with 75 MeV bremsstrahlung.

The neutron spectra obtained from time-of-flight measurements (Figs. D-3 and D-4) show humps at 2.25 and 6.75 MeV. They are probably related to the two maxima of the giant resonance in this deformed nuclide. The energy difference, thus interpreted, implies a quadrupole moment of 9 to 11 barns.

The angular distribution of the differential photoneutron cross sections obtained from the time-of-flight measurements showed that high energy neutrons arising from the (γ,n) and (γ,2n) processes are peaked at approximately 45° relative to the incident photo beam (Fig. D-5). Integration of these lower limits to the differential cross sections over the measured angular distributions gave lower limits to the total cross sections for these reactions of

7.9 mb and 0.12 mb for the (γ,2n) and (γ,n) processes, respectively, at 40 MeV. A higher energy measurement indicated that these lower limits have fallen to 0.9 mb and 0 mb at 60 MeV for the respective (γ,2n) and (γ,n) reactions if one assumes the same angular distributions.

The rising trends in the (γ,3n) and (γ,4n) cross sections after 60 MeV suggest that they might be the result of the semidirect emission of neutrons as a consequence of the nucleon collisions following a quasi-deuteron absorption. In an attempt to test this hypothesis the results of this experiment were compared with calculations by Gabriel and Alsmiller, Jr.[1] on thulium. They assumed γ -absorption by a quasi-deuteron, followed by an inter-nucleon cascade and subsequent particle evaporation. The calculation explicitly excludes absorption processes disallowed by the Pauli principle, but it disregards the inhibition of the quasi-deuteron mechansim at low energy due to healing-distance considerations. Comparison of the results of Gabriel and Alsmiller with those of this experiment indicated that the computation predicts more evaporation cross section than was found experimentally. A comparison of the computed cross sections with the measured ones is given in Table D1.

Although no calculations were made on the angular distribution of (γ,n) and (γ,2n) neutrons it seems unlikely that the quasi-deuteron theory would predict the extreme forward peaking found experimentally.

---

[1] T. A. Gabriel and R. G. Alsmiller, Jr., Oak Ridge National Laboratory Report ORNL-TM-2481, and private communication.

2. Bremsstrahlung Reactions with ^{51}V (I. L. Preiss, P. Wong, M. Weisfield and H. M. Clark)

Prior results indicated that it was likely that a form of fragmentation reaction would be possible in nuclei excited via absorption of high energy bremsstrahlung. If the cross sections for such reactions are appreciable, then it is highly likely that our program for producing new isotopes (expecially in low Z elements) would on the one hand become more complex, and on the other be enhanced by the addition of reaction mechanisms that may make it possible to form new radionuclides.

An experimental program was undertaken in which the radionuclides formed during high energy ($\sim$75 MeV) bremsstrahlung irradiations were studied. One limitation in this work should be noted, viz. that because these experiments were performed with only nominal control of the electron beam energy, the energy dependence of these reactions is merely qualitative. The preliminary results are summarized in Table D2. It should be noted that for convenience the yields are reported as integral yields with respect to the (γ, α) reaction which is known to be a giant dipole resonance phenomenon. These results were reported at the Fall 1968 meeting of the American Chemical Society.

3. Studies of ^{56}Ni (I. L. Preiss, J. Bon and H. M. Clark)

Preliminary experiments have indicated that rather large yields of ^{56}Ni can be obtained from the ^{58}Ni (γ, 2n) ^{56}Ni reaction. This isotope is of some interest since a small, but real, discrepancy exists in the published decay schemes. The study of the detailed decay scheme as well as the lifetimes of the lower states has been undertaken. Preliminary results would seem to indicate that two closely spaced levels exist in the region at about 1.0 MeV in ^{56}Co. This level could be 1+ state overlooked in the earlier experiments.

TABLE D1

	55 MeV		70 MeV	
	Gabriel and Alsmiller Calc.	This Experiment	Gabriel and Alsmiller Calc.	This Experiment
(γ,n)	.015 ± .01	.05	.007 ± .007	0
(γ,2n)	.31 ± .05	3.5	.11 ± .03	0
(γ,3n)	1.18 ± .04	0 ± 2	.60 ± .07	6 ± 4
(γ,4n)	3.03 ± .15	4 ± 1	1.19 ± .09	8 ± 3
(γ,5n)	16.5 ± .35	.6 ± .4	2.71 ± .14	0
(γ,6n)	3.73 ± .17	-	9.01 ± .26	-
(γ,7n)	- - -	-	7.38 ± .23	-
	24.4 mb	8 ± 2 mb	21.0 mb	14 ± 5 mb

Levinger's Modified Quasi-Deuteron Theory, $_{qd}$: 25 mb (60 MeV), 19.6 mb (80 MeV).

TABLE D2

$^{51}V(\gamma, x)$ PRODUCTS WITH 60-65 MeV e^-

Products	Q (MeV)	E (MeV)	Observed Half-Life	Relative Integrated Cross-Section
$(\gamma, 3n)^{48}V$	32	0.511, 0.990, 1.31	16d	8
$(\gamma, {}^3He)^{48}Sc$	22	0.990, 1.04, 1.31	46h	-
$(\gamma, \alpha)^{47}Sc$	14	.160	3.4d	1
$(\gamma, \alpha n)^{46}Sc$	26	0.890, 1.12	Long	3
$(\gamma, 2\alpha)^{43}K$	30	0.370, 0.610	22h	10^{-1}
*$(\gamma, 2\alpha n)^{42}K$	40	1.52	10.15h	-
$(\gamma, {}^{11}C)^{40}Cl$	36	2.75	1.4m	10^{-3}
$(\gamma, 2\alpha\, {}^3He)^{40}Cl$	35			

* Tentative assignment

4. Photo-Nuclear Reactions of Gadolinium (I. L. Preiss, G. Matthes and H. M. Clark)

Samples of Gd_2O_3 were irradiated at electron beam energies of $\lesssim$ 50 MeV. In these studies it was determined that the (γ, n) yield would not be so large as to interfere with the study of (γ, p) products at beam energies above 60 MeV.

E. LOW ENERGY NEUTRON INELASTIC SCATTERING

1. Epithermal Neutron Interactions with Uranium Carbide (C. Lajeunesse, W. E. Moore and M. L. Yeater)

The double-differential scattering cross section of polycrystalline natural uranium carbide has been measured for incident energies of 0.090, 0.092, 0.135 and 0.159 eV. Inelastic scattering peaks corresponding to excitation energies of 0.013 and 0.045 eV were observed, and are shown to belong to acoustic and optical modes of the UC lattice. A model has been developed using a normal mode analysis based on the Born and von Karman approximation, including non-central forces and considering up to third-nearest neighbors. Polarization-vector weighted frequency distributions and a theoretical scattering law have been derived based on this analysis. Resolution and multiple scattering corrections have been made using the above Monte Carlo approach. The application of these corrections to double-differential cross sections derived from the theoretical scattering law shows excellent agreement with the measurements. The variation of the specific heat with temperature is also accurately predicted by the model.

The scattering law and the elastic scattering component were submitted to the ENDF-B file. Since this scattering law reproduces the measured double-differential cross sections with good accuracy, it will provide better data for reactor calculations in UC-fueled systems.

The total cross section was also measured for the energy range 0.005 to 4 eV. The Bragg peaks due to coherent scattering were resolved up to 0.02 eV. The total cross section calculated from our non-central force model compares well with this measurement
The theoretical total cross section includes contributions from coherent elastic scattering, inelastic scattering (evaluated in the incoherent approximation), and the U-235 and U-238 absorption cross sections.

2. Multiple Scattering Code Development (F. Bischoff, W. E. Moore and M. L. Yeater)

A Monte Carlo code has been written to correct for multiple scattering effects in epi-thermal neutron differential scattering experiments. For a given incident energy, the scattered energy and angle at each collision are selected by sampling α and β from cumulative distribution functions generated from the scattering law, $S(\alpha, \beta)$.

The code has been extended recently to take into account the effects of experimental resolution. This treatment includes the effects of incident energy resolution, path length uncertainties, and finite analyzer time-channel width. In the Monte Carlo method the resolution and multiple scattering effects are computed on a neutron-by-neutron basis, so that the actual experimental conditions are duplicated with very little approximation. The program may provide correction factors to be applied to the data, or may apply adjustments directly to the theoretical cross-sections derived from $S(\alpha, \beta)$. The theory-data comparison is used to guide the development of an improved model describing the dynamical behavior of the scatterer.

The code exists in two versions, one for tubular geometry (MSCYL) and one for plane (MSCPL). MSCYL is applicable only to kernels such as water which include "quasielastic" scattering in the Scattering Law. MSCPL has options for coherent elastic scattering, for incoherent elastic (Debye-Waller) scattering, and for "quasielastic" scattering in the Scattering Law. These options are currently being used to interpret uranium carbide, polyethylene, and water data respectively. Elastic sampling and scoring is done using analytic expressions, and inelastic sampling and scoring is done using the alpha and beta sampling procedures described previously in WASH # 1124, p. 163.

FIGURE CAPTIONS

Figure A-1 ^{240}Pu Absorption Data from 2.5 to 100 keV.

Figure A-2 ^{240}Pu Absorption Data from 700 to 2000 eV.

Figure A-3 Yield divided by sample thickness for ^{60}Ni and ^{51}V (natural) in millibarns. A resolution of ~ 2.5 nsec/m was used for these measurements.

Figure A-4 ^{235}U $\bar{\nu}$ Variation for Incident Neutrons Below 1 eV.

Figure A-5 ^{235}U $\bar{\nu}$ Grouping for 13 Resonances Below 25 eV. The Ordinate is Arbitrarily Normalized.

Figure A-6 Transmission vs. Channel Number for a 2.54 cm Thick Copper Sample.

Figure B-1 Multilevel fit to vanadium total cross section data from 2-18 keV. The squares are the calculated cross sections and the diamonds are the experimental cross sections. The smooth curve is drawn through the calculated points.

Figure B-2 Neutron energy resolution function for a 30 nsec (FWHM) accelerator burst width, a 1 inch thick polyethylene moderator and a 25 meter flight path. The resolution function has been calculated for neutron energies of (a) 20 keV, (b) 10 keV, (c) 5 keV, (d) 1 keV, and (e) 500 eV.

Figure D-1 Cross-section shapes of ^{165}Ho (γ,n) and (γ,2n) processes as measured by Bergere et al. (Nucl. Phys. A 121, 463 (1968)) normalized so as to agree with the measured yield data for these processes in ^{169}Tm. Cross-section data for the ^{169}Tm (γ,5n) ^{164}Tm obtained by Penfold Leiss analysis of measured yield data. Errors shown reflect only statistical fluctuations.

Figure D-2 Cross-section data obtained by Penfold Leiss analysis of the yield data for the (γ,3n) and (γ,4n) processes. Yield data from the 670 keV and 296 keV peaks in the γ-ray spectra were multiplied by normalizaton factors of 1.23 and 2.2 respectively in order to obtain the cross section data shown. The dashed lines represent the average cross section as calculated from the two different peaks for each process. Errors shown reflect only statistical fluctuations.

Figure D-3 0.5-MeV-averaged relative yield of neutrons per unit energy, as a function of neutron energy, obtained from time-of-flight measurements of photo-neutrons from ^{169}Tm at angles of: A - 30°, B - 45°, and C - 67.5^{o} relative to the bremsstrahlung beam with endpoint energies of 50 MeV, 43.5 MeV, and 48.2 MeV respectively. The 67.5^{o}-data possibly are contaminated by stray neutrons originating from the electron beam collimator.

Figure D-4 0.5-MeV-averaged relative yield of neutrons per unit energy as a function of neutron energy, obtained from time-of-flight measurements of photoneutrons from ^{169}Tm at angles of: C - 90°, D - 133°, and E - 152° relative to the bremsstrahlung beam with endpoint energies of 45 MeV.

Figure D-5 Calculated lower limits to the differential cross sections for the (γ,n) and (γ,2n) processes in ^{169}Tm obtained from photoneutron energy spectra. Bremsstrahlung endpoint energies for the measurements at each angle are as indicated.

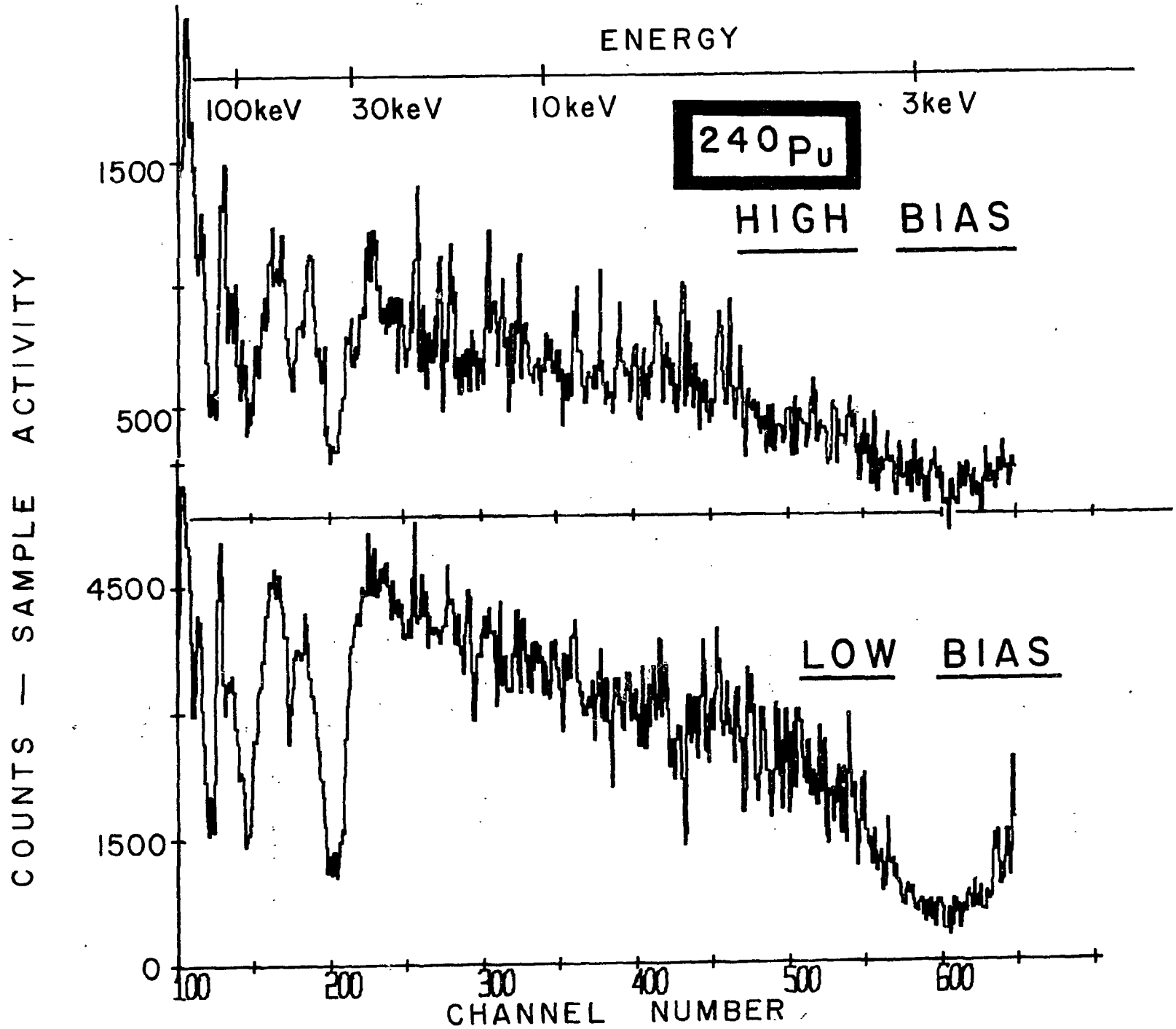

Figure A-1

DATA NOT FOR QUOTATION

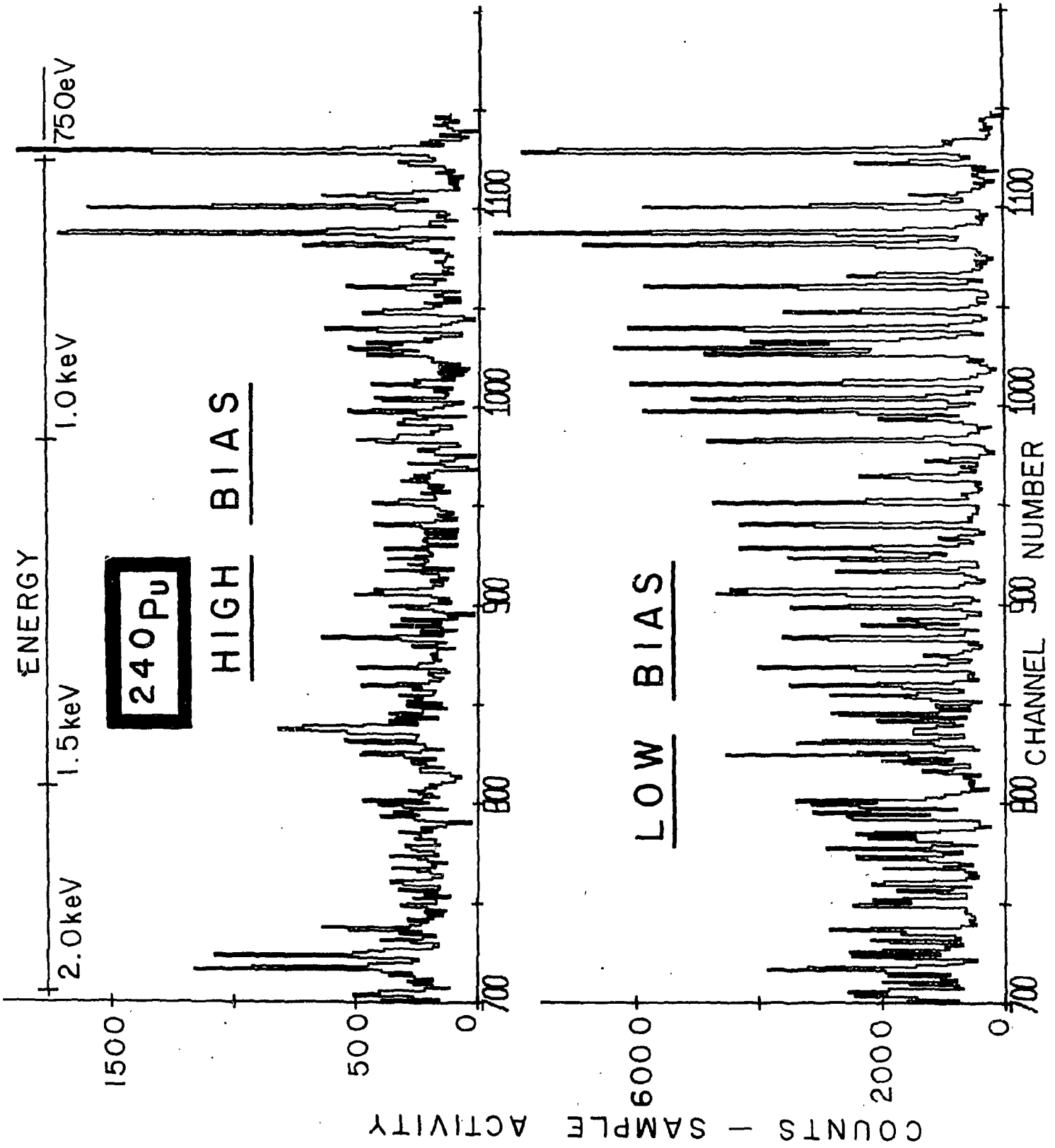

Figure A-2

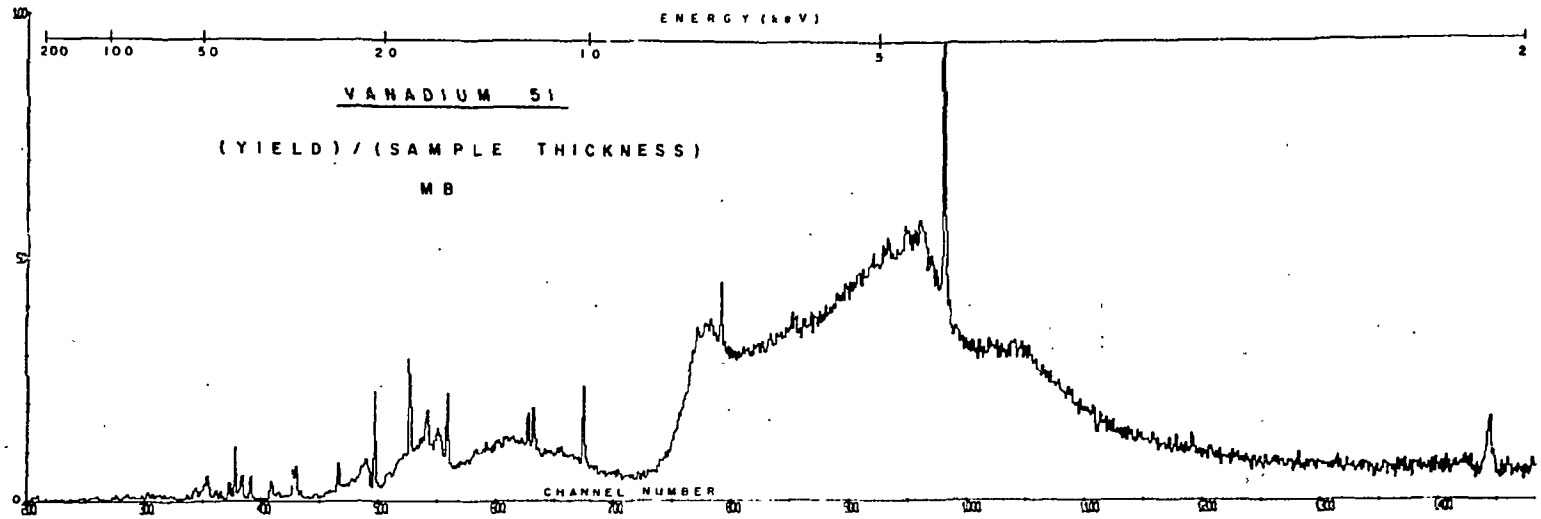

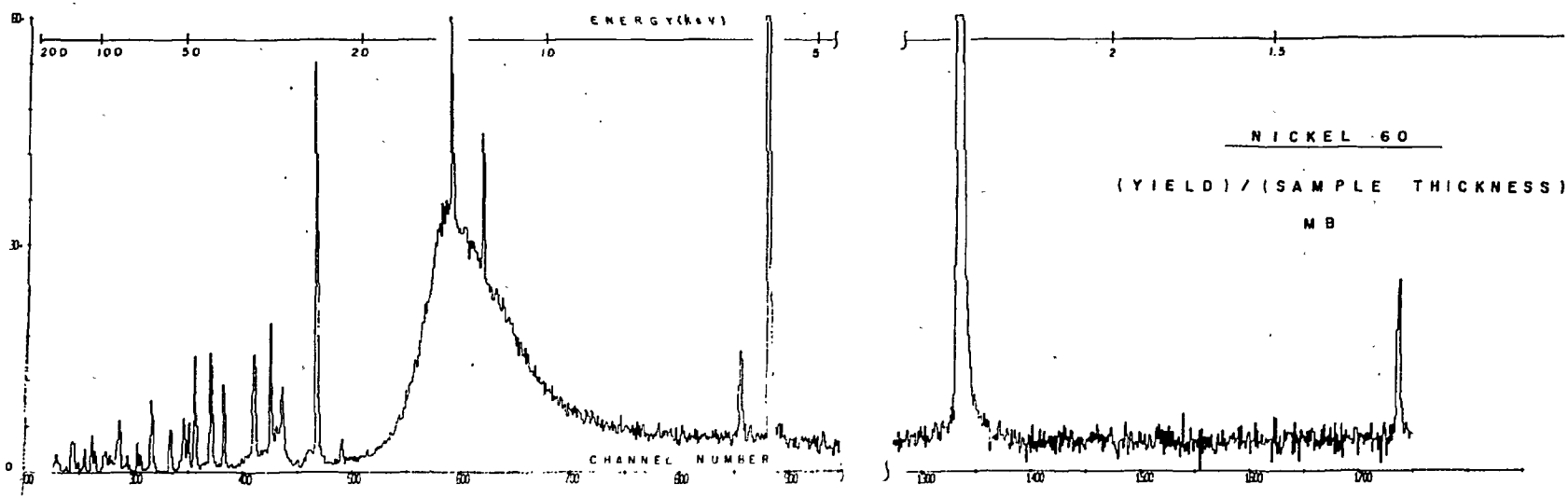

Figure A-3

page 165 follows after page 96

DATA NOT FOR QUOTATION

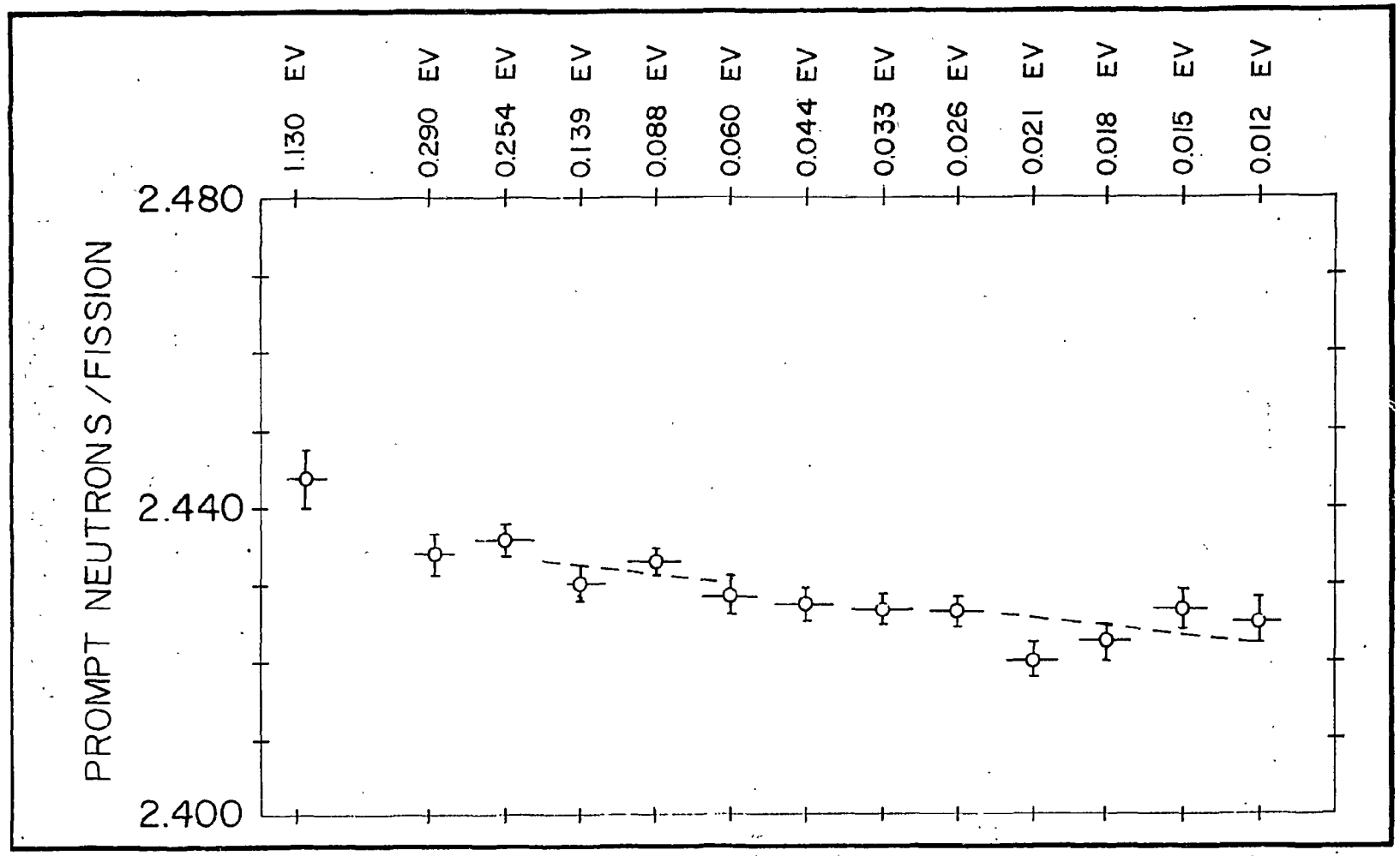

$\bar{\nu}$ (E) FOR U-235 , BELOW 1 EV

Figure A-4

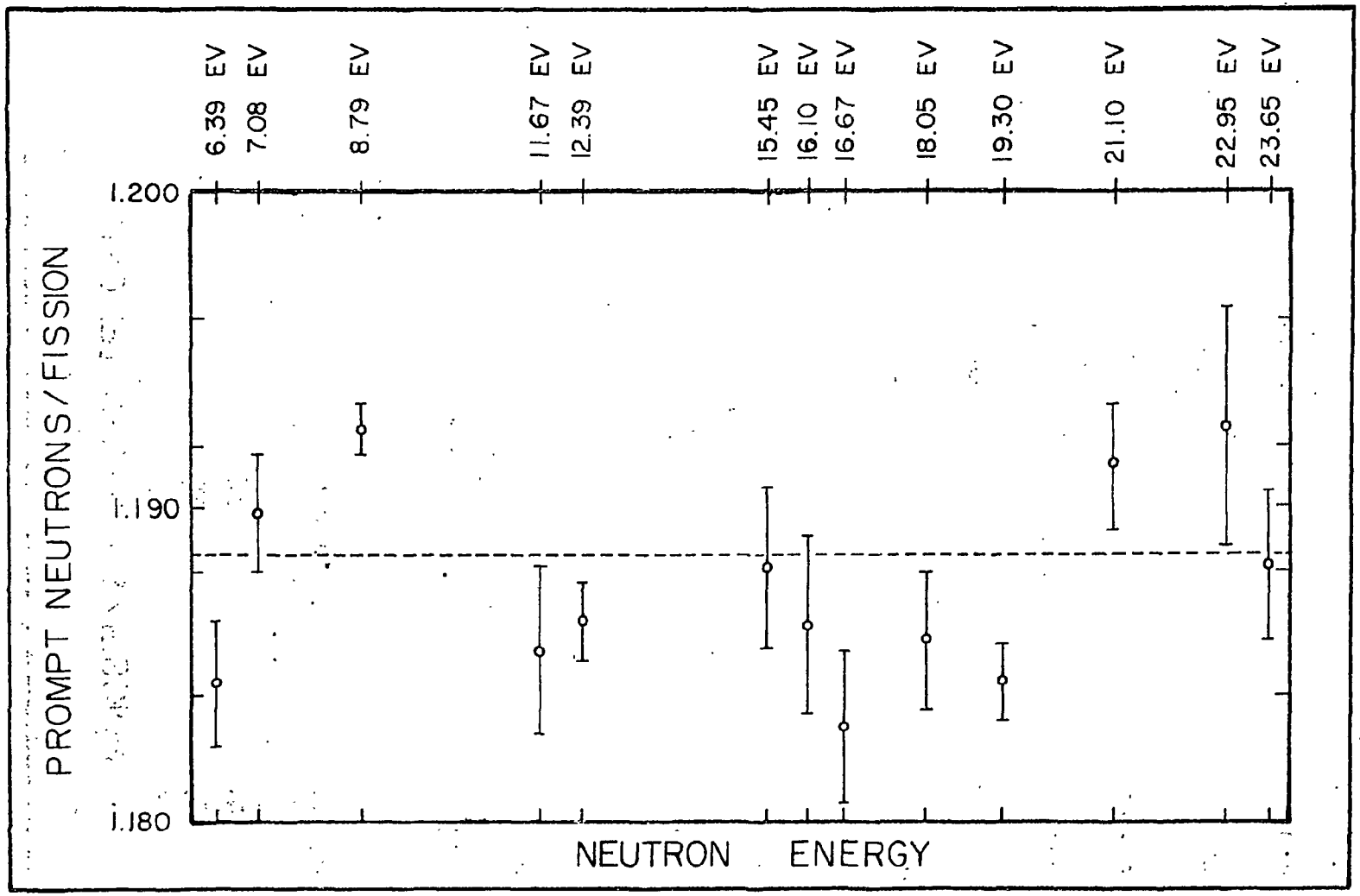

$\bar{\nu}$ (E) FOR U-235 , 6 TO 24 EV

Figure A-5

Figure A-6

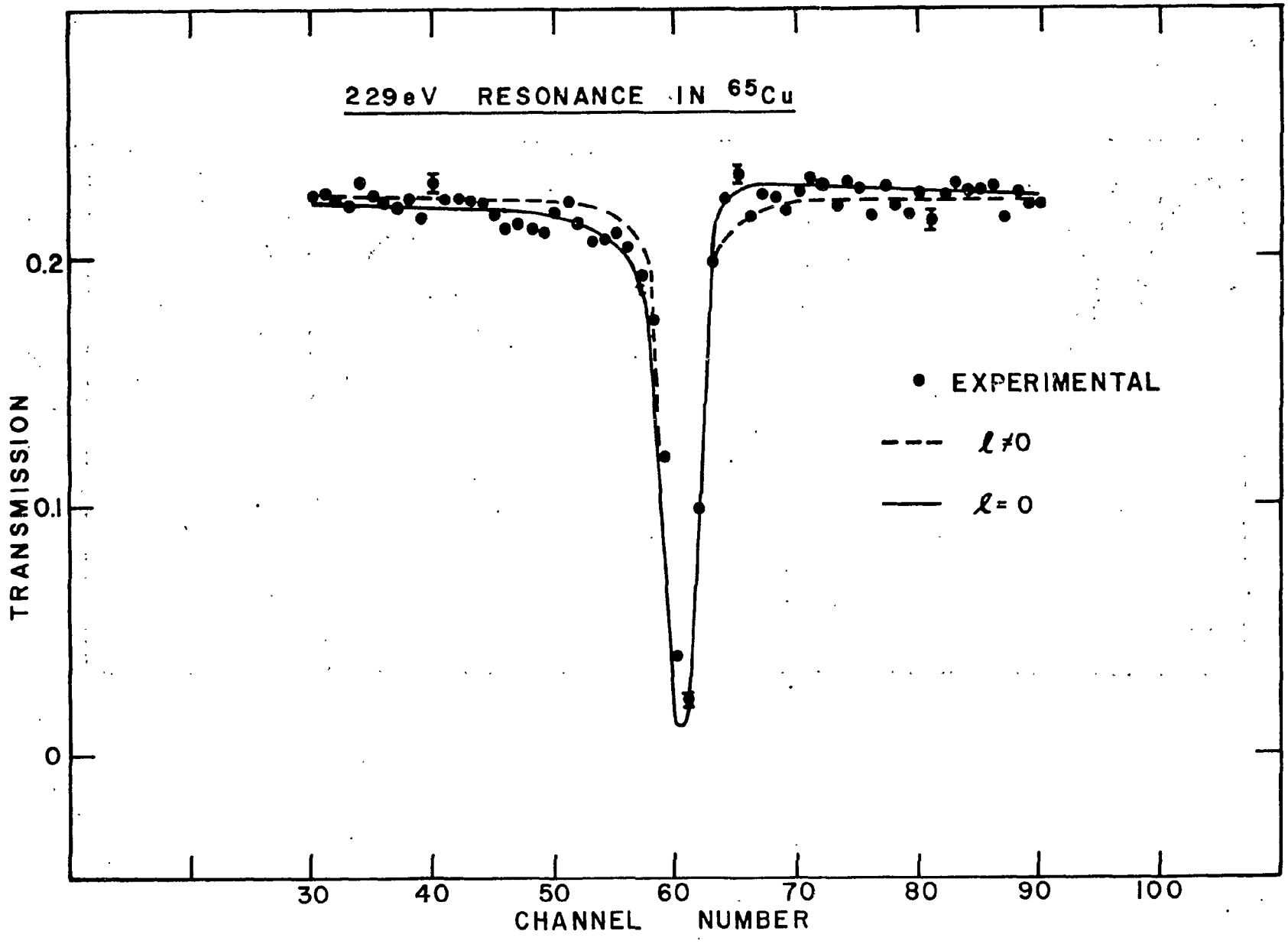

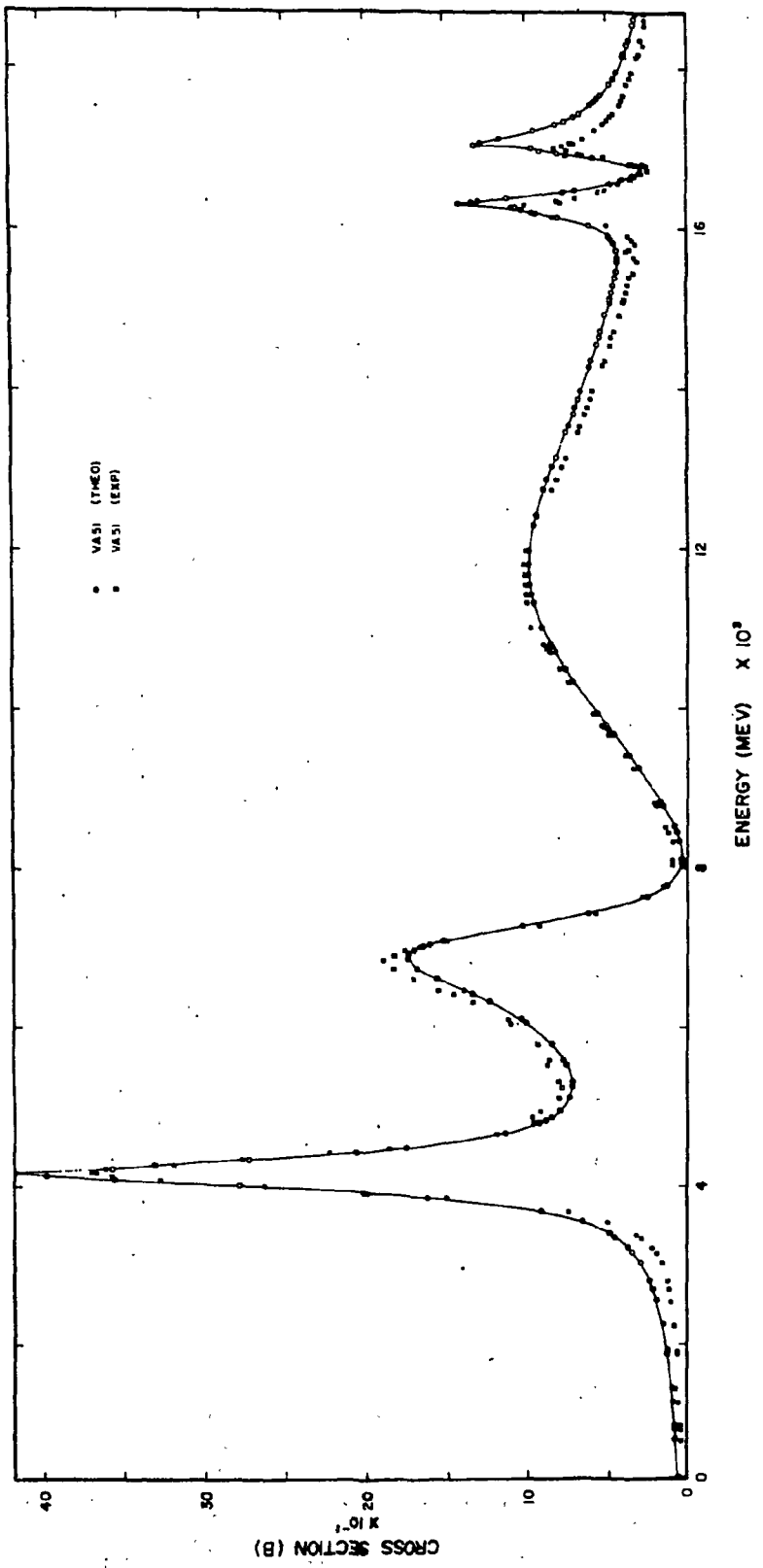

Figure B-1

DATA NOT FOR QUOTATION

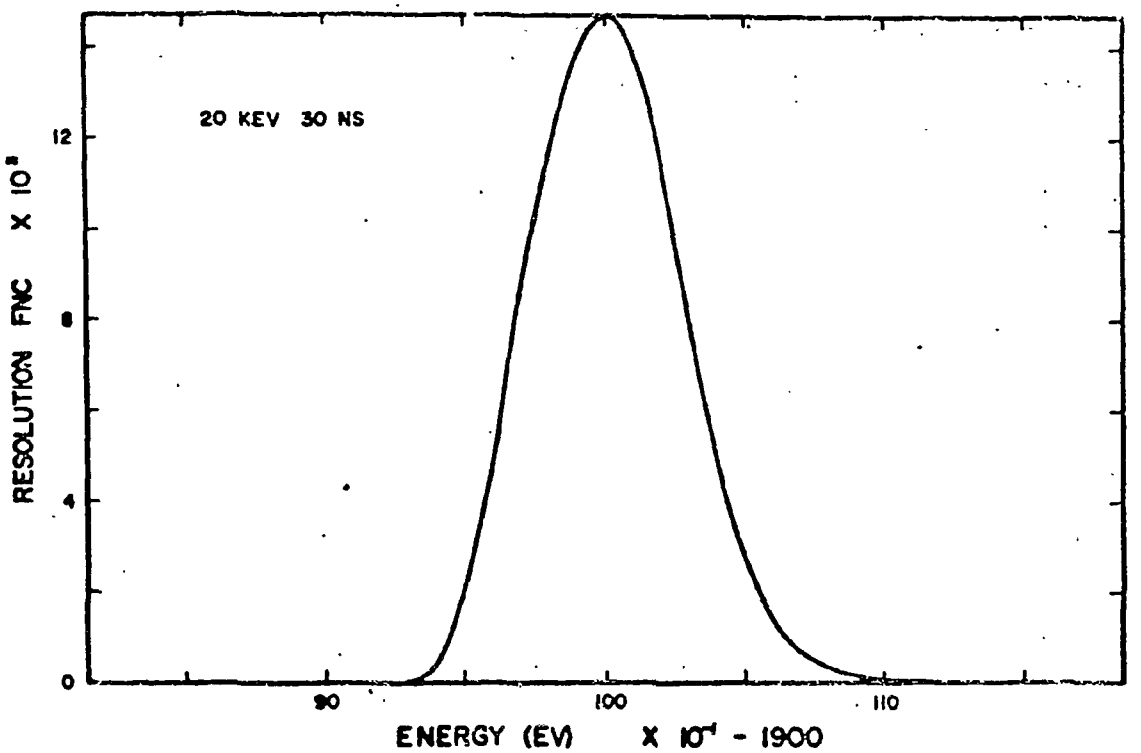

(a)

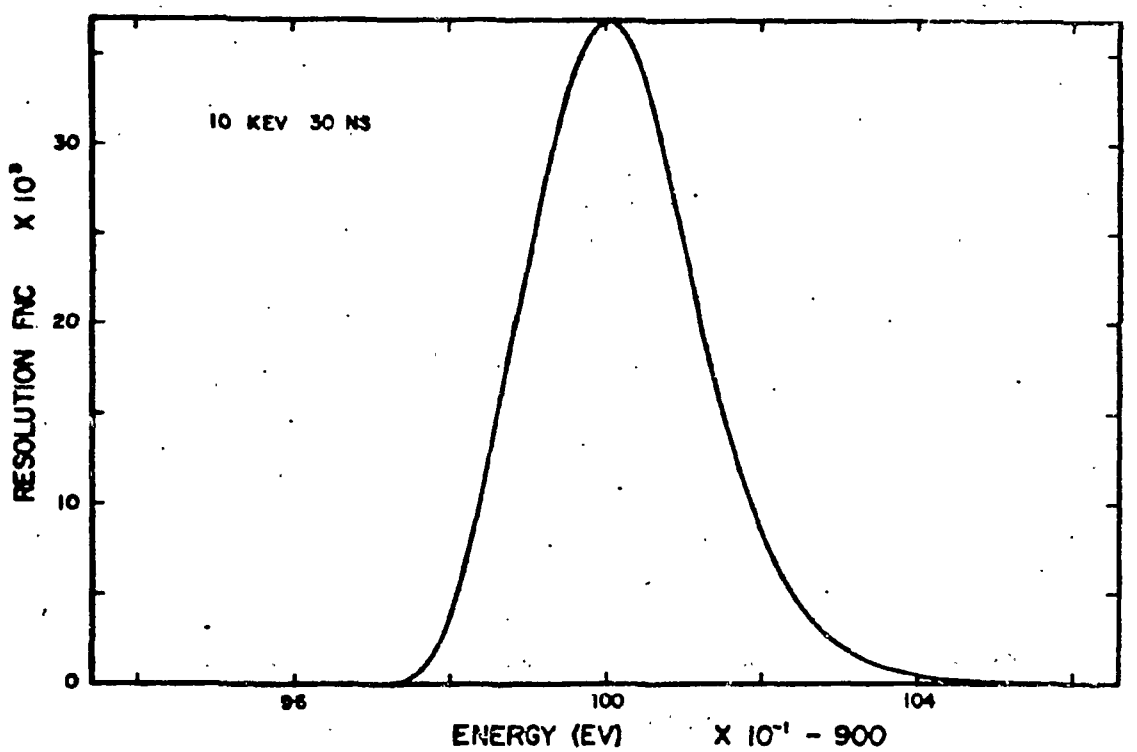

(b)

Figure B-2

DATA NOT FOR QUOTATION

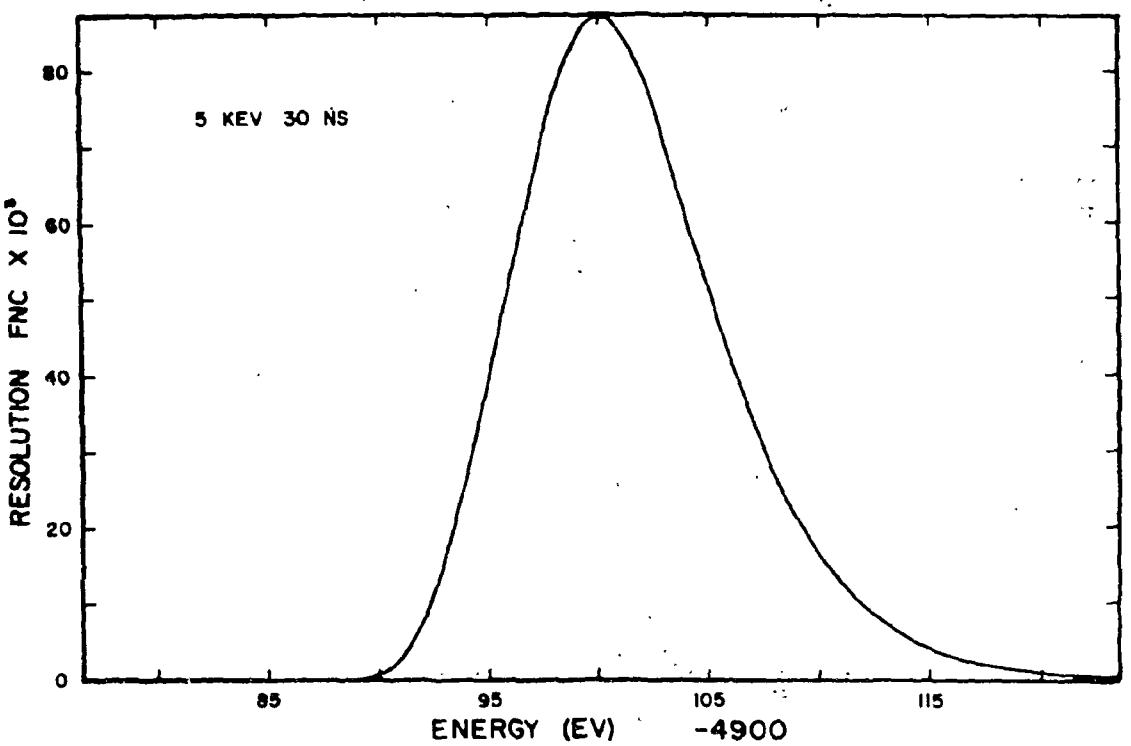

(c)

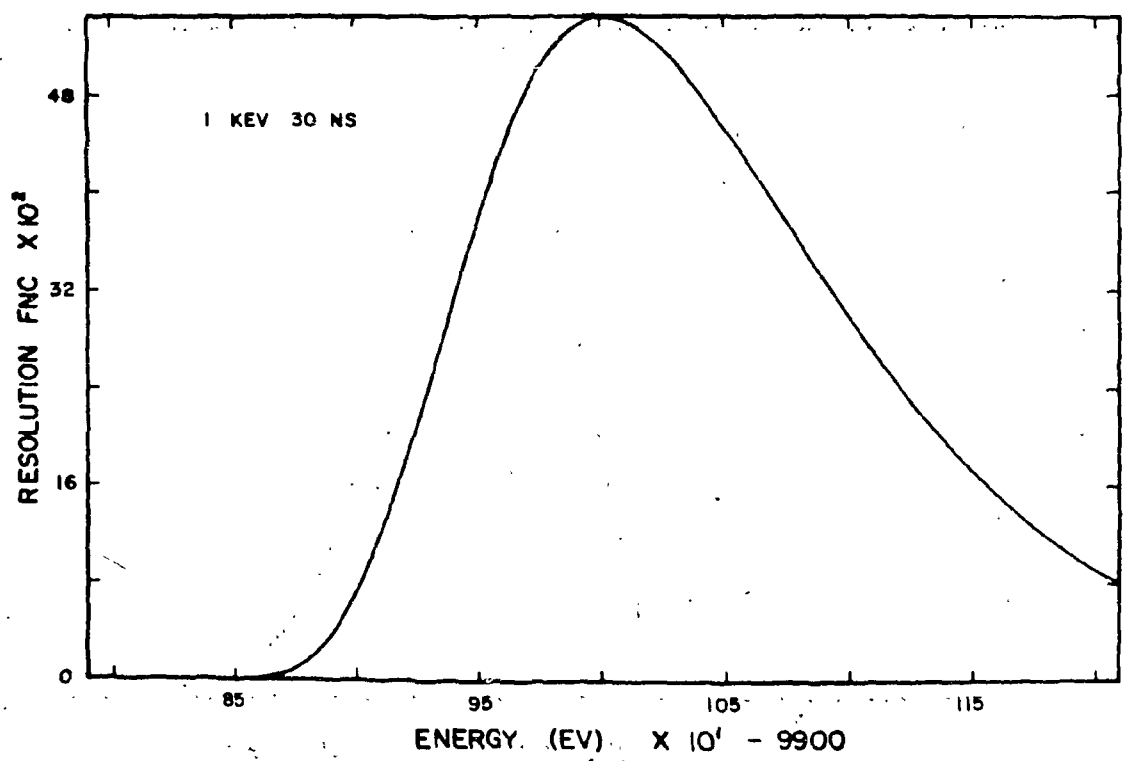

(d)

Figure B-2

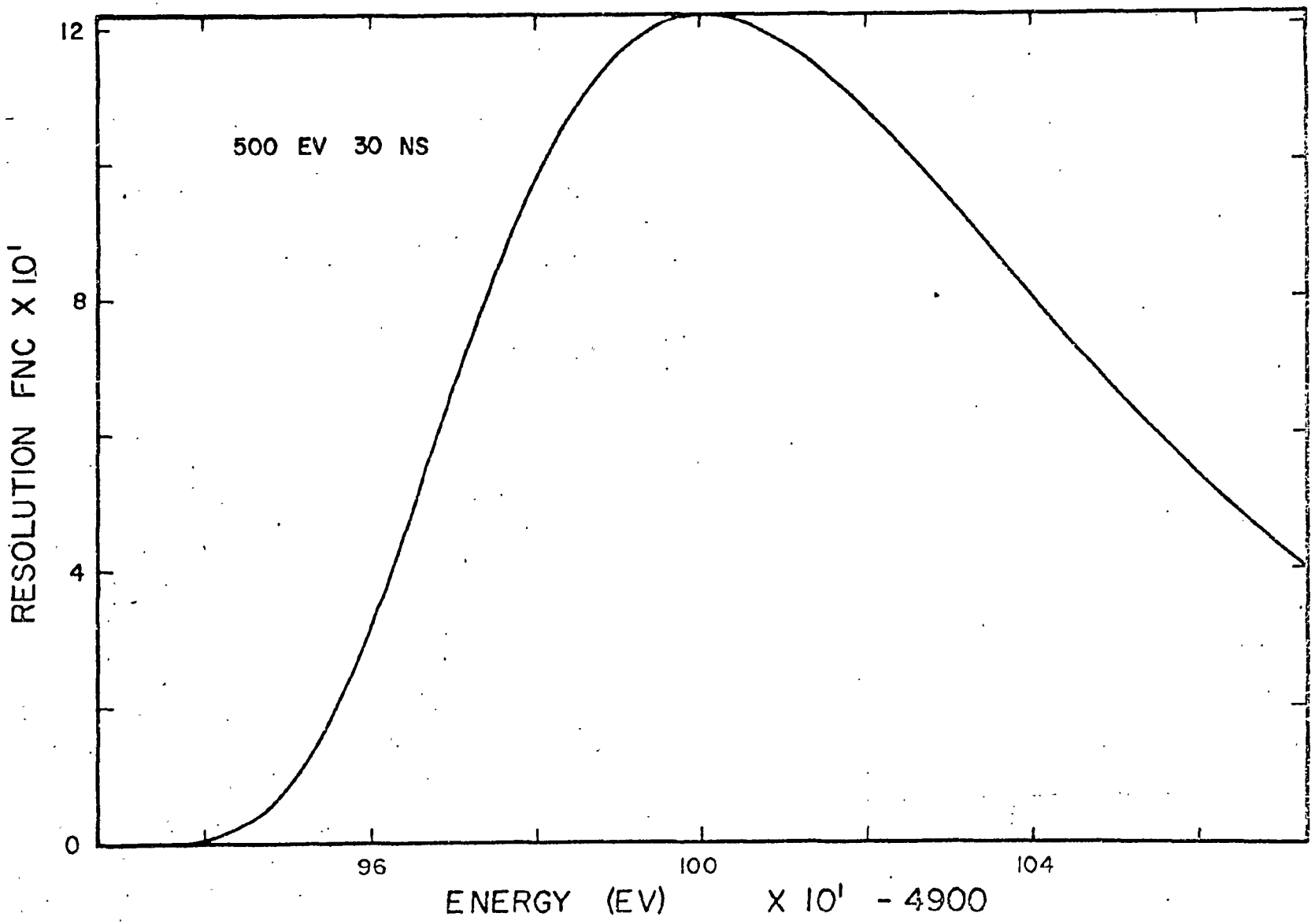

(e)

Figure B-2

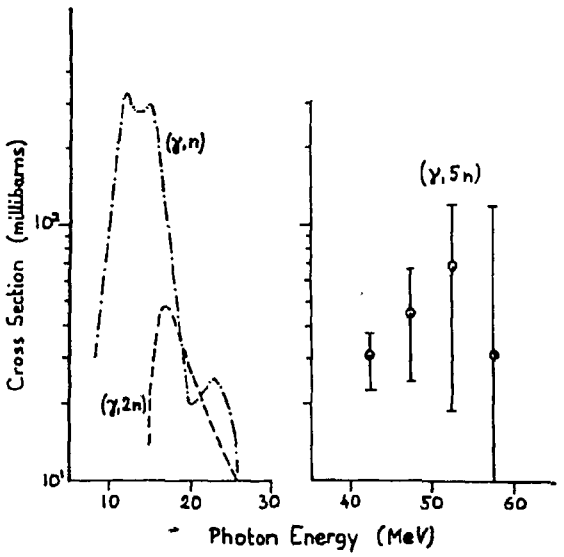

Figure D-1

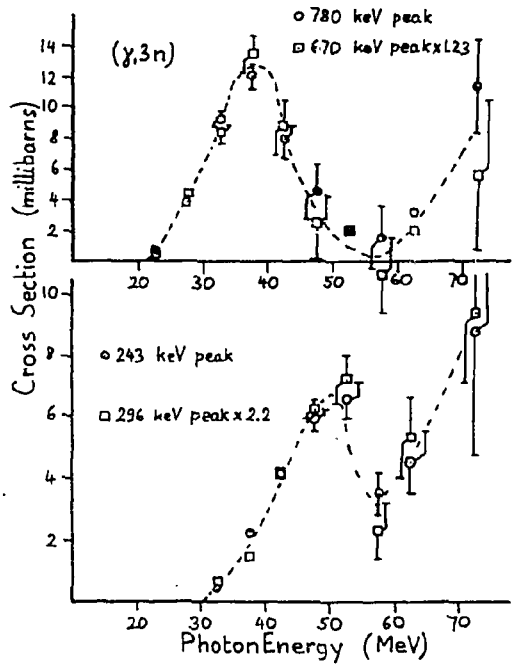

Figure D-2

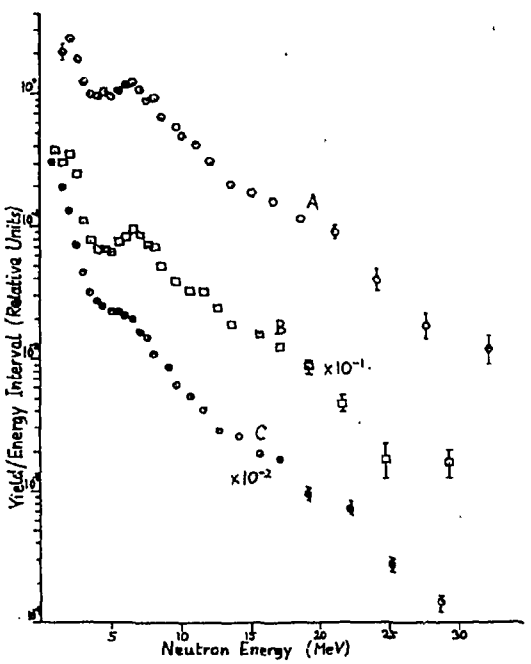

Figure D-3

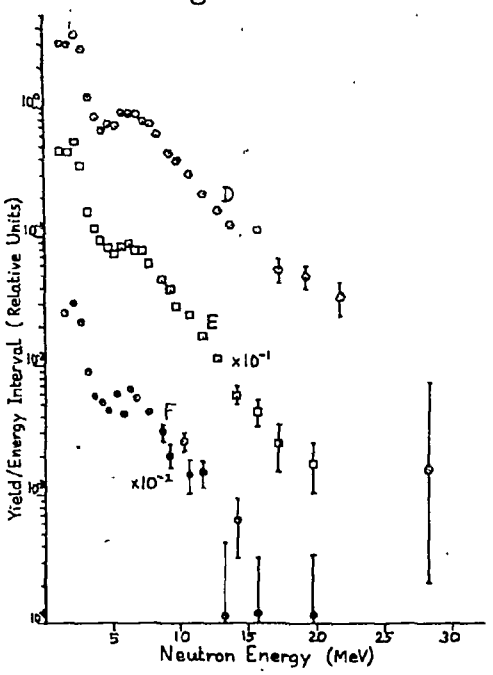

Figure D-4

DATA NOT FOR QUOTATION

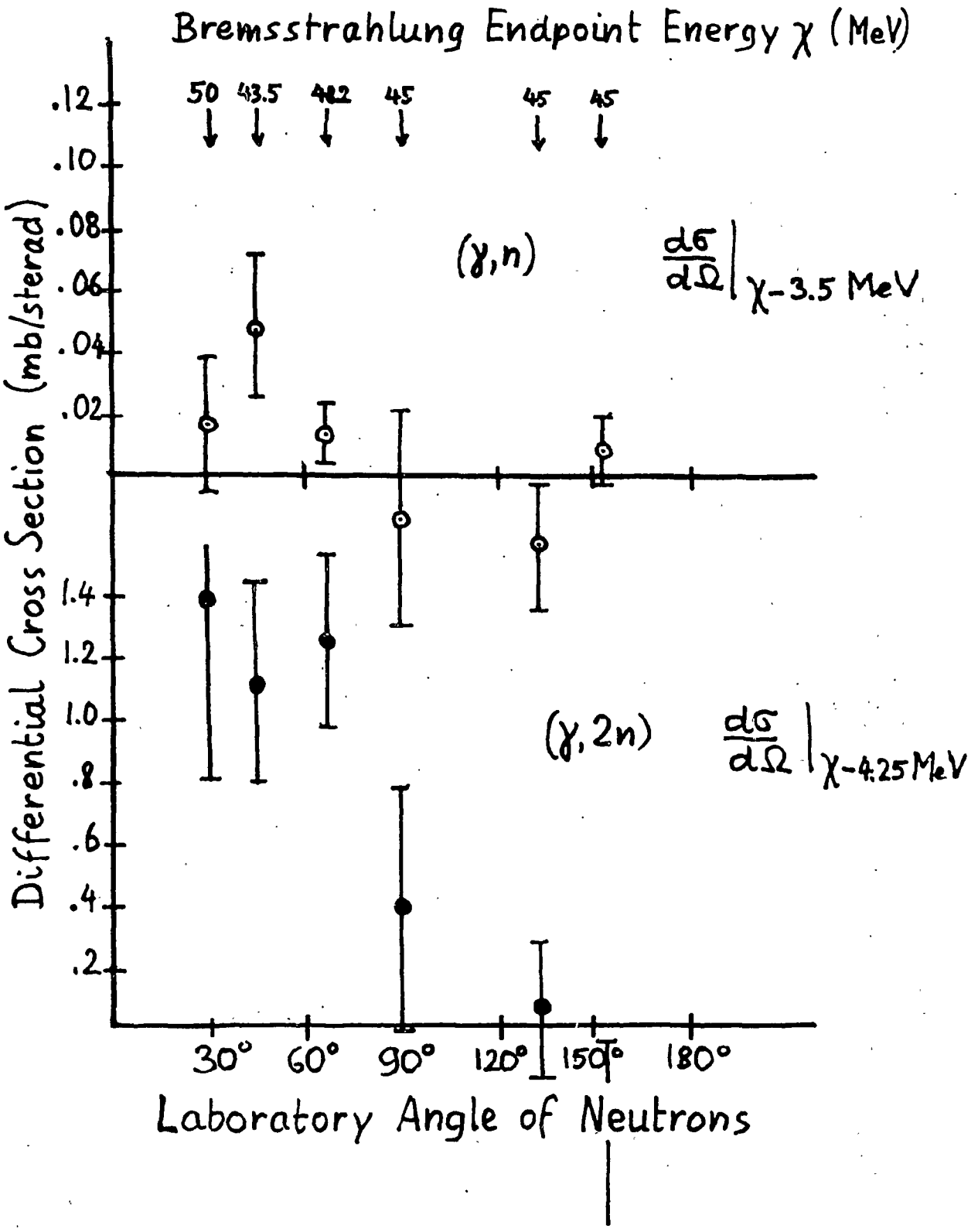

Figure D-5

DATA NOT FOR QUOTATION

BONNER NUCLEAR LABORATORIES, RICE UNIVERSITY

A. NEUTRON PHYSICS

1. Preparation of Monoenergetic Neutron Beam on the Tandem (A. Hochberg and G. C. Phillips)

A thin scintillator mounted on a very small photomultiplier tube is used for charged particle detection inside the low mass neutron production target chamber developed earlier. It will be applied to ^{3}He-N coincidence in the D(D,N) ^{3}He reaction using tandem pulsed-bunched beams. The purpose of this will be to produce a monoenergetic source of near forward-going ($\sim 20^\circ$ lab) d-d neutrons by requiring beam pulse-^{3}He delayed coincidences. The scintillator has its thickness adjusted to optimize the ^{3}He pulses.

2. Fast Neutron Spectroscopy (D. E. Velkley, G. S. Mutchler, D. Rendić, D. Bernard,* J. Sandler, and G. C. Phillips)

Using the fast neutron time-of-flight facilities, including a thin walled, low total mass scattering chamber, neutron measurements from ^{12}C(d,n) and ^{13}C(d,n) at a bombarding energy of 11.8 MeV have been made with the pulsed deuteron beam from the tandem Van de Graaff accelerator. By collecting the data in a multi-parameter format, excellent gamma ray discrimination was obtained without sacrificing neutron detection. Angular distributions from ^{12}C(d,n) to the first four levels in ^{13}N, and from ^{13}C(d,n) to the first three levels in ^{14}N have been measured from 12° to 135° in the center of mass. These angular distributions exhibit characteristic stripping patterns. DWBA calculations and the extraction of spectroscopic factors for the above mentioned angular distributions are in progress. Measurements of fast neutrons from ^{11}B(d,n) and ^{10}B(d,n) are presently being undertaken. Papers on the experimental techniques of beam pulsing-bunching, of the low-mass chamber, gamma ray discrimination, and neutron counter performance are being prepared.

---

* Present address: University of Southwestern Louisiana, Lafayette, Louisiana.

B. FEW NUCLEON PROBLEMS AND MANY-PARTICLE BREAK UP STUDIES

1. Investigation of the Reactions $^1H(d,pp)$ and $^1H(d,pn)$ (M. Ivanovich, E. V. Hungerford III, J. Sandler, W. von Witsch, and G. C. Phillips)

Some data at 12 MeV and 11 MeV incident energy have been obtained and data reduction is in the process. Computer codes for theoretical calculations utliizing Watson-Migdal, P.G.B., and PWBA theories have been developed. Further data taking is planned in order to enable us to conduct a more thorough analysis of the problem.

2. Reaction $d+d \rightarrow p+p+n+n$ (W. von Witsch, T.R.Canada, A. Niiler, J. Sandler, M. Ivanovich, and G.C.Phillips)

The reaction $d+d \rightarrow p+p+n+n$ is being investigated at 11-12 MeV bombarding energy, detecting the two protons in coincidence. A distinct locus in the E_1-E_2 plane has been observed, corresponding to events due to the kinematically completely determined reaction $d+d \rightarrow p+p+(2n)$. A missing mass analysis is being conducted to determine the energy and width of this n-n final state interaction. This reaction is of particular interest since the n-p and p-p final state interactions can be investigated in the same way, and a comparison with the n-n interaction is possible.

3. The Study of the d+t Reaction (G. S. Mutchler, J. Sandler, R. Spiger, and G. C. Phillips)

Hardware for this experiment has now been completed and tested. By recording charged particle-charged particle, and charged-particle - neutron time of flight coincidences simultaneously, it is hoped that final state interactions yielding insight into the mass-4 system will be observed.

4. Neutron-Proton Coincidence Measurements in the Reaction $^9Be(p,pn)^8Be$ (A. S. Wilson, J. Sandler, V. A. Otte, and G. C. Phillips)

Thin self-supporting and carbon-backed beryllium foils were bombarded with a 11.0, 11.5, and 12.0 MeV proton beam from the tandem Van de Graaff accelerator. Recoil protons at 110° or 88.4° (lab) and neutrons at 30° or 40° (lab), respectively, were detected in coincidence. This geometry was chosen to investigate low-lying states of ^9Be. Proton energy was determined with a solid state detector;

neutron energy was determined through time-of-flight techniques. Pulse shape discrimination between neutron and gamma scintillations in the neutron counter was employed. Spectra were stored and displayed on-line by the modified IBM 1800 1024 x 1024 channel computer-analyzer. Four spectra, with a typical accumulation time of 36 hours, were obtained. Peaking of counts was observed along the three-body locus $^{9}Be(p,pn)^{8}Be_{g.s.}$ at the expected positions of states in ^{9}Be and ^{9}B. The most striking feature of the spectra was an anomaly due to the population of $^{9}Be_{2.43}$ by inelastic proton scattering. The 2.43 state was found to decay to $^{8}Be_{g.s.}$ on the order of 5%, in agreement with the value of 12± 5% given by Marion et al.[1] Preliminary investigations of the mode of decay of the remainder of the anomaly, using density of states functions, have indicated a spatial localization of ^{8}Be in an S-wave "state," with suitable angular emission factors taken into consideration to account for the observed decay to the ground state of ^{8}Be.

5. Investigation of the Reactions $^{9}Be(p;p,\alpha)^{4}HeN$ and $^{9}Be(p;p,N)^{8}Be$ (E. V. Hungerford, M. Ivanovich, J. Sandler, and G. C. Phillips)

Interpretation and collection of data of the neutron and alpha decay of the 2.43 MeV level of ^{9}Be is in progress. Preliminary analysis shows a broad double peak in the decay particle spectra which cannot be described by either a simple sequential decay through ^{8}Be or ^{5}He. This experiment supplies additional information to that of $^{9}Be(p,pn)^{8}Be$ reported above.

6. Studies of the Reaction $^{13}C+p \rightarrow {}^{12}C+p+n$ (V.A. Otte, W. von Witsch, J. Sandler, D. Rendic, and G. C. Phillips)

Additional n-p correlation data have been obtained for proton energy 10.9 MeV, with both neutron and proton detectors at 30°, and for proton energy 7.9 MeV, with both detectors at 92°. Final analysis of the data is yet to be completed; preliminary reduction does not show any strong peaking in the region corresponding to low relative energy in the n-p final state system.

---

[1] J. B. Marion, J. S. Levin, and L. Cranberg, Phys. Rev. 114, 1584 (1959).

7. $d + {}^{12}C \rightarrow p + n + {}^{12}C$ (J. Sandler, V.A. Otte, E.V. Hungerford, D. Rendić, and G. C. Phillips)

Data at incident energies of 5.4, 8.8, 9.2, and 9.85 MeV have been collected for this reaction. Contrary to expectations, little evidence for singlet deuteron (T=1) production at the higher energies was observed. At 5.4 MeV, increased yields may be ascribed to either this or rescattering contributions. Work is being continued in an attempt to resolve this ambiguity.

8. Investigation of Coulomb Rescattering Process (D. Rendić, E. V. Hungerford, J. Sandler, and G.C.Phillips)

Rescattering in 3-body final state processes has thus far been investigated between neutrons and charged particles. In order to investigate such a process between two charged particles, the reactions $p + {}^{16}O \rightarrow \alpha + p + {}^{12}C$ and $d + {}^{14}N \rightarrow t + p + {}^{12}C$ are under consideration. Using gaseous targets, α-p and t-p coincidence spectra will be measured, respectively. Special care will be taken to see the distortion of charged particle spectrum induced by the presence of the other charged particle in the vicinity.

C. NUCLEAR SPECTROSCOPY AND NUCLEAR REACTION STUDIES

1. Cross Sections of the (p,γ) and the (p,α) Reactions with ${}^{40}Ca$ (R. Clark, L. R. Greenwood, R. W. Dougherty, and C. M. Class)

The ${}^{40}Ca(p,\gamma){}^{41}Sc$ and ${}^{40}Ca(p,\alpha){}^{37}K$ reactions are being studied in the energy range $E_p = 5.0$ — 12.5 MeV. The positron decays of the ${}^{41}Sc$ and ${}^{37}K$ ground states are detected, with the relative amounts being determined by a series of half life measurements. The (p,α) contribution is dominant above 9 MeV. Throughout the region strong resonances are superimposed on a continuum with the average cross sections varying from approximately 10 μb below 7 MeV to approximately 15 mb near 12.5 MeV.

2. Spin Determinations of Highly Excited Levels of ${}^{40}Ca$ (C. Sinex, R. Cox, and C. M. Class)

An investigation of the spins of highly excited states of ${}^{40}Ca$ is in progress using gamma ray angular correlation (Litherland and Ferguson geometry II). The effort at present

is directed to the study of the last levels below 7 MeV whose spins are unknown: those at 6.9 and 6.75 MeV and a triplet at 6.5 MeV. Suitable beam energies for the optimum population of these levels have been found by measuring excitation functions. Studies of the gamma ray decays of the levels are now being concluded, prior to undertaking the correlation measurements.

3. An Optical Model Analysis of $^{40}Ca(p,p)^{40}Ca$ Angular Distributions from 5.0 to 21.0 MeV (T. M. Jurgensen, C. M. Class, and J. S. Duval)

Angular distributions of protons elastically scattered by ^{40}Ca, measured at Rice and at Los Alamos, are being analyzed in terms of the Optical Model. Special emphasis is being placed on the interval of bombarding energies from 8.0 to 12.5 MeV where angular distributions and total reaction cross sections are available at 50 keV intervals.

4. Study of the $^{40}Ca(d,n)^{41}Sc^*(p)^{40}Ca$ Reaction (L.R. Greenwood, J. Sandler, R. Cos, and C. M. Class)

Angular distributions of the neutrons leading to the 1.71 MeV, $J^{\pi} = 3/2^-$ level of $^{41}Sc(Q = 3$ MeV) have been measured in the range $3.4 \leq E_D \leq 6.0$ MeV with the tandem time-of-flight apparatus. Characteristic $\ell = 1$ stripping patterns are observed at all energies. Measurements of the angular distributions of the protons from the break up of this level have been completed as well. These distributions, of the form $W(\theta) = 1 + a_2P_2(\cos\theta)$, show a strong attenuation of the a_2 coefficient as a function of energy. An explanation of this effect in terms of a DWBA analysis of both bodies of data will be sought.

D. POLARIZATION STUDIES

1. ^3He-^3He Elastic Scattering Using a Polarized ^3He Below 12 MeV (Wilber Boykin)

In view of the results at higher energies an investigation of ^3He-^3He polarization asymmetries with improved statistics has been undertaken. A target of optically pumped ^3He gas, and the $^3He^{++}$ beam from the 6 MV Van de Graaff accelerator is being employed. In addition to elastic scattering it is possible to observe the protons from the $^3He(^3He,p)^5Li_{g.s.}$ with the present apparatus.

2. Scattering of 7.5 to 17.9 MeV ^{4}He by Polarized ^{3}He (D. Hardy, S.D. Baker, R. Spiger, and T. A.Tombrello*)

Left-right asymmetries from an optically pumped ^{3}He target at 33°_{LAB} have been measured using ^{3}He and ^{4}He beams over the range 7.5 - 17.9 MeV which were supplied by the Caltech tandem. For ^{4}He-^{3}He elastic scattering two c.m. angles were observable. The forward angle $79^\circ_{c.m.}$ provided a verification of the high polarization >90% which persists over a large energy interval as predicted from the plane shifts of Spiger and Tombrello.** This region appears to be optimal from the standpoint of constructing a ^{4}He polarimeter for medium energy ^{3}He scattering experiments. The back angle ($114^\circ_{c.m.}$) polarization does not display the structure predicted from the plane shifts. The large discrepancies are probably accounted for by the sensitivity of the polarization to inelasticity in both resonant and non-resonant plane shifts.

3. ^{3}He(^{4}He,p)^{6}Li Reaction from 10.7-17.9 MeV (D. Hardy, S. D. Baker, R. Spiger, and T. A. Tombrello)

At the same time that the ^{3}He-^{4}He elastic scattering was being measured, asymmetries of the proton from the (^{4}He,p_0) and(^{4}He,p_1) reaction with a polarized ^{3}He target were also measured. Preliminary analysis shows that the analyzing power for this reaction at 33°_{Lab} has magnitudes comparable to the proton analyzing power in the inverse reaction.

4. Scattering of 4.3-17.5 MeV ^{3}He by Polarized ^{3}He (D. Hardy, S.D. Baker, R. Spiger, and T.A.Tombrello)

Using the same apparatus, the ^{3}He-^{3}He elastic scattering at $66^\circ_{c.m.}$ was observed. Within the accuracy of our experiment no left-right scattering asymmetry was observed in this energy range. Typical statistical errors were $\pm$ 0.05 in the analyzing power of this reaction.

---

* Present address: California Institute of Technology, Pasadena, California.

** R. J. Spiger and T. A. Tombrello, Phys. Rev. 163, 964 (1967).

5. Scattering of 6 to 10 MeV Deuteron by Polarized ^{3}He (D. H. McSherry, R. Spiger, S.D.Baker, and D. Hardy)

Asymmetry data taken at 55°c.m. and 111°c.m. indicate that the d-^{3}He elastic scattering produced ^{3}He polarized to approximate the same degree as the deuteron vector polarizations measured at Wisconsin. Further measurements at other angles are planned to provide angular distributions for ^{3}He polarization.

6. Proton Polarization in the ^{3}He(^{3}He,pp)^{4}He Reaction (M. Ivanovich)

This work is being planned at present with the purpose of acquiring information on the mechanism of the reaction as well as the level structure of the ^{5}Li nucleus which can be formed if the mechanism favors sequential decay. The completion of this work will depend on whether the negative Helium source becomes available on the tandem.

E. NUCLEAR THEORY

1. Nuclear Cluster Model Trial Wave Functions (J. E. Beam and K. Wildermuth*)

Under investigation is the possibility of simplifying nuclear cluster-model calculations by judiciously choosing trial functions so as to minimize the amount of antisymmetrization required.

2. Single-Separable Potential with Attraction and Repulsion (J. E. Beam)

A one-term separable interaction due to Tabakin[1] has been studied in the context of 2- and 3-body systems. It has been shown[2] that, contrary to a previous expectation, this potential cannot fit the nucleon-nucleon singlet-S phase shift, and is completely inappropriate for describing bound states of the 3-nucleon system.

---

*Present address: Institute for Theoretical Physics, Tübingen, Germany.

[1] F. Tabakin, Phys. Rev. 174, 1208 (1968).

[2] J. E. Beam, Phys. Lett. (in press).

F. INSTRUMENTATION

1. 1800 Computer System - Hardware (J. Buchanan)

The hardware is near completion with most circuits tested in all modes. Final tests are expected in the next reporting period.

2. Computer System - Software (H. Jones, M. Jones, and B. Smith)

The following progress has been made.

a. BONER Systems Development

Final stages of initial system implementation; some development of future system capabilities; and documentation of the system.

b. SREL Software Support

Implementation of system at the University of Houston 360-44 and program development and design.

3. Position Sensitive Proportional Counters (R. N. Persson, J. Windish, and G. C. Phillips)

Building and testing position sensitive, multiwire, proportional counters to be used at the SREL in October, 1969 are in progress. 6 one coordinate counters (204 wires/counter) and 2 two coordinate counters (408 wires/counter) are under fabrication. Each counter is of hexagonal shape, uses 3 or more planes of 2 mil wires with 50 mil spacing. These counters will also be used in the Bonner laboratories (see F-6 below).

4. Readout Electronics for Multiwire Proportional Counters (J. A. Buchanan)

In February, 1969 development of amplifiers and a readout system for the multiwire proportional chambers to be used in the SREL π^- experiment by the Rice-University of Houston High Energy Group started. After an initial small scale system was built and tested, design of the actual experiment was completed and construction is now partially finished. The final system will provide amplifier and logic for up to 3 planes of wires/counter with 204 wires/plane.

5. Multiwire Proportional Counter Camera for a Browne-Buechner Magnetic Spectrograph (R. Plasek, R. N. Persson, J. A. Buchanan, and G. C. Phillips)

A camera of 1000 proportional wires and a backing scintillation counter is being designed for the Bonner Nuclear Laboratories Brown-Buechner magnetic spectrograph. The position sensitive multiwire counter, coupled to the 1800 computer system will give $B\rho$ of the particles and the dE/dx is given by the linear signal. When used with a pulsed-bunched beam to measure time of flight to the scintillation detector the system will be capable of giving magnetic spectra versus Z and m.

6. A Large-solid Angle Reaction-chamber and Detector (D. Rendic and G. C. Phillips)

Design is completed on a chamber that will allow mounting two of the large hexagonal multiwire counters. Each will subtend about 1/2 steradian.

7. Installation of New 90° Energy Analyzing Magnet on Rice University 5.5 MV Van de Graaff Accelerator (W. Boykin, R. N. Persson, J. R. Risser, and G. C. Phillips)

A new 90° energy analyzing magnet has been installed on the 5.5 MV Van de Graaff accelerator. The magnet is mounted on a rotating base and is connected to the accelerator column by a rotating "O" ring seal which allows the beam tube to be oriented at any desired angle in the 100° permitted range. Rotation is accomplished without disturbing the vacuum in the beam tube and column. Energy calibration has been completed and is considered accurate to $\pm$ 0.1%.

8. Development of a Negative Helium Ion Source for the Tandem (M. Ivanovich)

The source has been operated successfully as an R-F facility and currents up to 1 mA of $^{4}He^{+}$ have been obtained. The exchange canal has been installed and good vacuum condition has been established. However, some unexpected technical difficulties have been encountered causing delay in completing this project.

9. Injection of Polarized ^{3}He Beam into a Cyclotron (S. D. Baker)

Nuclear structure and reaction mechanism studies should be very interesting with a polarized ^{3}He beam. It has been shown* that ^{3}He ions will suffer very little depolarization while being accelerated in a cyclotron such as the Berkeley and Texas A & M 88" cyclotrons. Modification of the method used at Berkeley** to inject polarized protons into the acceleration plane of the 88" cyclotron are being considered.

10. The Temperature Dependence of Electron-hole Pair Creation Processes in Silicon Nuclear Radiation Detectors (T. A. Rabson and J. R. Key)

The following goals were achieved:

a) A cryostat system capable of maintaining stable temperatures between 4.2-300 K was purchased, tested, and calibrated. The system has the facility of subjecting detectors in a controlled manner to radiation from natural sources.

b) A system was planned and the necessary equipment purchased or built to allow high-resolution spectra to be taken on a 2048 channel pulse-height analyzer. The system has been extensively calibrated (referred to the National Bureau of Standards) so that absolute measurements may be made. Final testing is currently in progress.

c) In a parallel effort directed toward the production of successful detectors, preliminary studies were made on quantitative tests for each step in the fabrication process.

11. Switching Phenomena in PIN Diodes (T.A. Rabson and T. L. Harmon)

The work will hopefully lead to a better understanding of the underlying principles governing the behavior of nuclear radiation detectors. The research has two aspects, one theoretical and the other experimental. The theoretical

---

* D. O. Findley, Ph.D. thesis, Rice University (unpublished)

** D. J. Clark, private communication.

study is expected to culminate in a computer solution of the switching problem. Empirical data will then be used as a check on the mathematical model proposed. The behavior of the diode as a radiation detector will be related to its switching properties. The past six months have been spent in assembling the necessary test apparatus and determining the mathematical method to be applied to the problem.

G. INTERMEDIATE ENERGY PHYSICS

1. Study of π^- Elastic, Inelastic, and Total Cross Sections from Nuclei Near the 3/2-3/2 Resonance (G. C. Phillips, E. V. Hungerford, and G. Mutchler)

An experiment has been designed to attain a high resolution π^- beam and to resolve groups of elastic and inelastically scattered pions from nuclei. The experiment employs the technique of time of flight and magnetic deflection of the pions with the straight line orbits of entering and emerging events determined accurately by thin, fast, multiwire proportional counters and scintillators. Energy resolution of 1% or better is desired. Goals of the experiments include: (a) studies of total cross sections and small angle scattering, (b) elastic and inelastic spectra and angular distributions, and (c) excitation curves of the above across the 3/2-3/2 resonance. Presently the counters, electronics, and computer interfacing logic have been designed and are under construction. The testing and investigation of beam profile, counter resolution, and efficiency are underway. The first physics measurement will be in October, 1969 and will include spectrometer resolution measurements and total cross section measurements.

TEXAS NUCLEAR

A. NEUTRON PHYSICS

1. Fluorescent and Low Energy Studies on W, ^{238}U, and Pu (D. O. Nellis, P. S. Buchanan, W. E. Tucker, and J. A. Stout)

(Work pertinent to requests #233, #310, and #338 WASH 1078)

Measurements of the yield of fluorescent X-rays and low energy gamma rays produced by the bombardment of high Z elements with 1 MeV incident neutrons are currently under way. A 2" x 1-3/4" NaI(Tl) crystal is used as the center detector in the anticoincidence spectrometer and time-of-flight gating is employed to reduce backgrounds. The time-of-flight gating turned out to be quite important in reducing the backgrounds from delayed activity in the detector and from the prompt gamma rays of iodine in the detector. The 59 keV gamma ray from the first excited state of iodine which has the same energy as the K-fluorescent X-ray from tungsten will interfere with the measurement of the fluorescent line unless it is eliminated by this gating technique.

A spectrum from fluorine (using a teflon scatterer) was first taken to test the operation of the electronics and to illustrate the operation of the time-of-flight gating. In addition, the only gamma-ray lines excited at this bombarding energy are at 110 keV and 198 keV, the first of which lies in the energy region of the K-fluorescent X-rays from the heavier elements. Figure 1.1 shows the positions of the time gates used (see insert on figure) and the spectra corresponding to these gates. The bottom spectrum is the difference of the upper two. The disappearance of the 198 keV peak in the difference spectrum is attributed to its rather long mean lifetime of 125 nanoseconds.

Spectra obtained from W and ^{238}U scattering samples are shown in Figs. 1.2 and 1.3. No measurements were made on Pu in this energy region since the high natural radioactivity of the sample produced large electronic dead times. In Fig. 1.2, the 59 keV peak is attributed to the fluorescent K X-ray line of W, while the peaks at 113 keV and 250 keV arise from the de-excitation of the first and second excited states in the three even isotopes of tungsten. Cross sections for the three peaks are shown in Table 1.1. The peak at 50 keV in

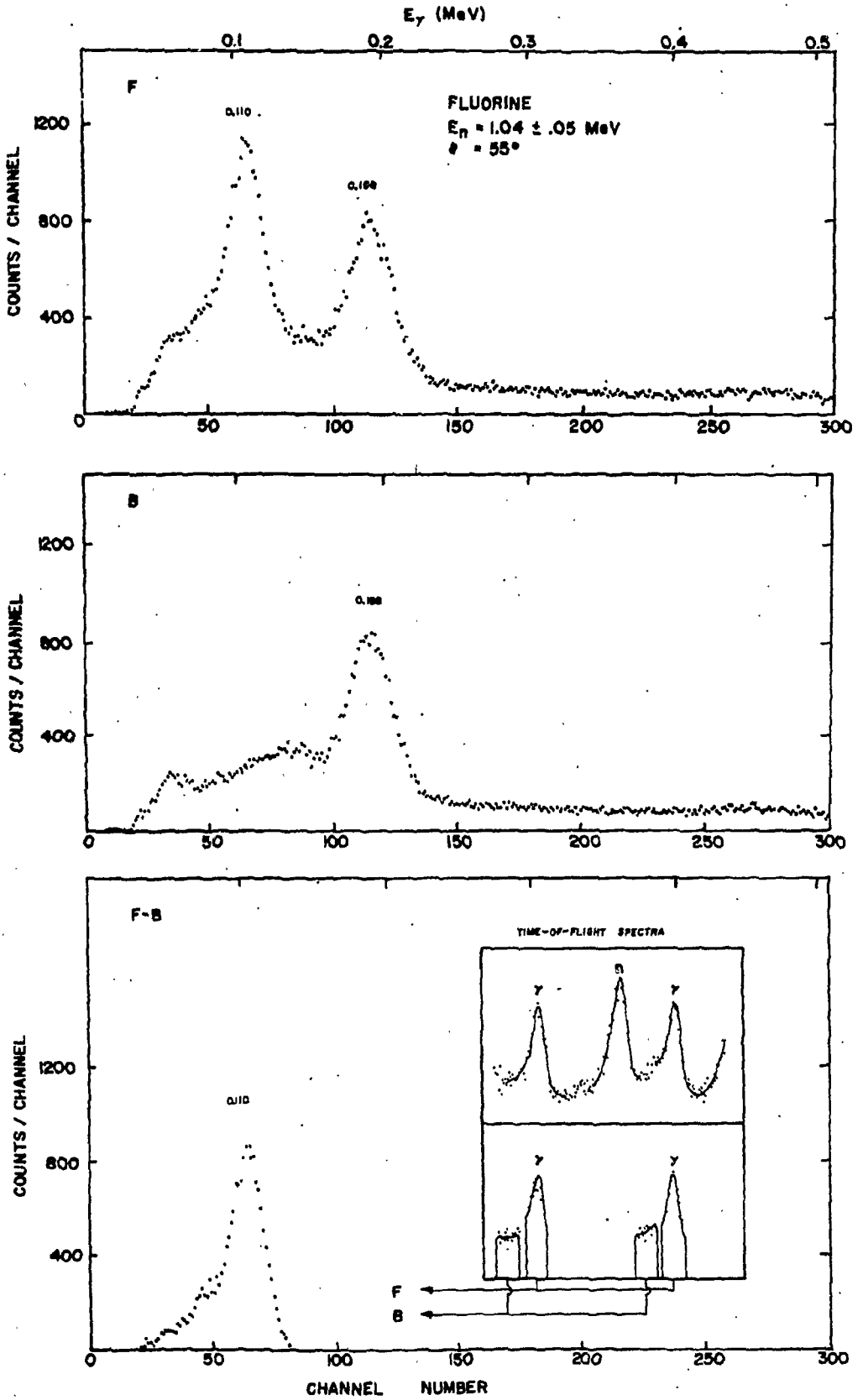

Figure 1.1

DATA NOT FOR QUOTATION

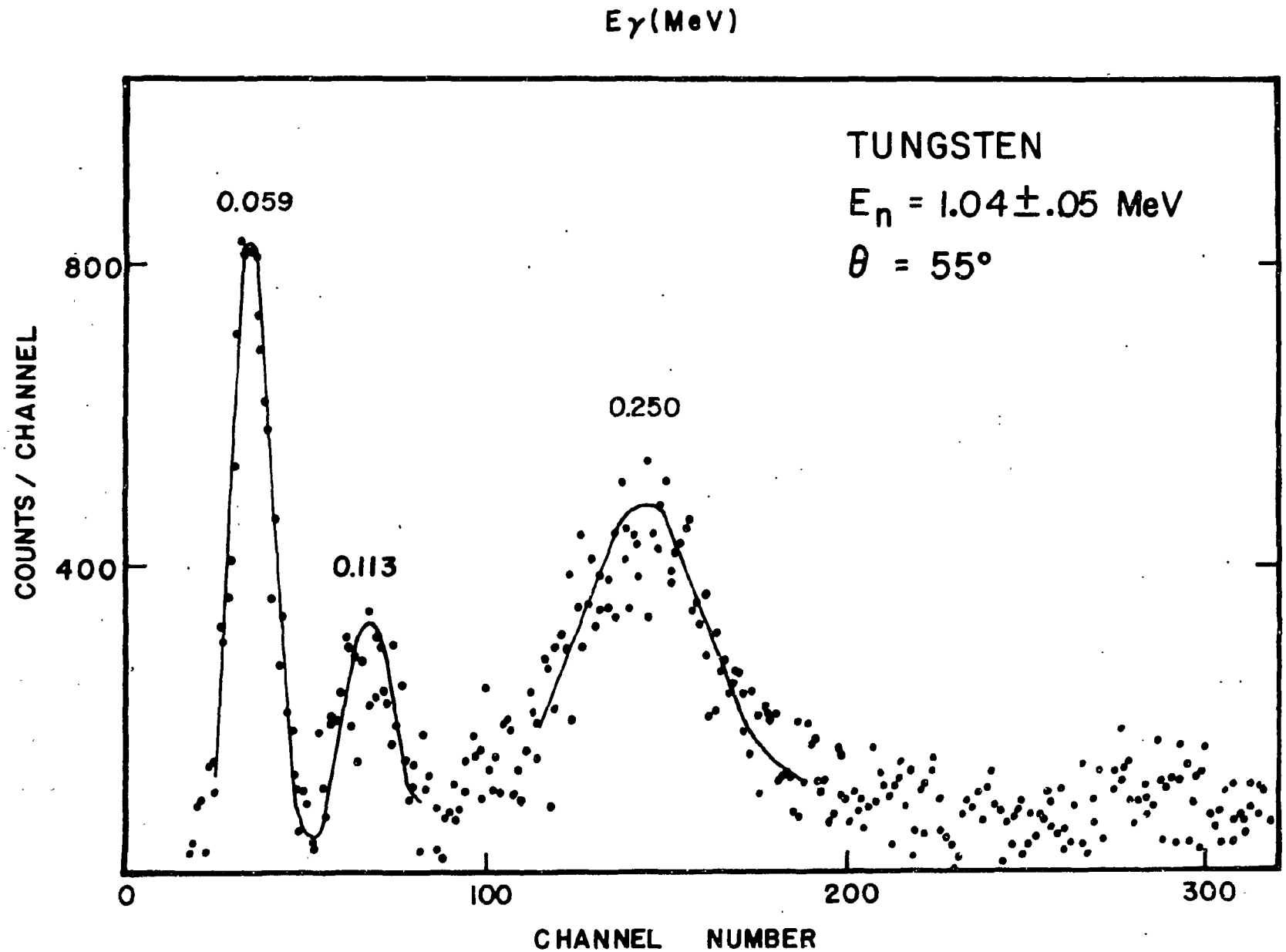

Figure 1.2

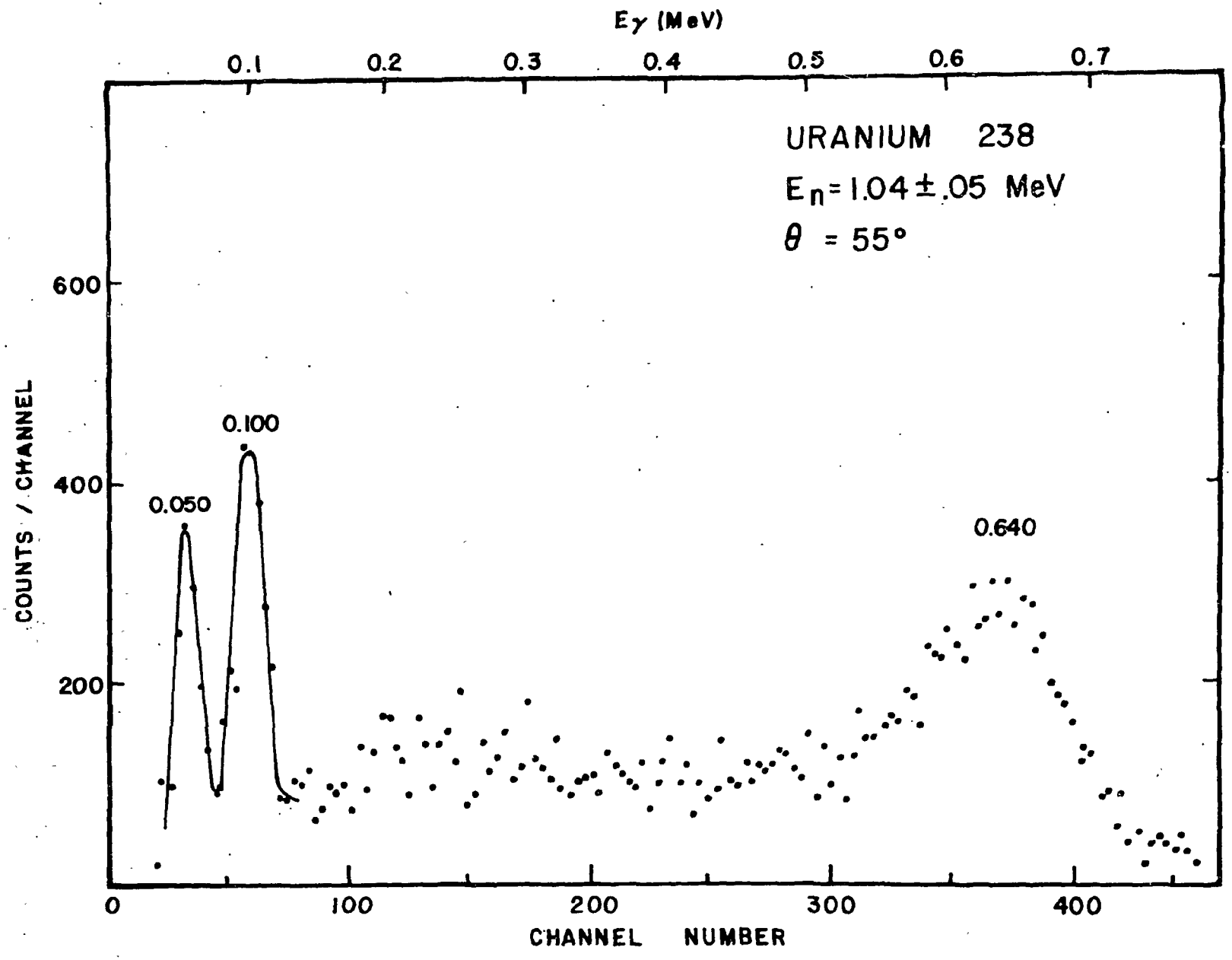

Figure 1.3

Fig. 1.3 is thought to be from the first excited state of ^{238}U and the 100 keV peak from a second to first excited state transition. The broad peak near 640 keV results from ground state transitions from the several levels reported in this energy region. Any uranium K fluorescent X-rays (98 keV) would be included in the 100 keV peak of Fig. 1.3. The small conversion coefficients associated with transitions from the higher levels however, imply that the fluorescent yield would be low. Cross sections for the peaks shown are listed in Table 1.2.

2. Capture Gamma-Ray Measurements (D. O. Nellis, W. E. Tucker, T. C. Martin, and J. A. Stout)

(Work pertinent to requests #233, #310, and #338 WASH 1078)

Additional measurements of the capture gamma-ray yield from W, ^{238}U, and Pu have been made using 300 keV incident neutrons. The spectra observed showed no evidence of high energy peaks associated with direct decays to the ground state. Cross sections for W and ^{238}U are listed in Tables 2.1 and 2.2. Comparisons of the integrated gamma-ray yield with reported (n,γ) cross sections indicate gamma-ray cascades consisting of approximately 7 gamma rays per capture event.

3. Silicon and Tungsten (W. E. Tucker, P. S. Buchanan, T. C. Martin, D. O. Nellis, G. H. Williams, and D. M. Drake*)

(Work pertinent to requests #71, #233, and #234 WASH 1078)

Gamma-ray production from natural silicon and tungsten has been measured at incident neutron energies between 5 and 11 MeV. Both the Texas Nuclear Van de Graaff facility and the Los Alamos tandem facility were used to make the measurements. Analysis of the data is complete and the results have appeared as report DASA-2333.

*Los Alamos Scientific Laboratory

TABLE 1.1

GAMMA-RAY PRODUCTION CROSS SECTIONS FOR TUNGSTEN

$E_n = 1.04 \pm 0.05$ MeV

E_γ (MeV)	$d\sigma(55^\circ)/d\Omega$ (mb/sr)	$4\pi \cdot d\sigma(55^\circ)/d\Omega$ (mb)
0.059	59.5	747
0.113	20.5	257
0.250	32.2	404

TABLE 1.2

GAMMA-RAY PRODUCTION CROSS SECTIONS FOR URANIUM 238

$E_n = 1.04 \pm 0.05$ MeV

E_γ (MeV)	$d\sigma(55^\circ)/d\Omega$ (mb/sr)	$4\pi \cdot d\sigma(55^\circ)/d\Omega$ (mb)
0.050	43.5	546
0.100	16.8	211
0.640	35.9	451

TABLE 2.1

GAMMA-RAY PRODUCTION CROSS SECTIONS FOR TUNGSTEN

$E_n = 0.302 \pm 0.06$ MeV

E_γ (MeV)	$d\sigma(55^\circ)/d\Omega$ (mb/sr)	E_γ (MeV)	$d\sigma(55^\circ)/d\Omega$ (mb/sr)
5.50-5.75	0.38	2.75-3.00	1.31
5.25-5.50	0.29	2.50-2.75	1.48
5.00-5.25	0.39	2.25-2.50	1.29
4.75-5.00	0.38	2.00-2.25	1.50
4.50-4.75	0.40	1.75-2.00	2.17
4.25-4.50	0.53	1.50-1.75	3.22
4.00-4.25	0.52	1.25-1.50	3.25
3.75-4.00	0.74	1.00-1.25	3.51
3.50-3.75	0.72	0.75-1.00	4.81
3.25-3.50	1.05	0.50-0.75	5.79
3.00-3.25	1.23	0.25-0.50	12.21
		TOTAL	47.07
		0.51	3.36

Total Continuum Less 0.51 MeV Peak = 43.71 mb/sr

$\times 4\pi$ = 549.0 mb

TABLE 2.2

GAMMA-RAY PRODUCTION CROSS SECTIONS FOR URANIUM 238

$E_n = 0.302 \pm 0.06$ MeV

E_γ (MeV)	$d\sigma(55^\circ)/d\Omega$ (mb/sr)	E_γ (MeV)	$d\sigma(55^\circ)/d\Omega$ (mb/sr)
5.50-5.75	0.07	2.75-3.00	1.78
5.25-5.50	0.15	2.50-2.75	1.70
5.00-5.25	0.12	2.25-2.50	2.34
4.75-5.00	0.15	2.00-2.25	3.61
4.50-4.75	0.04	1.75-2.00	4.89
4.25-4.50	0.32	1.50-1.75	5.22
4.00-4.25	0.05	1.25-1.50	5.69
3.75-4.00	0.34	1.00-1.25	6.52
3.50-3.75	0.38	0.75-1.00	6.83
3.25-3.50	1.10	0.50-0.75	13.14
3.00-3.25	1.22	0.25-0.50	16.62
		TOTAL	72.28
		0.51	4.27

Total Continuum Less 0.51 MeV Peak = 68.01 mb/sr
$\times 4\pi$ = 854.2 mb

4. Beryllium (D. O. Nellis and P. S. Buchanan)

(Work pertinent to requests #27 and #29 WASH 1078)

The gamma-ray production from Be has been measured using 14.8 MeV incident neutrons. The 478 keV gamma ray from the $^{9}Be(n,t\gamma)^{7}Li$ reaction was the only peak observed in the spectrum. Figure 4.1 shows the spectra obtained. The spectra marked F and B are those associated with the foreground and background gates in the time spectrum while the lower spectrum is the difference between the two. The continuum portion of the lower spectrum is due to room background and reduces to statistics when a no scatterer background is substracted. The cross section values obtained for the 478 keV peak are:

$$d\sigma(55^{o})/d\Omega = 0.79 \text{ mb/sr}$$

$$x4\pi = 9.95 \text{ mb}$$

This value is in close agreement with the results of Benveniste[1] at 14.1 MeV but is a factor of three lower than his result at 14.8 MeV.

5. Carbon (T. C. Martin and G. H. Williams)

(Work pertinent to request #37 WASH 1078)

Production cross sections for the 4.43 MeV gamma ray from carbon have been measured using incident neutron energies of 5.0 and 14.8 MeV. Spectra were taken using the 34cc Ge(Li) detector. Figure 5.1 shows the spectra obtained at 5 MeV and the insert illustrates the positioning of the time gates. The 2.23 MeV peak appearing in both spectra is from hydrogen capture in the detector shield and the other peaks are from the detector or background. The cross sections obtained are:

E_n (MeV)	$d\sigma(55^{o})/d\Omega$ (mb/sr)	$4\pi \cdot d\sigma(55^{o})/d\Omega$ (mb)
5.0	7.0	87.9
14.8	16.5	207.2

[1] J. Benveniste, A. D. Mitchell, D. C. Schrader, and J. H. Zenger, Nucl. Phys. 19, 52 (1960).

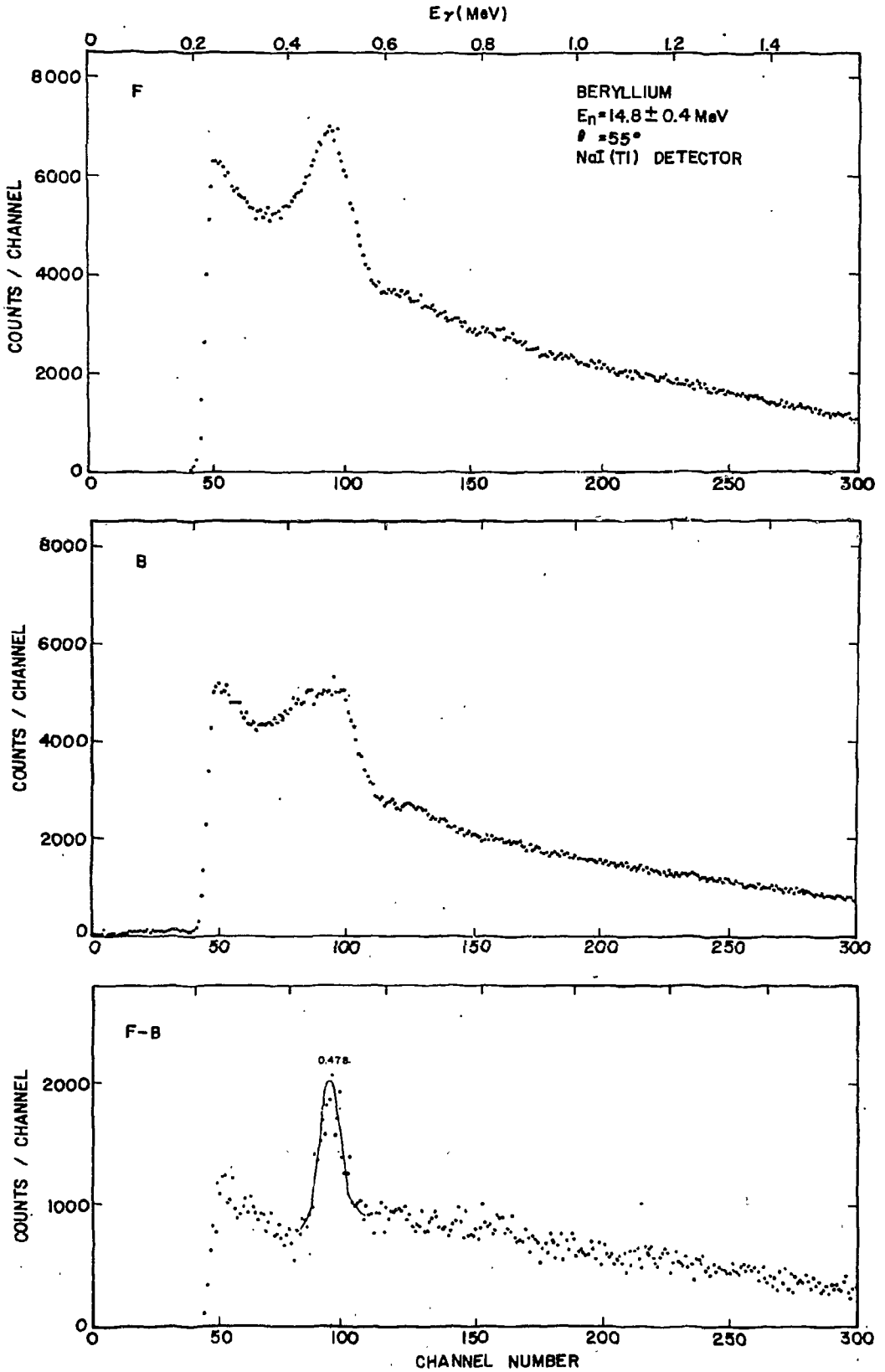

Figure 4.1

DATA NOT FOR QUOTATION

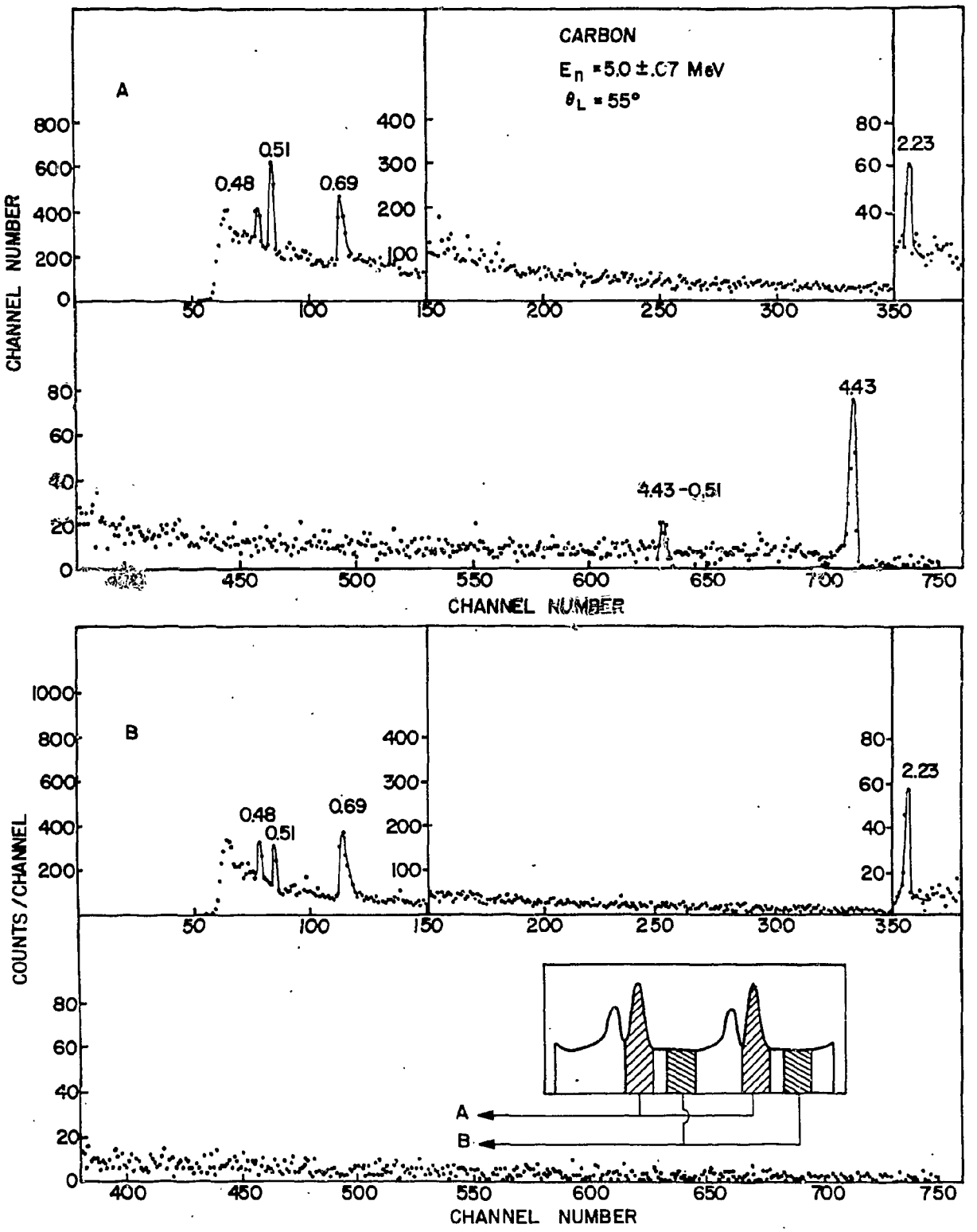

Figure 5.1

DATA NOT FOR QUOTATION

6. Nitrogen and Oxygen (P. S. Buchanan, W. E. Tucker, and D. O. Nellis)

(Work pertinent to requests #40, #41, #42, and #50 WASH 1078)

Several measurements at E_n = 14.8 MeV have been made and analysis and additional measurements are continuing. Lower energy measurements on N are planned. Figure 6.1 shows the spectrum obtained with a NaI(Tl) detector using slabs of BeO.

7. Chromium (P. S. Buchanan, D. O. Nellis, W. E.Tucker, and G. H. Williams)

(Work pertinent to request #88 WASH 1078)

Measurements have been made at neutron energies of 5.0 and 14.8 MeV. Figure 7.1 shows the spectrum obtained at 5 MeV using the Ge(Li) detector. Cross sections for the prominent gamma-ray peaks are given in Table 7.1. Theoretical calculations, including width fluctuation corrections, have been made over the neutron energy range 1.0 to 5.0 MeV. Comparison with the experimental values at 5 MeV are in excellent agreement for the most intense peaks at 0.936 and 1.434 MeV. Additional measurements at lower energy are planned.

8. Nickel (W. E. Tucker, P. S. Buchanan, T. C. Martin, and D. O. Nellis)

(Work pertinent to requests #115 and #116 WASH 1078)

Measurements were made at neutron energies of 4.0 and 14.8 MeV. Additional measurements at lower energies are planned. The spectrum obtained at 4 MeV, using a Ge(Li) detector, is shown in Figure 8.1 and cross sections for the more prominent gamma rays are listed in Table 8.1. Theoretical calculations similar to those mentioned under chromium have been made. Comparison with the 4 MeV data indicates only fair agreement. Comparisons are to be made at lower energies when data becomes available.

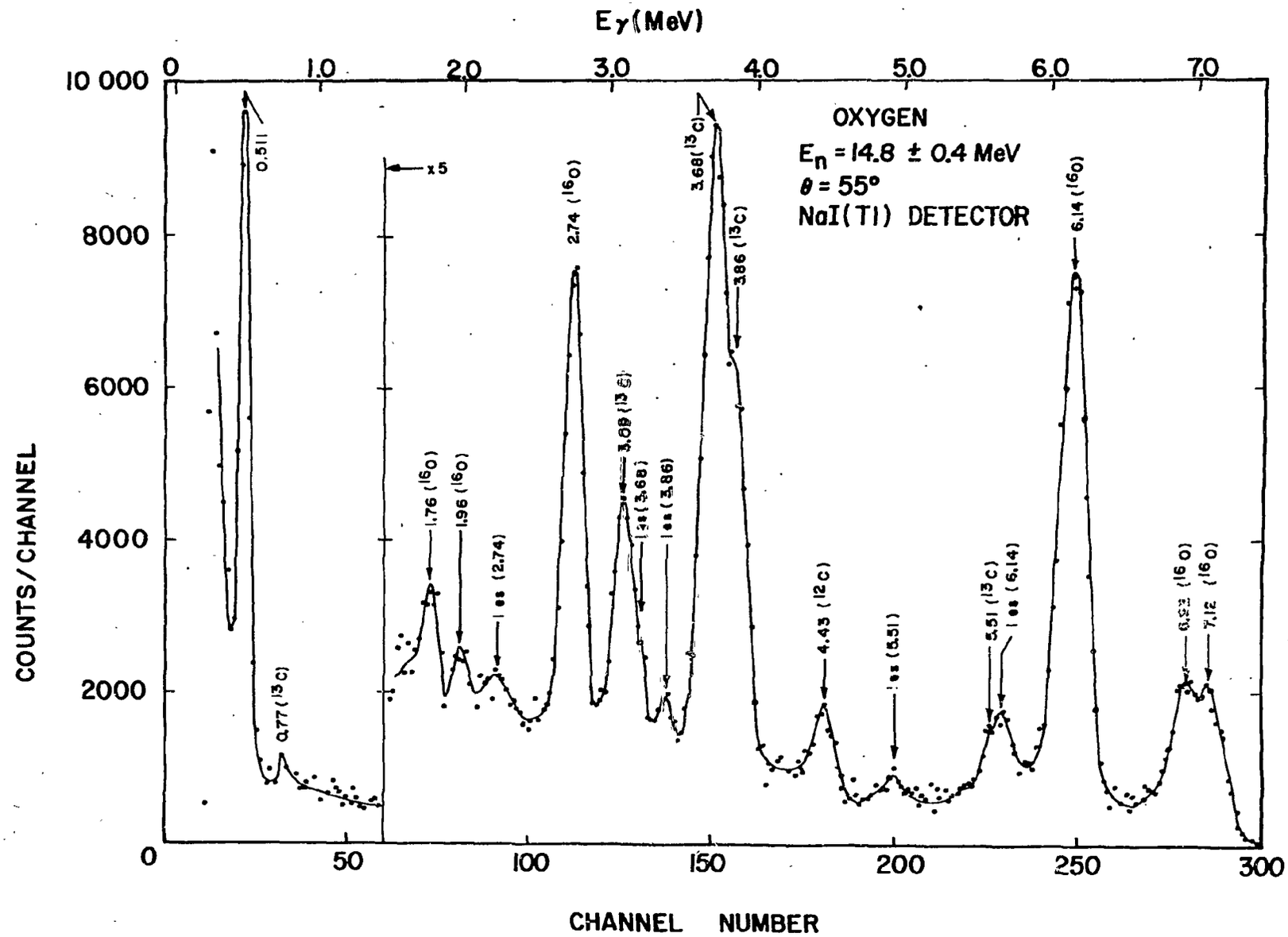

Figure 6.1

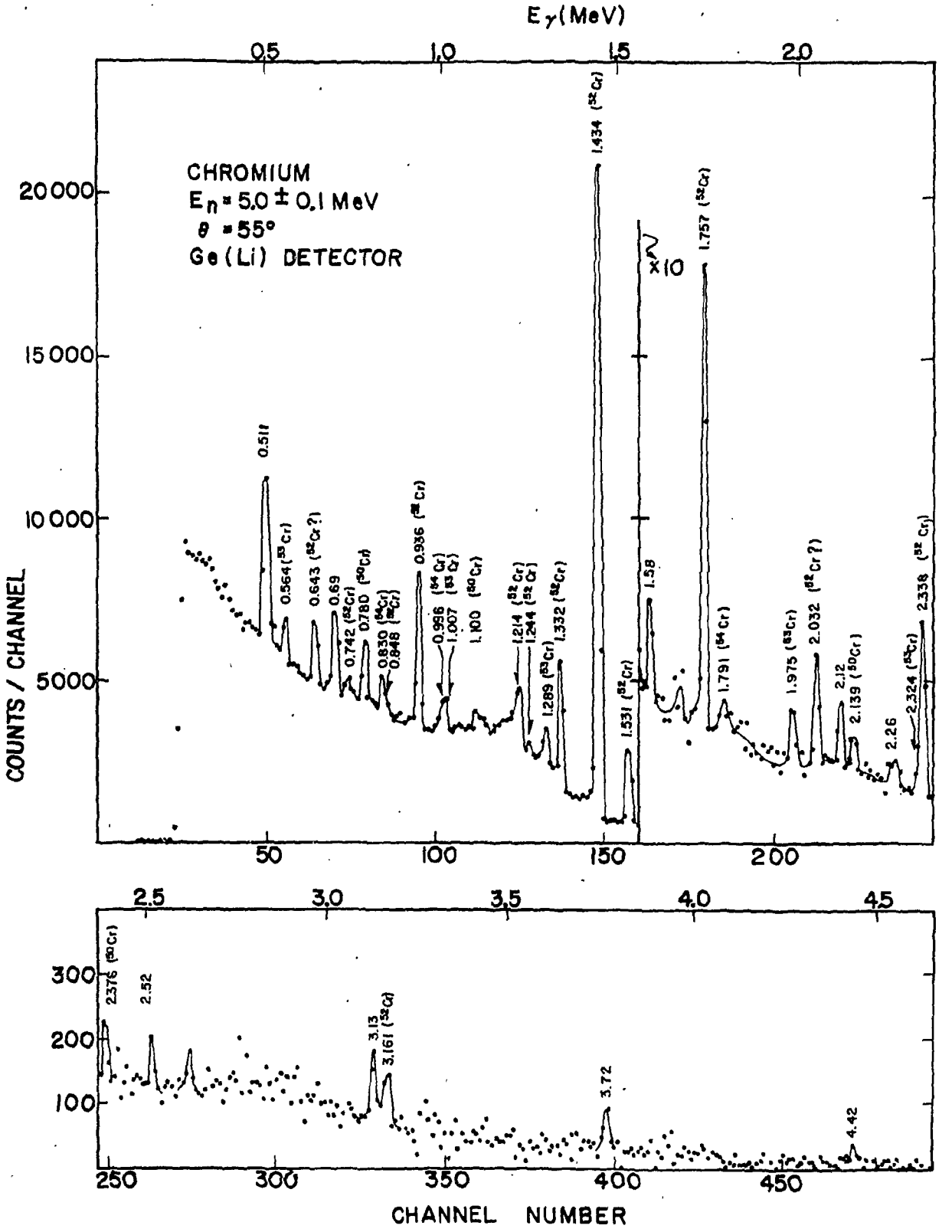

Figure 7.1

DATA NOT FOR QUOTATION

TABLE 7.1

GAMMA-RAY PRODUCTION CROSS SECTIONS FOR CHROMIUM

$E_n = 5.0 \pm 0.1$ MeV

E_γ (MeV)	$d\sigma(55^\circ)/d\Omega$ (mb/sr)	E_γ (MeV)	$d\sigma(55^\circ)/d\Omega$ (mb/sr)
0.511	0.58	1.727	5.89
0.564	2.50	1.975	0.80
0.643	3.05	2.032	1.32
0.690	4.19	2.12	0.98
0.780	3.17	2.139	0.70
(0.83)[a]	3.44	2.26	0.89
0.936	9.48	(2.33)	3.33
(1.00)	2.99	2.376	0.35
(1.10)	2.68	2.52	0.35
1.214	8.60	2.63	0.59
1.289	4.70	3.13	1.16
1.332	15.91	3.161	0.87
1.434	56.84	3.72	0.73
1.531	8.81	4.42	0.56
1.58	1.28		

[a] Parentheses indicate a possible gamma-ray multiplet. The energy given is an average over the component lines (see Figure 7.1).

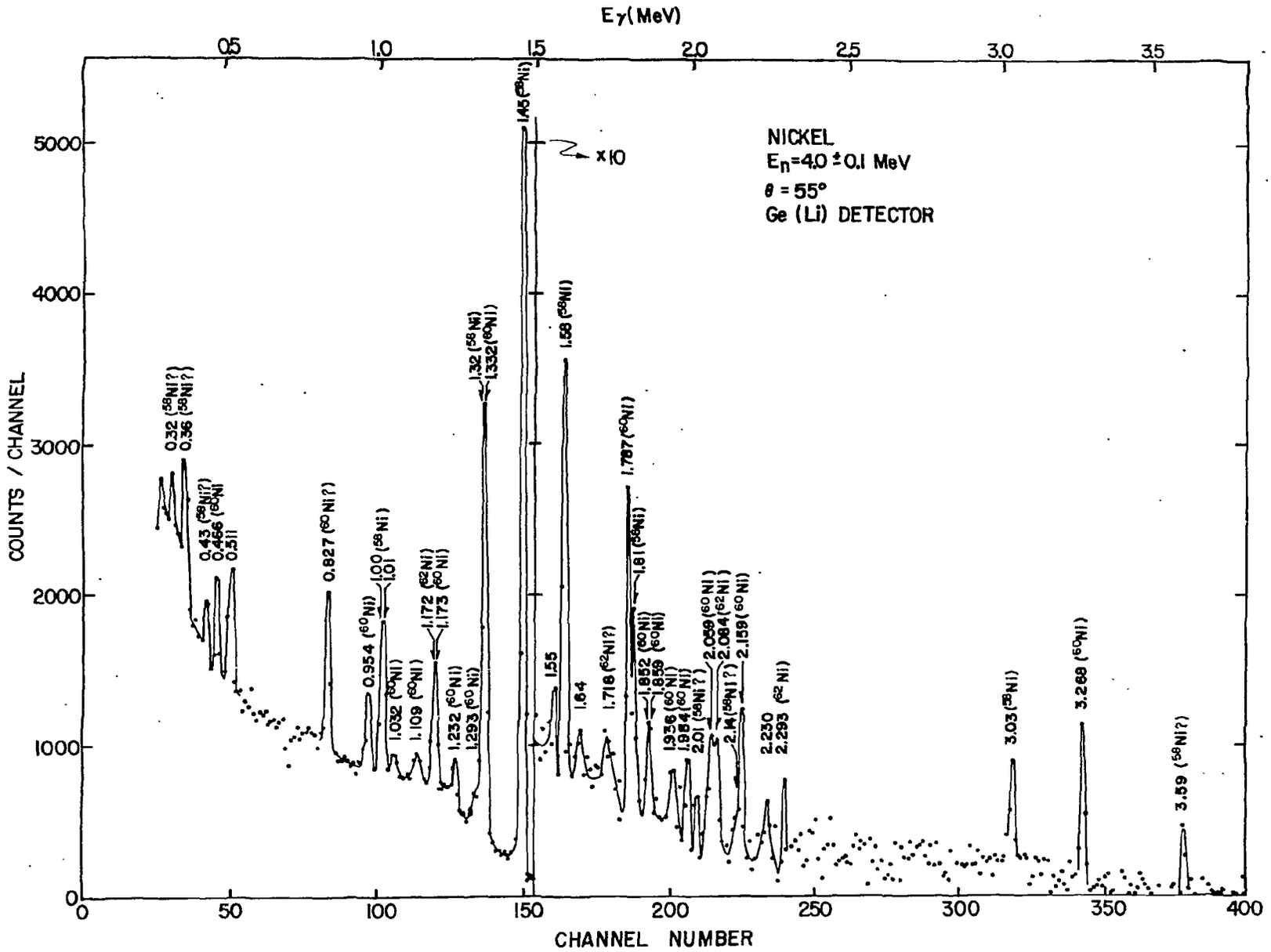

Figure 8.1

TABLE 8.1

GAMMA-RAY PRODUCTION CROSS SECTIONS FOR NICKEL

$E_n = 4.0 \pm 0.1$ MeV

E_γ (MeV)	$d\sigma(55^\circ)/d\Omega$ (mb/sr)	E_γ (MeV)	$d\sigma(55^\circ)/d\Omega$ (mb/sr)
0.38	3.41	1.232	5.02
0.43	1.65	(1.33)	29.76
0.466	1.84	(1.45)	41.84
0.511	3.03	1.58	1.77
0.827	6.26	(1.80)	3.39
0.954	4.43	(1.85)	1.42
(1.01)[a]	7.66	(2.07)	2.31
1.032	1.52	(2.15)	1.21
1.109	2.71	3.03	1.74
(1.17)	6.92	(3.26)	2.94
		3.59	1.07

[a] Parentheses indicate a possible gamma-ray multiplet. The energy given is an average over the component lines (see Figure 8.1).

9. Zirconium (T. C. Martin, W. E. Tucker, and P. S. Buchanan)

(Work pertinent to request #125 WASH 1078)

Gamma-ray yields of natural zirconium have been measured at neutron energies of 1.63, 4.0, 5.0, and 14.8 MeV. Figure 9.1 shows the spectrum obtained at 4 MeV using a Ge(Li) detector. Cross sections obtained at 1.63 and 4.0 MeV are listed in Tables 9.1 and 9.2. Theoretical calculations showed good agreement with some of the more prominent peaks in the 4 MeV experimental spectrum.

10. Niobium (G. H. Williams)

(Work pertinent to requests #153 and #154 WASH 1078)

Additional measurements have been made in the region between 0.75 and 1.9 MeV in order to establish the decay scheme which now appears to be more complex than reported in the literature. Specifically, measurements have been made at thirteen energies between 0.75 and 1.9 MeV and the yields of the observed gamma rays are given in Table 10.1. Angular distributions were also taken at 1.10 and 1.60 MeV. Analysis is continuing and a new level scheme is proposed. Theoretical calculations using this new level scheme are underway.

11. Tungsten (D. O. Nellis, T. C. Martin, P. S. Buchanan, and W. E. Tucker)

(Work pertinent to requests #233 and #234 WASH 1078)

In addition to the low energy measurements mentioned in sections 1 and 2, other measurements have been made at 4.0, 5.0, and 14.8 MeV. The spectra, all taken with a NaI(Tl) detector, consisted of a continuum with no prominent peaks other than that from the 0.511 MeV annihilation radiation. A single spectrum at a neutron energy of 14.8 MeV taken with a Ge(Li) detector enhibited a continuum and two small peaks at 1.11 and 1.22 MeV. Additional measurements to overlap the energy region where the spectrum changes from discrete lines to a continuum are planned. Cross sections obtained at 5 MeV are listed in Table 11.1.

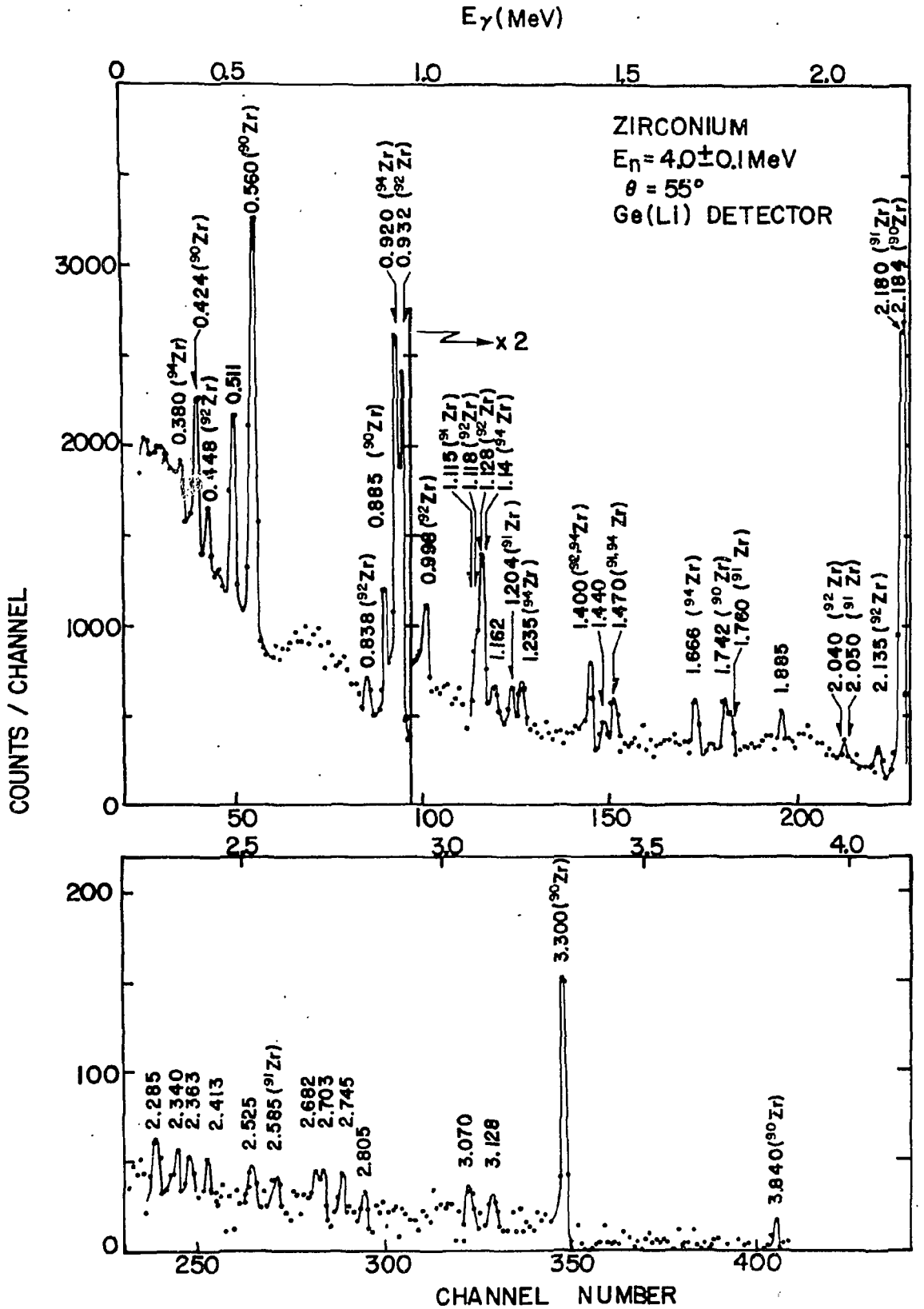

Figure 9.1

DATA NOT FOR QUOTATION

TABLE 9.1

GAMMA-RAY PRODUCTION CROSS SECTIONS FOR ZIRCONIUM

$E_n = 1.63 \pm 0.03$ MeV

E_γ (MeV)	$d\sigma(55^\circ)/d\Omega$ (mb/sr)
0.250-0.500	9.1
0.560	3.9
0.600-0.850	2.7
0.920, 0.935	18.8
1.025-1.275	1.8
1.275-1.525	1.6
TOTAL	37.9

Total $\times 4\pi$ = 476.0 mb

TABLE 9.2

GAMMA-RAY PRODUCTION CROSS SECTIONS FOR ZIRCONIUM

$E_n = 4.0 \pm 0.1$ MeV

E_γ (MeV)	$d\sigma(55^\circ)/d\Omega$ (mb/sr)	E_γ (MeV)	$d\sigma(55^\circ)/d\Omega$ (mb/sr)
0.380	0.7	1.885	1.2
0.424	3.7	2.040, 2.050	0.5
0.448	1.4	2.135	2.1
0.511	8.5	2.180, 2.184	38.0
0.560	22.5	2.285	0.7
0.838	37.0	2.340	0.6
0.885	9.9	2.363	0.6
0.920, 0.932	52.4	2.413	0.5
0.998	4.2	2.525	0.5
1.125	9.8	2.585	0.5
1.162	2.2	2.682, 2.703	1.5
1.204	2.0	2.745	0.5
1.235	2.9	2.805	1.2
1.400	4.5	3.070	8.8
1.440	0.7	3.128	1.5
1.470	2.5	3.300	9.8
1.666	2.6	3.840	0.8
1.742, 1.760	3.9		
		TOTAL	240.7

Total $x4\pi$ = 3023.2 mb

TABLE 10.1

GAMMA-RAY PRODUCTION CROSS SECTIONS FOR NIOBIUM 93

$d\sigma(55^{o})/d\Omega$ (mb/sr)

E_n (MeV)	0.75	0.85	0.90	0.95	1.00	1.05	1.10	1.30	1.40	1.50	1.60	1.70	1.90
E_γ (MeV)													
0.655		0.49	0.74	0.83	0.78	0.86	1.24	1.14	1.14	1.41	1.93	2.56	5.09
0.743		2.42	5.37	10.00	15.00	15.70	19.20	23.40	28.20	30.40	30.50	30.50	33.10
0.780			0.62	0.44	1.76	2.44	2.80	4.25	4.64	5.10	5.88	7.71	8.82
0.809			0.95	2.07	3.88	4.98	7.19	9.39	9.53	10.20	10.10	10.30	10.80
0.950					0.27	1.98	5.11	15.20	17.80	19.70	20.00	22.42	26.90
0.980						0.91	3.64	19.20	23.00	23.50	23.60	22.74	22.00
0.338								4.84	7.78	9.07	8.76	8.64	7.91
1.081								2.01	3.27	3.66	4.07	3.67	3.76
1.296									0.66	2.54	4.35	5.70	5.96
0.317									0.88	1.90	2.84	3.30	3.64
0.553									0.91	2.26	3.30	4.44	5.12
0.384										1.13	2.12	2.99	4.28
0.569										1.12	1.62	2.72	3.69
0.584											1.78	2.47	3.17
0.543												1.88	3.67
1.482												1.91	4.00
1.497												1.63	3.87
0.364													0.67
0.624													1.18
1.252													0.45
1.600													0.85
1.682													1.88
TOTAL	0	2.91	7.68	13.34	21.69	26.87	39.18	79.43	97.81	111.99	120.85	135.58	160.81

TABLE 11.1

GAMMA-RAY PRODUCTION CROSS SECTIONS FOR TUNGSTEN

$E_n = 5.0 \pm 0.1$ MeV

E_γ (MeV)	$d\sigma(55^\circ)/d\Omega$ (mb/sr)	E_γ (MeV)	$d\sigma(55^\circ)/d\Omega$ (mb/sr)
4.50-4.75	1.5	2.25-2.50	28.2
4.25-4.50	1.5	2.00-2.25	32.3
4.00-4.25	6.2	1.75-2.00	32.8
3.75-4.00	6.1	1.50-1.75	35.3
3.50-3.75	7.6	1.25-1.50	48.2
3.25-3.50	10.3	1.00-1.25	63.0
3.00-3.25	15.2	0.75-1.00	83.2
2.75-3.00	20.3	0.50-0.75	101.9
2.50-2.75	24.1	0.25-0.50	164.2
		TOTAL	681.9
		0.51	23.1

Total Continuum Less 0.51 MeV Peak = 658.8 mb/sr
$\times 4\pi$ = 8274.5 mb

TRIANGLE UNIVERSITIES NUCLEAR LABORATORY

A. NEUTRON PHYSICS

1. Resonance Cross Section Measurements with Continuous Beam (F. T. Seibel,* E. G. Bilpuch, H. W. Newson)

The total neutron cross section measurements of A^{40}, S^{34}, and Ca^{48} are now being prepared for publication. The non-s-wave resonances may be mostly due to d- rather than p-waves. See 6 below.

2. Average Total Neutron Cross Sections (W. F. E. Pineo, M. Divadeenam,** E. G. Bilpuch, H. W. Newson)

Previous cross section measurements made on the separated isotopes of neodymium and samarium have been corrected for the contamination by water and carbon dioxide and analyzed according to the methods described elsewhere.[1]

The results have been combined with those for the natural samples of cerium, neodymium, samarium, gadolinium, terbium, dysprosium, and holmium as well as mercury and several other samples scattered throughout the periodic table. Results indicate a larger variation in the scattering length, R', in the lighter rare earth region ($140 < A < 160$) than was previously thought. The cross sections of the rare earth samples averaged over the energy region 350-650 keV show good agreement with calculations done earlier at Oak Ridge using Tamura's coupled channel code, JUPITOR I.[2]

JUPITOR I is now running at the Triangle University Computer Center on the IBM 360/75 and the calculations are being extended into the vibrational region ($50 < A < 140$). Preliminary results indicate good agreement with experimental average cross sections is obtained by using Perey's optical model parameters[3] together with deformation parameters compiled by Stelson and Grodzins.[4]

---

* Los Alamos Scientific Laboratory, Los Alamos, New Mexico.

** Prairie View A. and M. College, Prairie View, Texas.

[1] M. Divadeenam, Ph.D. Thesis, 1967, unpublished.

[2] M. Divadeenam, Ph.D. Thesis, 1967, unpublished.

[3] F. Perey and B. Buck, Nuclear Physics 32, 352 (1962).

[4] P. H. Stelson and L. Grodzins, Nuclear Data Tables, 1, 21 (1965).

3. Average Total Neutron Cross Sections and Strength Functions (M. Divadeenam, E. G. Bilpuch, H. W. Newson)

A paper based on the thesis of M. Divadeenam is still in preparation for publication.

4. A Multi-Level Analysis of ^{92}Mo + n Resonances (5 - 60 keV) (M. Divadeenam, E. G. Bilpuch, H. W. Newson)

Preliminary results of this analysis follow. Any lower energy resonances were too weak for interpretation.

E_o(keV)	J^π	Γ_n (keV)
8.5	$\frac{1}{2}-$	.0113
11.3	$\frac{1}{2}+$	.022
13.5	$\frac{1}{2}+$	.057
16.3	$\frac{1}{2}+$	.072
18.8	$\frac{1}{2}-$	.0251
20.8	$\frac{1}{2}+$	.05
23.4	$\frac{1}{2}+$	.035
25.6	$\frac{1}{2}+$	.090
28.4	$\frac{1}{2}-$	.040
29.4	$\frac{1}{2}+$	.047
30.8	$\frac{1}{2}+$	.07
32.1	$\frac{1}{2}-$	.022
34.3	$\frac{1}{2}-$	.045
36.2	$\frac{1}{2}-$	.10
37.8	$\frac{1}{2}-$	.03
39.8	$\frac{1}{2}+$	.065
45.9	$\frac{1}{2}-$	.03
48.5	$\frac{1}{2}+$	.02
49.7	$\frac{1}{2}+$	.05
52.8	$\frac{1}{2}+$	.014
53.6	$\frac{1}{2}-$	.05
54.4	$\frac{1}{2}+$	.055
58.1	$\frac{1}{2}-$	.02

5. Theoretical Calculation of the Low-Lying Negative Parity Levels in ^{51}Ti (M. Divadeenam, W. P. Beres, H. W. Newson)

Inactive.

6. *Shell Model Calculation of the Neutron Resonances and Strength Functions* (M. Divadeenam, W. P. Beres, H. W. Newson)

The results for ^{49}Ca, ^{89}Sr, and ^{91}Zr are being compared to experiment. This comparison is encouraging enough to suggest additional experiments and calculations. The results on Ca^{48} + n are particularly interesting as mentioned above.

7. Polarization of Neutrons Produced in (d,n) Reactions on Nuclei in The 1p Shell (M. M. Meier, R. S. Thomason, G. Spalek, R. L. Walter)

Tabulations of the polarization for one or more neutron groups for (d,n) reactions on B^{10}, B^{11}, C^{13}, N^{14} and N^{15} have been reported in the Ph.D. dissertation of M. M. Meier (August 1969) and on Li^6 and Li^7 in the dissertation of R. S. Thomason (August 1969). DWBA calculations have been made for the $p_{3/2}$ $Li^7(d,n_0)$ and the $p_{3/2}$ $Li^6(d,n_1)$ groups with optical model parameters obtained from published values. Reasonable agreement with the cross-section data was obtained and some resemblance to the polarization for angles less than about 90° was found. The lengthy program of optical model studies of $N^{14}(d,d)$ and DWBA calculations for the 1p shell is described in section A-12. A paper on the j-dependence of the polarization in the $B^{11}(d,n_0)$ and $B^{11}(d,n_1)$ reactions was submitted to the "Symposium on Direct Reaction Mechanisms and Polarization Phenomena", University of Laval, Quebec (1969).

The dissertation abstract of M.M.M. appears below:

"Neutron polarization data for eleven (d,n) reactions, each involving the transfer of an $\ell = 1$ proton, have been obtained in the bombarding energy range 2.8 to 4.0 MeV for the target nuclei ^{10}B, ^{11}B, ^{13}C, ^{14}N and ^{15}N. Also, an earlier measurement by Sawers (1966) of the $^{12}C(d,n_0)$ reaction over this energy range was extended down to 1.80 MeV. The polarimeter utilized a spin precession solenoid and 132° (c.m.) scattering from a helium gas scintillation cell. A new automatic search program which extracts asymmetry data from spectra with partially resolved groups is discussed.

Most of the polarization distributions obtained have qualitative features which do not change appreciably as a function of bombarding energy, implying the dominance of a direct mechanism for these transitions. Also, similarities in the polarization patterns of some of the $j = \frac{1}{2}$ transitions were observed.

"The $^{14}N(d,n_o)$ reaction is chosen as a subject for analysis, and deuteron optical model wavefunctions for a DWBA analysis are generated by an extensive analysis of existing elastic scattering data for $^{14}N(d,d)$. An automatic search program, which corrects the experimental cross section for average compound elastic effects is described. This code was used to extract numerous sets of optical model parameters.

Subsequent DWBA calculations show that the parameter sets may be classified into several families, each family being comprised of a number of parameter sets which give rise to similar DWBA predictions. One of these families, corresponding to an optical potential with $V_o \sim 100$ MeV, $r_o \sim 1.6$ fm, when used for DWBA calculations, predicts polarization which is in reasonable agreement with experiment. Spectroscopic factors derived from calculations using sets from this family are in reasonable agreement with theoretical values.

A study of calculational sensitivities of the DWBA cross section and polarization to variations of other parameters provides a critique of the assumptions involved in the calculations as well as some insight into the features observed in several of the other (d,n) reactions.

The sign of the polarization at forward angles is not consistently j - dependent. This point seems to be partially explained by the fact that an extremely diverse set of Q-values (-0.2 to 13. MeV) is sampled in this data.

The j-dependence of the polarization at forward angles was seen in the experiment and the calculations to be somewhat ambiguous. Experimentally, five of six $j = \frac{1}{2}$ transfers are observed to have large negative polarizations at forward angles. The sixth, a reaction with a very high Q-value (13.73 MeV) exhibits a polarization with the opposite sign. Such an effect is suggested in the DWBA calculations."

8. Optical Model Analysis for Nucleon-He^4 Scattering (R. L. Walter, G. R. Satchler (ORNL), Th. Stammbach)

This work has appeared in Nuclear Phys. A112, 1 (1968). It may be reactivated if the data from Part A-14 require a new study.

9. Polarization in the $Be^9(He^3,n)$ Reactions (R. S. Thomason, L. A. Schaller, R. L. Walter, R. M. Drisko ((ORNL)).

A tabulation of these data appears in the Ph.D. dissertation of R. S. Thomason (August 1969). Optical model fits to the 6 MeV $Be^9(He^3,He^3)$ data of Earwaker were performed and the parameters were used in DWBA, two-nucleon stripping calculations. The $Be^9(He^3,n)$ cross section could be reproduced in these calculations but not the polarization data. All other available sets of Be^9 optical model parameters were tried, but none suitably reproduced both polarization and (He^3,n) cross section. The calculations appear in the dissertation of Thomason.

The dissertation abstract of R. S. T. follows:

"Angular distributions of the neutron polarizations were measured for the n_o and n_1 groups from the $^6Li(d,n)$ and $^7Li(d,n)$ reactions for deuteron energies from 2.5 to 3.8 MeV; for the n_o, n_1, and unresolved $(n_2 + n_3)$ groups from the $^9Be(^3He,n)$ reaction for ^3He energies from 2.1 to 3.9 MeV; and for the n_o groups from the $^{11}B(^3He,n)$ and the $^{13}C(^3He,n)$ reactions from 3.0 to 3.8 MeV. Targets were used that were generally about 200 keV in thickness to the incident ions. Helium was used as a polarization analyzer and a spin precession solenoid was used to simulate interchange of the "side" detectors. Data was accumulated by use of an automatic routine under control of an on-line computer. A computer code was written for use in the extraction of polarization asymmetries from unresolved peaks in gated helium recoil spectra, and this code was used in the analysis of most of the reactions studied.

The polarization distributions for the four groups from the (d,n) reactions have shapes that are very constant with energy over the energy range studied. The maximum absolute value of the measured polarizations is greater than about 0.40 for all of these reactions except $^7Li(d,n_1)$. Distorted wave Born approximation calculations in which capture of the proton in the 1p-shell with $j = 3/2$ was assumed were made for the

$^6Li(d,n_1)$ and $^7Li(d,n_0)$ reactions at 3.7 MeV. Optical model parameters were obtained from published values. Reasonable agreement with cross section data was obtained; the predicted polarizations resembled the measured data.

The shapes of the distributions for the measured groups from the $^9Be(^3He,n)$ reactions show a small gradual change with energy, and the absolute value of the measured polarizations is less than about 0.40 for all three groups. The polarization distributions for the $^{11}B(^3He,n_0)$ group have shape that is constant with energy within the experimental uncertainties; the polarization averaged over the energy range measured has a minimum of about -0.12 and a maximum of about +0.24. The shapes of the distributions for the $^{13}C(^3He,n_0)$ reaction between 3 and 4 MeV have moderate fluctuations about the average shape; the magnitude ranges from -0.64 to +0.34 over this range. Distorted wave Born approximation calculations in which transfer of the diproton with S = 0 was assumed were made for the $^9Be(^3He,n_0)$, $^{11}B(^3He,n_0)$, and $^{13}C(^3He,n_0)$ reactions at the highest energy at which each was measured. Fits to ^3He-^9Be elastic scattering data were made to obtain some of the optical model parameter sets used; other sets were obtained from the most applicable published values. Reasonable agreement with cross section data was obtained in all cases except for $^{11}B(^3He,n_0)$; the predicted polarizations for $^{13}C(^3He,n_0)$ resembled the measured data, but the results for $^9Be(^3He,n_0)$ were less encouraging."

10. Polarization in the $C^{13}(He^3,n)$ Reaction (R. S. Thomason, Th. Stammbach, J. Taylor, R. L. Walter)

This work appeared in Phys. Rev. 174, 1119 (1968). More recently, DWBA calculations using available $C^{13}(He^3,He^3)$ optical model parameters have been made and are reproduced in Thomason's thesis. Reasonable agreement to the (He^3,n) cross-section and polarization data was found for some of the calculations. A paper on this work was submitted to the Quebec Symposium on Nuclear Reaction Mechanisms and Polarization Phenomena.

11. Polarization in the $B^{11}(He^3,n)$ Reaction (R. S. Thomason, Th. Stammbach, J. Taylor, R. L. Walter)

These data have been reanalyzed using PROMETHEUS. DWBA calculations have been performed but no agreement to the forward peaked cross-section data was obtained using an $\ell = 2$ diproton transfer. Some other mechanism seems to be necessary to explain the data.

12. A DWBA Study of Polarization Produced in (d,n) Stripping Reactions Proceeding Via 1p Proton Transfers (M. M. Meier, R. L. Walter, R. G. Seyler ((OSU)), T. R. Donoghue ((OSU)), R. M. Drisko ((ORNL)) .

Associated with the work in section A-7, the sensitivity of DWBA predictions for cross sections and polarizations in (d,n) reactions on 1p shell targets has been studied. Since the last report the emphasis has been on fitting the N^{14} elastic deuteron scattering data of Flinner. A code for Hauser-Feshbach cross-sections for spin 1 particles was written by one of the authors (M. M. M.) and has been incorporated into the optical model fitting program JIB of Perey. The number of sets of OM parameters now has been reduced to about four, only one of which gives a suitable representation of the experimental $N^{14}(d,n)$ polarization when used in the DWBA calculation. This work is reported in the thesis of M. M. Meier (August 1969). Spectroscopic information for the $N^{14}(d,n)$ reaction is also discussed.

13. Polarization in the $Mg^{24}(d,n)$ and the $Si^{28}(d,n)$ Reactions (J. Taylor, Th. Stammbach, G. Spalek, R. L. Walter)

Six polarization angular distributions have been obtained from 2.2 to 4.0 MeV for the $Mg^{24}(d,n)$ and the $Si^{28}(d,n)$ reactions. The data are being analyzed with the fitting code PROMETHEUS. Only cursory DWBA calculations have been made so far.

14. Scattering of 8 MeV Polarized Neutrons from He^4 (Th. Stammbach, J. Taylor, G. Spalek, R. Hardekopf and R. L. Walter)

Eight MeV polarized neutrons from the $Be^9(\alpha,n)$ reaction were scattered from He in a gas scintillator and the asymmetry was observed at ten angles. With a polarization of 0.54, the polarization analyzing power was measured to better than $\pm$ 0.016. These data were reported at the Miami APS meeting. All of the corrections have finally been calculated. The results are consistent with the phase shifts of Satchler et al.[1] This work is being prepared for publication.

[1] G. R. Satchler, L. W. Owen, A. J. Elwyn, G. Morgan, and R. L. Walter, Nuclear Physics A112, 1 (1968).

15. Scattering of Polarized 8 MeV Neutrons from Deuterons (J. Taylor, Th. Stammbach, G. Spalek, R. L. Walter)

At the February 1969 APS meeting in New York the authors reported the angular distribution of the polarization for the scattering of 7.8 MeV neutrons from deuterons for angles from 60° L to 150° L. The wide angle data compared favorably to the p-d polarization data and the n-d calculation of Purrington and Gammel.[1] Because the 60° and 70° data indicated some differences to the charge symmetric p-d reaction, the range from 40° to 70° has been measured with a time-of-flight technique which reduced the background level to a negligible amount. Analysis of the new data is complete and it appears that the n-d and p-d data agree within the ± 0.015 uncertainty of this work. This work is being prepared for publication.

16. The $Be^9(\alpha,n)$ Reaction as a Source of Polarized Neutrons (Th. Stammbach, J. Taylor, G. Spalek, R. L. Walter)

Knowledge of the phase shifts for n-He^4 elastic scattering permits the authors to place accurate values on the $Be^9(\alpha,n_0)$ and $Be^9(\alpha,n_1)$ polarization. Measurements were made for the angular region from 40° to 60° for He^4 energies from 2.35 to 2.75. The usefulness of this reaction as a source of 7.8 MeV neutrons with a polarization of 0.54 is discussed in a paper being prepared for publication in Nuclear Instruments and Methods.

17. A DWBA Analysis of the $Ca^{40}(d,n)Sc^{41}$(G.S.) Reaction (J. Taylor, G. Spalek, R. Hardekopf, Th. Stammbach, R. L. Walter)

The neutron polarization was measured at 3.8 MeV for the $Ca^{40}(d,n)Sc^{41}$(G.S.) reaction. This reaction is an $\ell = 3$ transfer and the polarization was seen to be small as expected. DWBA calculations of the (d,n) cross section and polarization have been performed at 3.8 and 6.0 MeV using optical model parameters which fit the $Ca^{40}(d,d)$ cross section. Some parameter variation was also tried neglecting the effect which the variation had on the elastic scattering. The final fits to the cross section and polarization were encouraging but still not quite good. No more calculations are planned until the effects of the deuteron D- state and strongly coupled channels are known.

---

[1] R. D. Purrington, J. L. Gammel, Phys. Rev. 168, 1174 (1967).

18. Polarization of Neutrons from The $Be^9(d,n)B^{10}$ Reactions (J. Taylor, G. Spalek, R. Hardekopf, Th. Stammbach, R. L. Walter)

The polarization of the neutrons from the $Be^9(d,n)$ reaction to the ground, first-excited, third-excited, and fourth-excited states of B^{10} have been measured for angles from 10° to 135° at 3.0 and 3.5 MeV by scattering from He^4. The polarization was usually less than 0.2 in magnitude. The distributions at 3.0 were similar to those for the same neutron groups at 3.5 MeV. Other than C^{14}, Be^9 was the last stable target for study of the polarization in 1p shell neutron transfer reactions. DWBA calculations will be attempted.

B. CHARGED PARTICLE REACTIONS

1. Fine Structure of Isobaric Analog States in Medium-Weight Nuclei (D. P. Lindstrom, J. D. Moses, N. H. Prochnow, J. C. Browne, W. M. Wilson, W. C. Peters, G. E. Mitchell, H. W. Newson, E. G. Bilpuch)

a. The Chromium Isotopes

Investigations of the resonance structure of some Mn isotopes through elastic proton scattering on the even Cr isotopes are nearing completion. The following excitation functions have been measured:

$^{50}Cr(p,p)$ from 1.80 MeV to 3.30 MeV at 160°, 135°, 120°, and 90°.

$^{50}Cr(p,p_1)$ from 2.31 MeV to 3.30 MeV at 160°, 135°, 120°, and 90°.

$^{52}Cr(p,p)$ from 2.00 MeV to 3.23 MeV at 160°, 135°, 120°, and 90°.

$^{54}Cr(p,p)$ from 1.81 MeV to 2.90 MeV at 160°, 135°, 120°, and 90°.

$^{54}Cr(p,n)$ total cross section from threshold (~2.20 MeV) to 2.90 MeV.

Resolution of from 300 to 400 eV has been achieved in every case. The fine structure of several analog states, as well as other resonance structure, is observed in the data. Analysis of the data is in progress.

b. The Iron Isotopes

Elastic proton scattering experiments on ^{54}Fe, ^{56}Fe, and ^{58}Fe have been completed. The fine structure of the isobaric analogs of the 6th, 9th, and 11th excited states in ^{55}Fe has been analyzed. Detailed analysis of data corresponding to the ground state and the first and second excited states in ^{59}Fe, as

well as the 7th, 9th, and 10th excited states in ^{57}Fe is now in progress. Some inelastic scattering on ^{56}Fe and ^{58}Fe was also observed. Energy resolution in the above experiments was 300-400 eV.

c. The Nickel Isotopes

The proton elastic scattering measurements on ^{60}Ni, ^{62}Ni, and ^{64}Ni have been completed. The $^{64}Ni(p,n)$ total cross-section measurement has also been completed from threshold (approximately 2.50 MeV) to 3.30 MeV. The results of these experiments are included in a Ph.D. dissertation by one of the above authors. An abstract of this dissertation is presented below.

Fine Structure of Analog States in ^{61}Cu, ^{63}Cu and ^{65}Cu (J. C. Browne)

"Differential cross-sections were measured at laboratory angles of 160°, 135°, 120° and 90° for $^{60}Ni(p,p)$, $^{62}Ni(p,p)$ and $^{64}Ni(p,p)$ at energies ranging between 1.8 and 3.3 MeV. The $^{64}Ni(p,n)$ total cross-section was measured from threshold (~2.50 MeV) to 3.3 MeV. All data were taken using the high resolution electrostatic analyzer-homogenizer system in the 3 MV Van de Graaff laboratory which is part of the Triangle Universities Nuclear Laboratory. A total resolution of 300-400 eV was realized using thin solid targets of the enriched nickel isotopes.

The analogs of the second, sixth and eighth excited states of ^{61}Ni were identified in the $^{60}Ni(p,p)$ experiment. The analogs of the ground state, second and third excited states of ^{63}Ni were observed in the $^{62}Ni(p,p)$ experiment. The analog of the first excited state of ^{65}Ni was identified in the $^{64}Ni(p,p)$ experiment. In all cases, the analog state was fragmented into individual fine-structure resonances. The resonance parameters were obtained by an R-matrix analysis. Only $\ell = 1$ analog states were observed. Spectroscopic factors were obtained using the resonance parameters extracted from the data and the calculated single-particle widths for these states. Single-particle widths were estimated by calculations using an optical-model code. The spectroscopic factors disagree in many cases with the spectroscopic factors for the parent states extracted from (d,p) measurements.

The analog of the second excited state of ^{63}Ni was also observed by elastic proton scattering on a thick ^{62}Ni target. A comparison between these gross-structure results and the averaged fine-structure data was made. The spectroscopic factor for the thick target data is consistent with the spectroscopic factor obtained from the fine-structure measurements. Both numbers, however, disagree with the results of other gross-structure measurements (Gaarde et al., 1966).

Coulomb energy differences were calculated for the seven $\ell = 1$ analog states and their parents. Very consistent results were obtained assuming a $Z/A^{1/3}$ variation for the Coulomb energy."

d. The Zinc Isotopes

Preliminary investigations of elastic proton scattering on ^{64}Zn and ^{66}Zn have begun. The excitation functions for $^{64}Zn(p,p)$ and $^{66}Zn(p,p)$ have been measured at 160° (laboratory) from 1.86 MeV to 2.87 MeV and 2.74 MeV to 2.86 MeV, respectively. Initial results indicate a resolution of about 400 eV. Further investigations on these isotopes are continuing.

2. $Mg^{24}(He^3,\alpha\gamma)\,Mg^{23}$ Angular Correlation Measurements (L. C. Haun,* N. R. Roberson, D. R. Tilley, R. V. Poore)

This work has been submitted for publication in Nuclear Physics.

3. $Si^{30}(\alpha,p\gamma)\,P^{33}$ Angular Correlation Measurements (C. E. Moss, R. V. Poore, L. C. Haun,* C. E. Ragan, G. P. Lamaze, N. R. Roberson, D. R. Tilley)

This work has been published in the Physical Review 174, 1333 (1968).

4. $^{26}Mg(\alpha,p\gamma)^{29}Al$ Angular Correlation Measurements (C. E. Moss, R. V. Poore, L. C. Haun,* C. E. Ragan, G. P. Lamaze, D. M. Peterson, R. A. Hilko, N. R. Roberson, D. R. Tilley)

The method-II angular correlation technique of Litherland and Ferguson has been applied to the reaction $^{26}Mg(\alpha,p\gamma)^{29}Al$. The first three excited states

* Now at the Center for Naval Analyses, Arlington, Virginia.

were studied. The results agree with, and add nothing new to, recently reported results[1,2] and will not be published.

5. $^{29}Si(\alpha,p\gamma)^{32}P$ Angular Correlation Measurements (C. E. Moss,* R. V. Poore, C. E. Ragan, G. P. Lamaze, D. M. Peterson, R. A. Hilko, N. R. Roberson, D. R. Tilley)

The Method II angular correlation of Litherland and Ferguson was applied to the reaction $^{29}Si(\alpha,p\gamma)^{32}P$. The spin of the 1.755 MeV level in ^{32}P was determined to be J= 3. The results for several other low lying levels were in agreement with the known spins. This work, together with the ^{34}S results below, have been submitted to Nuclear Physics.

6. $^{31}P(\alpha,p\gamma)\,^{34}S$ Angular Correlations Measurements (C. E. Moss, R. V. Poore, C. E. Ragan, G. P. Lamaze, R. A. Hilko, N. R. Roberson, D. R. Tilley)

The method-II angular correlation technique of Litherland and Ferguson has been applied to the reaction $^{31}P(\alpha,p\gamma)^{34}S$. In ^{34}S the state at 4.07 MeV was determined to have J = 1, and the state at 4.88 MeV, J = 2. For other low lying levels, the present results are in agreement with the known spin assignments. Some mixing ratios and branching ratios were also determined. Accurate excitation energies were determined with a Ge(Li) detector. A paper describing the work on ^{34}S and ^{32}P has been submitted to Nuclear Physics.

7. The $(^3He,\alpha)$ Reaction at 8 MeV with Nuclei in the S-D Shell (J. McQueen, J. Joyce, E. J. Ludwig)

Attempts to fit the $(^3He,\alpha)$ angular distributions with ^3He optical-model real-well potentials of approximately 165 MeV yielded the most satisfactory agreement with both elastic scattering and $(^3He,\alpha)$ angular distributions for these nuclei. Good comparisons with $(^3He,\alpha)$ angular distributions were obtained for ^{30}Si and ^{26}Mg targets but not for those of ^{24}Mg, ^{28}Si and ^{32}S although the α-particle yields for these latter nuclei were greater. The spectroscopic factors extracted from the best fits for the ^{24}Mg, ^{28}Si and ^{32}S data were generally a factor of 2 or so higher than would be expected on the basis of theoretical estimates. Attempts will be

---

[1] D. C. Kean et al., Nucl. Phys. A132, 241 (1969).

[2] R. G. Hirko et al., Bull. Am. Phys. Soc. 13, 1371 (1968).

* Now at the University of Colorado, Boulder, Colorado 80302.

made to compare these data with calculations based on α-particle knockout mechanism.

Spectroscopic factors were obtained for the ^{30}Si and ^{26}Mg data using several sets of ^{3}He parameters. The spectroscopic factors were generally independent of the parameters and in agreement with the factor obtained at other energies and with other neutron pickup studies.

This work is being readied for publication.

8. ^{3}He Scattering And Polarization Studies (W. McEver, E. J. Ludwig, T. Clegg, J. Joyce and R. Walter)

a. Polarization

A system for analyzing ^{3}He particle polarization has been built and calibrated using recoil ^{3}He from the α-particle bombardment of a cell filled with ^{3}He gas. The analyzer consists of a cell containing ^{4}He which is viewed by detector telescopes. The analyzing power was measured to be approximately 0.67 and was fairly constant over a 1 MeV energy range.

Using the gas cell analyzer the polarization of ^{3}He particles scattered from ^{12}C has been measured at 18 MeV at several forward angles.

b. Elastic Scattering and Reactions

The elastic scattering angular distributions of ^{3}He particles from targets of ^{12}C, ^{16}O, and ^{28}Si have been obtained using E-ΔE detector telescopes and particle identification circuiting. Angular distributions have been obtained for ^{12}C targets at 18 and 21 MeV, for ^{16}O targets at 18 MeV and for ^{28}Si targets at 18 MeV. These data will be analyzed using an optical model search code.

The angular distribution of deuterons and α-particles resulting from the bombardment of ^{16}O by 18 MeV ^{3}He particles have also been obtained and will be compared to predictions using distorted wave code DWUCK.

9. Gamma Decay of Isobaric Analog Resonances (S. M. Shafroth, J. M. Joyce, G. J. F. Legge,* H. Ejiri,** T. Hain, W. McEver, E. J. Ludwig)

a. The $^{90}Zr(p,\gamma)^{91}Nb$ Reaction

A new beam line at 38° has been installed at the Cyclo-Graaff laboratory expressly for the purpose of doing (p,γ) work. A new target chamber lined with sheet tantalum has been made and found to be satisfactory for (p,γ) work of the kind reported on here. We have studied the $d_{5/2}$ resonance at 4.735 MeV in the $Zr^{90}(p,\gamma)Nb^{91}$ reaction using the 80 cc Ge(Li) detector. Peaks due to capture gamma rays to most of the low lying levels in Nb^{91} below 2.35 MeV have been identified. Preliminary analysis of the excitation curve data indicates that the resonance effect in gamma transitions to the 1.312 MeV $(3/2^-)$ level is almost as strong as for transitions to the 1.613 MeV $(3/2^-)$ level even though $Zr^{90}(He^3,d)$ results indicate twice the spectroscopic factor for the 1.613 MeV level. An invited talk entitled "Gamma Decay of Analog Resonances in the Giant Dipole Region" was given by S. M. Shafroth at the Washington meeting of the American Physical Society.

b. The $^{51}V(p,\gamma)^{52}Cr$ Reaction

This work which was done at the 3 MeV laboratory is being prepared for publication.

10. Gamma-Ray Studies Using the 80 cc Ge(Li) Detector (S. M. Shafroth, J. Montgomary, A. Seila, T. Hain, J. M. Joyce, G. J. F. Legge)

An efficiency calibration for the full energy peak has been done up to 2.6 MeV. A point at 10.76 MeV using the .991 MeV resonance in the $^{27}Al(p,\gamma)^{28}Si$ reaction was taken and the efficiency for the 2 escape peaks was found to be 4.8×10^{-5} at 12.5 cm assuming the width of this resonance to be as in Endt and Van der Leun.[1] However recent work at Cal. Tech.[2] indicates that Γ_γ may be less by a factor of two in which case the efficiency is increased by two.

---

* Visiting scientist from the University of Melbourne, Melbourne, Australia.

** Visiting scientist from the University of Washington, Seattle, Washington.

[1] Nuclear Physics A105, 140 (1967).

[2] Nuclear Physics A130, 1 (1969).

Voltage breakdown caused the detector to become noisy so it was sent back to Princeton for a new high voltage connector. This seems to have corrected the trouble.

11. Yields of K-x-rays as a Function of Proton Bombarding Energy (G. A. Bissinger, J. M. Joyce, W. McEver, E. J. Ludwig, S. M. Shafroth)

This work is being prepared for publication. It will be reported on at the New York American Physical Society meeting. The abstract appears in Appendix XIII .

12. Energies of Some ^{25}Al Levels from The ^{24}Mg $(p,\gamma)^{25}$Al Reaction (F. Everling, G. L. Morgan, D. W. Miller, L. W. Seagondollar, P. W. Tillman, Jr.)

This work is being prepared for publication.

13. Levels in ^{25}Al from The ^{24}Mg$(^3$He$,d)^{25}$Al Reaction (F. Everling, G. L. Morgan, D. W. Miller, P. W. Tillman, Jr.)

A self-supporting ^{24}Mg target and ^{24}Mg on carbon and formvar backings were bombarded by a 22 MeV ^{3}He beam from the tandem accelerator. The deuteron spectrum was recorded by using a detector-telescope and particle-identification circuit. The work is in progress.

14. Gamma Decay of The 2.138 MeV Resonance in The ^{20}Ne$(p,\gamma)^{21}$Na Reaction (G. L. Morgan and F. Everling)

The excitation energy and branching ratio of the 2.138 MeV resonance at 4.468 MeV excitation energy in ^{21}Na were measured with a 20 ccm Ge(Li) detector using the 4 MeV Van de Graaff accelerator. Analysis of the data is in progress.

15. Lifetime Measurements by The Doppler Shift Attenuation Method (C. E. Ragan, G. Lamaze, G. E. Mitchell, C. E. Moss, R. V. Poore, N. R. Roberson, D. R. Tilley)

The first experiment utilizing the DSAM method of measuring lifetimes of electromagnetic transitions has been completed. The following is the abstract of a paper submitted for publication:

"The mean lifetimes of the levels of ^{33}S below 3.3 MeV excitation energy have been measured by the Doppler shift attenuation method. The $^{30}Si(\alpha,n)^{33}S$ reaction was used to populate these states. SiO_2 targets (enriched to 95% in ^{30}Si) evaporated onto Ni backings were bombarded with α-particles ranging in energy from 5.5 to 9.0 MeV. γ-ray spectra were recorded with a 20-cc Ge(Li) detector at 0°, 90°, and 150° to the beam. The following mean lifetimes were found: T(0.842 MeV level) = 1.65 ± 0.34 psec, T(1.968) = 150 ± 20 fsec, T(2.313) = 158 ± 24 fsec, T(2.869) < 17 fsec, T(2.937) < 4 psec, T(2.970) = 69 ± 12 fsec, T(3.221) < 55 fsec. The branching ratios of the 2.970 MeV level were determined to be 90 ± 5% to the ground state and 10 ± 5% to the second excited state."

Further experiments in this mass region are planned for the near future.

16. $^{14}C + \alpha$ Reactions (R. A. Hilko, G. E. Mitchell, G. L. Morgan, N. R. Roberson, D. R. Tilley)

Measurements of the $^{14}C(\alpha,\alpha)\,^{14}C$ reaction have been extended. The present work was performed on the tandem accelerator, using the large scattering chamber. Eight angles (zeros of the first seven Legendre polynomials and one back angle) were measured simultaneously. Spectra were collected with the on-line computing system and processed following each run, thus providing eight constantly updated excitation functions. The spectra were also recorded on magnetic tape for possible reanalysis.

Excitation functions have been measured from 3.5 to 16.5 MeV. Above approximately 8 MeV the excitation functions are rather complex; the cross sections do not appear to be dominated by single resonances. Below 8 MeV, an analysis is being attempted considering these data as a superposition of individual levels. Twelve angular distributions have been measured in the lower energy region to assist in this analysis.

Further experimental work as well as efforts at detailed analysis is planned for the near future.

17. The $C^{13}(He^3,d)N^{14}$ Reaction (R. A. Hilko, H. R. Weller,* G. P. Lamaze, N. R. Roberson, D. R. Tilley)

The investigation of the $^{13}C(He^3,d)^{14}N$ reaction will be continued by one of the authors (H.R.W.) at the University of Florida in Gainesville. No further work on this experiment is planned at TUNL.

18. The $^{54}Fe(p,t)^{54}Fe$ Reaction (R. Nelson, N. R. Roberson)

The 30-MeV proton beam from the TUNL Cyclo-Graaff is being used to study the $^{54}Fe(p,t)$ reaction. The scattered particles are detected in two ΔE-E detector telescopes. The on-line computer is operated in the two-parameter mode and is programmed to select four mass windows and to store from 1024-channel energy spectra. Preliminary runs have been completed. The Bayman two-nuclear DWBA code is being debugged on the TUCC 360/75 and will be available for analysis of these data.

C. GENERAL

1. Nuclear Binding Energy Systematics Including Excited States (F. Everling)

A revised systematics of Coulomb-energy differences of the single-particle states of $T_z = \pm\frac{1}{2}$, $A = 4n + 1$ nuclei has been completed and is being prepared for publication.

2. IBM Systems 360 Programming (B. H. Choi, T. B. Clegg, R. A. Hilko, J. M. Joyce, M. M. Meier, R. O. Nelson, A. Seila)

The major analysis codes JIB3 (F. G. Perey) for optical model analysis of elastic scattering data and DWUCK (P. D. Kunz) for DWBA analysis of particle transfer reactions continue to be used in the analysis of many experiments. Two Hauser-Feshbach subprograms have been written and checked with hand calculations and with the calculations of Wilmore and Hodgson.[1] The first computes average compound nucleus cross sections using externally generated transmission coefficients. The second is used in conjunction with the optical model search code JIB3 and corrects the experimental data under analysis for compound elastic contributions. Transmission coefficients for the elastic channel are internally generated. Both programs include the width-fluctuation correction.

* Now at the University of Florida, Gainesville, Florida.

The optical model search code SNOOPY has been obtained from Dr. P. Schwandt at the University of Colorado. The code can be used for optical model or phase shift analyses of data when a spin-$\frac{1}{2}$ or spin-1 projectile is incident on a spin-0 target. Both vector and tensor spin-orbit potential parameters may be used when necessary in addition to the more common central potential parameters.

This program is now running at TUCC and analyses have begun on recent Wisconsin results of deuteron ^{4}He elastic scattering cross section and polarization measurements.

Taro Tamura's code JUPITOR-2 for coupled-channel, optical model, and optical model plus resonance analysis has been modified to run on the 360/75 system. David Sellin's code MULTI, which is a multi-channel, multi-level R-matrix analysis program, was expanded to handle ℓ-values to 9 and 10 different J^π values.

A two-particle transfer DWBA code (B. Bayman) is being modified to run on the Systems 360.

A non-linear least squares program for extracting analog-state resonance parameters from experimental excitation curves in the presence of interfering amplitudes has been written. Also, a copy of the program Oak Ridge General Least Squares (ORGLS) which will fit a linear or non-linear function of an arbitrary number of parameters to an arbitrary number of data points has been obtained and is running on the Systems 360.

3. Journals - Midstream Evaluation Conference (K. Way, S. M. Shafroth, J. Y. Park, H. W. Newson)

The concept of the experimenter-meeting approach as a means of generating up-to-date summaries of nuclear level information was tested at TUNL last June 11-13 when eight active nuclear physicists,[1] each of whom had done considerable preliminary work discussed the data problems associated with 19

[1] The conference participants and assigned nuclei were: J. Ball, Oak Ridge National Laboratory (^{90}Zr), C. Goodman, Oak Ridge National Laboratory (^{88}Y, ^{88}Zr), T. Hughes, IBM Scientific Center, Houston (^{88}Sr), M. Johns, McMaster University, Hamilton, Ontario, Canada (^{88}Rb, ^{89}Kr, ^{89}Rb, ^{90}Rb, ^{90}Sr), J. Y. Park, N. C. State University and TUNL (^{89}Zr), S. M. Shafroth, UNC, Chapel Hill and TUNL (^{89}Sr), D. M. Van Patter, Bartol Research Foundation Swarthmore, Pa. (^{89}Y), and K. Way, Duke and TUNL (^{96}Sr, ^{90}Y, ^{90}Nb).

nuclei with atomic numbers A = 88, 89, and 90. All of them have about 50 neutrons. At this meeting, up-to-date level schemes, spin-parity assignments, spectroscopic factors, etc. were developed and are to be published this Fall with references to the experiments on which they are based. Such an effort should help to clarify and extend knowledge in this mass region which was last reviewed systematically in 1960. (Additional material on data journals is given in Appendix XIV.)

4. Germanium Detector Fabrication Program (J. M. Sanderson, R. E. Surratt, C. E. Long, and A. W. Waltner)

Work on the detector fabrication program is progressing with some improvement in detector performance. Multiple detector arrays are being developed including Si(Li) as well as Ge(Li) detectors. The Si(Li) detectors are obtained from commercial vendors.

5. Installation of An Electrostatic Analyzer for The 4 MeV Laboratory (L. W. Seagondollar, H. W. Newson, O. Meier, Jr., E. G. Bilpuch)

An electrostatic analyzer has been installed at the 4 MeV Van de Graaff accelerator. This analyzer was acquired from the University of Kansas with a complete set of components including the power supply, the high voltage supply, the control circuits, and the vacuum system. Originally they were constructed by the Westinghouse Electric Corporation and initially installed, about 1951, for use with the electrostatic generator in the Westinghouse Research Laboratories.

It is now connected to the left 17° 49' beam port of the 4 MeV Van de Graaff accelerator in a horizontal position so that the beam is deflected to the right.

Measurements made shortly after the construction of the electrostatic analyzer yielded the following results:

ϕ' (the deflection angle) = 127° 1' ± 1'

R (the mean radius of two circular plates) = 39.990 inches ± 0.005 inch

a (the gap between plates) = 0.2855 inch ± 0.0005 inch

The high voltage supply provides a potential difference between the plates of 60 kV maximum. It is arranged to place +30 kV on the outer plate and -30 kV on the inner plate. The supply voltage is continuously variable over the total range, and up to 0.001% stability over short periods of time has been obtained.

Beams of single charged ions of any kind emerging from the 4 MeV Van de Graaff accelerator can thus be analyzed at somewhat greater than the rated 4 MeV of the accelerator. It is hoped that, when a homogenizer circuit is used with this analyzer, high resolution beams can be used at greater energies than are now available with the 3 MeV machine.

6. Computer Control of the 4 MeV Van de Graaff Accelerator (R. V. Poore, C. E. Moss*)

The on-line computer has been used to monitor and control the operation of the 4 MeV Van de Graaff accelerator during long low-count-rate experiments. This automatic operation allowed the accelerator to be left unattended during the night.

Active control of the accelerator by the computer was of a simple nature, involving only "on-off" operation of the main power, belt charge, control slits and beam stop. The beam was monitored by a meter relay, and tank sparks were detected by sensing a sudden change in the column resistor current. Using these variables a computer program was developed which sensed the stability of the accelerator by examining the beam and attempted to restore the stability by switching the control slits and belt charge off and on again. If a stable beam could not be obtained within a specified number of trys the main power was shut off. With this procedure the accelerator could be left unattended overnight with about a 50% probability of finding the accelerator on the following morning.

7. Table of Weighted Averages (F. Everling, J. Taylor, P. W. Tillman, Jr.)

In order to simplify the current compiling activity concerning level energies and Q-values as needed for systematics studies in the light element region, a table of weighted averages was developed by F. Everling and J. Taylor. In its present form, the table has just 520 print-out pages and yet allows weighted averaging of any pair of values with consistency $Re/Ri \leq 3$. Due to the successful testing in practice and the wide applicability in all fields of science where measurements of the same quantity with comparable standard deviation occur, the work is being prepared for publication.

---

* Now at the University of Colorado, Boulder, Colorado.

D. REPORTS OF PROJECT COMMITTEES

1. On-line Data Acquisition and Analysis (R. V. Poore, Chairman, S. E. Edwards, N. R. Roberson, J. M. Joyce, J. Boyce)

The new DDP-224 computer purchased by the University of North Carolina at Chapel Hill on a grant from the National Science Foundation has been installed and is operational. The new DDP-224 computer now shares the paper-tape punch and reader, the line printer, and the card reader with the older DDP-224 computer. Work is progressing on interfacing of a magnetic tape drive and controller and a 20 cm by 25 cm display scope. The plans are to use the new machine initially for preliminary raw data analysis and for debugging for the time-sharing on-line DDP-224. As more funds become available, the construction of a data acquisition interface as a back-up system for the time-sharing computer is planned.

Two 4-input routers have been installed on the time-sharing computer for the multiplexing of up to eight detector spectra through two ADC's.

Data-taking programs are now exclusively written in the FORTRAN IV language. This greatly simplifies the program writing and debugging and reduces the time required to get a program running. Many general purpose programs have been written for single-parameter and multi-parameter data accumulation and data analysis. These programs are easily changed by the experimenter to suit his particular needs.

2. The 24" Scattering Chamber (E. J. Ludwig, T. Clegg, W. McEver, J. Joyce, N. R. Roberson)

The 24" scattering chamber has been used heavily during the past months with few apparent troubles. Modifications have or will include:

1. Track Cooling - The tracks on which detectors and collimators are mounted are now insulated from the chamber plates and cooled with freon. New fittings are being installed in the chamber to allow the rapid warming of these tracks with warm freon gas.

2. Remote detector rotation - Motor devices will soon be installed to position the particle detectors remotely.

3. Slit system - A new slit system is being installed in the 24" scattering chamber in anticipation of using the chamber for experiments with polarized

beams. The new system has electrically isolated slits left, right, up and down to define the beam. The openings defined by the slits are rectangular and of easily variable size. Beam currents will be monitored on the horizontal and vertical pairs of slits. The difference in currents on the slits of a pair will be used to drive automatically a set of magnetic steerers before the chamber to balance the currents on each pair of slits. The beam will thus be held automatically on center through the slits even while the operator is focussing the beam with quadrupole lenses.

3. Polarized Ion Source (T. B. Clegg, G. Bissinger)

The Lamb-shift polarized ion source for the tandem accelerator is now under construction in Chapel Hill. Major hardware items and assembly are about 80% complete. The ion source is of hybrid design, including features from the successful sources at Los Alamos and at the University of Wisconsin.

The positive ion duoplasmatron was assembled and tested to optimize the H^+ and D^+ ion currents at 500 eV and 1000 eV respectively. The cesium oven, 575 Gauss, uniform field solenoid, spin filter, all vacuum systems, and the high voltage isolation cage are complete. The major items yet to be assembled are two electrostatic mirrors, and two spin rotation solenoids.

Before October 1969 the ion source will be ready for checking the total polarized beam output and the tensor polarization of the deuteron beam. It is expected that the final installation on the tandem accelerator will come before the end of 1969.

4. Tandem Accelerator (R. L. Walter, Chairman, R. L. Rummel, S. M. Shafroth, J. M. Joyce, G. E. Mitchell, F. Everling, D. R. Tilley, and E. G. Bilpuch)

The tandem has been running reliably up to 7.5 MV. The tandem tank has not been opened since April 1969 and the down time due to equipment failure or ion source components has been very low.

5. Beam Transport System (F. O. Purser, H. W. Newson)

Four target areas in target room 1 are now outfitted with beam handling equipment. Power supplies for the various beam line components on the separate target extensions are centrally located and switched through a power patch board to avoid unnecessary duplication of power supplies. All necessary components to implement a fifth target area serving the cyclotron when operated singly are on hand and will be installed at the first extended accelerator maintenance

period.

Various power supplies and auxiliary lenses for the high resolution analyzing and beam transport system are on hand. The system supplier, Varian Associates, has encountered difficulties in fabrication and the principal magnets of the system are now scheduled for shipment in late October. Precision optical equipment to aid in aligning this system to the accuracy required to make full use of the expected resolving power available has been ordered.

Subsequent to the delivery of the high resolution system target legs in target rooms 4 and 5 will be outfitted to meet experimenter demand. One of the first uses of the high resolution capability will be a study of Cyclo-Graaff beam resolution to supplement measurements presently being made with solid state counters.

6. Injector Cyclotron (F. O. Purser, N. R. Roberson, J. R. Boyce, M. T. Smith, E. J. Ludwig, T. Hayward, H. W. Newson)

Installation of a partial deionizer in the closed cyclotron cooling system has resulted in reduced current drain from various high voltage supplies. Present operating characteristics indicate the desirability of increasing the cooling water flow to many of the cyclotron components to extend their operating life.

A second set of slits has been installed in the cyclotron vacuum chamber to decrease the R. F. phase acceptance for particles accelerated to full radius. As a result the cyclotron may be tuned for 30 keV energy spreads routinely, and energy spreads in the extracted beam of the order of 20 keV may be obtained with minimum beam. An additional advantage of the two slit combination has been an improvement in tuning reproducibility due to the additional constraint upon orbit pattern.

Measurements of output pulse time characteristics have been indicated using commercially available equipment and have proven to be of great value in achieving optimum tuning conditions. Installation of a separate cyclotron target area presently planned for late September will facilitate future cyclotron development work.

Major projects for the near future include continuing improvement of the reliability of individual cyclotron components, development of an external feedback system to improve the transverse stability of the extracted beam, and investigation of improved dee voltage control with various feedback possibilities. Work is presently underway in all of these areas. An improvement in resolution by

the Corona control system should be observed after sending the cyclotron beam through the tandem. This effect has been found in a preliminary measurement, but the effect is small.

2. Determination of the Cl(n,γ) Spectrum (D. W. Peak, A. W. Waltner)

The experimental phase of this investigation is complete and a thesis is now being prepared summarizing the results. A paper will be submitted for publication.

3. The Decay Scheme of As^{77} (A. J. Gandhi, A. W. Waltner)

The experiment is completed and a paper has been prepared for publication. An M.S. thesis summarizing the results has been written by A.J.G. The abstract appears below:

> "The gamma ray spectrum of As^{77} was investigated by a lithium-drifted germanium detector, which permitted observation of the following gamma rays energies (in kev): 87.6, 162.2, 238.9, 249.8, 271.5, 281.5, 519.9.
>
> A coincidence experiment was performed to measure the 271 kev line. These results are in good agreement with previous work in the field by other investigators who used different methods."

4. Gamma-Ray Pair Spectrometer (D. W. Peak, A. W. Waltner)

This project is inactive at present.

5. Radioactivity Studies Using The 80cc Ge(Li) Detector (S. M. Shafroth, J. Montgomary, A. Seila, J. Voltava, T. Hain, J. M. Joyce, J. G. F. Legge)

The TUNL tandem accelerator has provided microampere beams of protons at energies above (p,n) thresholds but below other thresholds (typically 8 MeV) to make radioactive sources with half-lives of a few minutes where the decay energy is high so that high energy gamma rays may be produced. (The 80 cc detector is particularly good in the 2-4 MeV region where most of the response is concentrated in the full energy peak.) So far sources of Ni^{90}, Mn^{52} and K^{38} have been produced and γ-ray spectra have been observed. The data is being analyzed and an abstract is being prepared for submission to the Southeastern Section meeting of the American Physical Society at Gainesville.

F. THEORY

1. Shell Model Calculations of Sc^{41} and F^{17} (M. Divadeenam,* W. P. Beres,** H. W. Newson)

These nuclei have been considered in an attempt to understand the 2p-1h nature of the bound and continuum levels. The calculations are being compared with the experimental data.

2. Theoretical Study of Sr^{89} Levels Via Allowed β-decay (M. Divadeenam,* W. P. Beres,** H. W. Newson)

This work is inactive at present.

3. Applications of Direct-Interaction Inelastic Scattering Theory (J. Y. Park)

This work is inactive at present and will be resumed later when more computer time becomes available.

4. Elastic Scattering of ^{3}He-Particles by ^{9}Be and ^{11}B between 4.0 and 18.0 MeV (J. Y. Park, J. L. Duggan ((ORAU)), P. D. Miller ((ORNL)), M. M. Duncan ((Univ. of Georgia)), R. L. Dangle ((Univ. of Georgia))

This work has been accepted for publication in Nuclear Physics and is now in press.

5. Shell Model Analysis of The ^{3}He And Triton Inelastic Scattering for Zr Including The Effects of Core Excitation (J. Y. Park, G. R. Satchler ((ORNL))

Computer programs required for numerical calculations have been successfully tested. Preliminary calculations without core polarization were carried out for the ^{90}Zr (^{3}He, ^{3}He') inelastic scattering at 43.7 MeV and for the ^{90}Zr(t,t') inelastic scattering at 20.0 MeV, both leading to the 2^+ excited state at 2.18 MeV. Results are compared with those using the collective model. Effects of radial cut-off and the non-locality of the bound states on the angular distributions are examined. Various types and ranges of phenomenological effective interaction are

* Now at Prairie View A. and M. College, Prairie View, Texas.
** Now at Wayne State University, Detroit, Michigan.

studied. Calculated differential cross sections are found to be sensitive to the range when the Yukawa interaction is used. Preliminary results seem to suggest a shorter interaction range for (^{3}He, ^{3}He$'$) scattering than for (t, t$'$) scattering. Further calculations including the core polarization effects are planned for the ^{3}He inelastic scattering on ^{90}Zr leading to other low lying excited states to study the effective interactions and the nuclear wave functions.

6. ^{3}He Elastic Scattering from ^{10}B and ^{14}C in The Range of 4.0 to 18.0 MeV (S. D. Danielopoulos, J. Y. Park, J. L. Duggan ((ORAU)), P. D. Miller ((ORNL)), M. M. Duncan ((Univ. of Georgia)), R. L. Dangle ((Univ. of Georgia))

An optical model analysis has been completed including new data on the ^{14}C(^{3}He, ^{3}He)^{14}C elastic scattering at 15 and 18 MeV. This work is being prepared for publication.

7. Analysis of (^{3}He, α) Reactions in Terms of The Knock-out Theory (S. D. Danielopoulos, J. Y. Park)

In order to reduce the run time of the numerical computation and to improve the accuracy of the results a new computer program was written for the computations of overlap radial integrals. The run time was reduced to 60%-70%. The program is now under numerical verification and extensive calculations of various (^{3}He, α) reactions on A = 4n nuclei, such as ^{16}O, ^{24}Mg, ^{28}Si and ^{32}S are planned.

8. A Systematic Study of the ^{3}He Optical Model Potential in Light Nuclei (J. Y. Park)

Optical model calculations are in progress for 10 MeV ^{3}He particles elastically scattered from ^{6}Li, ^{9}Be, ^{10,11}B, ^{12,14}C, ^{16}O, ^{22}Ne, ^{27}Al and ^{28}Si, especially to study the mass dependence of the potential.

9. The Deuteron Scattering by ^{4}He (J. Y. Park, R. M. Drisko ((Univ. of Pittsburgh))

Description of deuteron elastic scattering from ^{4}He in terms of the optical model is being attempted. Independent radius parameters for real and imaginary form factors are used to examine if the spin-orbit coupling effects could be replaced by the form factors whose imaginary part extends further than that of the real part. A coupled channel program JUPITOR I is being adopted to run on the TUCC System 360/75 computer.

10. A Feynman-graph Study of Knock-out Nuclear Reactions (S. D. Danielopoulos, J. Y. Park)

The contribution of the "knock-out" mechanism to direct reactions is studied, with analyticity and unitarity of the relevant S-matrix as the starting point. The knock-out process is a two-intermediate-particles contribution to the unitarity condition sum with a singularity (branch point) in the t-variable for unphysical values. This singularity is of the "anomalous" type. The contribution of the above process to the transition amplitude is conveniently studied through the corresponding Feynman graph. The vertex functions for the process $A \to c + b'$ and

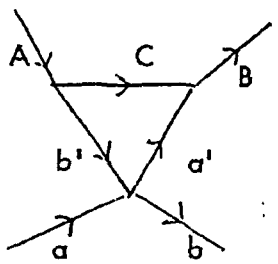

and $C + a' \to B$ were obtained through S-matrix reduction techniques and realistic bound state wave functions for nuclei A and B were employed. There are several options for the scattering vertex as, for example, the use of phase shifts obtainable from experimental data.

This kind of description of knock-out reactions eliminates some of the conceptual difficulties of conventional distorted wave theory, as the use of perturbation theory and optical model wave functions. The purpose is to find out whether, besides the sound theoretical basis, we have adequate quantitative results and to obtain means of improving them.

A code FDSKR which performs several suitable expansions and numerical integrations was written and is now under test on (p,n) reactions.

YALE UNIVERSITY

A. NEUTRON TIME-OF-FLIGHT STUDIES

1. Photoneutron Reactions--F.W.K. Firk, C.-P. Wu, G.W. Cole and R. Nath

The relative ground state cross section for the reaction $N^{14}(\gamma,n_0)N^{13}$ has been measured between 12 and 25 MeV (see Fig. A-1) using the nanosecond time-of-flight spectrometer. A new, low background cryostat has been constructed and will be used to obtain the cross section relative to the known deuterium cross section using an H_2O-D_2O difference technique. The results will then be compared with the $N^{14}(\gamma,p_0)C^{13}$ cross section (see section B1) in order to obtain information on the isospin purity of the states in N^{14}.

2. Photoneutron Polarization Studies--G.W. Cole and F.W.K. Firk

The polarization of photoneutrons from the reaction $O^{16}(\gamma,n)O^{15}$ has been measured with a time-of-flight resolution of 0.4 ns.m^{-1} using the $He^4(n,n)He^4$ reaction as an analyser (neutron scattering angles $\pm$ 130°. The scintillations from the liquid He are viewed in coincidence with the scattered neutrons thereby reducing the background to a negligible amount. Measurements have been made at 90° with bremsstrahlung end-point energies of 32 and 48 MeV. The preliminary results indicate very small values of polarization at 90°.

B. PHOTONUCLEAR REACTIONS (CHARGED PARTICLE EMISSION)

1. Angular Distribution of Photoprotons from N^{14*}--J.E.E. Baglin, R.W. Carr, C.-P. Wu

It is expected that the giant dipole resonance in N^{14} will derive much of its strength from the $p_{3/2} \rightarrow d_{5/2}$ and

---

*(see next page)

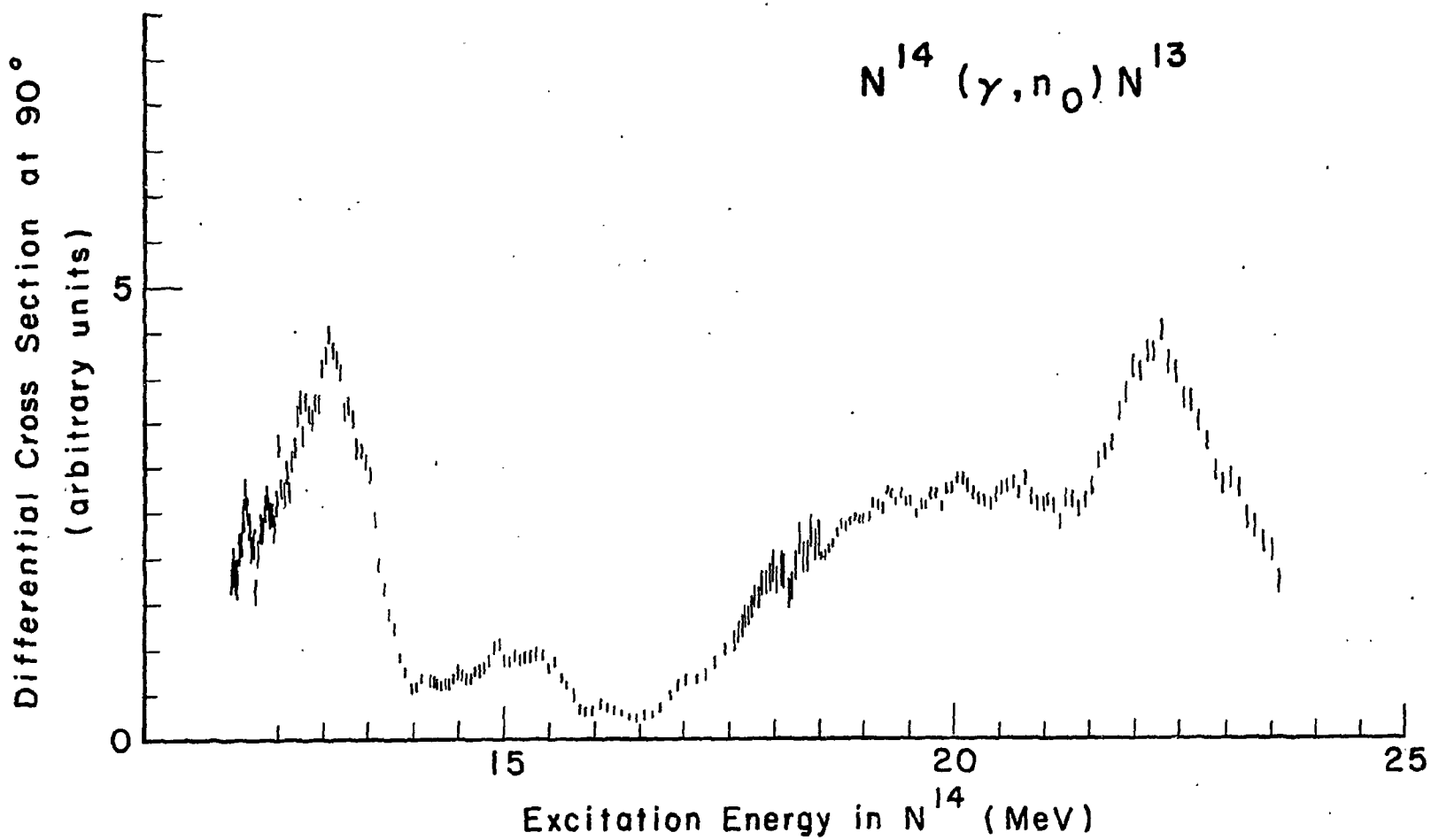

Fig.A-1

$p_{3/2} \rightarrow d_{3/2}$ single particle transitions. The same is true of the O^{16} giant resonance, and after our previous extensive studies of O^{16}, a comparative study of the N^{14} case should be informative.

In order to obtain (γ,p_o) angular distributions in 100 keV intervals over the giant resonance of N^{14}, a series of photoproton spectra were recorded using a nitrogen gas target irradiated with bremsstrahlung whose end point energy was set at 26.0, 24.5, 22.0 and 19.5 MeV respectively. By dividing out the bremsstrahlung weighting, and using the highest 2.5 MeV of each spectrum, only processes leading to the ground state of C^{13} are included. Spectra were recorded simultaneously with Si(Li) detectors placed at 45°, 65°, 90°, 115°, 135° and 160° to the photon beam.

Preliminary spectra indicate strong branching ratios to excited states of C^{13} from most of the N^{14} giant resonance. It also appears that the distributions for the (γ,p_o) protons are less forward peaked than were those of $O^{16}(\gamma,p_o)$.

The absolute cross section scale will be derived from spectra already taken with H^2 substituted for N^{14} in the

---

*The projects marked with an asterisk were undertaken wholly or partly at the Electron Prototype Accelerator, Los Alamos Scientific Laboratory, in collaboration with E.A. Knapp and D. Hagerman.

During a visit to that laboratory, we set up the (γ,p) and (γ,γ') experiments to take advantage of the 6% duty factor and high current of that accelerator. In these, and in numerous other exploratory runs, it was shown that no unexpected problems accompany the transfer of these experiments from the 0.1% duty cycle Yale Linac. Predictably, the data rate is increased, so that results equivalent to a month's continuous beam at the older machine can now be taken in 8 hours.

Further evident possibilities of the new machine lie in angular correlations studies, coincidence experiments and finely stepped excitation functions. Previously, these experiments have been impracticable. However, we now hope to explore such fields in the near future.

target chamber. The $H^2(\gamma,p)$ cross section will be a reference for this work.

2. Decay modes of N^{14} Giant Resonance States*--J.E.E. Baglin, E. Bentz, C.-P. Wu

Using a 7 mm deep planar Ge(Li) detector, we have studied the spectrum of γ-rays arising from the prompt decay of residual states following photodisintegration of N^{14}. The detector was placed at 135° to the bremsstrahlung beam whose end point was set at 26.0, 24.5, 22.0 and 19.5 MeV in four separate runs. A liquid nitrogen target was used.

It is evident that only two γ lines are important--the one at 3.68 MeV belonging to the $p_{3/2}$-hole state in C^{13}, and the 4.43 MeV line from the first excited state of C^{12}. The latter dominates, especially at the higher bremsstrahlung energies.

Further studies involving a complete excitation function and angular distribution work, will be undertaken.

3. P2 Reference Ionization Chamber*--J.E.E. Baglin, H.L. Schultz, C.-P. Wu, R.W. Carr, E. Bentz

The National Bureau of Standards "P2" ionization chamber has in the past been used as a general precision reference for measuring bremsstrahlung flux, having a minimal energy dependence between 5 and 100 MeV. However in present photoproton experiments at Yale and Los Alamos the instantaneous X-ray intensity used can exceed the specified 1000 μW per cm^2 beyond which recombination effects might spoil the chamber's response.

A precision study of this effect has been made, using as non-saturating reference monitors (i) activation of identical nickel samples and (ii) current from a photodiode viewing a plastic scintillator. Intensities of 5 mW per cm^2 were used, and with sensitivity to 0.5% we found no eividence of saturation. The study is proceeding.

4. Polarization of Photoprotons from Deuterium--H.L. Schultz and C.-P. Wu

Detailed studies of the optical properties of the quadrupole triplet lens system to momentum select and transport photoprotons to the He analyzer cell have been undertaken and are essentially complete. The next step will be the construction of an analyzer cell to test the performance of the entire system with thick target bremsstrahlung from the linac.

C. ELECTRON SCATTERING

1. Electron Scattering from the Nd Isotopes--D.W. Madsen, L. Cardman, J. Legg, R. Yen and C.K. Bockelman

Studies of the elastic and inelastic scattering of electrons from $Nd^{142,146,150}$ have been completed. The data were analyzed using theories which account for Coulomb distortion and finite size effects; results are summarized in Tables C1 and C2.

Table C1

Elastic Scattering Fermi Charge Distribution

Nucleus	c(F)	t(F)	$\langle r^2 \rangle^{1/2}$(F)
Nd^{142}	5.83 ± 0.02	1.79 ± 0.14	4.77 ± 0.04
Nd^{146}	5.96 ± 0.05	0*	4.61 ± 0.04
Nd^{150}	$5.82 {}^{+0.04}_{-0.03}$	$1.59 {}^{+0.18}_{-0.22}$	4.71 ± 0.06

*Final fit to a uniform distribution

Table C2

B(EL↑) Values Single Particle Units

Nucleus	State (MeV)	$\frac{B(EL\uparrow)}{B(EL\uparrow)sp}$
	+2 States	
Nd^{142}	1.57	13.1 ± 1.7
Nd^{142}	2.09	4.1 ± 1.1
Nd^{146}	0.45	30.9 ± 4.6
Nd^{150}	0.13	62.9 ± 10.5
	-3 States	
Nd^{142}	2.09	28.6 ± 5.0

For the 40-60 MeV electron energies used, a description in terms of a Fermi charge distribution with half-density radius $c = 1.1A^{1/3}$ and a 90%-10% skin thickness parameter t ranging from 2.3-2.5 F for spherical nuclei (and to larger values of t for deformed nuclei) is expected. A glance at Table C1 will show that unexpected (and thus extremely interesting!) results have been obtained. The skin thicknesses measured here for Nd nuclei range from 1.8 F to zero.

These small values of t reflect the fact that the cross sections are from 4-15% (depending on energy and angle) higher than predicted using conventional parameters. In these circumstances we have examined the normalization of the cross sections with great care, and we are convinced the cross sections are correct.

At this time we are not sure how to account for their results. The r.m.s. radii quoted in Table I differ from recent muonic X-ray results of Macagno, et al. at Columbia; high energy electron scattering results, normalized to the Columbia results indicate the expected range of c and t values. It is conceivable that the discrepancy results from the neglect in the scattering analysis of virtual transitions to nuclear excited states, equivalent to a distortion of the nucleus during the scattering process, i.e. neglect of the so-called "dispersion effect". The muonic X-ray results for Nd^{142} have been corrected for the dispersion effect; without that correction the muonic X-ray analysis indicated an anomalously small t not inconsistent with the values given in Table C1.

Application of a dispersion correction for electron scattering requires, in principle, knowledge of the energies and transition matrix elements to all nuclear states which can be reached at the electron energy used. Unfortunately, there are no experimental results or theoretical estimates of these quantities currently available for Nd. However, a start to solving the problem may be made using data of Table C2, which presents the B(E1↑) values expressed in single-particle units for the low-lying states extracted from a DWBA analysis of the inelastic electron scattering measured in this experiment. The values for $Nd^{142,146}$ are in reasonable agreement with those derived from other experiments; for Nd^{150} the value is a factor of two below the presently accepted value. The angular distribution of electrons inelastically scattered to the 2.09 MeV region in Nd^{142} indicates that a hitherto unreported even parity state exists within ~ 50 keV of the known 3^- level. It is interesting to note that the Nd^{150} 2^+ state is the lowest ever resolved from the elastic scattering peak in an electron scattering experiment. The data are shown in Figs. C-1 and C-2.

D. THEORETICAL DEVELOPMENTS

T.H. Schucan (in collaboration with J.N. Ginocchio and H.A. Weidenmuller)

The shell model theory of nucleon-nucleus scattering has

Raw Spectrum of Scattered Electrons

Nd^{150}

$E_0 = 60$ MeV

$\theta_{Lab} = 130°$

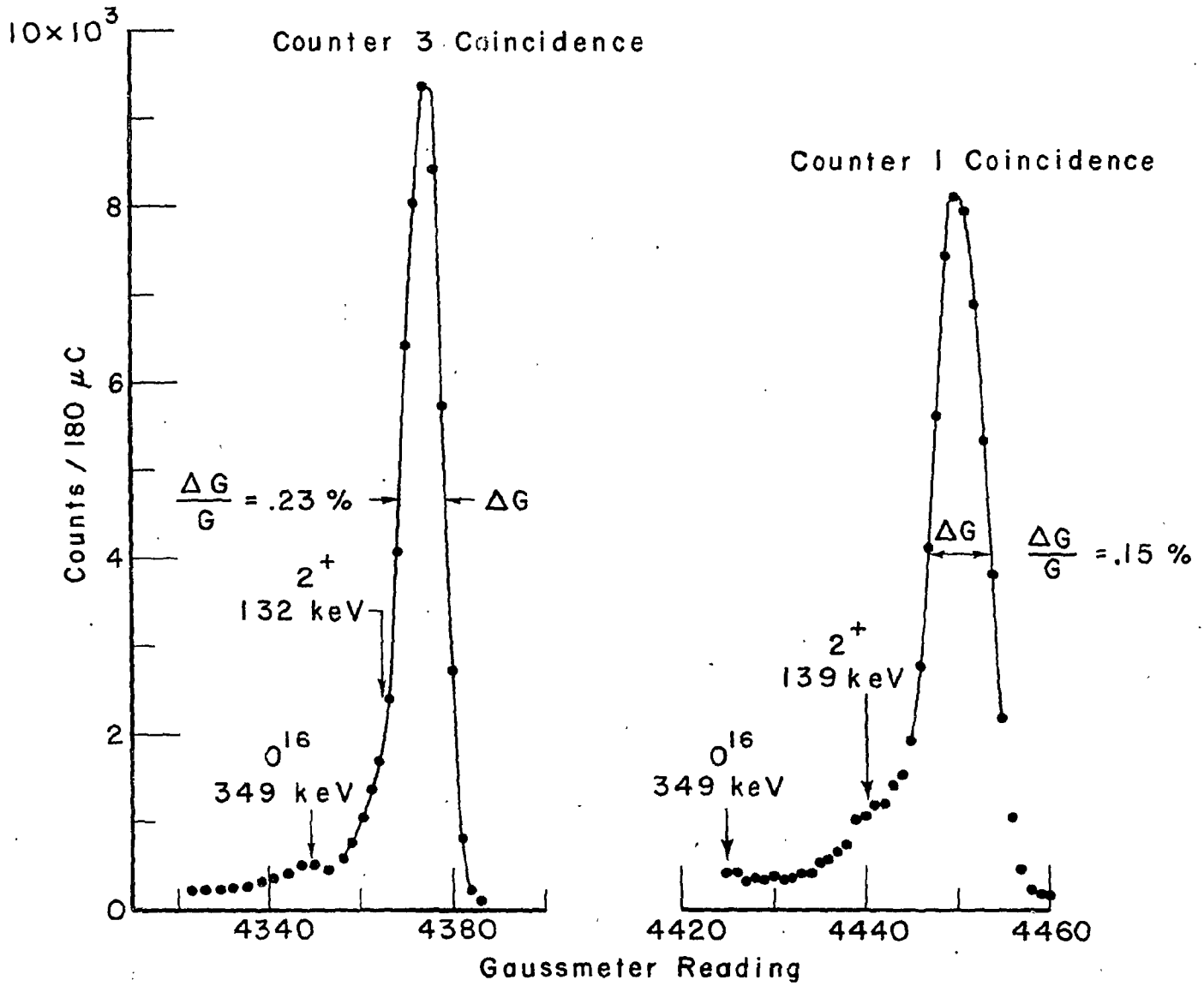

Fig.C-1

DATA NOT FOR QUOTATION

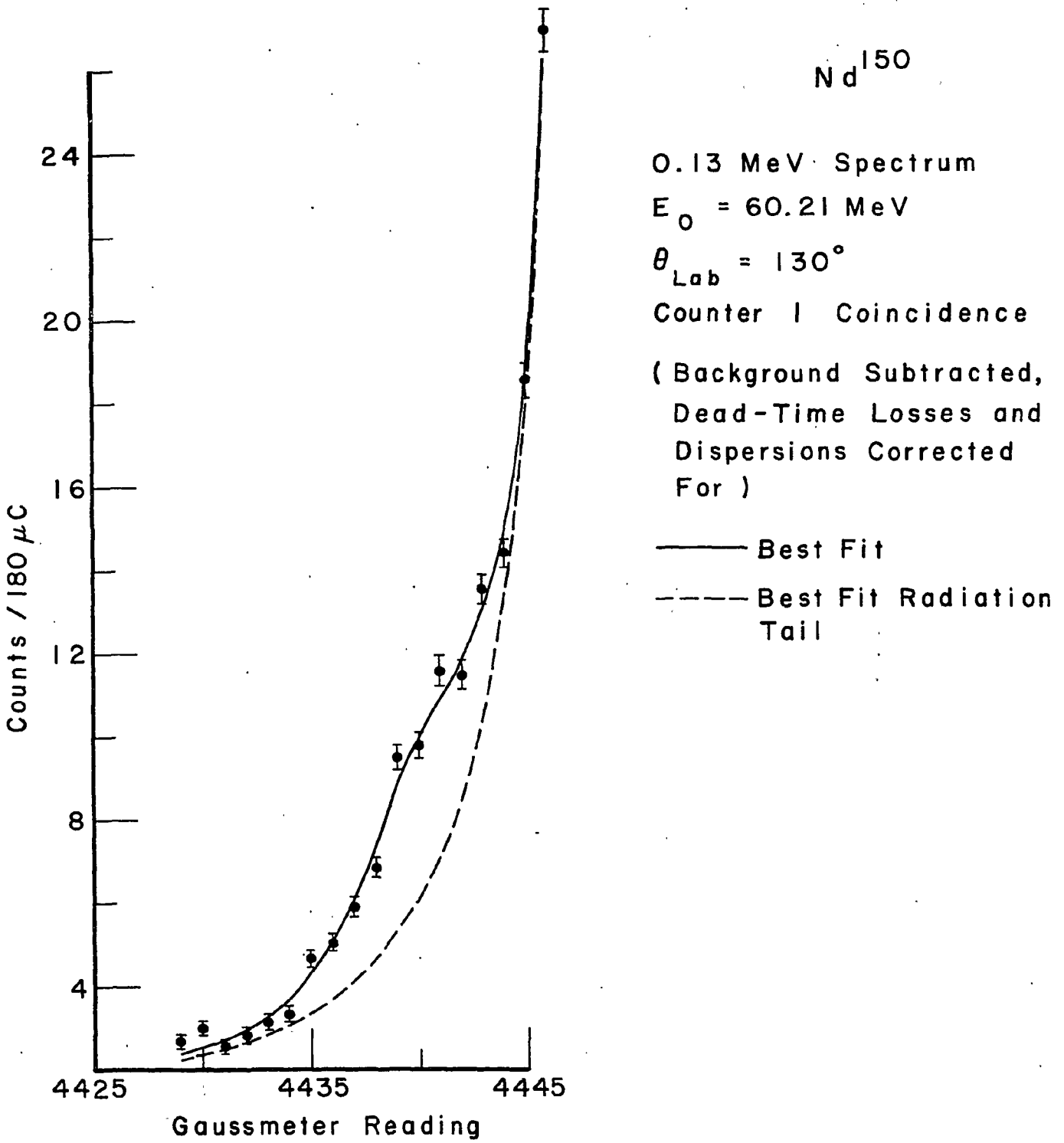

Fig.C-2

been extended to include ground state correlations. A general and yet explicit expression for the s-matrix has been obtained and the structure of this matrix has been investigated. In contrast to previous treatments it is not assumed that the residual interaction is separable.

APPENDIX

Recent Publications

ARGONNE NATIONAL LABORATORY

1. Nuclear Spectroscopy with Average Spectra from Neutron-Resonance Capture, L. M. Bollinger and G. E. Thomas, Contributions to IAEA Symp. on Nuclear Structure, Dubna, July 4—11, 1968. Joint Institute for Nuclear Research, Dubna, 1968, Publ. D-3893, p. 117.

2. Use of Ge(Li) Detectors in γ-Ray Spectroscopy: Applications and Basic Considerations, H. H. Bolotin, Semiconductor Nuclear-Particle Detectors and Circuits, Proc. Conf., Gatlinburg, Tennessee, May 15—18, 1967, Ed. W. L. Brown et al. Natl. Acad. Sci., Washington, D. C., 1969, Publ. No. 1593, pp. 660—683.

3. Effective-Interaction Formulation of Bound and Continuum Shell-Model Calculations, K. W. McVoy and W. J. Romo, Nucl. Phys. A126(1), 161—180 (1969).

4. Experimental Determination of the Efficiency of the Grey Neutron Detector, W. P. Poenitz, Nucl. Instr. and Methods 72, 120 (1969).

5. Studies of Fast Neutron Cross-Sections Through Integral Experiments, J. M. Kallfells, W. P. Poenitz, B. R. Sehgal, B. A. Zolotar, Transact. of ANS, Vol. 12, 187 (1969).

6. The Ratio $\sigma_\gamma(U238)/\sigma_f(U235)$ in the Neutron Energy Range 30—900 keV, W. P. Poenitz, Transact. of ANS 12, 279 (1969).

7. Radiative Transitions from Highly-Excited Nuclear States, L. M. Bollinger, Nuclear Structure, Proc. IAEA Symp., Dubna, 1968, Invited Papers. Intern. Atomic Energy Agency, Vienna, 1968, pp. 317—347.

8. Measurement of Internal-Conversion Coefficients of Neutron-Capture Gamma Rays with a Superconducting Spectrometer, S. B. Burson, Contributions to IAEA Symp. on Nuclear Structure, Dubna, July 4—11, 1968. Joint Institute for Nuclear Research, Dubna, 1968, Publ. D-3893, p. 174.

9. Properties of States Excited in ^{181}Re and ^{182}Re Following Orbital Electron Capture in $^{181}_{76}$Os (105 m) 75 and $^{182}_{76}$Os (22 h), S. B. Burson, Proc. Conf. on the Electron Capture and Higher Order Processes in Nuclear Decays, Debrecen, Hungary, July 15—18, 1968, Ed. D. Berenyi. Eötvös Lorand Phys. Soc., Budapest, 1968, Vol. 3, pp. 475—479.

10. Survey of Single-Particle and Collective States of the Actinides by Use of Transfer Reactions, J. R. Erskine, A. M. Friedman, T. H. Braid, and R. R. Chasman, Contributions to IAEA Symp. on Nuclear Structure, Dubna, July 4—11, 1968. Joint Institute for Nuclear Research, Dubna, 1968, Publ. D-3893, p. 61.

11. Generation and Statistical Analysis of Synthetic Cross Sections, P. Hoffman-Pinther, P. P. Singh, and D. W. Lang, Nucl. Phys. A127(2), 241—269 (1969).

12. Nuclear Structure Calculations, R. D. Lawson, Proc. Nuclear Physics and Solid State Physics Symp., 1968. Physics Committee, Indian Atomic Energy Authority, Bombay, 1968, 11. 17—31.

13. The Optics of Dipole Magnets, J. J. Livingood, Academic Press, New York, 1969.

14. Study of the $Ca^{48}(He^3,p)Sc^{50}$ Reaction, J. P. Schiffer and P. G. Roos, Phys. Rev. 177, 1695—1968 (1969).

15. (d,He^3) Reaction on the Chlorine Isotopes at 23.35 MeV, N. G. Puttaswamy and J. L. Yntema, Phys. Rev. 177, 1624—1628 (1969).

16. Analog Resonances in Heavier Nuclei, M. H. Macfarlane, Physics Division Informal Report PHY-1969D (June 1969).

17. Proton-Induced Analog Resonances, G. C. Morrison, Physics Division Informal Report PHY-1969C (April 1969).

18. Electromagnetic Transition Strengths in Pb^{206}, Pb^{207}, and Pb^{208} from Threshold Photoneutron Cross-Section Measurements, C. D. Bowman, B. L. Berman, and H. E. Jackson, Phys. Rev. 178, 1827—1836 (1969).

19. Delbrück Scattering of 10.8-MeV γ Rays, H. E. Jackson and K. J. Wetzel, Phys. Rev. Letters 22, 1008—1010 (1969).

20. Level Density of a Fermi System: Nonperiodic Perturbations of the Energy-Level Scheme, P. B. Kahn and N. Rosenzweig, J. Math. Phys. 10, 707—715 (1969).

21. Possible Spin Dependence in Proton Inelastic Scattering, J. C. Legg, Phys. Rev. Letters 22, 1005—1008 (1969).

22. Properties of the 3.39-MeV State in B^{12}, F. P. Mooring, J. E. Monahan, and R. E. Segel, Phys. Rev. 178, 1612—1615 (1969).

23. Study of the J Dependence in the (d,He^3) Reaction, H. Ohnuma and J. L. Yntema, Phys. Rev. 178, 1654—1662 (1969).

24. Experimental Study of the (d,t) Reaction on Even-Mass Mo Isotopes, H. Ohnuma and J. L. Yntema, Phys. Rev. 178, 1855—1863 (1969).

25. Neutron-Capture Gamma-Ray Studies of the Level Structure of the Te^{124} Nucleus, D. L. Bushnell, R. P. Chaturvedi and R. K. Smither, Phys. Rev. 179, 1113—1133 (1969).

26. Distribution of Charge in Th^{232} and U^{238} Determined by Measurements on Muonic X Rays, R. E. Coté, W. V. Prestwich, A. K. Gaigalas, S. Raboy, C. C. Trail, R. A. Carrigan, P. D. Gupta, R. B. Sutton, M. N. Suzuki, and A. C. Thompson, Phys. Rev. 179, 1134—1147 (1969).

27. Nuclear Models, D. R. Inglis, Phys. Today 22, 29—40 (1969).

28. Corrections to the Hartree-Fock Approximation for Homogeneous Nuclear Matter, J. J. Mackenzie, Phys. Rev. 179, 1002—1010 (1969).

29. Multipole Analysis of Particle-Particle or Particle-Hole Multiplets, M. Moinester, J. P. Schiffer, and W. P. Alford, Phys. Rev. 179, 984—995 (1969).

30. Study of the $Zr^{94}(He^3,d)Nb^{95}$ Reaction, H. Ohnuma and J. L. Yntema, Phys. Rev. 179, 1211—1213 (1969).

31. Neutron Resonances of Mo Isotopes, H. Shwe and R. E. Coté, Phys. Rev. 179, 1148—1153 (1969).

32. Level Structure of Low-Lying Excited States of Ga^{66} Populated by the Decay of 2.2-h Ge^{66}, H. H. Bolotin and D. A. McClure, Phys. Rev. 180, 987—996 (1969).

33. $B^{11}(He^{3},\alpha)B^{10}$ Reaction at 33 MeV, D. Dehnhard, N. Williams and J. L. Yntema, Phys. Rev. 180, 967—970 (1969).

34. Midwest Tandem Cyclotron—A Proposal for a Regional Accelerator Facility, D. S. Gemmell, T. K. Khoe, J. J. Livingood, W. J. Ramler, T. H. Braid, R. H. Siemssen, A. M. Friedman, A. H. Jaffey, F. P. Mooring, C. B. Wedster, P. R. Fields, J. P. Schiffer, L. M. Bollinger, and F. E. Throw, ANL-7582 (June 1969).

35. Coulomb Energies—An Anomaly in Nuclear Matter Radii, J. A. Nolen and J. P. Schiffer, Phys. Letters 29B(7), 396—398 (1969).

36. Precision Determination of the D-T Neutron Separation Energy, W. V. Prestwich and G. E. Thomas, Phys. Rev. 180, 945—947 (1969).

37. On Coulomb Energies, the Anomalous Isotope Shift of Nuclear Radii, and Core Polarization by the Neutron Excess, J. P. Schiffer, J. A. Nolen, and N. Williams, Phys. Letters 29B(7), 399—401 (1969).

38. Recoil Broadening of Secondary Transitions in Neutron-Capture Gamma-Ray Cascades, K. J. Wetzel, Phys. Rev. 101, 1465—1476 (1969).

Abstracts of contributions presented at recent meetings:

1. Direct Reactions on Be^{10}, D. L. Auton, B. Zeidman, H. T. Fortune, J. P. Schiffer and R. C. Bearse, Bull. Am. Phys. Soc. 14, 489 (1969).

2. States of Ho^{166} from Average Resonance Capture in $Ho^{165}(n,\gamma)Ho^{166}$, L. M. Bollinger and G. E. Thomas, Bull. Am. Phys. Soc. 14, 514 (1969).

3. Accurate Method of Determining Counting Losses in Nuclear Radiation Detection Systems, H. H. Bolotin, M. G. Strauss and D. A. McClure, Bull. Am. Phys. Soc. 14, 532 (1969).

4. Primary Gamma Rays in Sm^{150} Following Average Neutron Resonance Capture, D. J. Buss and R. K. Smither, Bull. Am. Phys. Soc. 14, 514 (1969).

5. Highly Excited States in C^{12}, N^{14}, and O^{16} from Li-Induced Reactions on B^{10} and C^{12}, J. R. Comfort, H. T. Fortune, G. C. Morrison, and B. Zeidman, Bull. Am. Phys. Soc. 14, 507 (1969).

6. Study of (α,t) Reactions on 1p-Shell Nuclei, H. T. Fortune, D. K. Dehnhard, R. H. Siemssen, and B. Zeidman, Bull. Am. Phys. Soc. 14, 487 (1969).

7. Delbrück Effect in Elastic Scattering of 10.8-MeV γ Rays, H. E. Jackson and K. J. Wetzel, Bull. Am. Phys. Soc. 14, 607 (1969).

8. Lifetime of the 11-keV Level in Cs^{134m}, F. J. Lynch and L. E. Glendenin, Bull. Am. Phys. Soc. 14, 629 (1969).

9. Study of the (He^3,d) Reaction for A = 31, R. A. Morrison, Bull. Am. Phys. Soc. 14, 567 (1969).

10. Coulomb Energies and Nuclear Radii, J. A. Nolen and J. P. Schiffer, Bull. Am. Phys. Soc. 14, 584 (1969).

11. O^{16} Elastic Scattering from $Mg^{24,26}$ and $Si^{28,30}$, R. H. Siemssen, H. T. Fortune, J. L. Yntema, and A. Richter, Bull. Am. Phys. Soc. 14, 548 (1969).

12. Average Resonance Capture in Cd^{113}, R. K. Smither, D. J. Buss, L. M. Bollinger, and G. E. Thomas, Bull. Am. Phys. Soc. 14, 513 (1969).

13. States of Pd^{106} from Average Resonance Capture in $Pd^{105}(n,\gamma)Pd^{106}$, G. E. Thomas and L. M. Bollinger, Bull. Am. Phys. Soc. 14, 515 (1969).

14. Computer-Controlled Multiple-Detector System for Heavy-Ion Scattering Experiments, J. W. Tippie, J. J. Bicek, H. T. Fortune, R. H. Siemssen, and J. L. Yntema, Bull. Am. Phys. Soc. 14, 533 (1969).

15. Method for DWBA Calculation of Stripping to Unbound States, C. M. Vincent and H. T. Fortune, Bull. Am. Phys. Soc. 14, 572 (1969).

16. Method for Determining Spins of Neutron Resonances, K. J. Wetzel, G. E. Thomas, L. M. Bollinger, and H. E. Jackson, Bull. Am. Phys. Soc. 14, 513 (1969).

17. Angular Distributions of Heavy Ions Produced by ^{3}He Bombardment of ^{12}C, B. Zeidman and H. T. Fortune, Bull. Am. Phys. Soc. 14, 507 (1969).

18. A System Approach to the Nuclear Shell Model, S. Cohen, Trans. Am. Nucl. Soc 12(1), 147 (1969).

BROOKHAVEN NATIONAL LABORATORY

1) R. E. Chrien, Experimental Studies of Resonance Neutron Capture γ Rays, Invited Talk presented at the International Symposium on Neutron Capture Gamma-Ray Spectroscopy, Studsvik, Sweden, August 11-15, 1969.

2) O. A. Wasson, Resonance Radiative Neutron Capture Studies at Brookhaven, presented at the International Nuclear Data Committee, Topical Conference, at Brookhaven, June 4, 1969.

3) M. Beer, Correlations and Distributions of Widths in Resonance Neutron Capture, Phys. Rev. 181, 1422 (1969).

4) S. F. Mughabghab and R. E. Chrien, S-wave Neutron Strength Functions of the Gd Isotopes, Physical Review 180, 1131 (1969).

5) O. A. Wasson, R. E. Chrien, M. A. Lone, M. R. Bhat, and M. Beer, Resonance Neutron Capture in $^{181}Ta(n,\gamma)^{182}Ta$, Nuclear Physics A132, 161 (1969).

6) S. F. Mughabghab, D. I. Garber, R. E. Chrien, and O. A. Wasson, Neutron Capture γ Rays from Pr^{142}, presented at the Spring Meeting of the American Physical Society, Washington, D. C. April 28, 1969.

7) O. A. Wasson, R. E. Chrien, and D. I. Garber, Resonance Neutron Capture in $La^{138}(n,\gamma)La^{139}$ and $La^{139}(n,\gamma)La^{140}$, presented at the Spring Meeting of the American Physical Society, Washington, D. C., April 28, 1969.

8) M. Beer and R. E. Chrien, Nuclear Structure and the Statistics of Resonance (n,γ) Partial Widths, presented at the Spring Meeting of the American Physical Society, Washington, D. C., April 28, 1969.

9) K. Rimawi, O. A. Wasson, R. E. Chrien, and D. I. Garber, Evidence for Channel Resonance Capture in $^{55}Mn(n,\gamma)^{56}Mn$, Contribution to International Conference on Properties of Nuclear States, Montreal, Canada, August 25-30, 1969.

10) P. H. M. Van Assche, H. Baader, H. R. Koch, B. P. K. Moler, U. Gruber, O. W. B. Schult, K. Rimawi, R. E. Chrien, O. A. Wasson, D. I. Garber, J. Comfort, and J. B. McGrory, Contribution to International Conference on Properties of Nuclear States, Montreal, Canada, August 25-30, 1969.

11) K. Rimawi, Thesis, State Univ. of N.Y. at Albany, "s-Wave and p-Wave Resonance Neutron Capture in Zr-91, Nb-93, and Rh-103", 8/69, Albany, N. Y.

GULF GENERAL ATOMIC

1. Neutron Capture Gamma-Ray Facility Using an Electron Linear Accelerator, V. J. Orphan, C. G. Hoot, A. D. Carlson, J. John and J. R. Beyster. To be published in Nuclear Instruments and Methods. GA-9221, Jan. 27, 1969.

2. A Computer System for Neutron Cross Section Measurements, W. M. Lopez. To be published in the Proceedings of Conference on Computer Systems in Experimental Nuclear Physics. GA-8293, Feb. 28, 1969.

3. A Facility for Measuring Cross Sections of (n, xγ) Reactions Using an Electron LINAC, V. J. Orphan, C. G. Hoot, A. D. Carlson, J. John and J. R. Beyster. To be published in Nucl. Inst. and Methods. GA-9274, Mar. 24, 1969.

4. Cross Sections for (n, xγ) Processes in Nitrogen and Oxygen, C. G. Hoot, V. J. Orphan, A. D. Carlson, J. John and J. R. Beyster, Bull. Am. Phys. Soc. 14, 494 (1969).

5. Neutron-Capture Cross Sections in the Energy Range 1-700 keV, W. M. Lopez, M. P. Fricke, S. J. Friesenhahn and D. G. Costello, Bull. Am. Phys. Soc. 14, 495 (1969).

6. Analysis of Average Neutron-Capture Cross Sections, M. P. Fricke, W. M. Lopez, S. J. Friesenhahn and D. G. Costello, Bull. Am. Phys. Soc. 14, 496 (1969).

7. ^{3}He(n, p)T Cross Section, D. G. Costello, M. P. Fricke, S. J. Friesenhahn and W. M. Lopez, Bull. Am. Phys. Soc. 14, 553 (1969).

8. Radiative Strength Function for Fast Neutron Capture, M. P. Fricke and W. M. Lopez, Physics Letters 29B, 393 (1969).

9. A Nearly Monoenergetic Source of 6.129-MeV Gamma Rays for Ge(Li) Detector Calibration, J. John, V. J. Orphan and C. G. Hoot. To be published in Nucl. Inst. and Methods. GA-9396, May 29, 1969.

10. Measurements of Resonance Neutron Capture γ-ray Spectra Using a Ge(Li)-NaI Spectrometer and an Electron LINAC, V. J. Orphan, J. John and C. G. Hoot. Presented at the International Symposium on Neutron Capture Gamma-Ray Spectroscopy which was held in Studsvik, Sweden, Aug. 11-15, 1969.

LOS ALAMOS SCIENTIFIC LABORATORY

The following papers have been submitted to The Physical Review:

1. H. C. Britt and J. D. Cramer, "(t,p) Q-Values for Th, U, and Pu Isotopes."

2. E. R. Flynn, D. D Armstrong, and J. G. Beery, "Inelastic Triton Scattering from ^{92,94,96}Zr."

3. E. R Flynn, D. D Armstrong, J. G. Beery, and A. G. Blair, "Triton Elastic Scattering at 20 MeV."

4. A. Niiler, "The D(p,d*)p Cross Section from the D(p,2p)n Reaction."

5. E. B. Shera and E. T. Jurney, "Energy Levels of ^{176}Lu."

6. G. Berzins, M. E. Bunker, and J. W. Starner, "Energy Levels of ^{100}Ru."

The following paper has been submitted to Physical Review Letters:

1. D. D. Armstrong, L. L Catlin, P. W. Keaton, Jr., and L. R. Veeser, "Polarization of ^{3}He Elastically Scattered from ^{4}He."

The following paper has been submitted to Nuclear Instruments and Methods:

1. G. G. Ohlsen, J. L. McKibben, R. R. Stevens, Jr., and G. P. Lawrence, "Depolarization and Emittance Degradation Effects Associated with Charge Transfer in a Magnetic Field."

Papers recently submitted for presentation at meetings included the following:

W. K. Brown G. A. Cowan	Scientific Applications of Nuclear Explosions	Symposium on Education for the Peaceful Uses of Nuclear Explosives, Univ. of Arizona, 3/31-4/2/69.
J. P. Shipley	Simple Pulse Shape Discriminator for Use with Ge(Li) Detectors and Organic Scintillators	Ispra Nuclear Electronics Symposium, Ispra, Italy, May 6-8, 1969.
M. Bolsterli E. O. Fiset J. R. Nix	Single Particle Calculations for Deformed Potentials Appropriate to Fission	Second Symposium on the Physics and Chemistry of Fission, Vienna, 7/28-8/1/69.

H. C. Britt S. C. Burnett J. D. Cramer	Fission Induced by the Pu-240(p,p'f) Reaction	Second Symposium on the Physics and Chemistry of Fission, Vienna, 7/28-8/1/69
L. V. East G. R. Keepin	Fundamental Fission Signatures and their Application to Nuclear Safeguards	" "
J. D. Seagrave	The Elastic Channel in Nucleon-Deuteron Scattering	Intl. Conf. on the Three-Body Problem in Nuclear and Particle Physics, Univ. of Birmingham, England, 7/8-10/69
E. T. Jurney	Excitation of Levels in ^{235}U by the $^{234}U(n,\gamma)^{235}U$ Reaction	Symposium on Capture γ-Ray Spectroscopy, Studsvik, Sweden, August 1969
J. L. Yarnell	Neutron Diffraction Study of Liquid 36-Argon	Gordon Research Conf. on the Chemistry and Physics of Liquids, Holderness, New Hampshire, 8/11-15/69
M. E. Bunker	Decay of 16-Sec ^{100}Tc	Intl. Conf. on Properties of Nuclear States, Montreal, 8/25-30/69
O. Hansen	Spectroscopic Information from Few Particle Transfer Reactions	" "
J. Terrell, Jr. K. H. Olsen	Luminosity Fluctuations of 3C 273	APS Honolulu Meeting, Sept. 2-5, 1969
J. E. Brolley D. A. Liberman	Diamagnetism of Helium and Gordon Scattering	" "
E. B. Shera E. T. Jurney	The $^{175}Lu(n,\gamma)^{176}Lu$ Reaction and the Energy Levels of ^{176}Lu	" "
P. W. Keaton L. Rosen	The Los Alamos Meson Factory	Symposium on Nuclear Reaction Mechanisms and Polarization Phenomena, Laval Univ., Quebec, 9/1-2/69
P. W. Keaton	Work with Polarized Tritons at Los Alamos	" "
R. C. Ragaini J. D. Knight W. T. Leland	Levels of ^{88}Sr from the $^{86}Sr(t,p)^{88}Sr$	APS Boulder Meeting, 10/30-11/1/69

D. G. Megli G. P. Agin V. R. Potnis C. E. Mandeville	Nuclear Energy States of ^{97}Niobium	APS Boulder Meeting, 10/30-11/1/69
E. R. Flynn	Paring Vibrations and Isospin	" "
D. R. Harris J. I. Sackett	Kinetic and Power Characteristics of Bare Pulsed Neutron Multipliers	ANS 1969 Winter Conf., San Francisco, 11/30-12/4/69
G. A. Cowan	Production of ^{252}Cf in Thermonuclear Explosions	ANS Symposium on Californium-252, New York, October 1968
G. R. Keepin R. B. Walton	Nuclear Safeguards Applications of ^{252}Cf	" "

The following have been published recently as Los Alamos reports:

1. A List of References on the Study of Liquids and Solids by Slow or Cold Neutron Scattering Experiments, Schuch, D-BIB-98.

2. Pulsed Neutron Research for Nuclear Safeguards. Quarterly Progress Report, January - March, 1969, Keepin, N-6-1016.

3. Monte Carlo Method Applied to an Estimation of Delayed Neutron Response, Turner, LA-DC-10515.

4. Nuclear Safeguards Research and Development Program. A Program Review Covering Calendar Year 1968, LA-MD-3005.

5. RAYMATH, A Fortran IV Code to Compile Simple Instructions for Array Mathematics and Manipulation, Harlow, Jr., and Neergaard, LA-4049.

6. Photon Energy Response of Several Commercial Ionization Chambers, Geiger Counters, Scintillators, and Thermoluminescent Detectors, Krohn, Chambers, and Storm, LA-4052.

7. Nuclear Safeguards Research and Development. Program Status Report, October - December, 1968, LA-4070-MS.

8. Fission Cross Section of ^{238}Pu from Persimmon, Silbert, LA-4108-MS.

9. Operation of a Radio-Frequency Nuclear Spin Filter, Ohlsen, McKibben, Stevens, Jr., Lawrence, and Lindsay, LA-4112.

10. Radiation Leakage through Pinhole Collimators, Moore, LA-4121.

11. Interactions of Nucleons with Deuterons, Tritons, ^{3}He, or ^{4}He Between 30 MeV and 1 GeV: A Bibliography, Seagrave and Jackson, LA-4143-MS.

12. Nuclear Safeguards Research and Development Program Status Report, January - March, 1969, LA-4162-MS.

13. EPUT Multiplexer Coder Driver and the EPUT Multiplex Decoder, Fullwood, LA-4175-MS.

14. Precision Staircase Calibrator for Field Use, Fullwood, LA-4178-MS.

15. Range-Energy Loss of Protons in Matter, Keaton, Jr., LA-4179-MS.

16. Quarterly Status Report on the Medium-Energy Physics Program for the Period Ending April 30, 1969, LA-4184-MS.

17. Fission Barriers and Transition-State Spectra for ^{232}Th, ^{234}Th, ^{238}U, ^{240}U, ^{242}Pu, and ^{244}Pu from (t,pf) Reactions, Cramer, LA-4198.

OAK RIDGE NATIONAL LABORATORY

Listed below is the title of a paper presented at the meeting of the New York Chapter of the American Nuclear Society, N. Y., N. Y., April 8-9, 1969.

Industrial Application of 14 MeV Neutron Generators, J. E. Strain.

Listed below is the title of a paper presented at the meeting of the American Physical Society, Washington, D. C., April 28 - May 1, 1969.

Nuclear Structure of Near Closed Shell Nuclei: I. Nuclei Near N = 50, J. B. Ball.

Listed below is the title of a paper presented at the meeting of the American Nuclear Society, Seattle, Washington, June 15-19, 1969.

The Dispersion Law of a Neutron Die-Away Experiment, R. S. Denning and R. B. Perez.

Listed below is the title of a paper presented at the meeting of the American Physical Society, Rochester, N. Y., June 18-20, 1969.

Soft X-Rays from Stripped O Beams, I. A. Sellin and Bailey Donnally.

Listed below is the title of a paper presented at the International Conference on the Three-Body Problem, Birmingham, England, July 8-10, 1969.

Radiative Capture of Protons by Deuterons, B. D. Belt, C. R. Bingham, M. L. Halbert, and A. Van der Woude.

Listed below is the title of a paper presented at the International Conference on Nuclear Reactions Induced by Heavy Ions, Heidelberg, Germany, July 15-18, 1969.

Multiple Coulomb Excitation of Medium-Weight and Rare-Earth Nuclei with ^{16}O Ions, R. L. Robinson, P. H. Stelson, F. K. McGowan, R. O. Sayer, and W. T. Milner.

Listed below is the title of a paper presented at the International Conference on Clustering Phenomena in Nuclei, Bochum, West Germany, July 21-24, 1969.

The $^{9}Be(p,p\alpha)^{5}He$ and $^{12}C(p,p\alpha)^{8}Be$ Reactions at 57 MeV, C. A. Ludemann, C. D. Goodman, P. G. Roos, H. G. Pugh, H. D. Holmgren, M. B. Epstein, M. Jain, and N. S. Wall.

Listed below is the title of a paper to be presented at the American Nuclear Society Conference on Reactor Operating Experience, San Juan, Puerto Rico, Oct. 1-3, 1969.

Measurement of the Neutron Flux within the HFIR Target Region, F. B. K. Kam and J. H. Swanks.

Listed below are titles of papers to be presented at the Second International Conference, Accelerator Dosimetry and Experience, Stanford Linear Accelerator Center, Stanford, California, Nov. 5-7, 1969.

1. Calculation of the Energy Deposited in Thick Targets by High Energy (1 GeV) Electron-Photon Cascades and Comparison with Experiment, R. G. Alsmiller and H. S. Moran.

2. Calculation of the Residual Photon Dose Rate Induced in Iron by 200-MeV Protons, T. W. Armstrong and J. Barish.

3. The Transport of Neutrons Produced by 3-GeV Proton-Lead Nucleus Collisions Through a Labyrinth and Comparison with Experiment, R. G. Alsmiller and E. Solomito.

Listed below are titles of papers to be presented at the meeting of the American Nuclear Society, San Francisco, California, Nov. 30 - Dec. 4, 1969.

1. Low-Energy Gamma-Ray Yields in ^{23}Na, ^{57}Fe, and ^{183}W, K. J. Yost, P. H. Pitkanen, and C. Y. Fu.

2. Gamma-Ray Spectra Arising from Thermal Neutron Capture in Titanium, Nickel, Zinc, Chlorine, Sulfur, and a Stainless Steel, R. E. Maerker and F. J. Muckenthaler.

3. Measurement of ^{235}U Capture to Absorption Ratio in the Molten Salt Reactor Experiment and Comparison with Calculations, G. L. Ragan, A. M. Perry, and B. E. Prince.

4. Evaluation of the Total Cross Section of Iron, D. C. Irving and E. A. Straker.

5. Statistical Properties of the Resonance Parameters of the Fissile Isotopes, G. de Saussure and R. B. Perez.

6. The Calculation of the Generalized Kapur-Peierls Parameters by Expansion of the Reich-Moore Multilevel Formula, R. B. Perez and G. de Saussure.

7. Proton Reaction Analysis for ^{12}C, ^{13}C, and ^{15}N Sensitivity and Biomedical Application, Enzo Ricci and J. H. Gibbons.

Listed below are titles of papers to be published.

1. Capture Cross Section Standards (or the Real Life Story of the Indian and the Turkey), J. H. Gibbons, Proc. Topical Conference on Neutron Capture Cross Sections and Gamma-Ray Spectra, Upton, L.I., N. Y., June 2-6, 1969.

2. Multiple Coulomb Excitation of Medium-Weight and Rare-Earth Nuclei with ^{16}O Ions, R. L. Robinson, P. H. Stelson, F. K. McGowan, R. O. Sayer, and W. T. Milner, Proc. International Conference on Nuclear Reactions Induced by Heavy Ions, Heidelberg, Germany, July 15-18, 1969.

3. Triple Angular Correlations, R. L. Robinson, Proc. International Conference on Radioactivity in Nuclear Spectroscopy, Vanderbilt University, Nashville, Tennessee, Aug. 11-15, 1969.

4. Coulomb Excitation of ^{152}Sm, $^{166,168,170}Er$, and ^{232}Th, F. K. McGowan, Proc. International Conference on Radioactivity in Nuclear Spectroscopy, Vanderbilt University, Nashville, Tenn., August 11-15, 1969.

5. Low-Lying Excited States of ^{204}Tl and ^{206}Tl Populated in Thermal Neutron Capture, C. Weitkamp, J. A. Harvey, G. G. Slaughter, and E. C. Campbell, Proc. International Symposium on Neutron Capture Gamma-Ray Spectroscopy, Studsvik, Sweden, August 11-15, 1969.

6. One Octupole-One Quadrupole Phonon States of ^{110}Pd, R. L. Robinson, J. A. Deye, J. L. C. Ford, Jr., P. H. Stelson, T. Tamura, and C. Y. Wong, Proc. International Conference on Properties of Nuclear States, Montreal, Quebec, Canada, Aug. 25-30, 1969.

7. Reaction List for Charged-Particle-Induced Nuclear Reactions Part A. Z = 3 to Z = 27 (Li to Co), F. K. McGowan, W. T. Milner, H. J. Kim, and Wanda Hyatt, Nuclear Data.

8. Reaction List for Charged-Particle-Induced Nuclear Reactions Part B. Z = 28 to Z = 99 (Ni to Es), F. K. McGowan, W. T. Milner, H. J. Kim, and Wanda Hyatt, Nuclear Data.

9. Periodic Intensity Fluctuations of Balmer Lines from Single Foil Excited Fast Hydrogen Atoms, I. A. Sellin, C. D. Moak, P. M. Griffin, and J. A. Biggerstaff, Phys. Rev.

10. Polarization of Neutrons from the $^{9}Be(d,n)^{10}B$ Reaction from 0.9 to 2.48 MeV, T. G. Miller and J. A. Biggerstaff, Phys. Rev.

11. Polarization of Neutrons from the $^{11}B(d,n)^{12}C$ Reaction, T. G. Miller and J. A. Biggerstaff, Phys. Rev.

12. Elastic and Inelastic Scattering of Protons from Krypton, H. J. Kim, J. K. Bair, C. M. Jones, and H. B. Willard, Phys. Rev.

13. Isobaric Spin Dependence in Proton Transfer Reactions, R. G. Couch, F. G. Perey, J. A. Biggerstaff, and K. K. Seth, Phys. Letters.

14. Elastic and Inelastic Proton Scattering from ^{110}Pd, R. L. Robinson, J. L. C. Ford, Jr., P. H. Stelson, T. Tamura, and C. Y. Wong, Phys. Rev.

15. Fast Neutron and Gamma-Ray Rise-Time Differences for 8 to 10 MeV Pulses in a Large NaI(Tl) Crystal, R. J. Jaszczak, R. Nutt, and R. L. Macklin, Rev. Sci. Instr.

16. Neutron Emission in the Fission of ^{213}At, F. Plasil, R. L. Ferguson, and H. W. Schmitt, Proc. International Atomic Energy Agency Symposium on the Physics and Chemistry of Fission, Vienna, Austria, July 28 - Aug. 1, 1969.

17. The $^{208}Pb(^{3}He,\alpha)^{207}Pb$ Reaction at 47.5 MeV, G. R. Satchler, W. C. Parkinson, and D. L. Hendrie, Phys. Rev.

18. $^{11}B(^{3}He,d)^{12}C$ Spectroscopic Factors, P. D. Miller, J. L. Duggan, M. M. Duncan, R. L. Dangle, W. R. Coker, and J. Lin, Nucl. Phys.

19. Penetration of a Double Barrier, C. Y. Wong and J. Bang, Phys. Letters.

20. Proton Strength Functions for Tin and the Optical Model Below the Coulomb Barrier, C. H. Johnson and R. L. Kernell, Phys. Letters.

21. Model for Fragment Mass vs Energy Correlations in Fission, H. W. Schmitt, Proc. International Atomic Energy Agency Symposium on the Physics and Chemistry of Fission, Vienna, Austria, July 28 - Aug. 1, 1969.

22. Statistical Tests for the Detection of Intermediate Structures in the Fission Cross Sections of ^{235}U and ^{239}Pu, R. B. Perez, G. de Saussure, and M. N. Moore, Proc. Second Symposium on the Physics and Chemistry of Fission, Vienna, Austria, July 28 - August 1, 1969.

23. Nuclear Structure of $^{91,92,93,95,97}Nb$ and ^{94}Mo with the (^{3}He,d) Reaction, M. R. Cates, J. B. Ball, and E. Newman, Phys. Rev.

24. The $^{4}He(t,p)^{6}He$ Reaction at Tritium Energy Equals 22 MeV, J. J. Malanify, Phys. Letters.

25. Total Reaction Cross Section Measurements with 60 MeV Protons, J. J. H. Menet, E. E. Gross, J. J. Malanify, and A. Zucker, Phys. Rev. Letters.

26. Calculated Energy Levels for ^{92}Mo and ^{94}Ru, J. B. Ball, J. B. McGrory, R. L. Auble, and K. H. Bhatt, Phys. Letters.

27. The (p,t) Reaction on the Even Zirconium Isotopes, J. B. Ball, R. L. Auble, and P. G. Roos, Phys. Letters.

28. A Large Scintillation Detector for Neutron Time-of-Flight Measurements, E. G. Silver, J. H. Todd, and J. Lewin, Proc. American Nuclear Society, San Francisco, Calif., Nov. 30 - Dec. 4, 1969.

29. Protons from 2.7-GeV Protons on Silver and Bromine, D. T. King, Phys. Rev.

30. The Transport of Neutrons Produced by 3-GeV Proton-Lead Nucleus Collisions through a Labyrinth and Comparison with Experiment, R. G. Alsmiller, Jr. and F. Solomito, Nucl. Instr. and Methods.

31. Photonucleon and Photopion Production from 400-MeV Electrons in Thick Copper Targets, T. A. Gabriel and R. G. Alsmiller, Nucl. Phys.

32. Shielding Against Neutrons in the Energy Range 50 to 400 MeV, R. G. Alsmiller, Jr., F. R. Mynatt, J. Barish, and W. W. Engle, Nucl. Instr. and Methods.

33. An Experimental Measurement of the High Energy Gamma Rays Produced by the Slowing Down of 14 MeV Neutrons in Air, J. H. Thorngate, Health Physics Journal.

34. A Sensitive Spectrometer for Fast Neutrons Using Europium Activated ^{6}Li Iodide, D. R. Johnson, J. H. Thorngate, and P. T. Perdue, Nucl. Instr. and Methods.

35. Nuclear Charge Distribution in Fission - Independent Yields of ^{132,133,134}I from Thermal Neutron Fission of ^{233}U, N. G. Runnals and D. E. Troutner, Phys. Rev.

36. The Thermal Neutron Capture Cross Section and Resonance Integral of ^{252}Cf, J. Halperin, C. E. Bemis, R. E. Druschel, and J. R. Stokely, Nucl. Sci. and Engineering.

37. Independent Yields of ^{95}Zr from Thermal Neutron Fission of ^{235}U and ^{233}U, L. H. Niece, D. E. Troutner, and R. L. Ferguson, Phys. Rev.

38. Performance of 140-MeV High Current Short Pulse Linac at ORNL, N. Pering and T. A. Lewis, Proc. 1969 National Particle Accelerator Conference, Washington, D. C., March 5-7, 1969.

39. ORELA Data Acquisition Into Greater than 10^5 Channels through A Priority Multiplexer Operating on a Direct Memory Access and a Program Controlled Device Interface, J. W. Reynolds, N. A. Betz, and D. A. McCully, Proc. 1969 Nuclear Science Symposium, San Francisco, Calif., Oct. 29-31, 1969.

Listed below are titles of Oak Ridge National Laboratory Reports.

1. Neutron Induced Background Effects in Gamma-Ray Spectrometers for Use in Space, R. L. Macklin, ORNL-TM-2675.

2. An Effective Nucleon-Nucleon Interaction for Use in Nuclear Hartree-Fock Calculations, C. W. Nestor, Jr., ORNL-TM-2556.

Listed below is the title of a National Academy of Sciences-National Research Council Report.

Calculations of the Penetration of Charged Particles Through Matter at Very High Energies, J. E. Turner.

YALE UNIVERSITY

ABSTRACTS

Washington APS Meeting, April, 1969, (B.A.P.S. 14, No.4)

"Estimate of the Direct Photonucleon E1 Transition Probability in O^{16} and C^{12}", M.G. Mustafa and F.B. Malik, p. 607.

"Isospin Mixing in the Giant Dipole States of Ca^{40}", C.-P. Wu, J.E.E. Baglin, F.W.K. Firk and T.W. Phillips, p. 607.

"Inelastic Electron Scattering from K^{39}", R.J. Peterson, H. Theissen and W.J. Alston (Boston University), p. 630.

CONFERENCE PROCEEDINGS

Gordon Conference on Photonuclear Reactions, August, 1969.

"High Resolution Polarization Studies of the $O^{16}(\gamma,n)O^{15}$ Reaction", G.W. Cole, F.W.K. Firk and T.W. Phillips.

"Photoprotons from O^{16}", J.E.E. Baglin and M.N. Thompson.

"Differential Cross Sections from Deuterium Photodisintegration Between 27 and 55 MeV", B. Weissman and H.L. Schultz.

INVITED PAPER:

"Giant Resonance Structure in p-shell Nuclei", J.E.E. Baglin, American Physical Society Meeting, Washington, April, 1969 (B.A.P.S. 14 506 (1969)).

YALE UNIVERSITY (cont.)

PUBLICATIONS

"Correlations in the Energies and Widths of Structure Observed in the Reactions $^{40}Ca(\gamma,n_0)^{39}Ca$ and $^{40}Ca(\gamma,p_0)^{39}K$." C.-P. Wu, J.E.E. Baglin, F.W.K. Firk and T.W. Phillips, Phys. Letters 29B (1969) 359.

"A Spectrometer for Photoprotons", J.E.E. Baglin and M.N. Thompson, Nuc. Instr. and Methods 71 71 (1969).

TO BE PUBLISHED:

"Polarization Studies of the $^{16}O(\gamma,n)^{15}O$ Reaction", G.W. Cole, F.W.K. Firk and T.W. Phillips, Phys. Letters.

"Quadrupole and Octupole Excitation of Even Tin Isotopes", T.H. Curtis, R.A. Eisenstein, D.W. Madsen, and C.K. Bockelman, Phys. Review.

"Elastic and Inelastic Scattering from Mn^{55}", H. Theissen, R.J. Peterson, W.J. Alston, and J.R. Stewart, Phys. Rev.

"Electron Scattering Studies on Ca^{40} and Ca^{48}", R.A. Eisenstein, D.W. Madsen, H. Theissen, L. Cardman, and C.K. Bockelman, Phys. Review.

"Model--Independent Analysis of Inelastic Electron Scattering from Nuclei. II. Monopole Excitation at Arbitrary Momentum Transfer", Thomas H. Schucan, Physical Review.

"A Study of $O^{16}(\gamma,p_0)$ Angular Distributions at Giant Resonance Energies", J.E.E. Baglin and M.N. Thompson, Nuclear Physics.

"Structure of the Nucleon-Nucleus Scattering Matrix in the Random-Phase Approximation", J.N. Ginocchio, T.H. Schucan and H.A. Weidenmuller.